Investigating the evolution and function of Wnt ligands

PhD Thesis

Submitted by

Michaela Holzem

In accordance with the requirements for the degree Doctor of philosophy

Awarded by Oxford Brookes University

December 2018

Oxford Brookes University, Oxford, UK

First supervisor: Prof. Alistair P McGregor

Second Supervisor: Dr. Maria Daniela Santos Nunes

Internal Examiner: Dr. Casper J Breuker, Oxford Brookes University, UK

External Examiner: Dr. Steffen Scholpp, University of Exeter, UK

Synopsis

Wnt genes encode secreted glycoproteins which play an important role in development of all animals. Overall, thirteen subfamilies of Wnt ligands are present and all of them can already be found in the most basal metazoans. The importance of this large gene family and its evolutionary conservation intrigued me to analyse Wnts with a variety of different approaches. Starting with a broad evolutionary approach, the losses, conservation and duplication within the Wnt gene repertoire throughout the metazoan phylogeny were studied to understand the underlying evolutionary constrains which were fundamental to create this diverse Wnt landscape.

I focussed on elucidating the Wnt gene losses and duplications in arthropods where I found support for the loss of *Wnt2* and *Wnt4* in all insects, loss of *Wnt16* in all insets except Hemiptera and loss of *Wnt8* and *Wnt9* in Hymenoptera, while Chelicerata, such as spiders and scorpions have lost *Wnt10*. In horseshoe crabs, spiders and scorpions, duplications of *Wnt7* and *Wnt11* were observed.

Taking some of the results from this broad evolutionary analysis, it would be interesting to understand on a finer scale how the expression or function of Wnt genes is conserved throughout more closely related species. Here, Lepidoptera became of certain interest due to their close relation toits sister groups Diptera and Coleoptera. The expression of Wnts is well known in *Drosophila* (Diptera) and *Tribolium* (Coleoptera) but relatively less is understood about Wnt gene expression in butterflies and moths (Lepidoptera). Showing the expression of Wnts in Lepidoptera and being able to compare these results with known patterns from closely related taxa could help to understand if also the function of Wnts could be conserved within phyla.

Interestingly, it was possible to show that some Wnts genes (*Wnt1*, *A* and *10*) have similar expression in all three analysed classes. This hints that in these closer related groups the function of Wnts could be conserved as well and therefore could also be able to influence the evolution of the ligands itself.

In the third part of this thesis, the exact function of Wnts was even more narrowed down. For this purpose, *Drosophila melanogaster* was used and puzzlingly, even in a well-studied model organism such as *Drosophila*, the function of some of the

Wnts is not fully understood. *wingless* for example is the most studied Wnt gene in *Drosophila*, while the role during development for *Wnt6* and *Wnt10* remains unclear. In the following analysis, the focus was on *Wnt6* due to its high sequence similarity to *wg*, close genomic location and overlapping expression. *Wnt6* is also highly conserved in all arthropods and additionally part of the conserved Wnt cluster (*Wnt1-6-9-10*). Hence, the function of *Wnt6* during development was studied and also these results were linked to the question of how and why Wnt genes are conserved and why so many Wnt ligands are still present in many species.

Previously, a potential role of *Wnt6* during maxillary palp development was described which was used as a starting point for the functional analysis. Further, a new *Wnt6* knockout line, using CRISPR/Cas9 was generated for comparison to a published knockout line. During the analysis a putative regulatory function of the first exon of *Wnt6* was found, which might influence a crucial *wg* signal during palp development. *Wnt6* itself might be involved in regulating the correct growth and pupariation signal during larval development. This analysis also added an additional components, including the regulation of Wnt ligands of the ancestral Wnt cluster to the potential evolutionary mechanisms.

Taking all of these results together it was possible to highlight the large diversity of the Wnt landscape in arthropods and indicate clues about the underlying evolutionary mechanisms. Analysing the exact function of *Wnt6* also revealed that the genomic location or the clustering of Wnts could play a role in constraining evolution on these genes due to regulatory region within the genes. Overall, this study contributes to increase our understanding of Wnt gene evolution as well as the function and regulation of Wnt ligands.

Table of content

Synopsis I

List of Figures V

List of Supplementary Figures VII

List of Supplementary Tables VII

1 | Wnt ligands and Wnt signalling pathways 1

1.1 Background 2

1.2 Processing, secretion and trafficking of Wnt ligands 5

1.3 Wnt signalling 7

The canonical Wnt signalling 7

The non-canonical Wnt pathways 8

1.4 Aims of this PhD thesis: Investigating the function and evolution of Wnt ligands 10

2 | Wnt gene evolution in arthropods 10

2.1 | Background 11

2.1.1 The Wnt repertoires of metazoans 12

Ctenophora 13

Porifera 13

Cnidaria 13

Acoela 14

Protostomia – Ecdysozoa - Nematoda 14

Protostomia – Ecdysozoa - Onychophora 14

Protostomia – Ecdysozoa - Arthropoda 15

Protostomia – Lophotrochozoa - Platyhelminthes 16

Protostomia – Lophotrochozoa - Annelida 16

Protostomia – Lophotrochozoa - Mollusca 16

Deuterostomia - Echinodermata 16

Deuterostomia - Chordata 16

2.2 | Methods 18

Phylogenetic analysis 18

2.3 | Results and Discussion 21

2.3.1 Analysing the maximum likelihood tree of arthropod Wnt genes 21

2.3.2 | Analysing the Wnt gene repertoire in small arthropod datasets 22

The Wnt genes in chelicerates 22

The Wnt genes in lepidopterans 28

2.3.2 The Wnt repertoire of newly sequenced arthropod species 31
2.3.4 The clustering of Wnt genes: Is the ancestral Wnt cluster conserved in arthropods? 39
2.4 | Conclusions and Outlook: Future study of Wnt genes in arthropods 42
2.5 | Supplement 43
3 | Wnt gene expression during embryogenesis in *Bicyclus anynana* . 59
3.1 | Background 60
3.1.1 Embryogenesis in Lepidoptera 61
3.1.2 Wnt genes in lepidopteran development 62
3.1.3 Aims 63
3.3 | Methods 64
Animal husbandry 64
In situ *hybridisation* 64
3.4 | Results and discussion 65
3.4.1 *Bicyclus anynana* embryogenesis 65
4-8 h AEL (0-10% development completed) 65
9-14h AEL (10-15 % development completed) 66
16-28 h AEL (20-30% development completed) 68
30-51 h AEL (35-50 % development completed) 70
3.4.2 Expression of Wnt genes during butterfly embryogenesis 72
Wnt1/wingless 72
Wnt5 and *Wnt6* 74
Wnt7 75
Wnt9 76
Wnt10 76
Wnt11 79
WntA 79
3.5 | Conclusions and future directions 82
3.6 | Supplement 85
4 | Investigating the functional role of *Wnt6* in *Drosophila melanogaster* 88
4.1 | Background 89
4.1.1 The *Wnt6* gene in *D. melanogaster* 89
4.1.2 The developmental regulation of maxillary palps 91

4.1.3 Aims 93

4.3 | Material and Methods 95
Fly husbandry and fly genetics 95
Dissections, measurements and statistics 95
Cloning the CRISPR construct for the Wnt6*{KO}* 96
Cloning the Wnt6 HA tag vector 99
In situ *hybridisation* 99
Immunohistochemistry and confocal microscopy 100
Developmental assays 101

4.4 | Results and Discussion: The role of *Wnt6* in *Drosophila melanogaster* 102

4.4.1 | Analysing the *Wnt6*{KOd} function 102
Analysing the phenotype of the Wnt6{KOd} fly line 102
Rescuing the Wnt6*{KOd} maxillary palp phenotype using the UAS/Gal4 system* 104

4.4.2 | Creating a *Wnt6* knockout fly using CRISPR/Cas9 mediated homologous recombination 110

4.4.3 Analysing the differences between the two *Wnt6* knockout lines 114
Analysis of the Wnt6*{KO} lines using deficiency lines* 114

4.4.3 | Analysing the Wnt6 and Wg protein distribution in *Wnt6* knockout lines ... 118
Is the first exon of Wnt6 *an active regulatory region during MP development?* 120
Which gene in the developmental MP pathway is potentially affected by the potential regulatory function of the first exon? 122

4.4.4 | Analysing the new *Wnt6*{KOmche} phenotype: developmental assays 124
Duration of larval development 125
Measuring larval size 126

4.5 | Conclusions and outlook 128
A potential regulatory role of the first exon of Wnt6*.* 128
Wnt6 might be involved in regulating the signal to pupate 129

4.6 | Supplement 130

5 | General Discussion 139

Acknowledgements 148

References 150

List of Figures

Figure 1.1 | Ribbon structures of Xenopus Wnt8 and Drosophila Wg. 3
Figure 1.2 | The canonical and non-canonical Wnt signalling pathways. 8
Figure 1.3 | Schematic connection of the three projects presented in this thesis. 11
Figure 2.1 | Summary of the Wnt gene diversity in selected metazoans. 12
Figure 2.2 | Maximum likelihood tree of chelicerates. 24
Figure 2.3 | Chelicerate maximum likelihood tree without *P. opilio*.. 27
Figure 2.4 | Overview of Wnt genes in chelicerates.. 28
Figure 2.5 | Phylogenetic analysis of lepidopteran Wnt genes. 29
Figure 2.6 | Summary of the Wnt gene repertoire in lepidopterans. 30
Figure 2.7 | Summary of the Wnt gene analysis in arthropods. 32
Figure 2.8 | Wnt gene clusters in arthropods. 40
Figure 3.1 | The African butterfly *B. anynana* and its distribution..... 60
Figure 3.2 | Early developmental stages of *B. anynana* from 4 to 8 hours..... 65
Figure 3.3 | Embryonic stages of *B. anynana* from 9 to 14 h AEL.. 67
Figure 3.4 | Embryonic development from 16 to 28 hours in *B. anynana*..... 69
Figure 3.5 | Developmental stages of *B. anynana* from 30 to 51 hours.. 71
Figure 3.6 | *Wnt1/wg* expression during embryogenesis in *B. anynana*. 73
Figure 3.7 | Expression of *Wnt7* during development in *B. anynana*. 75
Figure 3.8 | *Wnt10* expression during *Bicyclus anynana* embryogenesis. 78
Figure 3.9 | *Wnt11* expression during late embryogenesis in *B. anynana.* 79
Figure 3.10 | Expression of *WntA* during the development of *B. anynana.* 80
Figure 3.11 | Schematic summary of the Wnt expression pattern in early embryogenesis of *B. anynana*.. 83
Figure 4.1 | *Wnt6* structure and expression in imaginal discs of 3rd instar larvae of *D. melanogaster*..... 90
Figure 4.2 | Developmental pathways of antennal and MP development. 92
Figure 4.3 | Methodological overview about the CRISPR strategy for the *Wnt6*{KO} and the *Wnt6*{HA} fly lines. 98
Figure 4.4 | Analysis of the *Wnt6*{KOd} fly line. 103
Figure 4.5 | Rescuing the MP development using *elav*-Gal4. 105
Figure 4.6 | Rescuing the MP phenotype of *Wnt6*{KOd} using *hth*-Gal4. 107
Figure 4.7 | Rescuing the MP phenotype of *Wnt6*{KOd} using *dpp*-Gal4..... 109
Figure 4.8 | Confirming the successful knockout of *Wnt6* in the *Wnt6*{KOmche} line. 112

Figure 4.9 | Analysing the MP phenotype of the new CRISPR *Wnt6* knockout line.. 113
Figure 4.10 |Crosses of the two *Wnt6* knockout lines to the deficiency line Df(2L)BSC226. ... 115
Figure 4.11 | Cross between both *Wnt6* knockout lines.. 117
Figure 4.12 | Sequencing confirmation of correct insertion of the HA tag into *Wnt6* locus 119
Figure 4.13 | Wg and Wnt6-HA protein localisation in the pre-pupal antennal disc. 120
Figure 4.14 | Analysing the potential enhancer activity of the first exon of *Wnt6*. 121
Figure 4.15 | Distribution of Wingless protein in pre-pupal antennal discs in two *Wnt6* knockout lines..... 123
Figure 4.16 | Analysing the duration of larval development until pupariation. 125
Figure 4.17 | Analysis of the larval length over time in control and *Wnt6* knockout lines. 127
Figure 5.1 | The design of chimeric Wnt genes. 145

List of Supplementary Figures

Supplement Figure S2.1 | Maximum likelihood tree of all analysed arthropod species..... 58
Supplement Figure S4.1 | Crosses for rescuing the Wnt6{KOd} phenotype using the UAS/Gal4 system. 132
Supplement Figure S4.2 | Balancing and 'floxing' crosses of the CRISPR generated Wnt6KO and HA tag flies.. 133
Supplement Figure S4.3 | In situ hybridisations of 3rd instar larval discs for dfd, dpp, hth and elav. 134
Supplement Figure S4.4 | Antibody staining's of Wnt6-HA together with Wg protein localisation in different 3rd instar larval tissues.. 135
Supplement Figure S4.5 | Measurements of the 2nd leg tibia length for the lines from the UAS/Gal4 crosses.. 136
Supplement Figure S4.6 | Leg measurements of the deficiency line crosses and the cross between both Wnt6 knockout lines. 137
Supplement Figure S4.7 | q-q plots for non-normally distributed strains..... 138
Supplement Figure S4.8 | 2nd leg pair of the Wnt6{KOd};dpp>Wnt6 cross. 138

List of Supplementary Tables

Supplement Table S2.1 | Summary of all used Wnt gene sequences, their accession numbers or protein source code and the newly annotated Wnt subfamily association. 43
Supplement Table S2.2 | All genome accession data for the phylogenetic analysis of Arthropods.. 53
Supplement Table S3.1 | Primer sequences for all Wnt probes used in this study..... 86
Supplement Table S4.1 | Stocklist of all used fly lines with their full genotypes, commercial stock numbers and sources. 130
Supplement Table S4.2 | Primer list.. 131

Introduction

1 | Wnt ligands and Wnt signalling pathways

1.1 Background

Wnt proteins are signalling molecules which regulate important developmental processes, such as cell proliferation, differentiation, polarity and cell cycling e.g. Logan and Nusse (2004). Malfunction of the Wnt signalling can lead to severe diseases such as colorectal cancer, bone density defects or the Robinow syndrome (Nusse and Clevers, 2017; Zhan *et al*., 2017). This dramatic influence of Wnt signalling on development and health moved Wnt genes and all other pathway components into the research focus. The Wnt gene family is characterised by a pattern of 22-24 cysteine residues and within this family, thirteen Wnt subfamilies are described (*Wnt1-11, 16* and *A*) which are highly conserved throughout the metazoan phylogeny (Croce and McClay, 2008; Seto and Bellen, 2004). Most Wnt ligands can bind to the transmembrane receptors of the Frizzled (Fz in *Drosophila*; FZD in human) family and operate through either the canonical or non-canonical Wnt signalling pathways which are able to activate important target gene expression needed for e.g. cell cycle or proliferation (Figure 1.2) (Bhanot *et al*., 1996; Wodarz and Nusse, 1998).

wingless (*wg* or *Wnt1*) was the first Wnt gene discovered in *Drosophila melanogaster* due to mutation screenings by Sharma (1973). *wingless* is homolog to the vertebrate Wnt gene, the mouse *integrin-1* gene (Cabrera *et al*., 1987; Rijsewijk *et al*., 1987). Both gene names together were used to form the current family name: Wnt gene family (**w***ingless* and *i***nt***egrin*) (Nusse *et al*., 1991).

The structure of Wnt ligands resembles a U-shape, which has also been described as a “hand” structure with an extended “thumb” and “index finger” (Figure 1) and the cysteine pattern, characterising Wnts is involved in forming this structure (Janda *et al*., 2012). The Wnt ligand can bind to the Fz receptor at two interaction sites: (1) the palmitoleic acid lipid group on the “thumb” (PAM site) can interact with the deep groove in the extracellular cysteine rich domain (CRD) of Fz. (2) The other interaction happens via the “index finger” where hydrophobic amino acids contact the opposite site of the Fz CRD (Figure 1.1) (Janda *et al*., 2012).

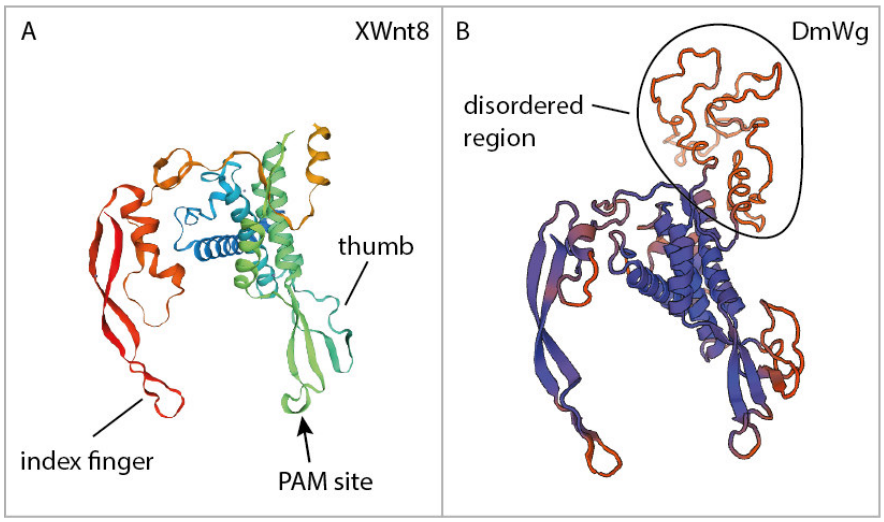

Figure 1.1 | Ribbon structures of *Xenopus* Wnt8 and *Drosophila* Wg. **(A)** The published structure of XWnt8 from *Xenopus* is shown with the "index finger" and "thumb". The palmitoleic acid group (PAM) site at the thumb is also indicated. **(B)** Modelled structure of Wg from *Drosophila* based on the published XWnt8 structure. The overall structure is similar with "thumb" and "index finger" whereas an additional disordered region is present. Ribbon structure models are obtained from SWISS-MODEL (Waterhouse *et al*., 2018) by using the published XWnt8 structure from Janda *et al.* (2013) as template.

It has been described, that some Wnt ligands are located next to each other in several species. This grouping of Wnts, normally involving *Wnt1-6-9-10* was considered to be an ancestral Wnt cluster (Guder *et al*., 2006; Nusse, 2001). In *D. melanogaster* this cluster is ordered in *Wnt9-1-6-10* (Nusse, 2001) which can be observed similarly in the flour beetle *Tribolium castaneum*, the silk moth *Bombyx mori* (Bolognesi *et al*., 2008), the honey bee *Apis mellifera* (Dearden *et al*., 2006), amphioxus *Branchiostoma floridae* (Putnam *et al*., 2008), the pearl oyster *Pinctata fucata* (Takeuchi *et al*., 2016) and the water flea *Daphnia pulex* (Janssen *et al*., 2010). In some species, the synteny of these genes has been broken up, for example in the sea anemone *Nematostella vectensis* (Sullivan *et al*., 2007), where only *Wnt*6 and *Wnt10* remain linked. The clustering of Wnt genes is one of the important evolutionary clues in understanding where Wnt genes have evolved from and how so many subfamilies have arisen. It is assumed, that the *Wnt1-6-9-10* cluster originated from tandem duplications (Holland *et al*., 1994) and further, gene duplications are considered to explain the rapid emergence of many Wnt genes at the base of the metazoan phylogeny. Until now, the origin of the "Ur-Wnt" gene remains unknown, but it is hypothesised that a gene fusion lead to the first Wnt at the very basis of the metazoans and this "Ur-Wnt" was then the founder of all Wnt

subfamilies. So far, no Wnt ligands were found in any organisms outside Metazoa whereas components of the Wnt signalling pathway were present, such as ß-catenin or proteins of the destruction complex (Holstein, 2012). It is assumed, that acquiring the Wnt signalling pathway was one of the key developmental novelties that lead to the diversification and evolution of the metazoan body plan (Holstein, 2012).

1.2 Processing, secretion and trafficking of Wnt ligands

For activation of the Wnt signalling pathway in a target cell, Wnt ligands need to be secreted into the extracellular (Figure 1.2). To be able to enter the secretory pathway Wnt ligands are located via their signal peptide sequence to the endoplasmic reticulum ER, where they are lipid modified by the membrane associated O-palmitoyleoyltransferase Porcupine (Por in *Drosophila* and Porcn in humans) (Kadowaki *et al*., 1996; Nusse, 2003; Tang *et al*., 2012; Willert *et al*., 2003). Por modifies Wnt ligands with palmitoleic acid at a serine residue (S239 in *Drosophila*) (Herr and Basler, 2012; Willert *et al*., 2003) which is required for the association of Wnt with Wntless (Wls/Evi/Sprinter in *Drosophila*; GPR177 in humans) (Banziger *et al*., 2006; Bartscherer *et al*., 2006; Goodman *et al*., 2006; Moti *et al*., 2019).

In *D. melanogaster* the Wg-Wls complex is trafficking from the ER to the Golgi apparatus from where it is secreted in endovesicles (Bartscherer and Boutros, 2008). The endovesicles traffic to the apical plasma membrane and Wg was released by fusion of the endovesicle with the membrane or multi vesicular bodies were formed which could also fuse with the membrane and set free exosomes (Bartscherer and Boutros, 2008). In a different study, it has been shown that Wg in *Drosophila* was trafficking within the cell from the apical to the basolateral membrane (Yamazaki *et al*., 2016). The endovesicles are transported via the protein Godzilla to the basolateral membrane where Wg could be secreted (Langton *et al*., 2016).

In *Drosophila*, *wg* is considered to be a morphogene which includes the ability to travel within an organism from an origin to a target cell and transmit therewith a signal (Aulehla *et al*., 2003; Aulehla *et al*., 2008; Gao *et al*., 2011; Kiecker and Niehrs, 2001). In the fruit fly, a short-range and a long-range signalling activity were described for *wg* and it was assumed that different transport mechanisms were involved in facilitating these two signalling ranges (Swarup and Verheyen, 2012; Zecca *et al*., 1996). Recently, the mechanisms of Wnt secretion and travelling in the extracellular space were highly researched (Chaudhary and Boutros, 2018; Pani and Goldstein, 2018; Takada *et al*., 2017). Due to their lipid modifications, Wnt ligands were highly hydrophobic and tend to stick to cell membranes which made simple diffusion as travel option unlikely (Willert *et al*., 2003). Coudreuse *et al*. (2006) hypothesised that secreted Wnt ligands associated

with multiprotein complexes, so called retromers which than could move freely in the extracellular space (Coudreuse *et al*., 2006). Further, the movement via exosomes or other vesicles was proposed (Greco *et al*., 2001; Gross *et al*., 2012; Korkut *et al*., 2009; Panakova *et al*., 2005) or the transport via cellular projections, so called cytonemes (or filopodia) which were cell protrusions that "hand over" the Wnt ligand to the neighbouring cell (Ramirez-Weber and Kornberg, 1999; Roy *et al*., 2011; Stanganello *et al*., 2015). Another publication identified a molecule named "secreted *wg* interacting molecule" (SWIM) which promoted the long-range signal of *wg* via binding of the Wnt ligand and transport it to its target cell, whereas the exact mechanism of how this protein was binding Wnts remains unclear (Mulligan *et al*., 2012).

Which of the above-mentioned mechanisms were involved in the Wg short- or long-range signalling in *Drosophila* was controversially discussed. It was acknowledged that only for the long-range function, Wg did need to move some distance through the ECM (Neumann and Cohen, 1997; Zecca *et al*., 1996), contrastingly a study using a membrane tethered Wg mutant in the wing imaginal disc indicated that a distribution of Wg in this disc was not needed for the long-range signal. This result was explained to be a potential tissue specific cell memory effect, where early ubiquitous expression of *wg* was sufficient for later *wg* signalling in the wing disc (Alexandre *et al*., 2014). However, the question remained of why a gradient of Wg could be detected in wing discs if it was not required for a long-range function. Very recently, this view was challenged by a study in *Caenorhabditis elegans*. Here, *Wnt/egl-20* was fluorescently tagged and live imaged during development, where a clear *egl-20* gradient formation was detected. Tethering of *egl-20* lead to a breakdown of the gradient and malformation phenotypes in the nematode (Pani and Goldstein, 2018). Another study showed, that Wg spreading was needed for the correct development of malphigian tubules in *Drosophila* (Beaven and Denholm, 2018). Intriguingly, another study in *Drosophila* showed that membrane tethered Wg was not restricted to its source cells and those directly adjacent but could be detected further away from its source. Also, it seems that Wg was able to directly activate Wnt signalling over a distance of 11 cells and even more distant signalling was observed in combination with the Fz2 receptor in *Drosophila* (Chaudhary and Boutros, 2018). Taking together, this illustrates the complexity of this

topic and also indicates that the processing and transport of Wnts has to be carefully considered in a species-specific and tissue-specific context.

1.3 Wnt signalling

Secreted Wnt ligands could activate the Wnt signalling pathways on target cells via binding to the Fz receptors (FZD in humans). These signalling pathways were classified in the literature into (1) the canonical Wnt pathway and (2) the non-canonical pathways, which included the planar cell polarity (PCP) and the calcium dependent pathways. The different signalling fates were mainly influenced by the combination of different co-factors with the Fz receptor (Kikuchi *et al*., 2009; Lapebie *et al*., 2011; McMahon and Moon, 1989; Nusse and Clevers, 2017) (Figure 1.2). An overview about the different Wnt signalling pathways will be given below and due to my later work with *Drosophila*, the nomenclature will be oriented on this species.

The canonical Wnt signalling

In the canonical Wnt pathway, reviewed by MacDonald *et al*. (2009) and Seto and Bellen (2004), the secreted extracellular Wnt ligand bound the transmembrane receptor Fz (Janda *et al*., 2012) and its co-receptor Arrow (Arr or LRP5/6 in humans). This extracellular receptor/co-receptor/Wnt complex activated the intracellular canonical signalling pathway (Figure 1.2 A and B) which started with the intracellular recruitment of Dishevelled (Dsh in *Drosophila* or DVL in humans) to the receptor complex. Before activation, Dsh was part of the degradation complex including Shaggi (Sgg or GSK3-ß in humans), adenomatosis polyposis coli (APC), casein kinase 1 (CK1) and Axin which facilitated the degradation of Armadillo (Arm or ß-catenin in humans). When Arm was degraded it could not translocate to the nucleus and the Wnt signalling pathway was off (Jenny and Basler, 2014) (Wnt-OFF) (Figure 1.2 A). The absence of Arm from the nucleus lead to binding of Pangolin (Pan or TCF/LEF in humans) and Groucho (Gro or Grg/TLE in humans) to transcription start sites of target genes and transcriptional repression (Figure 1.2 A) (Cavallo *et al*., 1998; Jenny and Basler, 2014).

Localisation of Dsh to the receptor complex Arr/Fz recruited the degradation complex also to the membrane (Figure 1.2 B). The degradation complex could now no

longer mediate the Arm degradation which was now free to translocate to the nucleus (Figure 1.2 B). In the nucleus, Arm released Pan and Gro from transcription start site and activated together with Legless (Lgs or BCL9 in humans) and Pygopus (Pygo or PYGO in humans) transcription of Wnt target genes (Figure 1.2 A and B) (Hoffmans *et al*., 2005; Jenny and Basler, 2014; Kramps *et al*., 2002).

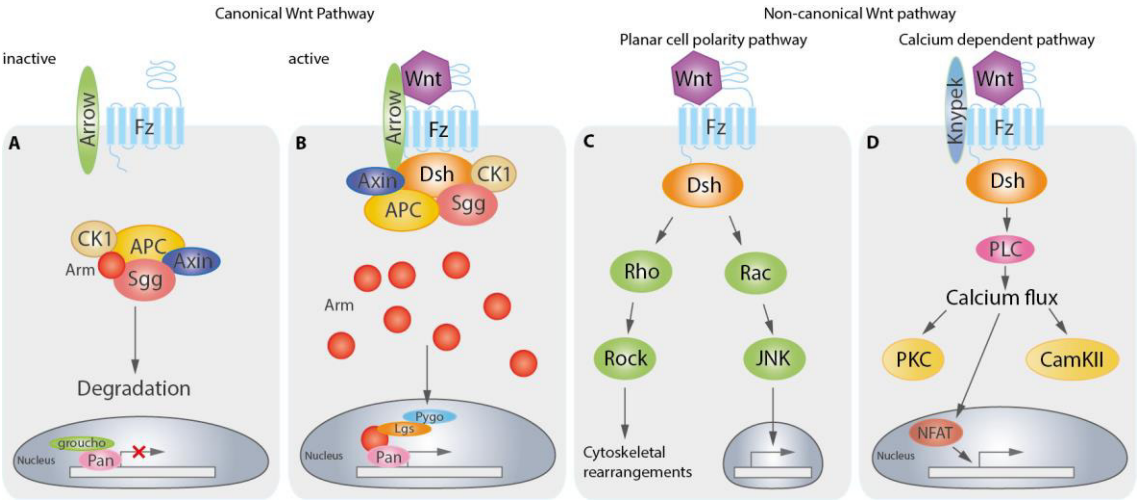

Figure 1.2 | The canonical and non-canonical Wnt signalling pathways. **(A)** The inactive state of the canonical pathway (WNT-OFF). **(B)** The active canonical pathway (WNT-ON). **(C)** The planar cell polarity pathway. **(D)** The calcium dependent Wnt pathway. Fz: Frizzled; CK1: casein kinase 1; APC: adenomatosis polyposis coli; Sgg: Shaggi; Pan: Pangolin; Pygo: Pygopus; Lgs: legless; Rho: small GTPase; Rock: serine/threonine kinase; Rac: small GTPase; JNK: c-Jun N-terminal kinases; PLC: phospholipase C; PKC: protein kinase C; CamKII: calmodulin kinase II; NFAT: Nuclear factor of activated T-cells (based on reviews from Seto & Bellen, 2004; MacDonald *et al*., 2009 and Niehrs, 2012; Nusse and Clevers, 2017).

The non-canonical Wnt pathways

Next to Arrow, several other co-receptors binding to Fz were described (reviewed in (Nusse and Clevers (2017) and references therein). These co-receptors were responsible for triggering a different downstream pathway which were all grouped under the non-canonical or ß-catenin independent Wnt pathways. An example would be the PCP pathway (Figure 1.2 C), which also functions via a Wnt ligand bound to the Fz receptor. Dsh was then recruited to Fz, which via the small GTPase Rac, lead to activation of the mitogen activated c-Jun N-terminal kinases (JNK). In parallel the small GTPase Rho could activate its associated kinase Rock which lead to cytoskeletal rearrangements to achieve planar cell polarity (Figure 1.2 C) (Amano *et al*., 2010; Lapebie *et al*., 2011). Several interactions of Fz with other transmembrane proteins were

assumed, such as Flamingo (Fmi) or VanGogh (Vang) whereas the exact PCP signalling seems to be highly tissue specific (Yang and Mlodzik, 2015).

Another non-canonical pathway would be the calcium dependent Wnt signalling pathway (Niehrs, 2012; Seto and Bellen, 2004). This pathway again requires the binding of a Wnt ligand to Fz, however the co-receptor was the proteoglycan receptor Knypek (Kny), which was recruited to the membrane (Figure 1.2 D). This binding again activates Dsh which leads to a Ca^{2+} flux due to phospholipase C (PLC), the activation of the protein kinase C (PKC) and the calmoduline kinase II (CamKII). The transcription of target genes was activated via the transcription factor Nuclear Factor of Activated T-cells (NFAT) (Figure 1.2 D) (Veeman *et al*., 2003). It has been suggested that these two non-canonical Wnt pathways were the same pathway with different functions and outcomes depending on the tissue, cofactors and the developmental timing of activation (Lapebie *et al*., 2011).

1.4 Aims of this PhD thesis: Investigating the function and evolution of Wnt ligands

In this thesis, an analysis of the role of Wnt ligands in the context of evolution and development is presented. In the first part, the evolutionary diversity of Wnt ligands, their conservation and losses were analysed to detail. This part of the study will be the basis for future analysis of the Wnt repertoire throughout the metazoans and will help to increase our understanding of the Wnt gene evolution (Chapter 1; Figure 1.3). Taking it from this broad evolutionary overview chapter, the potential underlying mechanisms of Wnt evolution were analysed further. Are Wnt genes conserved due to their functional role during development? To study this question, I choose to work with Lepidoptera, which are the sister group to Diptera and Coleoptera, both with relatively well understood Wnt gene expression and function (Chapter 2; Figure 1.3). Wnt expression during butterfly embryogenesis is poorly described and generating this data would make a comparison between these phylogenetically closely related groups possible. Finding similarities and differences in Wnt gene expression is the first step to understand the underlying function and therefore take a step forward in understanding the evolution of Wnt genes to a larger extend.

Further, extracting the exact function of a Wnt gene is not a trivial task to do but necessary to add to understand the evolution of this protein family. From the previous analysis in Chapter 1, it was shown that the ancestral Wnt cluster (*Wnt1-6-9-10*) is highly conserved in all arthropods (Figure 1.3). The function of *Wnt1* and 9 are very well understood whereas the role of *Wnt6* and *Wnt10* during development remain less clear. *Wnt6* is of particular interest due to its close genomic location, high sequence similarity and overlapping gene expression with *Wnt1*. Here, I focussed on determining the exact function and interactions of *Wnt6* during *Drosophila* development (Chapter 3). This analysis has the potential to facilitate further functional *Wnt6* studies in other arthropod species and therefore allow to compare the functional diversity of Wnts in an evolutionary context.

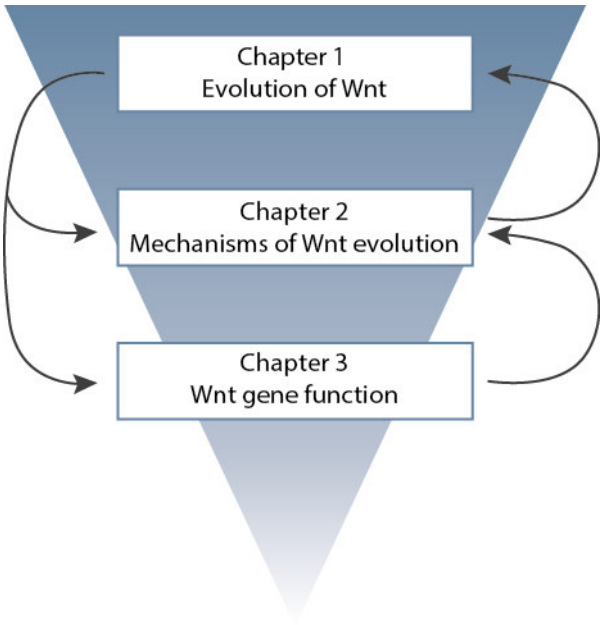

Figure 1.3 | Schematic connection of the three projects presented in this thesis. The broad overview about Wnt genes in arthropods (Chapter 1) will influence the questions asked in Chapter 2 and 3. Also the results from Chapter 2 and 3 are impacting the understanding of Wnt evolution analysed in Chapter 1.

Chapter 1 | Wnt gene evolution in arthropods

Thirteen Wnt subfamilies evolved at the base of metazoans, but subsequently losses and duplications have been observed throughout the phylogenetic tree of animals, and in particular, arthropods are characterised by losses of specific Wnt subfamilies. In this chapter of my PhD thesis, I investigated the Wnt gene repertoire among Arthropoda using recently sequenced genomes and transcriptomic data. Additionally, I analysed the conservation of the ancestral Wnt cluster. This project will contribute to a broad understanding of Wnt gene repertoires, conservations, losses and clustering and will therefore form the basis for several future studies regarding the evolution of Wnt genes.

Chapter 2 | Wnt gene expression during embryogenesis of Bicyclus anynana

From the previous phylogenetic analysis, studying the underlying evolutionary mechanisms of Wnt genes became of great interest. For this purpose, I choose to analyse the expression of Wnt genes in Lepidoptera and compared the results to expression data of the sister groups: Diptera (*D. melanogaster*) and Coleoptera (*T. castaneum*). Finding similarities or differences in the expression of Wnts during development could indicate, that the potential underlying function is involve in

conservation or loss of these Wnt genes. In the course of this study, I also will describe the embryogenesis of *B. anynana*, a well-established butterfly model, in detail.

Chapter 3 | Investigating the functional role of Wnt6 *in* Drosophila *melanogaster*

Leading from the two previous chapters, studying the exact function of Wnts cannot only contribute to understand the development of a specific species but also contribute to reveal underlying evolutionary mechanisms of Wnt genes. In Chapter 2 the focus was on three insect groups which included the Diptera with *D. melanogaster* as a great model organism to study function of Wnt genes further. Here, the function of *Wnt1* is very well analysed, whereas *Wnt6* and *Wnt10* are more neglected Wnt genes in *Drosophila*. Still, the function of both genes would be interesting in an evolutionary context, because they are part of the ancestral Wnt cluster (*Wnt1-6-9-10*). I focussed on studying *Wnt6* function during development due to its conservation in the cluster, but also due to its sequence and expression pattern similarities to *Wnt1*. Recently, a potential role of *Wnt6* in maxillary palp development was proposed which I will analyse in detail, also considering the position of *Wnt6* in this tissue specific developmental pathway and its interactions. This functional analysis will aid future studies on Wnt evolution in arthropods, understanding which mechanisms were involved in conservation or loss of Wnt ligands.

Chapter 1

2 | Wnt gene evolution in arthropods

2.1 | Background

Wnt ligands and their associated signalling pathways play an important role during development in metazoans. They are able to activate genes which are involved in many developmental processes, such as cell proliferation, differentiation, polarity or cell cycling (Logan and Nusse, 2004). Malfunction of the Wnt signalling could lead to severe diseases such as several types of cancer (Nusse and Clevers, 2017). This dramatic influence of Wnt signalling on development and health moved Wnt genes and all other pathway components into the research focus. Here, we were interested in the evolution of the Wnt ligands itself, which were able to activate the signalling pathway by binding to the Fz receptor (Bhanot *et al*., 1996; Janda *et al*., 2012; Kikuchi *et al*., 2007). Thirteen Wnt subfamilies were described within the Wnt protein family (*Wnt1-11, 16* and *A*), e.g. Prud'homme *et al*. (2002) and members from all subfamilies could already be found in basal metazoans such as cnidaria (Kusserow *et al*., 2005; Stefanik *et al*., 2014), whereas components of the signalling machinery were even found outside metazoans but no Wnt genes were ever detected in any non-metazoan species (Holstein, 2012). It remains unclear, which Wnt subfamily was ancestral to all other or how they have multiplied at the metazoan base, but it was assumed that duplications have played a role during this process (Holstein, 2012). Additionally, it remains unclear which underlying evolutionary constrains work on Wnt genes and influence their loss, conservation or duplication. One idea was, that the function of Wnts is conserved and crucial for correct development. Mutating or losing a particular Wnt would lead to severe developmental defect or would even be lethal.

In this chapter, all published data about the Wnt repertoire in metazoans were analysed first, to create a more complete picture of conserved, lost or duplicated Wnt genes. Furthermore, I focussed on arthropods, a phylum mainly characterised by losses of several Wnt gene subfamilies. Within the arthropods, eleven arthropod species have been analysed for their Wnt repertoire by Janssen *et al.* (2010) and Hogvall *et al*. (2014). However, these analyses left gaps in our understanding of losses, conservation and duplication of Wnt subfamilies in other arthropod families. Therefore, I analysed several newly sequenced arthropod specie genomes or transcriptomes and compared their putative Wnt genes with those of well-studied species. Moreover, this dataset was used

to analyse the clustering of Wnt genes with the focus on a presumably ancestral Wnt cluster containing *Wnt1-6-9-10* (Guder *et al*., 2006; Nusse, 2001).

2.1.1 The Wnt repertoires of metazoans

Wnt genes were present in all metazoans and some Wnt subfamilies were well conserved whereas others were lost. To better understand these dynamics, the published Wnt repertoire data was summarized for several metazoans. If for more than one species from one family the same Wnt repertoire was described, only one dataset was presented here for clarity. All findings were summarized in Figure 2.1 (with references provided therein) and the Wnt repertoires in each major lineage were discussed below.

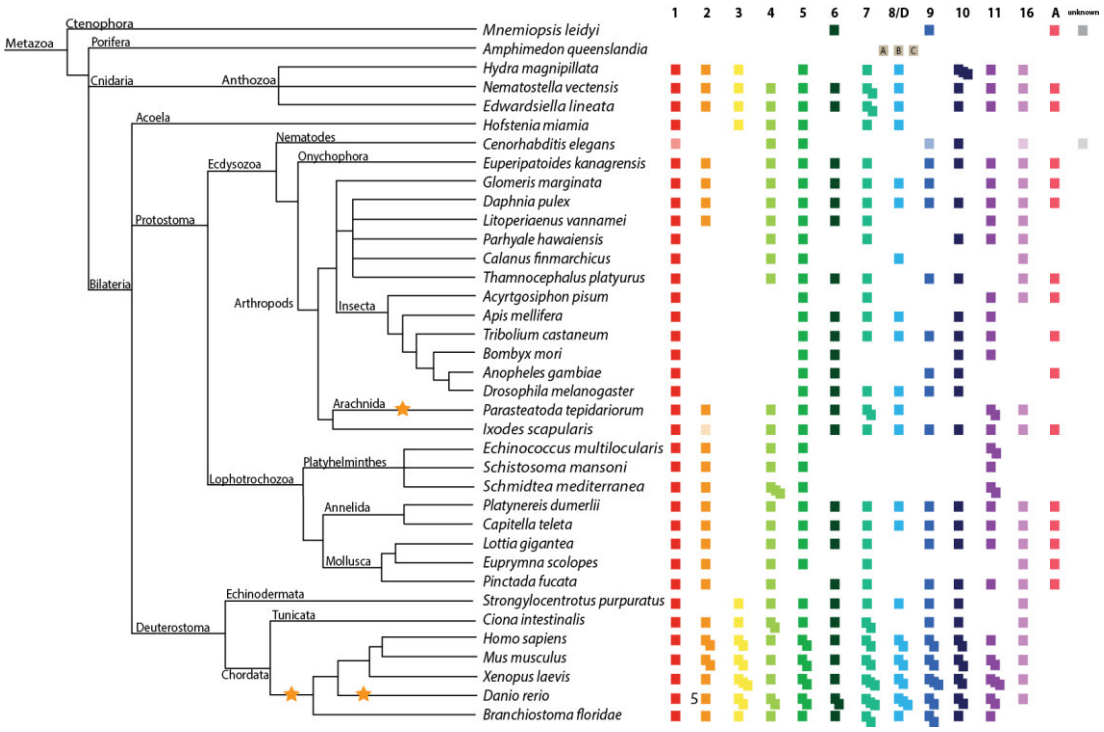

Figure 2.1 | Summary of Wnt gene diversity in selected metazoans. Shown are the thirteen Wnt subfamilies 1 to 11, 16 and A for several metazoan species. Duplicated Wnt genes were observed in deuterostomes, lophotrochozoans and chelicerates and were indicated by multiple coloured boxes or a number indicating the amount. Grey boxes: Wnts not assigned to subfamily. Yellow stars indicate whole genome duplications (WGD). (Based on: Pang *et al.,* 2010; Adamska *et al.,* 2010; Lengfeld *et al*., 2009; Hensel *et al.,* 2009; Stefanik *et al.,* 2014; Sirvastava *et al.,* 2014; Kusserow *et al.,* 2005; Hogvall *et al*., 2014; Janssen & Posnien, 2014; Kao *et al.,* 2016; Janssen *et al.,* 2010; Shigenobu *et al.*, 2010; Dearden *et al.,* 2006; Bolognesi *et al.,* 2008; Llimargas & Lawrence, 2001; Riddiford & Olson, 2011; Prud'homme *et al.,* 2002; Cho *et al.,* 2010; Setiamarga *et al.,* 2013; Croce *et al.,* 2006; Garriock *et al.,* 2007; Miller *et al.,* 2001)

Ctenophora

Four Wnt genes were found in the transcriptome of *Mnemiopsis leidyi*, the warty comb jelly (6, 9, A, unknown) (Figure 2.1) (Pang *et al*., 2010) and one of these Wnts could not be assigned to any of the subfamilies, which might be due to an incomplete sequence or a high mutation rate (Pang *et al*., 2010). It has been hypothesised that the Wnt genes in *M. leidyi* were involved in axis formation (Ryan *et al*., 2013) which might be an ancestral role of the Wnt signalling pathway (Petersen and Reddien, 2009).

Porifera

Several components of the Wnt signalling pathway were described in the sponge *Amphimedon queenslandia* including four Wnt genes however, their assignment to Wnt subfamilies has proven to be problematic (Adamska *et al*., 2010). Adamska *et al.* (2010) annotated three of these four Wnts as homologs of the *Wnt8* subfamily, leaving one still unclassified (Figure 2.1) (Adamska *et al*., 2010). The remaining unannotated Wnt gene "*Wnt"* was expressed at the anterior and posterior pole of the developing sponge. "*Wnt"* was antagonised by TCF at the posterior end, which contributes to formation of the anterior-posterior axis (Adamska *et al*., 2011; Adamska *et al*., 2007). More recently, it was described, that Wnt signalling in sponges was also responsible for development of the "aquiferous system", which leads to polarization and the organisation of the central part of the sponge (Windsor and Leys, 2010).

Cnidaria

The fresh water polyp *Hydra magnipillata* (Anthozoa) has eleven Wnt genes (*Wnt1*, *2, 3, 5, 7, 8, 10a, 10b, 10c, 11, 16*) (Figure 2.1) (Lengfeld *et al*., 2009). A few changes in the Wnt repertoire could be observed in comparison to *Hydractina sp*. (Hydrozoa), which has duplications of *Wnt5* and *Wnt11*, as well as only one *Wnt10* gene (Hensel *et al*., 2014). In *Edwardsiella lineata* (Anthozoa), a parasitic sea anemone and the sea anemone *Nematostella vectensis* (Anthozoa), all Wnt genes subfamilies were represented in the transcriptome except *Wnt9* (Figure 2.1) (Stefanik *et al*., 2014). Wnt signalling in cnidarians was involved in gastrulation and establishing the body axis (Kusserow *et al*., 2005; Petersen and Reddien, 2009; Sullivan *et al*., 2007). It is remarkable that a complete set of thirteen Wnt ligands is present in Cnidarians, which branch near the base of metazoans (Figure 2.1).

Acoela

The flatworm *Hofstemia miamia* has only four *Wnt* genes, which were assumed to belong to the subfamilies *Wnt1*, 3, 4 and 5 (Figure 2.1) (Srivastava *et al*., 2008). It remains unclear if there was a significant loss of *Wnt* genes in Acoela or if we were simply missing information about Wnt genes due to limited sequence data for these species.

Protostomia – Ecdysozoa - Nematoda

There were five Wnt genes described for *C. elegans*, but there have been a lot of amino acid changes in the genes of this nematode, so that a correct classification to the Wnt subfamilies was not straightforward (Figure 2.1) (Pan *et al*., 2006). *egl-20* (Forrester *et al*., 2004; Maloof *et al*., 1999) is a Wnt gene which is involved in the directional migration of neurons via activation of *mab*-5, a Hox gene (Forrester *et al*., 2004; Green *et al*., 2007). The other Wnt genes were *Lin-44* (Herman *et al*., 1995; Inoue *et al*., 2004; Maloof *et al*., 1999), *Mom-2, cwn-2* (Inoue *et al*., 2004) and *cwn-1* (Pan *et al*., 2006). *Lin-44* is involved in the control of polarity in the asymmetric cell divisions in the tail region of *C. elegans* (Herman *et al*., 1995; Takeshita and Sawa, 2005) and *Mom-2* might distinguish between endoderm and mesoderm in early development (Rocheleau *et al*., 1997; Thorpe *et al*., 2005). The above mentioned Wnt ligands were first annotated to correspond to *Wnt4, 5, 10(?)* and two unclassified Wnt genes (Prud'homme *et al*., 2002). Reanalysing the *C. elegans* sequences lead Kusserow *et al.* (2005) to the assumption that *Wnt1* and *Wnt5* together with three unclassified Wnts were present in the nematode (Figure 2.1). Further analysis by Janssen *et al*. (2010) lead to re-assignment into the Wnt subfamilies *Wnt4*, *5, 9, 10* and *16*. However, due to the derived amino acid sequences in *C. elegans* (Pan *et al*., 2006) it remains unclear to which Wnt subfamilies the five nematode Wnt genes belong, but it seems likely, that *Wnt4*, *5* and *10* are represented (Figure 2.1) (Janssen *et al*., 2010; Kusserow *et al*., 2005; Prud'homme *et al*., 2002).

Protostomia – Ecdysozoa - Onychophora

The velvet worm *Euperipatoides kanangrensis* has all described Wnt genes except *Wnt3* and *Wnt8* (Figure 2.1). Most of them were expressed in a segment polarity pattern and therefore might also play a functional role in onychophoran segmentation (Hogvall *et al*., 2014). This supports the conclusion that the last common ancestor of ecdysozoans had twelve of the Wnt subfamilies, only missing *Wnt3* (Figure 2.1).

Protostomia – Ecdysozoa - Arthropoda

In the pill millipede *Glomeris marginata* eleven *Wnt* genes (*Wnt1, 2, 4, 5, 6, 7, 8, 9, 11, 16, A*) have been described (Figure 2.1) (Janssen *et al*., 2010; Janssen and Posnien, 2014). In another myriapod, the centipede *Strigamia maritima,* a similar set of Wnt genes was found but a *Wnt10* gene was present and no *Wnt8* was detected (Hayden and Arthur, 2014). The crustacean *Daphnia pulex* contains representatives of all twelve protostome Wnt genes subfamilies except *Wnt3* (Figure 2.1) (Janssen *et al*., 2010) and recently it was described that *Wnt8* is duplicated in this water flea (Kao *et al*., 2016). The Wnt gene repertoires have also been described multiple other crustaceans: *Parhyale hawaiensis* (*Wnt1, 4, 5, 10, 11* and *16*) (Kao *et al*., 2016), *Litopenaeus vamamei* (*Wnt1, 2, 4, 5, 6, 7, 11* and *16*) (Kao *et al*., 2016), *Calanus finmarchicus* (*Wnt1, 4, 5, 8* and *16*) (Kao *et al*., 2016) and *Thamnocephals platyurus* (*Wnt1, 4, 5, 6, 7, 9, 10, 16* and *A*) (Constantinou *et al*., 2016) (Figure 2.1).

Among the insects, the pea aphid, *Acyrthosiphon pisum* has only six Wnt genes: *Wnt1, 5, 7, 11, 16* and *A* (Shigenobu *et al*., 2010), and thus showed a drastic reduction of Wnt genes. The loss of several Wnt genes could also be detected in other insects: the honeybee, *Apis mellifera* has seven Wnt genes (*Wnt1, 4, 5, 6, 7, 10, 11*) (Figure 2.1) (Dearden *et al*., 2006), *Tribolium castaneum* has nine (*Wnt1, 5, 6, 7, 8/D, 9, 10, 11, A)* (Figure 2.1), *Anopheles gambiae* has six (*Wnt1, 5, 6, 9, 10* and *A*) (Figure 2.1) (Bolognesi *et al*., 2008; Janssen *et al*., 2010; Murat *et al*., 2010) and seven Wnt ligands were present in *Drosophila melanogaster*: *wg* (*Wnt1*), *2 (7), 4 (9), 5, 6, 8, 10* (Figure 2.1) (Llimargas and Lawrence, 2001). *Drosophila* is one of the few species in insects which had lost the *WntA* gene. So far, it remains unclear why this was the case and which evolutionary mechanism was behind it.

The chelicerate *Parasteatoda tepidariorum* has eleven Wnt genes including duplicates of *Wnt7* and *Wnt11* and loss of *Wnt3, 9, 10* and *A* (Figure 2.1) (Janssen *et al*., 2010). In the Central American wandering spider *Cupiennius salei* a *WntA* gene has also been found and *Wnt7* is also duplicated (Damen, 2002; Janssen *et al*., 2010). *Ixodes scapularis*, a deer tick, has all Wnt subfamilies represented except *Wnt3* but none were duplicated (Janssen *et al*., 2010).

Protostomia – Lophotrochozoa - Platyhelminthes

The platyhelminth *Echinococcus multilocularis*, a cyclophyllid tapeworm, has the Wnt genes *Wnt1, 2, 4, 5, 11a* and *11b*, whereas *Schistosoma mansoni* (trematode) has *Wnt1, 2, 4, 5* and *11* with no duplication of *Wnt11*. *Schmidtea mediterranea* (Planaria) has *Wnt1*, *2, 4a, 4b, 4c, 5, 11a, 11b* and one unclassified *Wnt* gene (Figure 2.1) (Riddiford and Olson, 2011). Therefore, there had been significant loss of Wnt subfamilies in Platyhelminthes as well as duplications of *Wnt4* and *Wnt11*.

Protostomia – Lophotrochozoa - Annelida

The annelid *Platynereis dumerilii* contains all Wnt genes except *Wnt3* (Figure 2.1) (Janssen *et al*., 2010; Prud'homme *et al*., 2002; Raible *et al*., 2005). The marine annelid worm *Capitella teleta* shows the same Wnt repertoire, whereas the freshwater leech *Helobdella robusta* appeared to have lost *Wnt9* and had duplicates of *Wnt*5 and *Wnt16* and three copies of *Wnt11* (Figure 2.1) (Cho *et al*., 2010).

Protostomia – Lophotrochozoa - Mollusca

Lottia gigantea, the owl limpet, has all Wnt genes except *Wnt3* and *Wnt8* (Figure 2.1) (Cho *et al*., 2010), The pearl oyster, *Pinctata fucata* has a similar set of Wnt genes, but was missing *Wnt5* (Setiamarga *et al*., 2013), whereas the cephalopod *Euprymna scolopes* had only seven Wnt genes (*Wnt1, 2, 4, 5, 7, 16* and *A*) (Figure 2.1).

Deuterostomia - Echinodermata

Strongylocentrotus purpuratus, the sea urchin, is a well-studied echinoderm with all Wnt genes except *Wnt2* (Figure 2.1) (Croce *et al*., 2006; Robertson *et al*., 2008). *Wnt8* is involved in regulating gastrulation by interacting with and activating the canonical Wnt pathway. Wnt genes were also involved in the differentiation of ectoderm and mesoderm (Smith *et al*., 2008; Wikramanayake *et al*., 2004). A complex of *Wnt6*, *Wnt8* and *runx-1* was also involved in the regulation of cell proliferation (Robertson *et al*., 2008).

Deuterostomia - Chordata

The tunicate *Ciona intestinalis* has a large repertoire of Wnt genes: *Wnt1, 2, 3, 4a, 4b, 5, 6, 7a, 7b, 9, 10* and *16* (Figure 2.1) (Croce and McClay, 2008; Hino *et al*., 2003). Amphioxus, *Branchiostoma floridae* is a close invertebrate relative living to vertebrates

and has all Wnt subfamilies except *Wnt16* and *A* with a *Wnt9* duplication (Figure 2.1)(Putnam *et al*., 2008; Schubert *et al*., 2001).

The Wnt repertoire of vertebrates is characterised by multiple duplications due to two whole genome duplications (WGD) early in their evolution (Dehal and Boore, 2005). The teleost underwent an additional WGD (Jaillon *et al*., 2004) which lead to 27 Wnt genes in the zebrafish *Danio rerio* (Figure 2.1) (Garriock *et al*., 2007). The lineage leading to the frog *Xenopus laevis* also had an additional WGD producing a repertoire of 23 Wnt genes (Figure 2.1) (Garriock *et al*., 2007). In *Mus musculus* the gene *integrin-1* (*int-1*) was the first discovered murine Wnt gene (*Wnt1*). *M. musculus* has 19 Wnt genes and is only missing a *WntA* gene (Figure 2.1) (Miller, 2002) which is identical to the Wnt gene repertoire found in *Homo sapiens* (Garriock *et al*., 2007). Interestingly, *Wnt1* and *Wnt16* were never duplicated, not even in zebrafish.

From this literature review, it became clear that there is a large diversity in the Wnt repertoire (Figure 2.1) but its underlying evolutionary mechanisms remain unclear. Due to which constraints were Wnt genes conserved? How can they be lost, and which effects had duplicated Wnts on the development of the organism? Also, the origin of the Wnt family itself is not known and only speculations of how Wnt genes evolved can be made (see Introduction). In the following study, I wanted to investigate the Wnt gene repertoire focussing on arthropods to understand the dynamics of losses, conservation and duplication to a larger extend. This analysis would form a basis for further studies on the evolution of Wnt genes.

2.2 | Methods

Phylogenetic analysis

All sequences used in this analysis were obtained from NCBI or other genomic sources specified in the supplement (see below), using the tBlastN search tool with a consensus Wnt sequence as query (see Supplement). The consensus sequence was generated using Wnt gene sequences of *H. sapiens, D. melanogaster, T. castaneum* and *P. tepidariorum* which were aligned using ClustalX (Larkin *et al*., 2007). Wnt genes were mainly characterised by their conserved 22-23 cysteine pattern. Therefore, to be able to search for this cysteine pattern in the genomic data, an artificial consensus Wnt sequence was generated. This sequence excludes any biases of species specific Wnts and made it possible to search for Wnt genes mainly by their cysteine pattern. As a control, this query was used to search for Wnt genes in well described species throughout the metazoan phylogeny. This confirmed, that all described Wnts for all tested species could be detected. In several cases, as a control, a more specific search for Wnt subfamilies using Wnt amino acid sequences as the query from closely related species was included.

The newly analysed species were: the tardigrade, *Hypsibius dujardini* (water bear), the insects *Bemisa tabaci* (Silverleaf whitefly), *Diaphorina citri* (Asian citrus psyllid), *Halyomorpha halys* (brown marmorated stink bug), *Cimex lectularis* (Bed bug), *Trachymyrmex zeteki* (fungus growing ant), *Megachile rotundata* (leafecutter bee), *Fopius arsenius* (braconid wasp), *Nasonia vitripennis* (Jewel wasp), *Dufourea novaeangliae* (pickerel Bee), *Polistes dominula* (European paper wasp), *Aethina tumida* (Small hive beetle), *Nicrophorus vespilloides* (Burying beetle), *Bombyx mori* (silk moth), *Bicyclus anynana* (Squinting bush brown butterfly); the chelicerates *Limulus polyphemus* (Horseshoe crab), *Centruroides sculpturatus* (scorpion) and *Phalangium opilio* (harvestman) (see Supplement for genome references). The following species with known and published Wnt gene repertoires were included in the analysis: the onychophoran *Euperipatoides kanangrensis* (Velvet worm), the myriapods *Glomeris marginata* (Pill millipede) and *Strigamia maritima* (centipede), the crustacean *Daphnia pulex* (water flea), *Litoperiaenus vannamei* (Whiteleg shrimp) and *Parhyale hawaiensis* (amphipod crustacean), the insects *Acyrthosiphon pisum* (Pea aphid), *Heliconius melpomene* (Postman butterfly), *Apis mellifera* (Honeybee),

Tribolium castaneum (flour beetle), *Anopheles gambiae* (mosquito) and *Drosophila melanogaster* (fruit fly), the chelicerate *Parasteatoda tepidariorum* (common house spider) and *Ixodes scapularis* (deer tick), the lophotrochozoa *Platynerei dumerilii* (annelid) and the vertebrate *Homo sapiens* (human). All gene accession numbers can be found in Supplement Table S1.1 and genome sources in Supplement Table S1.2.

Sequences from *P. hawaiensis* were obtained from (Kao *et al*., 2016) and additional transcriptomic information was kindly provided by Anastasios Pavlopoulos. However, not all sequences of published Wnt genes were found and only a reduced set could be used in the analysis. Sequences for *H. melpomene* and *B. anynana* were extracted from Lepbase (Challis *et al*., 2016). Sequencing data for *I. scapularis* was extracted from sequence files in Janssen *et al.* (2010). Transcriptomic datasets for *P. opilio* (kindly provided by Prashant P. Sharma) and *C. sculpturatus* (kindly provided by Natascha Turetzek) were analysed by creating local blast databases for both transcriptomes using a consensus Wnt sequences as query (Code: makeblastdb –in phaop.fasta –out dbBLAST –dbtype prot –parse_seqids ; blastp –query consensusWnt.fasta –db dbBLAST –out hits.txt).

All nucleotide sequences were translated via EMBOSS Transeq (http://www.ebi.ac.uk/Tools/st/emboss_transeq/) and aligned using local ClustalX 2.1 (Larkin *et al*., 2007). The alignment was edited manually using SeaView version 4.6.1 (Gouy *et al*., 2010). A phylogenetic tree was created using RAxML including rapid bootstrapping with 1000 replicates (Stamatakis, 2014; Stamatakis *et al*., 2008) (example code: raxmlHPC – f a –x 12345 –p 12345 -#1000 –PROTGAMMAVT – s align.phy –n tree). This tree building method was used for all maximum likelihood trees generated for this study. RAxML analysis was chosen above Bayesian based methods due to the very diverse dataset, but small dataset where a suitable substitution model specific for this sequence data could be applied. While the Bayesian approach is based on a prior subjective assumption which can influence the outcome of the analysis, RAxML was a more objective approach. The best protein alignment model was detected using local ProtTest 2.4.3 (Abascal *et al*., 2005). For the complete arthropod dataset, the best fitting model for estimating the amino acid replacement frequencies during molecular

evolution was VT+G (Muller and Vingron, 2000). This model is an extension of the Markov model previously estimated by (Dayhoff *et al*., 1978) and allows to predict the amino acid substitution from more divergent alignments. The +G (Gamma) would add a category of change for each amino acid site and allow rating into low, medium and high rate of change (Yang, 1993).

2.3 | Results and Discussion

2.3.1 Analysing the maximum likelihood tree of arthropod Wnt genes

To contribute to the understanding of Wnt gene evolution, predicted Wnt gene sequences from annotated genomes and transcriptomic data were used to try to identify and characterise Wnt orthologues in several arthropod species, additional to those studied previously (see section 2.1.1). Here, predicted and known Wnt gene sequences from 32 arthropod species were aligned and phylogenetically analysed. From this analysis a phylogenetic tree was obtained which grouped all sequences by their potential corresponding Wnt subfamily.

Unfortunately, the bootstrap support (BS) of the Wnt subfamily branching was very weak (<32) when using the full dataset of 32 species, meaning that the assignment of predicted Wnt sequences to specific Wnt subfamilies was unreliable (see Supplement Figure S2.1). Additionally, this also indicated the sequence divergence observed in the Wnt subfamilies. All sequences maintained the 22-23 cystein residue pattern while only a small amount of the remaining sequence is conserved. This results in quite diverse sequences which made it difficult to compare subfamilies this data across distantly related species. Species which were closer related have shown less divergent sequences (data not shown) and comparing my phylogenetic tree to previous phylogenetic studies on Wnt genes in arthropods (Hogvall *et al*., 2014; Janssen *et al*., 2010), it was shown that a smaller dataset with good sequence quality could produce a robust tree with good BS support (e.g. above 80) (Janssen *et al*., 2010). It has also been shown, that adding one species to this phylogenetic Wnt tree could already change the relationship between Wnt subfamilies as well as the branch support (Hogvall *et al*., 2014).

The 32 arthropod species included in this analysis represent a three-fold increase in the sample size compared to Janssen *et al.* (2010) and Hogvall *et al*. (2014) and the bootstrap support values obtained were between 0 and 98, shown in the following in brackets (Supplement Figure S2.1). Especially, the tree branching between Wnt subfamilies was not well supported (0-32). These low BS values made the whole relationship between the Wnt subfamilies unclear and any connection between Wnt subfamilies with this large and diverse dataset could not be confidently concluded. Higher BS support could be seen within *Wnt3* (98), *Wnt8* (72) and *Wnt2* (79) and all of

these subfamilies contained very few sequences due to losses in all (*Wnt3*) or many (*Wnt2* and *Wnt8*) arthropod species (Supplement Figure S2.1). All other Wnt subfamilies also shown very low BS support within their subfamilies (Supplement Figure S2.1).

It was assumed, that the amount and quality of data used in this analysis was negatively influencing the overall support of the maximum likelihood tree. To exclude any bias of the method, the here used analysis was repeated using a published dataset from Janssen *et al*. (2010) (data not shown). Here, a very similar tree with very good BS values and all Wnt sequences clustering with the previously published Wnt subfamilies could be produced. Therefore, it was assumed, that the tree building method used was working well, but that the input data was influencing the quality of the phylogenetic tree. Therefore, it was decided to analyse smaller subsets of the full dataset, to decrease the diversity of sequences in the tree runs.

2.3.2 | Analysing the Wnt gene repertoire in small arthropod datasets

The Wnt genes in chelicerates

As a first sub-dataset, it was chosen to analyse the Wnt genes in chelicerates. Chelicerata are one of the large orders in arthropods, next to the insects and crustaceans and the only arthropod groups with known Wnt gene duplications (namely *Wnt7* and *Wnt11*). Here, all chelicerate species from the above analysed dataset were used, additionally including the scorpion *Mesobuthus martensii* and the spider *Pholcus phalangoides*. Several insect species as well as humans and Platyhelminthes were added as outgroups with well-known Wnt gene sequences.

The BS support of the chelicerate Wnt subfamilies was overall higher then observed for the full dataset (Figure 2.2). The Wnt subfamilies *Wnt1* (88)*, 2* (77)*, 3* (98)*, 4* (88)*,* and *A* (95) were now well supported, although the branch support for most other Wnt subfamilies was still quite poor (Figure 2.2). The *Wnt16* (59) and *Wnt6* (44) subfamilies show intermediate BS support which was increased compared to the full dataset support for these Wnt subfamilies. Interestingly, the sequences from the harvestman *P. opilio* often gave very long branch lengths which indicated a high number of substitutions in these sequences compared to all other sequences and subfamilies containing these long branches (*Wnt9, 10, 7* and *5*) had still a very low BS value between 4 and 30 (Figure 2.2). In addition, although the BS values for the relationships between

Wnt subfamilies were generally low, while *Wnt1* and *Wnt6* were still closely related, consistent with previous trees (Figure 2.2) (Hogvall *et al*., 2014; Janssen *et al*., 2010).

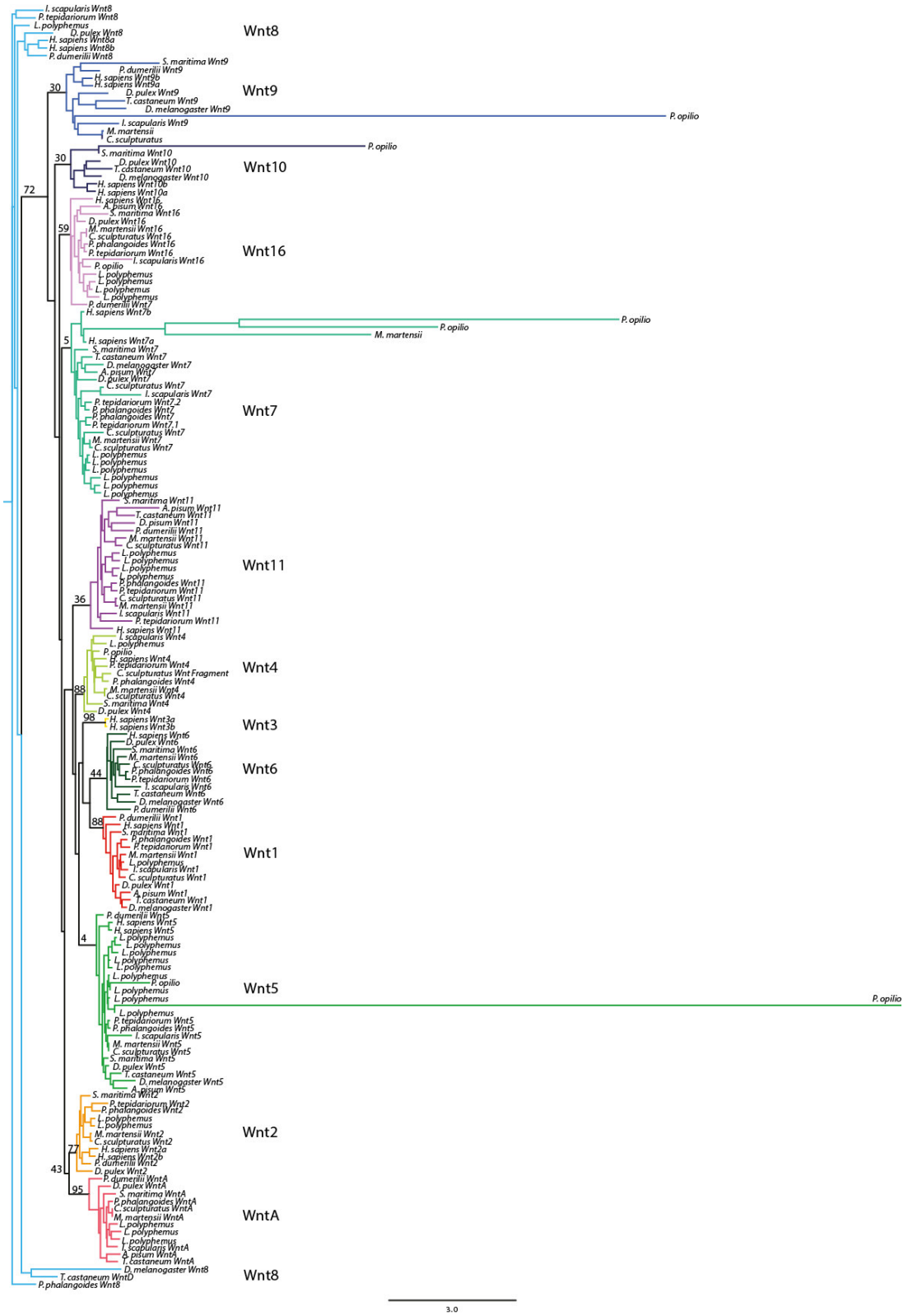

Figure 2.2 | Maximum likelihood tree of chelicerates. ML tree based on amino acid sequences analysed using RAxML with 1000 bootstrapping repeats. BS values shown on branches. Number of substitutions indicates by the scale bar.

In a second analysis of the chelicerate subset, sequences from *P. opilio* were excluded to erase the effect of the long branches on the BS support. Interestingly, all

Wnt subfamilies which had previously long *P. opilio* branches were now very well supported by the BS values (Figure 2.3): *Wnt5* (87), *Wnt7* (91), *Wnt9* (58) and *Wnt10* (92) (Figure 2.3). This increase in the branch support indicates, that the fragmented sequences from *P. opilio* did have a negative effect on the BS values for these subfamilies. Other subfamilies, which included *P. opilio* sequences with short branches did not change dramatically in their support values. Here, *Wnt4* still had the same BS value of 88 and *Wnt16* with 63 was just slightly higher than the previous 59 BS value (Figure 2.3). The BS support of subfamilies which did not include *P. opilio* sequences previously increased or remained the same, *Wnt1* (88), *Wnt2* (98), *Wnt3* (100), *Wnt6* (94), *Wnt8* (84) and *WntA* (94). The only exception was *Wnt11* that was previously supported with a BS value of 36 was now forming a polyphyletic outgroup of the whole tree and did show very low BS support (Figure 2.3). Additionally, *Wnt1* and *Wnt6* as well as *Wnt9* and *Wnt10* were grouping together, which was previously seen for these Wnt subfamilies (Hogvall *et al*., 2014; Janssen *et al*., 2010).

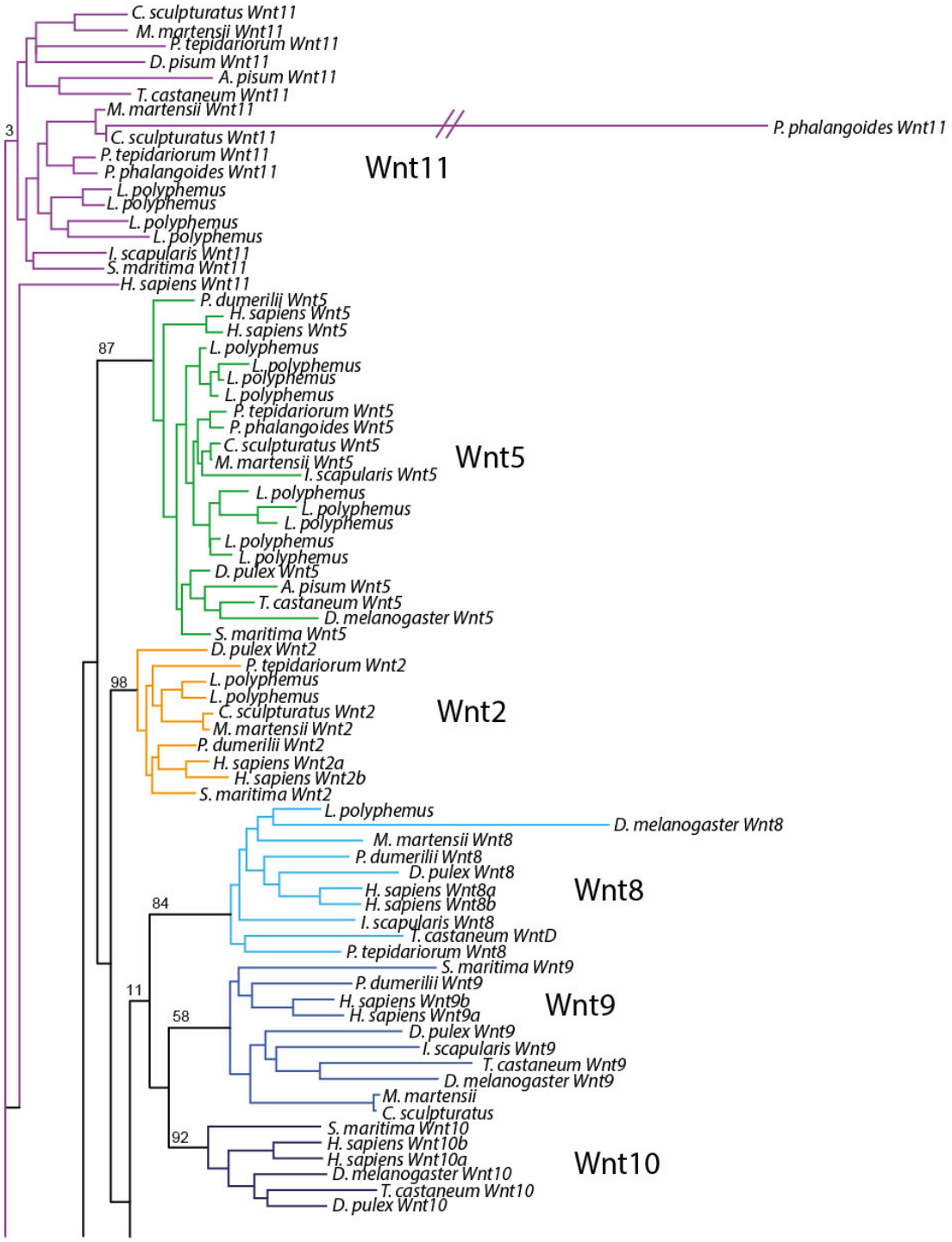

Figure continued on next page

Figure 2.3 | Chelicerate maximum likelihood tree without *P. opilio*. ML tree based on amino acid sequences analysed using RAxML with 1000 bootstrapping repeats. BS values shown on branches. Number of substitutions indicated by the scale bar.

Overall, the exclusion of the fragmented *P. opilio* sequences increased the reliability and BS support of the maximum likelihood tree for chelicerates. However, it was assumed that *P. opilio* had a similar Wnt gene repertoire to its close relative

I. scapularis, and faint boxes indicate these assumptions for the harvestman *P. opilio* (see Figure 2.2 and Figure 2.3). Comparing both chelicerate trees, all analysed predicted Wnt sequences clustered with the same Wnt subfamilies in both trees. The Wnt gene repertoire for all chelicerates from the sub dataset was summarized in Figure 2.4.

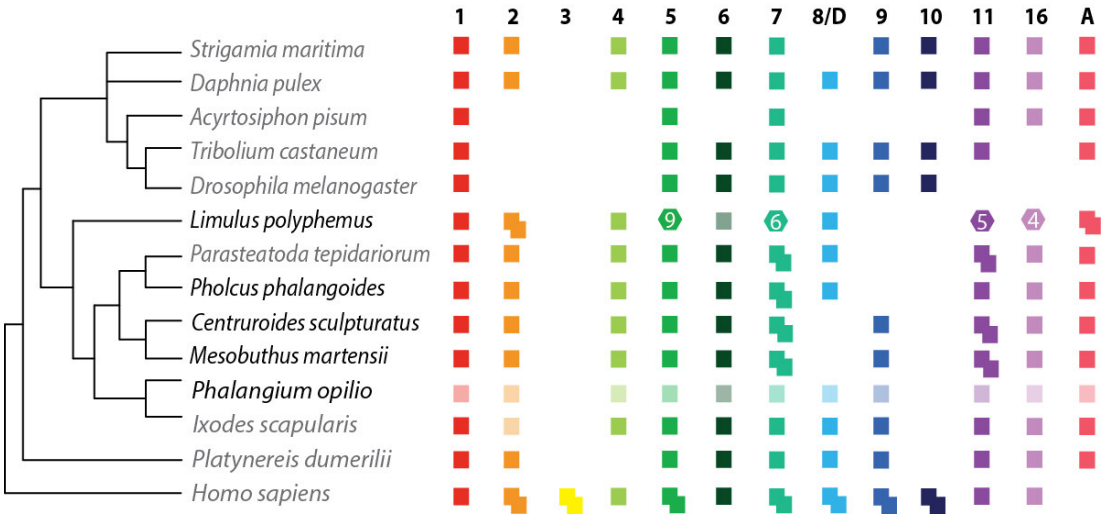

Figure 2.4 | Overview of Wnt genes in chelicerates. The newly analysed chelicerate species are written in black. Duplications of Wnt genes are represented by multiple coloured boxed or numbers within the boxes. Not confirmed Wnts are shown in faint colours.

The Wnt genes in lepidopterans

As a second sub-dataset, it was chosen to look more closely into lepidopteran (butterflies and moths) Wnts because there had been little analysis of the Wnt genes in these animals and they provide an interesting comparison to other insects like beetles (Coleoptera) and flies (Diptera) where more is known about Wnts. In addition to relevant species used in the large dataset, the butterfly *Papilio glaucus* and the moth species *Manduca sexta* were added to the sub-dataset.

The BS support was very high for all Wnt subfamilies (93-100) which made the annotation of Wnts for several insect species, including the lepidopterans, quite reliable (Figure 2.5). Compared to the subtree from the chelicerate datasets, much shorter branch lengths were obtained (Figure 2.5) and this shows, that the sequences were quite similar to each other and not many substitutions happened. Overall, the sequence input in this dataset was of high quality.

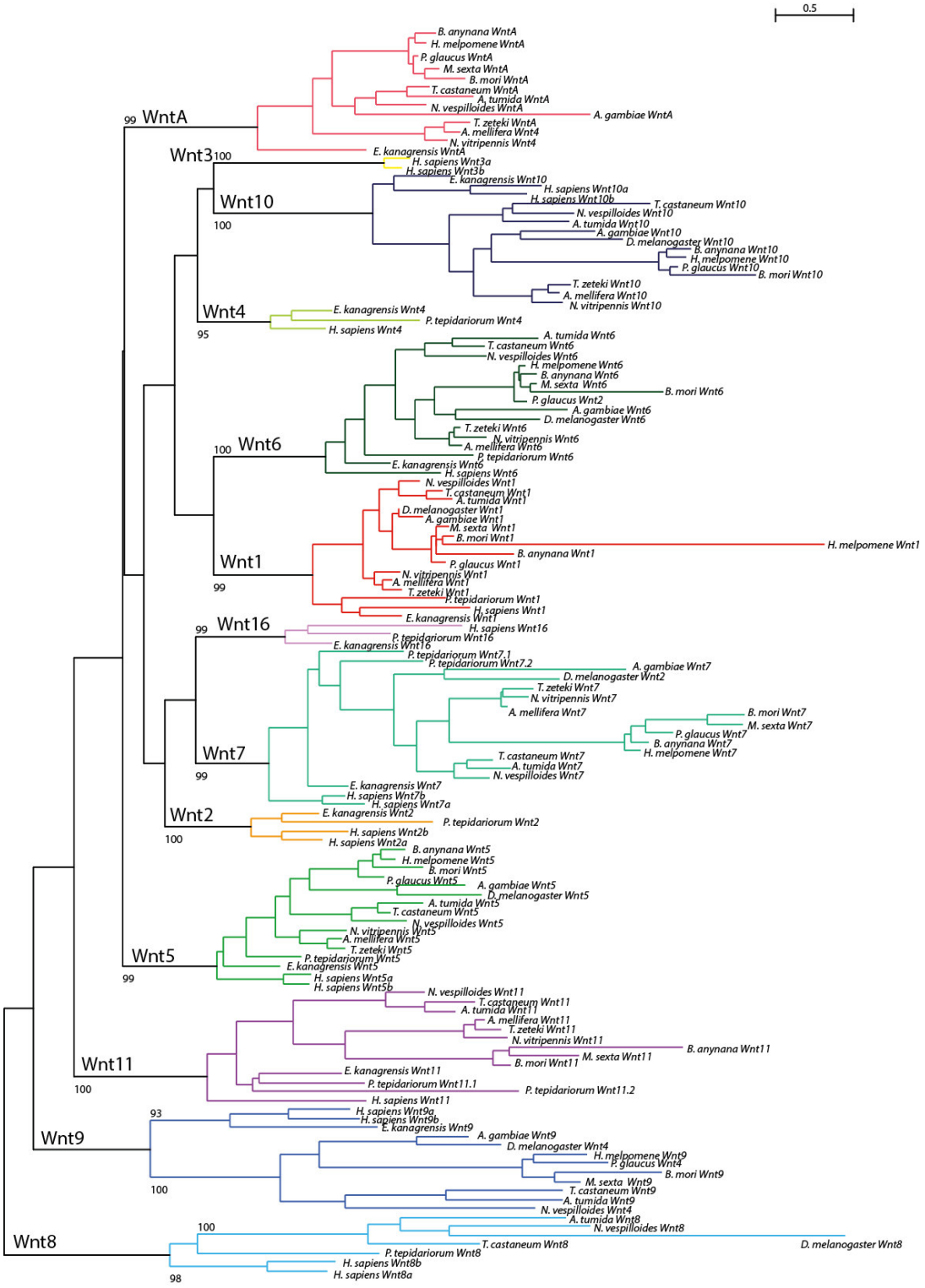

Figure 2.5 | Phylogenetic analysis of lepidopteran Wnt genes. Maximum likelihood tree based on amino acid sequences of all Wnt genes analysed with RAxML including 1000 bootstrap repeats. Bootstrap values are indicated on the subfamily branches. All values are high and therefore the branch support of the Wnt subfamilies is high.

This tree was compared with the previous full dataset tree to find out if the same predicted Wnt sequences were grouped into the same Wnt subfamilies. Interestingly,

all Wnts from the analysed species clustered with the same Wnt subfamily in this subtree (very high BS support) as previously assigned in the full maximum likelihood tree with the low BS support (Supplement Figure S2.1). For all butterflies, seven Wnt genes appeared conserved, *Wnt1, 5, 6, 7, 9, 10* and *A* (Figure 2.5 and 2.6), but *Wnt11* appeared to display a complex pattern of loss and retention. In butterflies, *Wnt11* was only detected in *B. anynana*, but was present in both analysed moth species (Figure 2.5 and 2.6). Therefore, it was hypothesised that *Wnt11* was present in the last common ancestor of lepidopterans but subsequently lost in some butterfly families.

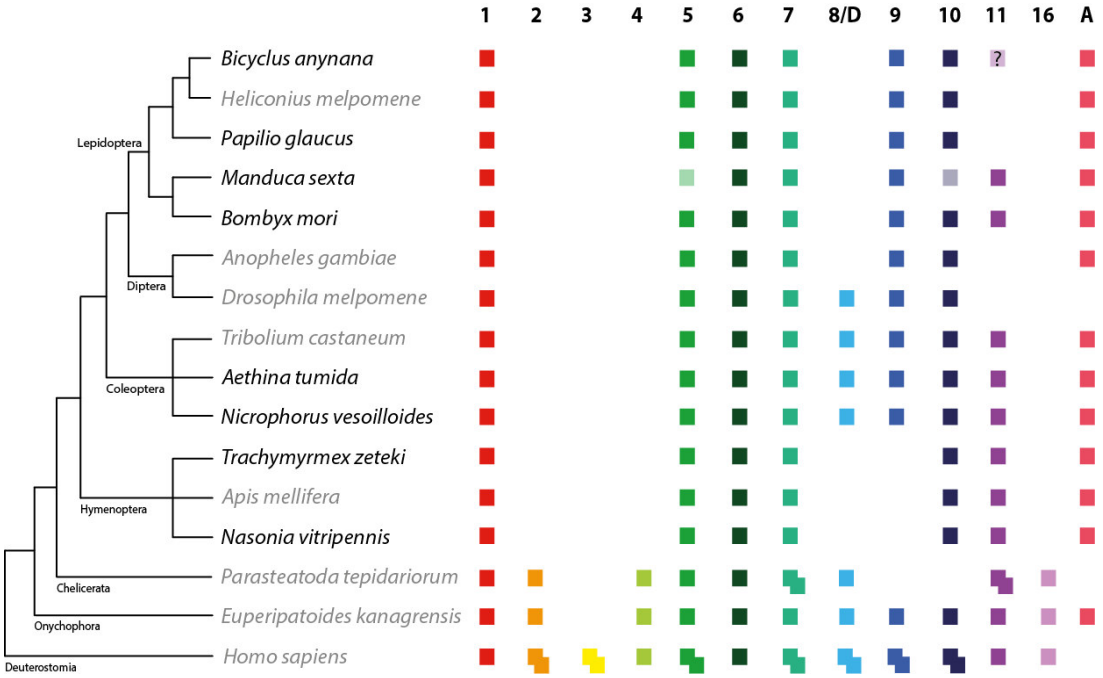

Figure 2.6 | Summary of the Wnt gene repertoire in lepidopterans. The newly analysed species are indicated in black font. Presumed Wnt genes in *M. sexta* are indicated with faint boxes (*Wnt5* and *Wnt10*). Duplicated Wnt genes are indicated by multiple coloured boxes.

In the moths, *Wnt1*, *6, 7, 9, 11* and *A* were present in both analysed species, while *Wnt5* and *Wnt10* were not found in *M. sexta* but appeared to be present in *B. mori* (Figure 2.6). *M. sexta* was the only species where a transcriptome was used to find Wnt gene sequences and although the transcriptomic data used for *M. sexta* was extensive, it was not exhaustive for all developmental time points and tissues, and therefore, it was possible that these two Wnt genes were not expressed at the developmental time points included in this transcriptomic data.

Overall, the analyses of the smaller sub-datasets of arthropods greatly increased the BS values and more reliably allowed the assignment of the new annotations into

Wnt subfamilies. However, this analysis also confirmed the annotation of Wnt genes obtained from the large dataset even though the BS values for this larger tree were generally unreliable.

2.3.2 The Wnt repertoire of newly sequenced arthropod species

In the following section, the newly annotated Wnt repertoires for the analysed arthropod species were summarized from all tree data mentioned above (Figures 2.4, 2.5 and S2.1).

Wnt1

A gene belonging to the *Wnt1* or *wingless* gene subfamily was found in all of the analysed arthropod species except in three, *P. opilio* (see above) *L. vannamei*, and *H. dujardini* (Figure 1.3). These findings were consistent for all three trees. For the white leg shrimp *L. vannamei, Wnt1* is reported in a previous publication (Kao *et al*., 2016), but it was not possible to obtain the published *Wnt1* sequence from any of the published sources (see Methods), and therefore this gene was not included (Figure 2.7). Furthermore, *Wnt1* was not identified for the tardigrade *H. dujardini* whose genome was just recently annotated and several Wnt gene sequences reported. However, due to low sequence quality (Yoshida *et al*., 2017), it was likely that not all Wnt genes were annotated in the genome and were therefore missing from my dataset.

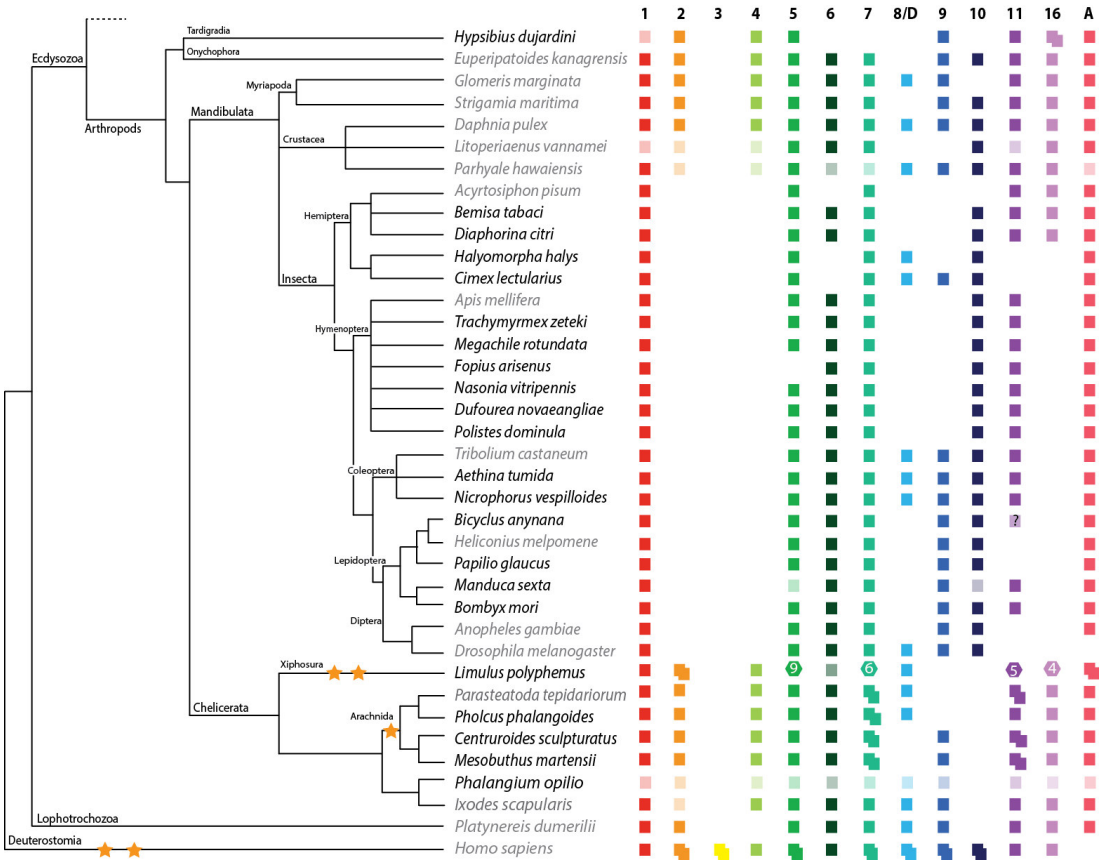

Figure 2.7 | Summary of the Wnt gene analysis in arthropods. Included are all results from the maximum likelihood tree obtained for the full dataset of 37 arthropod species. Numbers of duplicated Wnt genes are indicated with multiple boxes, or by numbering within the boxes. Yellow stars indicate WGD event. Based on: Jansson *et al.,* 2010; Garriock *et al.,* 2007; Prud'homme *et al.,* 2002; Llimargas & Lawrence, 2001; Bolognesi *et al*., 2008; Dearden *et al.,* 2006; Shigenobu *et al.,* 2010; Kao *et al.,* 2016; Janssen & Posnien, 2014; Hogvall *et al.,* 2014).

The BS support of the *Wnt1* subfamily was very poor in the large dataset but increased in the two subsets. However, the same sequences group with the *Wnt1* subfamily in all three trees. Therefore, a reliable annotation for *Wnt1* was possible from the newly analysed species (Supplement Table S2.1).

Wnt2

It was previously suggested that the *Wnt2* gene subfamily had been lost in insects (Janssen *et al*., 2010). Consistent with this, I did not detect a *Wnt2* gene in any of the additionally analysed insect species in the full dataset tree analysis or in the lepidopteran subtree (Figure 2.7). The BS support was very high in all three trees (Full tree: 79, Chelicerate tree: 98 and Lepidopteran tree: 100).

Wnt2 sequences have been found in myriapods, onychophorans, tardigrades, crustaceans and chelicerates as well as in lophotrochozoans and deuterostomes. It was found that *L. polyphemus* had a duplication of *Wnt2* (Figure 2.7) presumably because of the WGDs in horseshoe crabs (Kenny *et al*., 2016). A duplication of *Wnt2* was also detected in the tardigrade *H. dujardini*, most likely resulting from a tandem duplication (Yoshida *et al*., 2017). No *Wnt2* sequences were detected for the deer tick *I. scapularis* which was already described in Janssen *et al.* (2010) (Figure 2.7).

Wnt3

It was previously shown that all Wnt subfamilies were present in arthropods except *Wnt3* and therefore it was likely that the *Wnt3* subfamily was lost in the last common ancestor of protostomes (Janssen *et al*., 2010). This was consistent with my analysis where none of the analysed arthropod sequences group with the human *Wnt3* genes in all analysed trees (Figure 2.7) where the support of the *Wnt3* subfamily was in all cases very high (98-100).

Wnt4

The *Wnt4* subfamily also appeared to be lost in all insects (Figure 2.7), as suggested previously by Janssen *et al.,* (2010). The BS support of this subfamily was low in the full dataset (32) but became more reliable in the chelicerate (88) and in the lepidopteran (95) subtrees. In addition, no duplication of *Wnt4* was observed in any of the species (Figure 2.7) and indeed, even in *L. polyphemus* no duplication of *Wnt4* was detected while also in humans only one copy of *Wnt4* was present, despite two rounds of WGD (Dehal and Boore, 2005) (Figure 2.7). The only duplications seen for *Wnt4* were detected in the zebrafish (Figure 2.1).

Wnt5

Wnt5 was present in all arthropod species used in this analysis except the bracoid wasp *F. arsenius* (Figure 2.7). This Wnt subfamily had an intermediate BS support in the full dataset (54) and was therefore somewhat unreliable. The support in the chelicerate (87) and lepidopteran (99) tree was very good. However, the same predicted Wnt sequences cluster with this subfamily in all three trees. Therefore, the annotation of newly found *Wnt5* sequences in arthropods seemed to be reliable.

Duplication of *Wnt5* had only been observed in vertebrates and the horseshoe crab *L. polyphemus,* where nine predicted *Wnt5* sequences were seen. When aligning all these horse shoe crab fragments with known *Wnt5* gene sequences were aligned, five of these sequences were fragments either of the 5' or 3' section of *Wnt5*. Four *L. polyphemus* sequences aligned with the other *Wnt5* orthologs on the full length. None of the sequences were identical to each other, which would lead to a maximum amount of nine *Wnt5* genes present in *Limulus* (Figure 2.7).

Wnt6

As well as *Wnt5*, the *Wnt6* gene subfamily was present in most metazoan species (Figure 2.1 and Figure 2.7). The very week support in the full dataset (11) was increased in the chelicerate subtree (94) while a good support of this subfamily could be seen in the lepidoptera tree (100) as well. Again, all predicted Wnt sequences, grouped in this subfamily, were similar in all analysed trees. Therefore, it seems reliable to annotate the predicted Wnt sequences accordingly.

Among arthropods, *Wnt6* was only missing in the stink bug *H. halys*, the bed bug *C. lectularis*, the pea aphid *A. pisum* and water bear *H. dujardini* (Figure 2.7). These missing sequences could be true losses of *Wnt6* or caused by missing sequence data. Further analysis, such as blasting transcriptomes (when available) could help to determine if *Wnt6* was truly lost in these species. No duplications of *Wnt6* were observed in any arthropod species and the only known species so far with duplicated *Wnt6* genes was the zebrafish *D. rerio*, which had three WGDs (Figure 2.1) (Jaillon *et al*., 2004).

Wnt7

Wnt7 was not found in tardigrades but at least one copy was found in all other analysed arthropods (Figure 2.7). This Wnt subfamily was very poorly supported in the full data tree (0), whereas good BS support was observed in the lepidopteran (99) and the chelicerate subtree (91). Comparison of all sequences clustering in all analysed trees with the *Wnt7* subfamily showed that the same predicted sequences were grouped for this subfamily.

A *Wnt7* gene was detected in the mosquito *A. gambiae* and the silk moth *B. mori,* which were not described previously (Janssen *et al*., 2010) (Figure 2.7). Aligning the newly found *Wnt7* sequences of both species with previously characterised arthropod Wnt7 amino acid sequences showed a high similarity between all aligned sequences (data not shown). Therefore, it seemed to be likely that the detected sequences were indeed part of the *Wnt7* gene subfamily. Duplication of *Wnt7* could be seen in the Arachnida which was likely to have happened due to the WGD in this class (Kenny *et al*., 2016; Schwager *et al*., 2017). For the horseshoe crab seven *Wnt7*-like sequences were found. Aligning all found *Limulus* sequences to well-known Wnt7 protein sequences revealed, that most of them aligned to the templates but showed amino acid differences, whereas one of the detected sequences seemed to be a fragment which did not align to any of the predicted or template *Wnt7* sequences and was therefore excluded. This leaves six predicted *Wnt7* sequences present in *L. polyphemus* (Figure 2.7). It was assumed, that some of them were still fragments of the same Wnt gene but with the current analysis none of the sequences could be confidentially excluded.

Wnt8

The *Wnt8* subfamily had been lost in various arthropod species analysed but it could still be detected in several classes throughout the phylogeny (Figure 2.7). A *Wnt8* gene was found in all newly analysed beetles as well as the stink bugs (*H. halys*) and bed bugs (*C. lectularis*) (Figure 2.7). The *Wnt8* gene subfamily was well supported by a BS value of 72 in the full dataset, with BS values between 98-100 in the lepidopteran subset and with 84 in the chelicerate tree. Overall, the high BS support from the two other trees, again showed the same sequences cluster in the *Wnt8* subfamily, were reliable enough for annotating predicted *Wnt8* sequences. In all Chelicerata *Wnt8* was present, except in both scorpions *C. sculpturatus* and *M. martensii* (Figure 2.4 and 2.7), suggesting it had been lost in these arachnids.

Wnt 9

The BS support of the *Wnt9* subfamily in the full dataset (42) and in the chelicerate tree (58) were low, whereas the support in the lepidopteran tree was very high (93-100). *Wnt9* was newly detected in three of the four lepidopteran species, the silk moth *B. mori,* and the butterflies *B. anynana* and *P. glaucus* (Figure 2.7). Previously, *Wnt9* was

only described for *H. melpomene* (Martin *et al*., 2012) but it was conserved in all analysed lepidopterans. However, *Wnt9* might have been lost from all hymenopterans, such as bees, wasps and ants (Figure 2.7) while it was newly detected in the bed bug *C. lectularis*, the beetles *A. tumida* and *N. vespilloides*, and the scorpions *C. sculpturatus* and *M. martensii*.

Wnt10

The *Wnt10* subfamily was not supported in the full data tree (0), while the BS increased in the chelicerate subtree (92) and became very high in the lepidopteran tree (100). Analysing which sequences were clustering in all trees with the *Wnt10* subfamily showed that similar predicted Wnt sequences were present in all analysed trees. Also, based on the very high support in the subtrees, sequences clustered with this subfamily were annotated as *Wnt10* genes.

The *Wnt10* subfamily was lost in all chelicerates analysed in this study (Figure 2.7) whereas it was present in all Mandibulata. *Wnt10* also appeared to be missing in the tardigrade *H. dujardini*, however, this may just be a result of incomplete sequence data for this species.

Wnt11

This subfamily was represented in most arthropod species and it only appeared to be lost in the dipterans, such as the fruit fly *D. melanogaster* and mosquito *A. gambiae* (Figure 2.7). The support for this Wnt subfamily was very low (0) in the full arthropod tree, whereas the BS support increases in the chelicerate subtree (with *P. opilio*) (30) and was very high in the lepidopteran tree (100). Especially taking the lepidopteran dataset into account it was assumed that the clustering of predicted Wnt sequences with *Wnt11* was reliable and indeed, the same sequences were grouped in this subfamily in all trees.

Wnt11 was detected in one of the butterfly species *B. anynana* (see 1.3.1) while it was not fond in the two other butterfly species (Figure 2.7). *Wnt11* was present in both moths so it was assumed, that it might be lost in several butterfly species but present in the last common ancestor of Lepidoptera. *Wnt11* was only duplicated in the chelicerates, such as in the spiders and scorpions (Figure 2.7), while no duplication could

be found for the harvestman *P. opilio*, or the deer tick *I. scapularis.* The Wnt gene repertoire for *P. phalangoides* was very similar to *P. tepidariorum*, but no duplication of *Wnt11* was found (Figure 2.4). Re-analysing the *P. phalangoides* transcriptome also did not reveal any second *Wnt11* sequence. To my knowledge, this transcriptome was generated from embryonic stages and it was known from *P. tepidariorum* that during embryogenesis only one *Wnt11* gene was expressed. Thus, it still could be possible that a second *Wnt11* gene was present in *P. phalangoides* considering later stages. Further, duplications were observed in the horseshoe crab, where five different *Wnt11* sequences were found (Figure 2.7). Aligning these sequences showed, that they were all different from each other but aligning with previously characterised *Wnt11* genes. Again, several Wnts were found in this species, where it remains unclear which genes were fragments of maybe the same Wnt gene or which ones were true duplicates.

Wnt16

This Wnt subfamily was not supported in the full data tree (0), while the support was reasonable high in the chelicerate (63) and very high in the lepidopteran subtrees (99). Therefore, it was assumed that the clustering of sequences with this subfamily was reliable, also due to the fact that the same sequences could be found in all trees for this subfamily.

Wnt16 was lost in most of the insect species, except the hemipterans such as the aphid (*A. pisum)*, the white fly (*B. tabaci)* and the psyllid (*D. citri)* (Figure 2.7). This Wnt subfamily seemed to be duplicated in the water bear *H. dujardini* and in the horse shoe crab *L. polyphemus* where five different *Wnt16* gene sequences were detected (Figure 2.7). Again, aligning all *L. polyphemus* sequences showed that they all align clearly with known *Wnt16* sequences, whereas they were all different to each other. Therefore, none of these sequences could be excluded from the analysis at this point.

WntA

All analysed arthropod species had a *WntA* gene, except *D. melanogaster,* which was described previously, and it remains unclear why *Drosophila* has lost *WntA* (Figure 2.7). All *WntA* sequences were found at the base of the full data tree in a polyphyletic manner. Therefore, no BS support was obtained for the full tree, whereas the support

of the subfamily was very high in the chelicerate (94) and lepidopteran subtrees (99). Focussing on the subtrees, it was assumed that the annotation of predicted Wnt genes for this Wnt subfamily was reliable.

In spiders, *WntA* was previously described for the wolf spider *Cupiennus salei* (Damen, 2002) but it could not be detected in *P. tepidariorum* (Janssen *et al*., 2010). However, a recent Blast search in the genome revealed a "predicted *Wnt1*-Like isoform X1" (accession number: XP_015915580.1) sequence with a 99% coverage and a 68% identity to the *Ixodes WntA* sequence. This sequence was not included in the phylogenetic analysis, but it could be assumed that *WntA* was also present in *P. tepidariorum*. Duplications again, were only observed in the horseshoe crabs, where two different copies of the *WntA* gene were found (Figure 2.7). Overall, it could be concluded, that *WntA* was highly conserved throughout arthropods but losses occurred in specific lineages. In Deuterostomia, no *WntA* was present so far, whereas *WntA* could be found in Acoela, Cnidaria and possibly in sponges (Figure 2.1). Therefore, it might be possible, that the whole subfamily of *WntA* was lost in the common ancestor of deuterostomes but was still present in the last common ancestor of all metazoans.

2.3.4 The clustering of Wnt genes: Is the ancestral Wnt cluster conserved in arthropods?

An ancestral Wnt cluster was previously described consisting of *Wnt1, 6, 9, 10* and potentially *Wnt3* (Guder *et al*., 2006). *Wnt3* was lost in all protostomes which leaves four genes potentially clustered in arthropods. In addition to analysing the Wnt repertoire in several recently sequenced arthropod species, also the clustering of these Wnt genes was analysed (Figure 2.8). The clustering of Wnts could be an important factor in Wnt gene evolution.

In the tardigrade *H. dujardini* only *Wnt9* was found in this study. Therefore, it remains unresolved if other Wnt genes, such as *Wnt1* and *Wnt6,* were also present but not annotated in the most recent public available genome (see 2.3.1). The onychophoran *E. kanangrensis* had *Wnt1*, *6, 9* and *10*, but it was not possible to find the exact genomic locations of these genes and therefore it could not be determined if these genes were clustered in the velvet worm. For the myriapod, *S. maritima, Wnt1-6-10* were found on the same scaffold and were therefore clustered. However, the exact relative orientation of the Wnt genes could not be obtained from the available genomic data due to missing information about the gene locus and its structure. In Crustacea, the genomic locations of Wnts could only be found for the water flea *D. pulex* as previously described (Janssen *et al*., 2010). Here, *Wnt9, 1, 6* and *10* were potentially clustered but interspersed by other genes (Figure 2.8). In the hemipterans *B. tabaci* and *D. citri Wnt1-6-10* were clustered and orientated in the same relative directions but no *Wnt6* was found for *H. halys* or *C. lectularius* (Figure 2.8). Still, *Wnt1* and *Wnt10* could be found in close proximity to each other in both species (according to the obtained genomic coordinates), while no information about other genes between *Wnt1* and *Wnt10* was found. In *C. lectularius Wnt9* seemed to be located next to *Wnt10*, which was not observed in any other arthropod species and therefore probably represents a genomic rearrangement in this species.

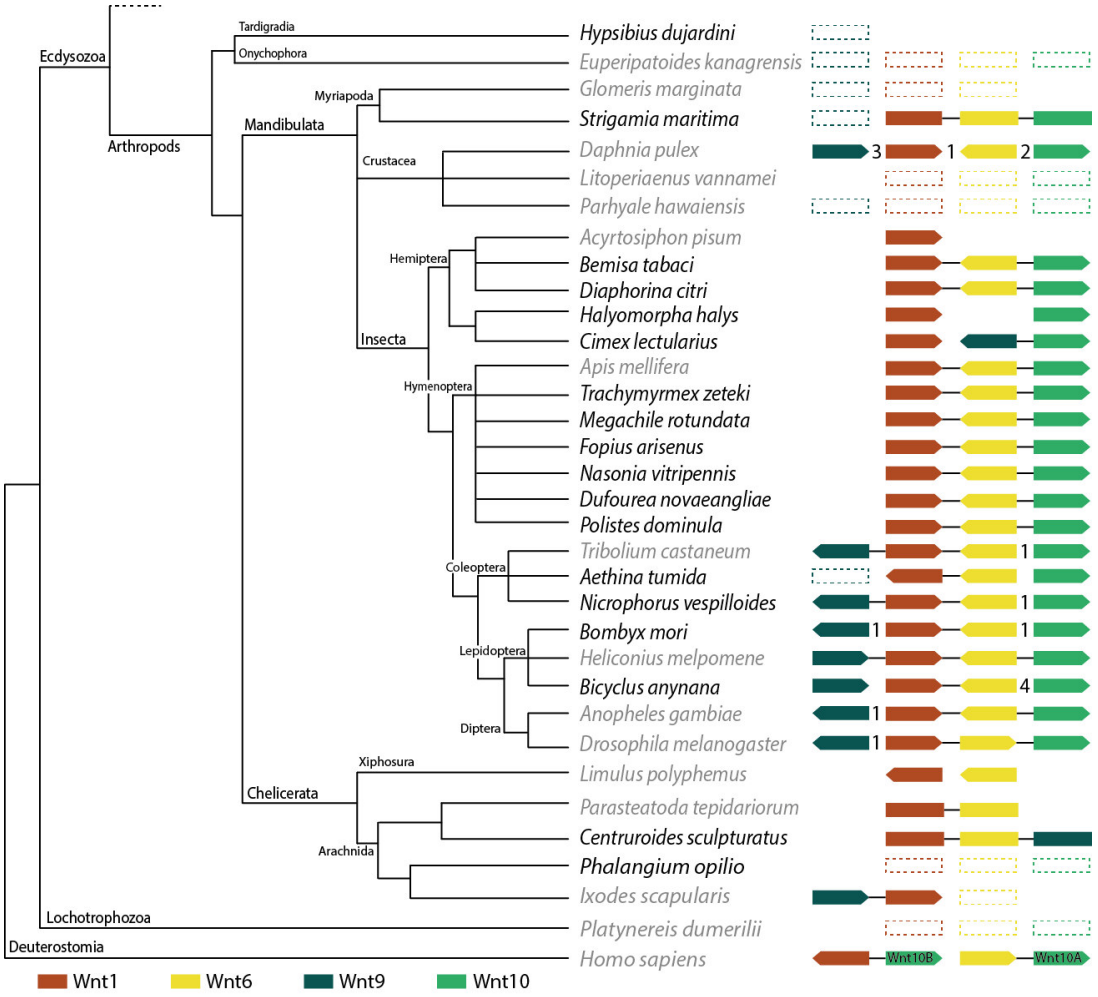

Figure 2.8 | Wnt gene clusters in arthropods. The ancestral Wnt gene cluster containing *Wnt1-6-9-10* is partially conserved throughout arthropods. Wnt genes present in the species but with no known location in the genome or not in the cluster are indicated by boxes with dashed lines. Clustered Wnt genes are connected via a black line. The arrow head of the box indicates the relative direction of this gene in the genome to the other genes in the cluster. If known, numbers between Wnt genes indicate the number of other genes located here. Newly analysed species in this study are printed in black, with previously studied species in light grey.

A very consistent picture of Wnt gene synteny was observed among Hymenoptera where *Wnt1-6-10* were always clustered and orientated in the same directions. In Coleoptera, *Wnt9-1-6* were clustered and orientated in the same way as in *T. castaneum* and *N. vespilloides,* and *Wnt10* was also found after an intervening gene between *Wnt6* and *Wnt10*. In the third analysed beetle, *A. thumida* only *Wnt1* and *Wnt6* were clustered (Figure 2.8) but orientated in the same direction and thus the orientation of *Wnt1* switched compared to most other species.

Wnt1 and *Wnt6* were clustered in the Lepidoptera *B. mori* and *B. anynana* and in *H. melpomene Wnt9-1-6-10. Wnt1*, 6 and *Wnt10* were also orientated in the same

directions in all analysed lepidopteran species. Orientation of *Wnt9* in *H. melpomene* and *B. anynana* was like the orientation of *Wnt1,* whereas the orientation of *Wnt9* in *B. mori* was the same as *Wnt6* (Figure 2.8). In the Diptera, *A. gambiae* and *D. melanogaster, Wnt1-6-10* were clustered while *Wnt9* was also still closely linked; but separated from *Wnt1* by one gene in both species (Figure 2.8).

In chelicerates *Wnt1* and *Wnt6* were juxtaposed in *P. tepidariorum* and *Wnt1, 6* and *9* were clustered in the scorpion *C. sculpturatus* as well as *Wnt9* and *Wnt1* in *I. scapularis* (Figure 2.8). Interestingly, in *H. sapiens* the remains of this cluster were also still detectable: while *Wnt1* and *Wnt6* were no longer linked, both are still syntenic with a *Wnt10* paralog.

Overall, *Wnt1* and *Wnt6* were still juxtaposed in most of the analysed species, while *Wnt10* often remains close to *Wnt6* and was therefore in most cases also part of the cluster. *Wnt1* and *Wnt6* were mostly orientated head to head whereas *Wnt10* was found tail to tail with *Wnt6*.

This analysis showed that the ancestral Wnt cluster was still highly conserved throughout arthropods. It could be speculated, that the genomic location of the Wnt genes could influence their evolution (conservation/loss/function) but on the other hand it might also be likely that Wnt genes became dependent on regulatory sequences near other Wnt genes. This had been shown in a previous study by Koshikawa *et al.* (2015). Here, several Wnt genes of the same cluster shared several enhancer elements (Koshikawa *et al*., 2015). Until now, however, no enhancers are known in *Wnt1* or *Wnt6* that were able to regulate the other Wnt gene. An overall analysis of this locus, searching for other enhancer regions could be a first step in further understanding a potential dependency between Wnts in the ancestral cluster.

2.4 | Conclusions and Outlook: Future study of Wnt genes in arthropods

In this analysis, it has been shown which Wnt genes were conserved, lost or duplicated in arthropods. However, the question remains as to why some Wnt ligands were conserved while others were lost and what makes these conserved subfamilies so important. Further analysis of the function of Wnt genes in several arthropod species could help to find out more about these questions. A first step into this direction was done in Chapter 2 where the expression of Wnts and their potential function in insect development will be compared between the three sister groups of Diptera, Lepidoptera and Coleoptera (See Chapter 2). One idea would be that these subfamilies have a conserved function with important roles during development in these species. This conserved function could then protect a particular Wnt gene from getting lost or changed too dramatically during evolution (Koshikawa *et al*., 2015). Here, not the function of the Wnt gene would be the reason for conservation, but its regulation. This could especially be the case for the Wnt genes in the ancestral Wnt cluster. Alternatively, Wnts could replace the function of other Wnts in some species which could result in the loss of a Wnt gene. This functional shuffling (e.g. Somorjai *et al*. (2018)) could be seen for example in *P. tepidariorum* where *Wnt8* overtakes the segmentation role of *wg* (Janssen *et al*., 2010).

Further, questions still unanswered include which Wnt gene was the first one or which of the Wnt subfamilies was the ancestor of all other Wnts. It was known that from very early in metazoans evolution all Wnt gene subfamilies were present, while in sponges or ctenophora only fragments have been found (Adamska *et al*., 2010; Pang *et al*., 2010). Therefore, it would be very interesting to continue the screening for Wnt genes in these very early metazoans and to compare the sequences systematically with those in other metazoans. Ancestral reconstruction could be used to find out the ancestral state of Wnt sequences to understand their possible ancestral structure and function and how they evolved and diversified. Such an approach has recently been used successfully to understand the evolution of *bicoid* (Liu *et al*., 2018) and the *atonal* gene family (Zhou *et al*., 2016). This analysis could build on my findings to further contribute to the understanding of the Wnt gene evolution and function.

2.5 | Supplement

>consensusWNT

LSPKQRRLCRRNPDVMPSVAEGARLAISECQHQFRNRRWNCSTLDGAPVFGKILKRGTRETAFVY

AISSAGVAHAVTRACSLGELTSCGCDRSPRGRSPDEDWEWGGCSDNIDFGMRFSRKFLDARERK

RSDARALMNLHNNEAGRKAVKSNMRTECKCHGVSGSCSVKTCWKQLPDFREVGDRLKEKYDGA

VKVVRRVRNRGKRLLPRSRFKPPTKTDLVYLEKSPDYCERNPKLGSLGTQGRECNKTSTGPDGCDL

LCCGRGYNTRTVTVTERCNCKFHWCCYVKCKTCRRTVEVYTCK

Supplement Table S2.1 | Summary of all used Wnt gene sequences, their accession numbers or protein source code and the newly annotated Wnt subfamily association.

Species	Gene accession number or protein bank code	Annotated Wnt
C. lectularius	XM_014401938.1_2_PREDICTED:_Cimex_lectularius_Wnt-5a-like	*Wnt5*
C. lectularius	XM_014394181.1_3_PREDICTED:_Cimex_lectularius_wingless	*Wnt1*
C. lectularius	XM_014401901.1_3_PREDICTED:_Cimex_lectularius	*WntA*
C. lectularius	XM_014401758.1_2_PREDICTED:_Cimex_lectularius_Wnt-7b	*Wnt7*
C. lectularius	XM_014394318.1_1_PREDICTED:_Cimex_lectularius_Wnt-10a	*Wnt10*
C. lectularius	XM_014405439.1_1_PREDICTED:_Cimex_lectularius_Wnt-8b-like	*Wnt8*
C. lectularius	XM_014394108.1_1_PREDICTED:_Cimex_lectularius_Wnt-4-like	*Wnt9*
H. halys	XM_014419236.1_1_PREDICTED:_Halyomorpha_halys_Wnt-5b-like	*Wnt5*
H. halys	XM_014426235.1_3_PREDICTED:_Halyomorpha_halys_wingless	*Wnt1*
H. halys	XM_014421726.1_1_PREDICTED:_Halyomorpha_halys_Wnt-1-like	*WntA*
H. halys	XM_014422068.1_1_PREDICTED:_Halyomorpha_halys_Wnt-7b-like	*Wnt7*
H. halys	XM_014426216.1_1_PREDICTED:_Halyomorpha_halys_Wnt-10b	*Wnt10*
H. halys	XM_014435114.1_1_PREDICTED:_Halyomorpha_halys_Wnt-8a-like	*Wnt8*
D. citri	XM_017444469.1_1_PREDICTED:_Diaphorina_citri_Wnt-6-like	*Wnt6*
D. citri	XM_017444468.1_3_PREDICTED:_Diaphorina_citri_Wnt-1-like	*Wnt1*
D. citri	XM_008489903.1_1_PREDICTED:_Diaphorina_citri_Wnt-7c-like	*Wnt5*
D. citri	XM_008479326.2_3_PREDICTED:_Diaphorina_citri_Wnt-4-like	*Wnt16*
D. citri	XM_008486682.2_1_PREDICTED:_Diaphorina_citri_Wnt-5a-like	*Wnt11*
D. citri	XM_008484931.1_1_PREDICTED:_Diaphorina_citri_Wnt-5b-like	*Wnt5*
D. citri	XM_008470765.2_1_PREDICTED:_Diaphorina_citri_Wnt-5b-like	*WntA*
D. citri	XM_008486259.1_1_PREDICTED:_Diaphorina_citri_Wnt-10b-like	*Wnt10*
D. citri	XM_017443218.1_2_PREDICTED:_Diaphorina_citri_uncharacterized	*Wnt10*
B. tabaci	XM_019062440.1_3_PREDICTED:_Bemisia_tabaci_wingless-like	*Wnt1*
B. tabaci	XM_019051165.1_1_PREDICTED:_Bemisia_tabaci_Wnt-5b-like	*Wnt5*
B. tabaci	XM_019058231.1_2_PREDICTED:_Bemisia_tabaci_Wnt-2	*Wnt7*
B. tabaci	XM_019058833.1_3_PREDICTED:_Bemisia_tabaci_Wnt-1-like	*WntA*
B. tabaci	XM_019062466.1_2_PREDICTED:_Bemisia_tabaci_Wnt-6-like	*Wnt6*

B. tabaci	XM_019062435.1_1_PREDICTED:_Bemisia_tabaci_Wnt-10a-like	*Wnt10*
B. tabaci	XM_019062009.1_1_PREDICTED:_Bemisia_tabaci_Wnt-16-like	*Wnt11*
B. tabaci	XM_019062437.1_2_PREDICTED:_Bemisia_tabaci_Wnt-10a-like	*Wnt16*
F. arisanus	XM_011300877.1_3_Fopius_arisanus_wingless	*Wnt1*
F. arisanus	XM_011300876.1_2_Fopius_arisanus_Wnt-6	*Wnt6*
F. arisanus	XM_011304797.1_3_Fopius_arisanus_Wnt-4-like	*WntA*
F. arisanus	XM_011300874.1_1_Fopius_arisanus_Wnt-10b	*Wnt10*
F. arisanus	XM_011306172.1_2_Fopius_arisanus_Wnt-11b-2-like	*Wnt11*
F. arisanus	XM_011316200.1_1_Fopius_arisanus_Wnt-2	*Wnt7*
L. polyphemus	XM_013926410.1_1_PREDICTED:_Limulus_polyphemus_Wnt-4-like	*Wnt4*
L. polyphemus	XM_013928174.1_1_PREDICTED:_Limulus_polyphemus_Wnt-5b-like	*Wnt5*
L. polyphemus	XM_013926362.1_1_PREDICTED:_Limulus_polyphemus_Wnt-2b-A-like	*Wnt2*
L. polyphemus	XM_013918353.1_1_PREDICTED:_Limulus_polyphemus_Wnt-5b-like	*Wnt5*
L. polyphemus	XM_013918356.1_1_PREDICTED:_Limulus_polyphemus_Wnt-7b-like	*Wnt7*
L. polyphemus	XM_013930964.1_1_PREDICTED:_Limulus_polyphemus_Wnt-2b-like	*Wnt2*
L. polyphemus	XM_013928173.1_1_PREDICTED:_Limulus_polyphemus_Wnt-7b-like	*Wnt7*
L. polyphemus	XM_013922669.1_1_PREDICTED:_Limulus_polyphemus_Wnt-5a-like	*Wnt5*
L. polyphemus	XM_013919848.1_1_PREDICTED:_Limulus_polyphemus_Wnt-16-like	*Wn16*
L. polyphemus	XM_013929412.1_1_PREDICTED:_Limulus_polyphemus_Wnt-4-like	*WntA*
L. polyphemus	XM_013922594.1_1_PREDICTED:_Limulus_polyphemus_Wnt-7b-like	*Wnt16*
L. polyphemus	XM_013922563.1_1_PREDICTED:_Limulus_polyphemus_Wnt-7b-like	*Wnt7*
L. polyphemus	XM_013935585.1_1_PREDICTED:_Limulus_polyphemus_Wnt-11-like	*Wnt11*
L. polyphemus	XM_013926485.1_1_PREDICTED:_Limulus_polyphemus_Wnt-11b-2-like	*Wnt11*
L. polyphemus	XM_013925512.1_1_PREDICTED:_Limulus_polyphemus_Wnt-11b-2-like	*Wnt11*
L. polyphemus	XM_013927740.1_1_PREDICTED:_Limulus_polyphemus_Wnt-2b-like	*WntA*
L. polyphemus	XM_013937883.1_1_PREDICTED:_Limulus_polyphemus_Wnt-7b-like	*Wnt7*
L. polyphemus	XM_013932682.1_3_PREDICTED:_Limulus_polyphemus_wingless-like	*Wnt1*
L. polyphemus	XM_013937282.1_1_PREDICTED:_Limulus_polyphemus_Wnt-5b-like	*Wnt5*
L. polyphemus	XM_013936661.1_3_PREDICTED:_Limulus_polyphemus_Wnt-16-like	*Wnt16*
L. polyphemus	XM_013929750.1_1_PREDICTED:_Limulus_polyphemus_Wnt-7b-like	*Wnt7*
L. polyphemus	XM_013927622.1_1_PREDICTED:_Limulus_polyphemus_Wnt-8b-like	*Wnt8*
L. polyphemus	XM_013935495.1_3_PREDICTED:_Limulus_polyphemus_Wnt-6-like	*Wnt6*
L. polyphemus	XM_013929552.1_1_PREDICTED:_Limulus_polyphemus_Wnt-11b-1-like	*Wnt11*
L. polyphemus	XM_013936197.1_1_PREDICTED:_Limulus_polyphemus_Wnt-5b-like	*Wnt5*
L. polyphemus	XM_013919287.1_1_PREDICTED:_Limulus_polyphemus_Wnt-16-like	*Wnt16*
L. polyphemus	XM_013933553.1_1_PREDICTED:_Limulus_polyphemus_Wnt-7b-like	*Wnt7*
L. polyphemus	XM_013923053.1_1_PREDICTED:_Limulus_polyphemus_Wnt-2b-A-like	*WntA*
L. polyphemus	XM_013923140.1_1_PREDICTED:_Limulus_polyphemus_Wnt-5b-like	*Wnt5*
L. polyphemus	XM_013936832.1_2_PREDICTED:_Limulus_polyphemus_Wnt-5a-like	*Wnt5*
L. polyphemus	XM_013916700.1_1_PREDICTED:_Limulus_polyphemus_Wnt-11-like	*Wnt11*

L. polyphemus	XM_013937817.1_1_PREDICTED:_Limulus_polyphemus_Wnt-5b-like	*Wnt5*
L. polyphemus	XM_013938103.1_1_PREDICTED:_Limulus_polyphemus_Wnt-5b-like	*Wnt5*
L. polyphemus	XM_013928576.1_1_PREDICTED:_Limulus_polyphemus_Wnt-3a-like	*Wnt16*
M. rotundata	XM_003707837.2_1_PREDICTED:_Megachile_rotundata_Wnt-1	*Wnt1*
M. rotundata	XM_012280855.1_1_PREDICTED:_Megachile_rotundata_Wnt-5b-like	*Wnt5*
M. rotundata	XM_003706539.2_3_PREDICTED:_Megachile_rotundata_Wnt-1-like	*WntA*
M. rotundata	XM_003707840.2_2_PREDICTED:_Megachile_rotundata_Wnt-10a	*Wnt10*
M. rotundata	XM_012296265.1_1_PREDICTED:_Megachile_rotundata_Wnt-6	*Wnt6*
M. rotundata	XM_012283819.1_1_PREDICTED:_Megachile_rotundata_Wnt-11b-1-like	*Wnt11*
M. rotundata	XM_012289594.1_2_PREDICTED:_Megachile_rotundata_Wnt-7b	*Wnt7*
N. vitripennis	XM_008214294.2_1_PREDICTED:_Nasonia_vitripennis_Wnt-5b-like	*Wnt5*
N. vitripennis	XM_008204199.2_3_PREDICTED:_Nasonia_vitripennis_Wnt-1	*Wnt1*
N. vitripennis	XM_001603301.4_1_PREDICTED:_Nasonia_vitripennis_Wnt-6	*Wnt6*
N. vitripennis	XM_016989866.1_2_PREDICTED:_Nasonia_vitripennis_Wnt-7b	*Wnt10*
N. vitripennis	XM_001606292.4_1_PREDICTED:_Nasonia_vitripennis_Wnt-7b	*Wnt7*
N. vitripennis	XM_003424864.3_3_PREDICTED:_Nasonia_vitripennis_Wnt-11b-1-like	*Wnt11*
N. vitripennis	XM_008204197.2_1_PREDICTED:_Nasonia_vitripennis_Wnt-10b	*Wnt10*
N. vitripennis	XM_008205746.2_2_PREDICTED:_Nasonia_vitripennis_Wnt-4-like	*WntA*
P. opilio	P.opilio_comp180159_c1_seq1_1_1	*Wnt7*
P. opilio	P.opilio_comp180159_c1_seq2_2_6	*Wnt16*
P. opilio	P.opilio_comp175018_c0_seq1_3_4	*Wnt4*
P. opilio	P.opilio_comp179026_c1_seq4_10_5	*Wnt1*
P. opilio	P.opilio_comp183805_c0_seq8_17_6	*Wnt5*
P. opilio	P.opilio_comp71692_c0_seq1_18_2	*Wnt16*
P. opilio	P.opilio_comp175768_c0_seq10_28_4	*Wnt6*
P. opilio	P.opilio_comp183805_c0_seq3_34_2	*Wnt7*
P. opilio	P.opilio_comp142605_c0_seq1_35_6	*Wnt7*
D. novaeangliae	XM_015577499.1_1_Dufourea_novaeangliae_Wnt-1	*Wnt1*
D. novaeangliae	XM_015578961.1_1_Dufourea_novaeangliae_Wnt-5b-like	*Wnt5*
D. novaeangliae	XM_015577483.1_1_Dufourea_novaeangliae_Wnt-6-like	*Wnt6*
D. novaeangliae	XM_015582721.1_1_Dufourea_novaeangliae_Wnt-1-like	*WntA*
D. novaeangliae	XM_015577482.1_1_Dufourea_novaeangliae_Wnt-10b-like	*Wnt10*
D. novaeangliae	XM_015576447.1_1_Dufourea_novaeangliae_Wnt-11b-like	*Wnt11*
D. novaeangliae	XM_015577775.1_1_Dufourea_novaeangliae_Wnt-7b-like	*Wnt7*
D. melanogaster	wg_dm_aa	*Wnt1*
D. melanogaster	Wnt2_dm_aa	*Wnt7*
D. melanogaster	Wnt4_dm_aa	*Wnt9*
D. melanogaster	Wnt5_dm_aa	*Wnt5*
D. melanogaster	Wnt6_dm_aa	*Wnt6*
D. melanogaster	Wnt8_dm_aa	*Wnt8*
D. melanogaster	Wnt10_dm_aa	*Wnt10*
H. sapiens	sp|P41221|WNT5A_HUMAN_Wnt-5a_Homo_sapiens	*Wnt5*

H. sapiens	sp|P56704|WNT3A_HUMAN_Wnt-3a_Homo_sapiens	*Wnt3*
H. sapiens	sp|P56705|WNT4_HUMAN_Wnt-4_Homo_sapiens	*Wnt4*
H. sapiens	sp|O00755|WNT7A_HUMAN_Wnt-7a_Homo_sapiens	*Wnt7*
H. sapiens	sp|P04628|WNT1_HUMAN_Proto-oncogene_Wnt-1_Homo_sapiens	*Wnt1*
H. sapiens	sp|O96014|WNT11_HUMAN_Wnt-11_Homo_sapiens	*Wnt11*
H. sapiens	sp|P09544|WNT2_HUMAN_Wnt-2_Homo_sapiens	*Wnt2*
H. sapiens	sp|O00744|WN10B_HUMAN_Wnt-10b_Homo_sapiens	*Wnt10*
H. sapiens	sp|P56703|WNT3_HUMAN_Proto-oncogene_Wnt-3_Homo_sapiens	*Wnt3*
H. sapiens	sp|Q9GZT5|WN10A_HUMAN_Wnt-10a_Homo_sapiens	*Wnt10*
H. sapiens	sp|P56706|WNT7B_HUMAN_Wnt-7b_Homo_sapiens	*Wnt7*
H. sapiens	sp|O14905|WNT9B_HUMAN_Wnt-9b_Homo_sapiens	*Wnt9*
H. sapiens	sp|Q9UBV4|WNT16_HUMAN_Wnt-16_Homo_sapiens	*Wnt16*
H. sapiens	sp|Q93097|WNT2B_HUMAN_Wnt-2b_Homo_sapiens	*Wnt2*
H. sapiens	sp|Q9Y6F9|WNT6_HUMAN_Wnt-6_Homo_sapiens	*Wnt6*
H. sapiens	sp|Q9H1J7|WNT5B_HUMAN_Wnt-5b_Homo_sapiens	*Wnt5*
H. sapiens	sp|O14904|WNT9A_HUMAN_Wnt-9a_Homo_sapiens	*Wnt9*
H. sapiens	sp|Q9H1J5|WNT8A_HUMAN_Wnt-8a_Homo_sapiens	*Wnt8*
H. sapiens	sp|Q93098|WNT8B_HUMAN_Wnt-8b_Homo_sapiens	*Wnt8*
P. dominula	XM_015323048.1_1_PREDICTED:_Polistes_dominula_Wnt-1	*Wnt1*
P. dominula	XM_015324085.1_3_PREDICTED:_Polistes_dominula_Wnt-5b-like	*Wnt5*
P. dominula	XM_015330508.1_3_PREDICTED:_Polistes_dominula_Wnt-1-like	*WntA*
P. dominula	XM_015322923.1_3_PREDICTED:_Polistes_dominula_Wnt-6-like	*Wnt6*
P. dominula	XM_015322921.1_3_PREDICTED:_Polistes_dominula_Wnt-10b	*Wnt10*
P. dominula	XM_015326943.1_1_PREDICTED:_Polistes_dominula_Wnt-11b-1-like	*Wnt11*
P. dominula	XM_015330978.1_2_PREDICTED:_Polistes_dominula_Wnt-7b	*Wnt7*
H. melpomene	heliconius_melpomene_core_32_85_1_cds_HMEL022606-RA_1	*Wnt5*
H. melpomene	heliconius_melpomene_core_32_85_1_cds_HMEL022601-RA_1	*Wnt1*
H. melpomene	heliconius_melpomene_core_32_85_1_cds_HMEL011436-RA_1	*Wnt6*
H. melpomene	heliconius_melpomene_core_32_85_1_cds_HMEL018100-RA_1	*WntA*
H. melpomene	heliconius_melpomene_core_32_85_1_cds_HMEL011434-RA_1	*Wnt10*
H. melpomene	heliconius_melpomene_core_32_85_1_cds_HMEL011441-RA_1	*Wnt9*
H. melpomene	heliconius_melpomene_core_32_85_1_cds_HMEL022591-RA_1	*Wnt7*
T. zeteki	XM_018461916.1_3_PREDICTED:_Trachymyrmex_zeteki_Wnt-1	*Wnt1*
T. zeteki	XM_018448384.1_1_PREDICTED:_Trachymyrmex_zeteki_Wnt-5b-like	*Wnt5*
T. zeteki	XM_018461920.1_3_PREDICTED:_Trachymyrmex_zeteki_Wnt-6-like	*Wnt6*
T. zeteki	XM_018461918.1_1_PREDICTED:_Trachymyrmex_zeteki_Wnt-10a	*Wnt10*
T. zeteki	XM_018456288.1_3_PREDICTED:_Trachymyrmex_zeteki_Wnt-4-like	*WntA*
T. zeteki	XM_018445643.1_1_PREDICTED:_Trachymyrmex_zeteki_Wnt-7b	*Wnt7*
T. zeteki	XM_018460491.1_3_PREDICTED:_Trachymyrmex_zeteki_Wnt-11b-1-like	*Wnt11*
A. tumida	XM_020012776.1_1_PREDICTED:_Aethina_tumida_Wnt-2-like	*Wnt7*
A. tumida	XM_020021341.1_1_PREDICTED:_Aethina_tumida_Wnt-1	*Wnt1*
A. tumida	XM_020010480.1_3_PREDICTED:_Aethina_tumida_Wnt-5b-like	*Wnt5*

A. tumida	XM_020023863.1_2_PREDICTED:_Aethina_tumida_Wnt-1-like	*WntA*
A. tumida	XM_020021386.1_1_PREDICTED:_Aethina_tumida_Wnt-6-like	*Wnt6*
A. tumida	XM_020021383.1_2_PREDICTED:_Aethina_tumida_Wnt-10a-like	*Wnt10*
A. tumida	XM_020011652.1_3_PREDICTED:_Aethina_tumida_Wnt-11b-1-like	*Wnt11*
A. tumida	XM_020014760.1_2_PREDICTED:_Aethina_tumida_Wnt-8b-like	*Wnt8*
A. tumida	XM_020021337.1_1_PREDICTED:_Aethina_tumida_Wnt-4-like	*Wnt9*
N. vespilloides	XM_017918062.1_1_PREDICTED:_Nicrophorus_vespilloides_Wnt-5b-like	*Wnt5*
N. vespilloides	XM_017922415.1_3_PREDICTED:_Nicrophorus_vespilloides_Wnt-1	*Wnt1*
N. vespilloides	XM_017921306.1_2_PREDICTED:_Nicrophorus_vespilloides_Wnt-7b	*Wnt7*
N. vespilloides	XM_017922392.1_1_PREDICTED:_Nicrophorus_vespilloides_Wnt-6	*Wnt6*
N. vespilloides	XM_017915392.1_2_PREDICTED:_Nicrophorus_vespilloides_Wnt-4-like	*WntA*
N. vespilloides	XM_017922431.1_2_PREDICTED:_Nicrophorus_vespilloides_Wnt-10b	*Wnt10*
N. vespilloides	XM_017925713.1_1_PREDICTED:_N_vespilloides_Wnt-11b2-like	*Wnt11*
N. vespilloides	XM_017930403.1_1_PREDICTED:_Nicrophorus_vespilloides_Wnt-8a-like	*Wnt8*
N. vespilloides	XM_017922385.1_1_PREDICTED:_Nicrophorus_vespilloides_Wnt-4	*Wnt9*
B. mori	sp|P49340|WNT1_BOMMO_Wnt-1_Bombyx_mori	*Wnt1*
B. mori	tr|H9JW73|H9JW73_BOMMO_Wnt_Bombyx_mori	*WntA*
B. mori	tr|H9JDI3|H9JDI3_BOMMO_Wnt_Bombyx_mori	*Wnt11*
B. mori	tr|H9JWR7|H9JWR7_BOMMO_Wnt_Bombyx_mori	*Wnt7*
B. mori	tr|H9J9F2|H9J9F2_BOMMO_Wnt_Bombyx_mori	*Wnt9*
B. mori	tr|H9J9F5|H9J9F5_BOMMO_Wnt_Bombyx_mori	*Wnt10*
B. mori	tr|H9J912|H9J912_BOMMO_Wnt_Bombyx_mori	*Wnt6*
B. mori	tr|M4B151|M4B151_BOMMO_Wnt_Bombyx_mori	*Wnt5*
B. mori	tr|H9J9F4|H9J9F4_BOMMO_Wnt_Bombyx_mori	*Wnt7*
T. castaneum	tr|D7EKY4|D7EKY4_TRICA_WntD_Tribolium_castaneum	*Wnt8*
T. castaneum	tr|D6WK67|D6WK67_TRICA_Wnt_Tribolium_castaneum	*Wnt6*
T. castaneum	tr|D6WK65|D6WK65_TRICA_Wnt_Tribolium_castaneum	*Wnt9*
T. castaneum	tr|D6WK66|D6WK66_TRICA_Wnt_Tribolium_castaneum	*Wnt1*
T. castaneum	tr|D6WK69|D6WK69_TRICA_Wnt_Tribolium_castaneum	*Wnt10*
T. castaneum	tr|A0A139WF66|A0A139WF66_TRICA_Wnt_Tribolium_castaneum	*WntA*
T. castaneum	tr|D6WRU0|D6WRU0_TRICA_Wnt_Tribolium_castaneum	*Wnt5*
T. castaneum	tr|D6WT32|D6WT32_TRICA_Wnt_Tribolium_castaneum	*Wnt7*
T. castaneum	tr|D6WKY7|D6WKY7_TRICA_Wnt_Tribolium_castaneum	*Wnt11*
A. gambiae	tr|Q5TP56|Q5TP56_ANOGA_Wnt_Anopheles_gambiae_	*Wnt1*
A. gambiae	tr|A0NG52|A0NG52_ANOGA_Wnt_Anopheles_gambiae	*Wnt7*
A. gambiae	tr|Q7PM75|Q7PM75_ANOGA_Wnt_(Fragment)_Anopheles_gambiae	*Wnt9*
A. gambiae	tr|Q7PM77|Q7PM77_ANOGA_Wnt_Anopheles_gambiae	*Wnt10*
A. gambiae	tr|Q7Q1L2|Q7Q1L2_ANOGA_Wnt_(Fragment)_Anopheles_gambiae	*Wnt6*
A. gambiae	tr|Q5TS73|Q5TS73_ANOGA_Wnt_Anopheles_gambiae	*WntA*
A. gambiae	tr|Q7Q0K5|Q7Q0K5_ANOGA_Wnt_(Fragment)_Anopheles_gambiae	*Wnt5*

A. gambiae	tr|A0NFU3|A0NFU3_ANOGA_Wnt_Anopheles_gambiae	*Wnt7*
A. mellifera	tr|A0A088ANQ7|A0A088ANQ7_APIME_Wnt5_Apis_mellifera	*Wnt5*
A. mellifera	tr|A0A088A2M8|A0A088A2M8_APIME_Wnt6_Apis_mellifera	*Wnt6*
A. mellifera	tr|A0A087ZZX9|A0A087ZZX9_APIME_Wnt11_Apis_mellifera	*Wnt11*
A. mellifera	tr|A0A088A2M9|A0A088A2M9_APIME_Wnt1_Apis_mellifera	*Wnt1*
A. mellifera	tr|A0A088A2N0|A0A088A2N0_APIME_Wnt10_Apis_mellifera	*Wnt10*
A. mellifera	tr|A0A087ZZP2|A0A087ZZP2_APIME_Wnt7_Apis_mellifera	*Wnt7*
A. mellifera	tr|A0A088A0Q5|A0A088A0Q5_APIME_Wnt4_Apis_mellifera	*WntA*
A. pisum	tr|J9K970|J9K970_ACYPI_Wnt_Acyrthosiphon_pisum	*Wnt7*
A. pisum	tr|J9JSF9|J9JSF9_ACYPI_Wnt_Acyrthosiphon_pisum	*Wnt1*
A. pisum	tr|J9JT78|J9JT78_ACYPI_Wnt_Acyrthosiphon_pisum	*Wnt5*
A. pisum	tr|J9JK28|J9JK28_ACYPI_Wnt_Acyrthosiphon_pisum	*Wnt16*
A. pisum	tr|J9JLW9|J9JLW9_ACYPI_Wnt_Acyrthosiphon_pisum	*WntA*
A. pisum	tr|J9JXJ2|J9JXJ2_ACYPI_Wnt_Acyrthosiphon_pisum	*Wnt11*
E. kanangrensis	A0A097ZRW5|A0A097ZRW5_9BILA_Wnt_E_kanangrensisWnt6	*Wnt6*
E. kanangrensis	A0A097ZRP0|A0A097ZRP0_9BILA_Wnt_E_kanangrensis_Wnt2	*Wnt2*
E. kanangrensis	A0A097ZRN9|A0A097ZRN9_9BILA_Wnt_E_kanangrensisWnt5	*Wnt5*
E. kanangrensis	A0A097ZRP1|A0A097ZRP1_9BILA_Wnt_E_kanangrensisWnt11	*Wnt11*
E. kanangrensis	A0A097ZRP8|A0A097ZRP8_9BILA_Wnt_E_kanangrensisWnt10	*Wnt10*
E. kanangrensis	A0A097ZRP4|A0A097ZRP4_9BILA_Wnt_E_kanangrensis_Wnt4	*Wnt4*
E. kanangrensis	A0A097ZRP2|A0A097ZRP2_9BILA_Wnt_E_kanangrensis_Wnt7	*Wnt7*
E. kanangrensis	A0A097ZRW6|A0A097ZRW6_9BILA_WntE_kanangrensisWnt16	*Wnt16*
E. kanangrensis	A0A097ZRP3|A0A097ZRP3_9BILA_Wnt_E_kanangrensis_Wnt9	*Wnt9*
E. kanangrensis	A0A097ZRP6|A0A097ZRP6_9BILA_Wnt_E_kanangrensisWntA	*WntA*
E. kanangrensis	B0FRJ8|B0FRJ8_9BILA_Wnt_(Fragment)_Euperipatoides_kanangrensis	*Wnt1*
G. marginata	tr|H6QXV0|H6QXV0_GLOMR_Wnt_(Fragment)_G_marginata_wnt11	*Wnt11*
G. marginata	tr|X5JAR0|X5JAR0_GLOMR_Wnt_Glomeris_marginata_Wnt4	*Wnt4*
G. marginata	tr|H6QXU9|H6QXU9_GLOMR_Wnt_(Fragment)_G_marginata_wnt8	*Wnt8*
G. marginata	tr|Q708C6|Q708C6_GLOMR_Wnt_(Fragment)_G_marginata_wnt-7	*Wnt16*
G. marginata	tr|X5JAY7|X5JAY7_GLOMR_Wnt_(Fragment)_Glomeris_marginata_Wnt5	*Wnt5*
G. marginata	tr|X5JA62|X5JA62_GLOMR_Wnt_Glomeris_marginata_Wnt9	*Wnt9*
G. marginata	tr|X5JAE1|X5JAE1_GLOMR_Wnt_Glomeris_marginata_Wnt2	*Wnt2*
G. marginata	tr|Q708C8|Q708C8_GLOMR_Wnt_(Fragment)_Glomeris_marginata_wg	*Wnt1*
G. marginata	tr|Q708C7|Q708C7_GLOMR_Wnt_(Fragment)_G_marginata_wnt-5	*WntA*
G. marginata	tr|H6QXU8|H6QXU8_GLOMR_Wnt_(Fragment)_G_marginata_wnt7	*Wnt7*
G. marginata	tr|H6QXU7|H6QXU7_GLOMR_Wnt_(Fragment)_G_marginata_wnt6	*Wnt6*
D. pulex	tr|E9G214|E9G214_DAPPU_Wnt_Daphnia_pulex_WNT1	*Wnt1*
D. pulex	tr|E9GSF2|E9GSF2_DAPPU_Wnt_Daphnia_pulex_WNTY	*Wnt11*
D. pulex	tr|E9GB34|E9GB34_DAPPU_Wnt_Daphnia_pulex_WNT8.2	*Wnt8*
D. pulex	tr|E9G208|E9G208_DAPPU_Wnt_Daphnia_pulex_WNT10	*Wnt10*
D. pulex	tr|E9H794|E9H794_DAPPU_Wnt_(Fragment)_Daphnia_pulex_WNT4	*Wnt4*

D. pulex	tr|E9HP52|E9HP52_DAPPU_Wnt_Daphnia_pulex_WNT7	*Wnt7*
D. pulex	tr|E9G217|E9G217_DAPPU_Wnt_Daphnia_pulex_WNT9	*Wnt9*
D. pulex	tr|E9HE78|E9HE78_DAPPU_Wnt_(Fragment)_Daphnia_pulex_WNTX	*WntA*
D. pulex	tr|E9FZU6|E9FZU6_DAPPU_Wnt_(Fragment)_Daphnia_pulex_WNT2	*Wnt2*
D. pulex	tr|E9HP53|E9HP53_DAPPU_Wnt_(Fragment)_Daphnia_pulex_WNT5	*Wnt5*
D. pulex	tr|E9G212|E9G212_DAPPU_Wnt_Daphnia_pulex_WNT6	*Wnt6*
D. pulex	tr|E9GBP2|E9GBP2_DAPPU_Wnt_Daphnia_pulex_WNT16	*Wnt16*
P. tepidariorum	tr|B5TTU9|B5TTU9_PARTP_Wnt8_Parasteatoda_tepidariorum	*Wnt8*
P. tepidariorum	tr|Q75PH4|Q75PH4_PARTP_Wnt2_Parasteatoda_tepidariorum	*Wnt2*
P. tepidariorum	tr|Q75PH6|Q75PH6_PARTP_Wnt7-2_Parasteatoda_tepidariorum	*Wnt7*
P. tepidariorum	tr|Q75PH5|Q75PH5_PARTP_Wnt16_Parasteatoda_tepidariorum	*Wnt16*
P. tepidariorum	tr|E5Q9H0|E5Q9H0_PARTP_Wnt_(Fragment)_P_tepidariorum	*Wnt11*
P. tepidariorum	tr|Q75PH8|Q75PH8_PARTP_Wnt7-1_Parasteatoda_tepidariorum	*Wnt7*
P. tepidariorum	tr|Q75PH7|Q75PH7_PARTP_Wnt5_Parasteatoda_tepidariorum	*Wnt5*
P. tepidariorum	tr|Q75PH9|Q75PH9_PARTP_wg_(Fragment)_Parasteatoda_tepidariorum	*Wnt1*
P. tepidariorum	tr|E5Q9G7|E5Q9G7_PARTP_Wnt_(Fragment)_P_tepidariorum	*Wnt4*
P. tepidariorum	tr|E5Q9G9|E5Q9G9_PARTP_Wnt_(Fragment)_P_tepidariorum	*Wnt11*
P. tepidariorum	Wnt6_1_Pt	*Wnt6*
I. scapularis	tr|B7PG71|B7PG71_IXOSC_Wnt_Ixodes_scapularis	*Wnt11*
I. scapularis	tr|B7PV27|B7PV27_IXOSC_Wnt_Ixodes_scapularis	*Wnt9*
I. scapularis	tr|B7PV28|B7PV28_IXOSC_Wnt_(Fragment)_Ixodes_scapularis	*Wnt1*
I. scapularis	tr|B7P8N6|B7P8N6_IXOSC_Wnt_(Fragment)_Ixodes_scapularis	*WntA*
I. scapularis	tr|B7PQK1|B7PQK1_IXOSC_Wnt_Ixodes_scapularis	*Wnt4*
I. scapularis	tr|B7QGH6|B7QGH6_IXOSC_Wnt_Ixodes_scapularis	*Wnt7*
I. scapularis	tr|B7PH10|B7PH10_IXOSC_Wnt_(Fragment)_Ixodes_scapularis	*Wnt16*
I. scapularis	tr|B7P9G6|B7P9G6_IXOSC_Wnt_(Fragment)_Ixodes_scapularis	*Wnt5*
I. scapularis	tr|B7PYK6|B7PYK6_IXOSC_Wnt_Ixodes_scapularis	*Wnt5*
L. vannamei	tr|A0A1L2A1N4|A0A1L2A1N4_LITVA_Wnt7_Litopenaeus_vannamei	*Wnt7*
L. vannamei	tr|A0A1L2A1N8|A0A1L2A1N8_LITVA_Wnt4_Litopenaeus_vannamei	*WntA*
L. vannamei	tr|A0A1L2A1P3|A0A1L2A1P3_LITVA_Wnt5_Litopenaeus_vannamei	*Wnt5*
L. vannamei	tr|A0A1L2A1P1|A0A1L2A1P1_LITVA_Wnt16_Litopenaeus_vannamei	*Wnt16*
L. vannamei	tr|A0A1L2A1N5|A0A1L2A1N5_LITVA_Wnt10_Litopenaeus_vannamei	*Wnt10*
L. vannamei	tr|A0A1L2A1P6|A0A1L2A1P6_LITVA_Wnt6_Litopenaeus_vannamei	*Wnt6*
B. anynana	bicyclus_anynana_BANY.1.2.t00712_1_Wnt-5a	*Wnt5*
B. anynana	bicyclus_anynana_BANY.1.2.t05290_1	*Wnt7*
B. anynana	bicyclus_anynana_BANY.1.2.t03758_1_Wnt-4	*Wnt1*
B. anynana	bicyclus_anynana_BANY.1.2.t03771_1_Wnt-10a	*Wnt10*
B. anynana	bicyclus_anynana_BANY.1.2.t03759_1_Wnt-2	*Wnt6*
B. anynana	bicyclus_anynana_BANY.1.2.t07631_1	*WntA*
B. anynana	bicyclus_anynana_BANY.1.2.t04594_1	*Wnt11*
S. maritima	tr|T1IJF2|T1IJF2_STRMM_Protein_Wnt_OS=Strigamia_maritima	*Wnt16*
S. maritima	tr|T1IPH0|T1IPH0_STRMM_Protein_Wnt_OS=Strigamia_maritima	*Wnt10*

S. maritima	tr|T1JI07|T1JI07_STRMM_Protein_Wnt_OS=Strigamia_maritima	*Wnt11*
S. maritima	tr|T1IPG8|T1IPG8_STRMM_Protein_Wnt_OS=Strigamia_maritima	*Wnt1*
S. maritima	tr|T1JPJ6|T1JPJ6_STRMM_Protein_Wnt_OS=Strigamia_maritima	*WntA*
S. maritima	tr|T1IPG9|T1IPG9_STRMM_Protein_Wnt_OS=Strigamia_maritima	*Wnt6*
S. maritima	tr|T1JL28|T1JL28_STRMM_Protein_Wnt_OS=Strigamia_maritima	*Wnt9*
S. maritima	tr|T1IT71|T1IT71_STRMM_Protein_Wnt_OS=Strigamia_maritima	*Wnt7*
S. maritima	tr|T1IJF2|T1IJF2_STRMM Protein Wnt OS=Strigamia maritima	*Wnt7*
S. maritima	tr|T1ITD0|T1ITD0_STRMM_Protein_Wnt_OS=Strigamia_maritima	*Wnt2*
S. maritima	tr|T1J4F4|T1J4F4_STRMM_Protein_Wnt_OS=Strigamia_maritima	*Wnt5*
S. maritima	tr|T1JIR6|T1JIR6_STRMM_Protein_Wnt_OS=Strigamia_maritima	*Wnt4*
H. dujardini	OQV25062.1 Protein Wnt-5b [Hypsibius dujardini]	*Wnt5*
H. dujardini	OQV22138.1 Protein Wnt-4 [Hypsibius dujardini]	*Wnt16*
H. dujardini	OQV21261.1 Protein Wnt-11 [Hypsibius dujardini]	*Wnt11*
H. dujardini	OQV20568.1 Protein Wnt-4 [Hypsibius dujardini]	*Wnt4*
H. dujardini	OQV19782.1 Protein Wnt-4 [Hypsibius dujardini]	*Wnt16*
H. dujardini	OQV17790.1 Protein Wnt-3a [Hypsibius dujardini]	*WntA*
H. dujardini	OQV11710.1 putative Protein Wnt-9a [Hypsibius dujardini]	*Wnt9*
H. dujardini	OWA52741.1 Protein Wnt-2 [Hypsibius dujardini]	*Wnt2*
I. scapularis	ISCW022384PA protein wingless, putative	*Wnt7*
I. scapularis	ISCW004707PA AmphiWnt4, putative	*Wnt11*
I. scapularis	Is_Wnt8	*Wnt8*
I. scapularis	Is_Wnt6	*Wnt6*
C. sculpturatus	CSCU004622-PA	*Wnt2*
C. sculpturatus	CSCU004625-PA	*Wnt16*
C. sculpturatus	CSCU018371-PA	*Wnt7*
C. sculpturatus	CSCU014631-PA	*WntA*
C. sculpturatus	CSCU004232-PA	*Wnt6*
C. sculpturatus	CSCU007733-PA	*Wnt6*
C. sculpturatus	CSCU011488-PA	*Wnt4*
C. sculpturatus	CSCU007735-PA	*Wnt1*
C. sculpturatus	CSCU004233-PA	*Wnt1*
C. sculpturatus	CSCU009514-PA	*Wnt11*
C. sculpturatus	CSCU007732-PA	*Wnt9*
C. sculpturatus	CSCU017121-PA	*Wnt11*
C. sculpturatus	CSCU014540-PA	*Wnt5*
C. sculpturatus	CSCU014543-PA	*Wnt7*
C. sculpturatus	CSCU014539-PA	*Wnt5*
C. sculpturatus	CSCU011489-PA	*Wnt4*
C. sculpturatus	CSCU004234-PA	*Wnt1*
C. sculpturatus	CSCU014538-PA	*Wnt5*
C. sculpturatus	CSCU007734-PA	*Wnt1*
C. sculpturatus	CSCU014541-PA	*Wnt7*
P. durmelii	Pd_Wnt11	*Wnt11*

P. durmelii	Pd_Wnt16	*Wnt16*
P. durmelii	Pd_Wnt2	*Wnt2*
P. durmelii	Pd_WntA	*WntA*
P. durmelii	Pd_Wnt1	*Wnt1*
P. durmelii	Pd_Wnt6	*Wnt6*
P. durmelii	Pd_Wnt5	*Wnt5*
P. durmelii	Pd_Wnt9	*Wnt9*
P. durmelii	Pd_Wnt8	*Wnt8*
P. hawaiensis	phaw_30_tra_m.012090	*Wnt1*
P. hawaiensis	phaw_30_tra_m.023054	*Wnt5*
P. hawaiensis	phaw_30_tra_m.022810	*Wnt10*
P. hawaiensis	phaw_30_tra_m.015031	*Wnt11*
P. hawaiensis	phaw_30_tra_m.021731	*Wnt16*
P. phalangoides	>c100839_g1_i1_3 len=1949	*Wnt2*
P. phalangoides	>c100246_g1_i3_3 len=1958	*Wnt5*
P. phalangoides	>c104722_g2_i2_2 len=3071	*Wnt4*
P. phalangoides	>c104855_g3_i1_2 len=1735	*Wnt1*
P. phalangoides	>c103422_g2_i1_3 len=1698	*Wnt7*
P. phalangoides	>c111004_g2_i1_4 len=4356	*Wnt16*
P. phalangoides	>c47853_g1_i2_3 len=1331	*Wnt7*
P. phalangoides	>c105403_g1_i2_1 len=5557	*WntA*
P. phalangoides	>c111740_g4_i1_2 len=2060	*Wnt6*
P. phalangoides	>c110869_g1_i1_2 len=2747	*Wnt11*
P. phalangoides	>c93728_g1_i2_4 len=1922	*Wnt8*
M. martensii	MMa37570	*Wnt2*
M. martensii	MMa45995	*Wnt5*
M. martensii	MMa00727	*Wnt16*
M. martensii	MMa04980	*Wnt7*
M. martensii	MMa13725	*Wnt1*
M. martensii	MMa47532	*WntA*
M. martensii	MMa40874	*Wnt6*
M. martensii	MMa16104	*Wnt4*
M. martensii	MMa52170	*Wnt11*
M. martensii	MMa40873	*Wnt9*
M. martensii	MMa16972	*Wnt11*
M. martensii	MMa42852	*Wnt7*
M. sexta	TCONS_00052657_2 XLOC_029656	*Wnt1*
M. sexta	TCONS_00052567_2 XLOC_029629	*Wnt6*
M. sexta	TCONS_00053691_1 XLOC_030097	*Wnt7*
M. sexta	TCONS_00029570_3 XLOC_018721	*WntA*
M. sexta	TCONS_00052659_3 XLOC_029657	*Wnt9*
M. sexta	TCONS_00036310_2 XLOC_021899	*Wnt11*

P. glaucus	papilio_glaucus_v1x1_core_32_85_1__cds__pgl185.18.mrna_1 Protein Wnt-5a OS=Homo sapiens GN=WNT5A PE=1 SV=2 [Source:UniProtKB/TrEMBL;Acc:P41221]	*Wnt5*
P. glaucus	papilio_glaucus_v1x1_core_32_85_1__cds__pgl3243.3.mrna_1 Protein Wnt-1 OS=Xenopus laevis GN=wnt1 PE=2 SV=1 [Source:UniProtKB/TrEMBL;Acc:P10108]	*Wnt1*
P. glaucus	papilio_glaucus_v1x1_core_32_85_1__cds__pgl3243.1.mrna_1 Protein Wnt-2 OS=Muntiacus muntjak GN=WNT2 PE=3 SV=1 [Source:UniProtKB/TrEMBL;Acc:Q09YJ6]	*Wnt6*
P. glaucus	papilio_glaucus_v1x1_core_32_85_1__cds__pgl501.3.mrna_1 Protein Wnt-1 OS=Danio rerio GN=wnt1 PE=2 SV=1 [Source:UniProtKB/TrEMBL;Acc:P24257]	*WntA*
P. glaucus	papilio_glaucus_v1x1_core_32_85_1__cds__pgl917.1.mrna_1 Protein Wnt-10a OS=Homo sapiens GN=WNT10A PE=1 SV=1 [Source:UniProtKB/TrEMBL;Acc:Q9GZT5]	*Wnt10*
P. glaucus	papilio_glaucus_v1x1_core_32_85_1__cds__pgl185.1.mrna_1 Protein Wnt-7a OS=Aotus trivirgatus GN=WNT7A PE=3 SV=1 [Source:UniProtKB/TrEMBL;Acc:Q1KYK4]	*Wnt7*
P. glaucus	papilio_glaucus_v1x1_core_32_85_1__cds__pgl3243.4.mrna_1 Protein Wnt-4 OS=Drosophila *melanogaster* GN=Wnt4 PE=2 SV=2 [Source:UniProtKB/TrEMBL;Acc:P40589]	*Wnt9*

Supplement Table S2.2 | All genome accession data for the phylogenetic analysis of Arthropods. Grey are species where the genome was used to find new Wnt genes species. Black are species that were used as reference sequences.

Species	**Trivial name**	**Genome Reference or BioProject Number NCBI genomes**
Acyrthosiphon pisum	Pea aphid	(Shigenobu *et al*., 2010)
Aethina tumida	Small hive beetle	PRJNA361278, PRJNA256171
Anopheles gambiae	Mosquito	(Holt *et al*., 2002)
Apis mellifera	Honeybee	(The Honeybee Genome Sequencing, 2006)
Bemisia tabaci	Silverleaf whitefly	PRJNA352527, PRJNA312470
Bicyclus anynana	Squinting bush brown butterfly	LepBase v4, 2017
Bombyx mori	Silkworm	International Silkworm genome consortium (2008)
Centruroides sculpturatus	Arizona bark scorpion	Kindly provided by Natascha Turetzek
Cimex lectularius	Bed bug	(Rosenfeld *et al*., 2016)
Daphnia pulex	Water flea	PRJNA12756
Diaphorina citri	Asian citrus psyllid	PRJNA251515, PRJNA29447
Drosophila melanogaster	Fruit fly	(Adams *et al*., 2000)
Dufourea novaeangliae	Pickerel Bee	PRJNA311229, PRJNA279825
Euperipatoides Kanangrensis	Velvet worm	(Hogvall *et al*., 2014)
Fopius arisanus	Braconid Parasitoid Wasp	PRJNA274979, PRJNA258104 (Geib *et al*., 2017)
Glomeris marginata	Pill millipede	(Janssen and Posnien, 2014)
Halyomorpha halys	Brown marmorated stink bug	PRJNA298780, PRJNA168118
Heliconius melpomene	Postman butterfly	LepBase v4, 2017
Homo sapiens	Human	(Venter *et al*., 2001)
Hypsibius dujardini	Water bear	(Boothby *et al*., 2015) PRJNA360553 (annotated genome from April 2017)
Ixodes scapularis	Head lice	PRJNA34667, PRJNA16232
Limulus Polyphemus	Horseshoe crab	(Nossa *et al*., 2014) (WGD)
Litoperiaenus vannamei	Whiteleg shrimp	(Kao *et al*., 2016)
Megachile rotundata	leafcutter bee	PRJNA87021, PRJNA66515
Nasonia vitripennis	Jewel wasp	PRJNA20073, PRJNA13660
Nicrophorus vespilloides	Burying beetle	PRJNA339573, PRJNA284849
Parasteatoda tepidariorum	Common house spider	PRJNA167405
Parhyale hawaiensis	Crustacean	(Kao *et al*., 2016) Transcriptomic data provided by Anastasios Pavlopoulos
Phalangium opilio	Harvestman	Provided by Prashant P. Sharma, Wisconsin, United States (unpublished data)
Polistes dominula	European paper wasp	PRJNA307991, PRJNA234105
Strigamia maritima	Centipede	PRJNA20501
Trachymyrmex zeteki	Fungus growing ant	PRJNA343251, PRJNA292628
Tribolium castaneum	Flour beetle	(Kim *et al*., 2010) PRJNA15718, PRJNA12540

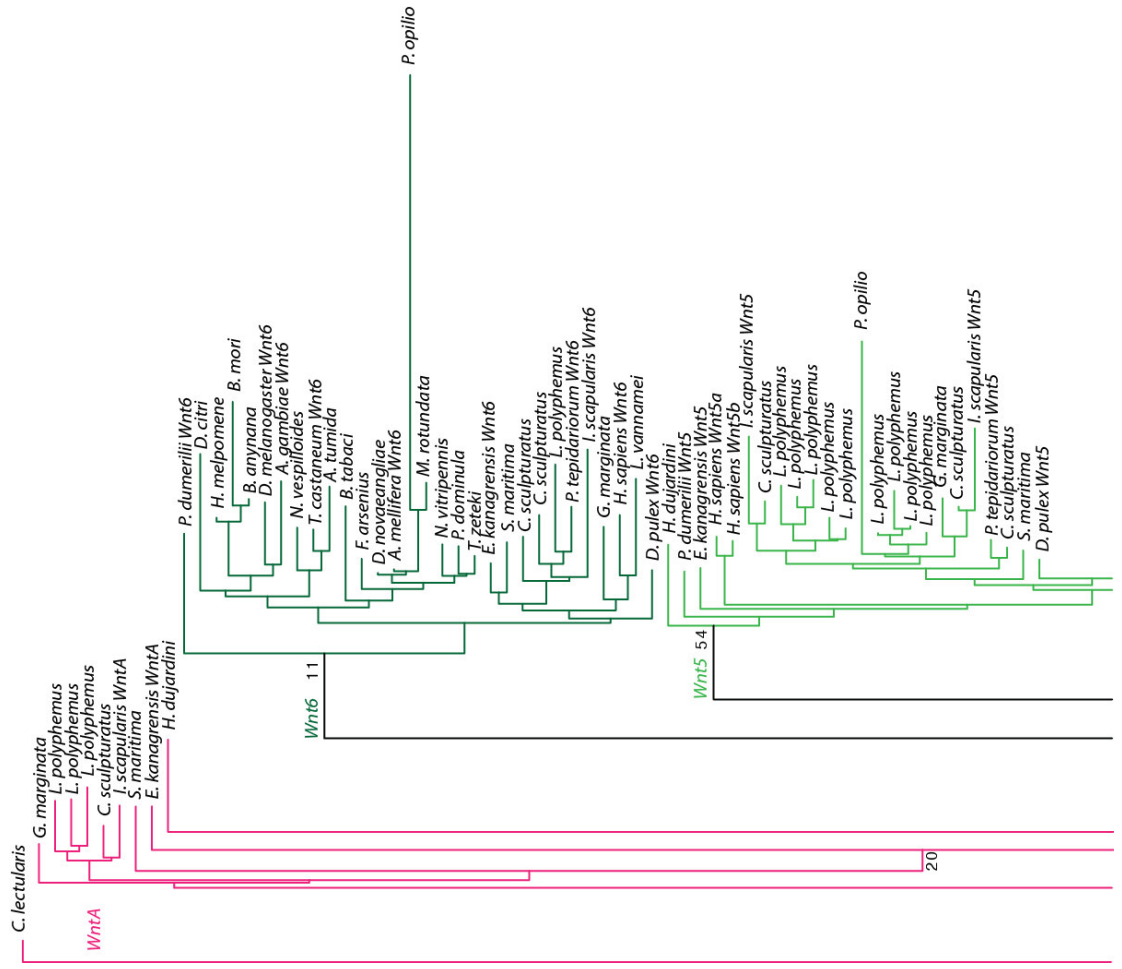
C. lectularis
G. marginata
L. polyphemus
L. polyphemus
L. polyphemus
C. sculpturatus
I. scapularis WntA
S. maritima
E. kanagrensis WntA
H. dujardini
WntA
20
P. dumerilii Wnt6
D. citri
H. melpomene
B. mori
B. anynana
D. melanogaster Wnt6
A. gambiae Wnt6
N. vespilloides
T. castaneum Wnt6
A. tumida
B. tabaci
F. arsenius
D. novaeangliae
A. mellifera Wnt6
M. rotundata
N. vitripennis
P. dominula
T. zeteki
E. kanagrensis Wnt6
S. maritima
C. sculpturatus
C. sculpturatus
L. polyphemus
P. tepidariorum Wnt6
I. scapularis Wnt6
G. marginata
H. sapiens Wnt6
L. vannamei
D. pulex Wnt6
H. dujardini
Wnt6 11
P. opilio
P. dumerilii Wnt5
E. kanagrensis Wnt5
H. sapiens Wnt5a
H. sapiens Wnt5b
I. scapularis Wnt5
C. sculpturatus
L. polyphemus
L. polyphemus
L. polyphemus
L. polyphemus
P. opilio
L. polyphemus
L. polyphemus
L. polyphemus
L. polyphemus
G. marginata
C. sculpturatus
I. scapularis Wnt5
P. tepidariorum Wnt5
C. sculpturatus
S. maritima
D. pulex Wnt5
Wnt5 54

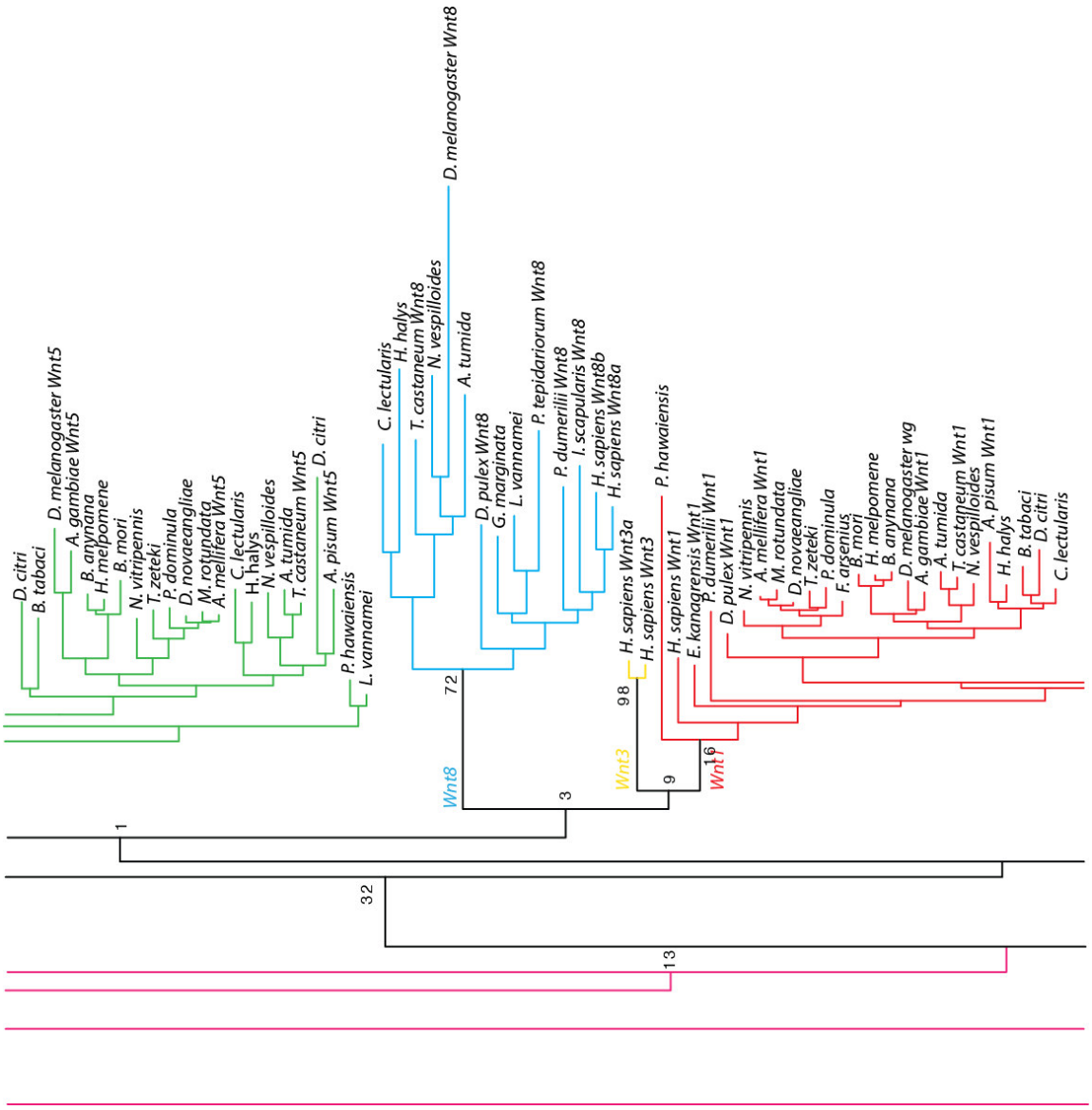
D. citri
B. tabaci
D. melanogaster Wnt5
A. gambiae Wnt5
B. anynana
H. melpomene
B. mori
N. vitripennis
T. zeteki
P. dominula
D. novaeangliae
M. rotundata
A. mellifera Wnt5
C. lectularis
H. halys
N. vespilloides
A. tumida
T. castaneum Wnt5
A. pisum Wnt5
D. citri
P. hawaiensis
L. vannamei
C. lectularis
H. halys
T. castaneum Wnt8
N. vespilloides
A. tumida
D. melanogaster Wnt8
D. pulex Wnt8
G. marginata
L. vannamei
P. tepidariorum Wnt8
P. dumerilii Wnt8
I. scapularis Wnt8
H. sapiens Wnt8b
H. sapiens Wnt8a
H. sapiens Wnt3a
H. sapiens Wnt3
P. hawaiensis
H. sapiens Wnt1
E. kanagrensis Wnt1
P. dumerilii Wnt1
D. pulex Wnt1
N. vitripennis
A. mellifera Wnt1
M. rotundata
D. novaeangliae
T. zeteki
P. dominula
F. arsenius
B. mori
H. melpomene
B. anynana
D. melanogaster wg
A. gambiae Wnt1
A. tumida
T. castaneum Wnt1
N. vespilloides
A. pisum Wnt1
H. halys
B. tabaci
D. citri
C. lectularis
72
98
16
3
9
1
32
13
Wnt8
Wnt3
Wnt1

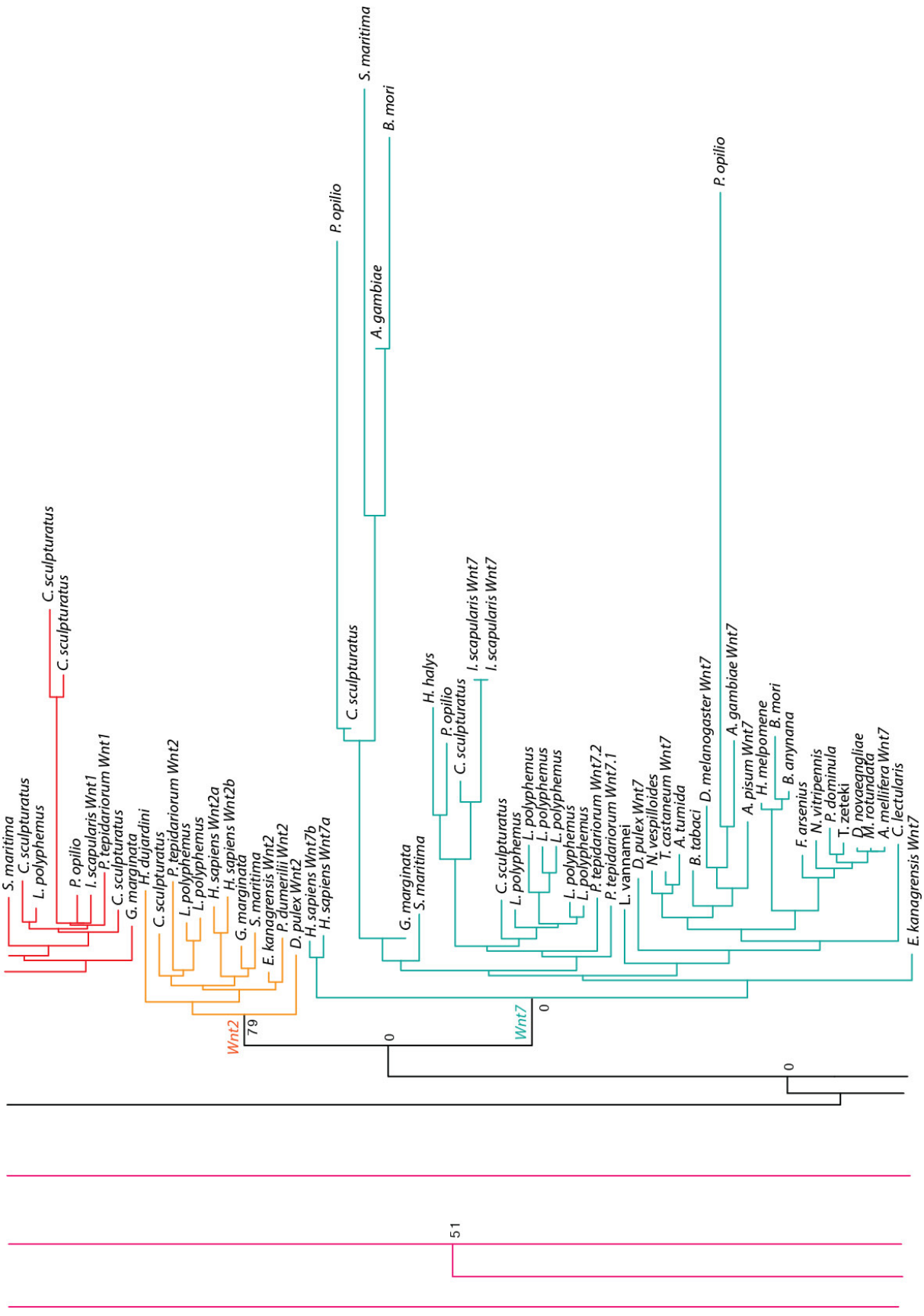
S. maritima
C. sculpturatus
L. polyphemus
P. opilio
I. scapularis Wnt1
P. tepidariorum Wnt1
C. sculpturatus
G. marginata
H. dujardini
C. sculpturatus
P. tepidariorum Wnt2
L. polyphemus
L. polyphemus
H. sapiens Wnt2a
H. sapiens Wnt2b
G. marginata
S. maritima
E. kanagrensis Wnt2
P. dumerilii Wnt2
D. pulex Wnt2
H. sapiens Wnt7b
H. sapiens Wnt7a
C. sculpturatus
C. sculpturatus
P. opilio
S. maritima
A. gambiae
B. mori
G. marginata
S. maritima
H. halys
P. opilio
C. sculpturatus
I. scapularis Wnt7
I. scapularis Wnt7
C. sculpturatus
L. polyphemus
L. polyphemus
L. polyphemus
L. polyphemus
L. polyphemus
P. tepidariorum Wnt7.2
P. tepidariorum Wnt7.1
L. vannamei
D. pulex Wnt7
N. vespilloides
T. castaneum Wnt7
A. tumida
B. tabaci
D. melanogaster Wnt7
P. opilio
A. gambiae Wnt7
A. pisum Wnt7
H. melpomene
B. mori
B. anynana
F. arsenius
N. vitripennis
P. dominula
T. zeteki
D. novaeangliae
M. rotundata
A. mellifera Wnt7
C. lectularis
E. kanagrensis Wnt7
Wnt2
79
Wnt7
0
0
0
51

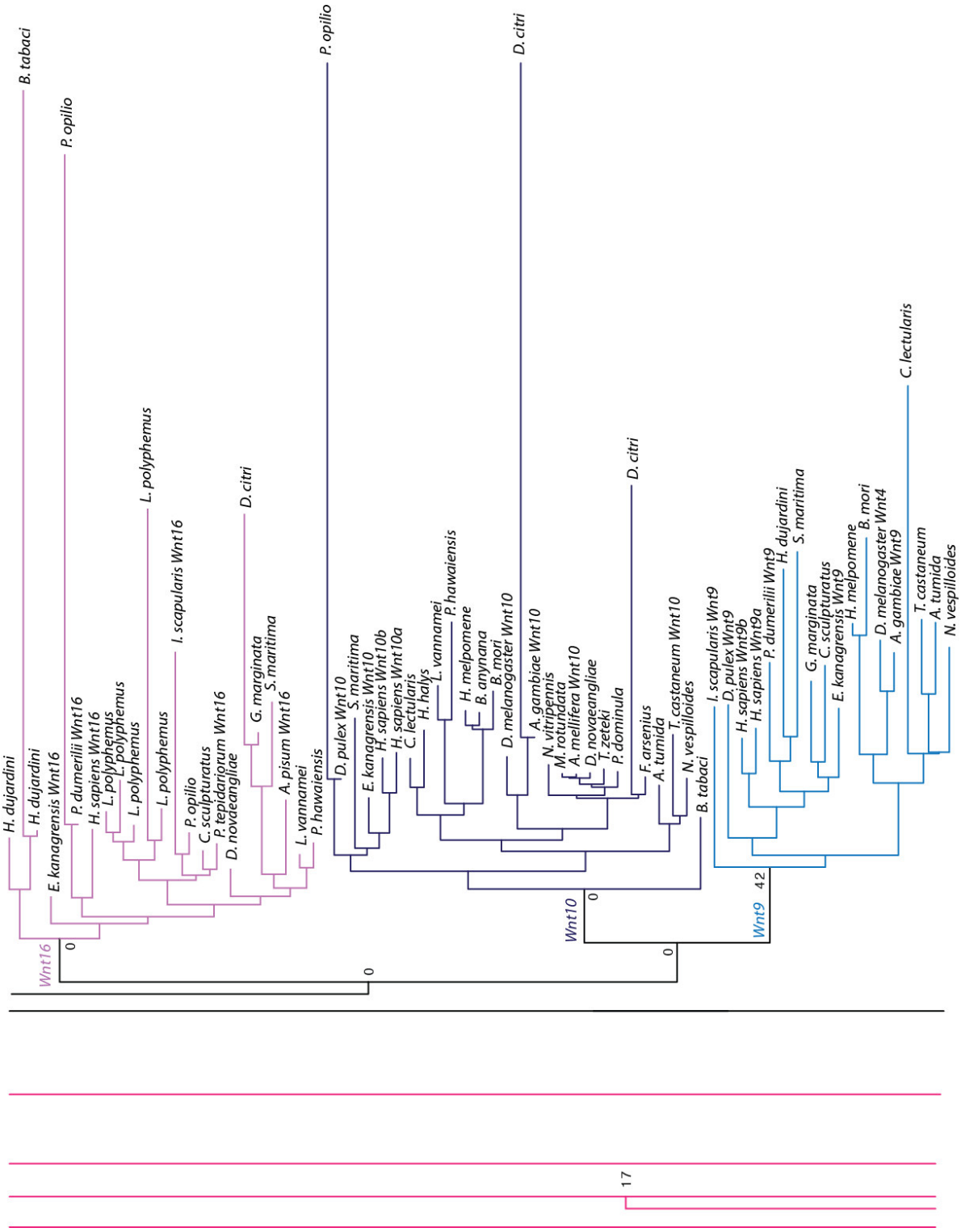
B. tabaci
P. opilio
H. dujardini
H. dujardini
E. kanagrensis Wnt16
P. dumerilii Wnt16
H. sapiens Wnt16
L. polyphemus
L. polyphemus
L. polyphemus
L. polyphemus
I. scapularis Wnt16
P. opilio
C. sculpturatus
P. tepidariorum Wnt16
D. novaeangliae
D. citri
G. marginata
S. maritima
A. pisum Wnt16
L. vannamei
P. hawaiensis
P. opilio
D. pulex Wnt10
S. maritima
E. kanagrensis Wnt10
H. sapiens Wnt10b
H. sapiens Wnt10a
C. lectularis
H. halys
L. vannamei
P. hawaiensis
H. melpomene
B. anynana
B. mori
D. melanogaster Wnt10
D. citri
A. gambiae Wnt10
N. vitripennis
M. rotundata
A. mellifera Wnt10
D. novaeangliae
T. zeteki
P. dominula
D. citri
F. arsenius
A. tumida
T. castaneum Wnt10
N. vespilloides
B. tabaci
I. scapularis Wnt9
D. pulex Wnt9
H. sapiens Wnt9b
H. sapiens Wnt9a
P. dumerilii Wnt9
H. dujardini
S. maritima
G. marginata
C. sculpturatus
E. kanagrensis Wnt9
H. melpomene
B. mori
D. melanogaster Wnt4
A. gambiae Wnt9
C. lectularis
T. castaneum
A. tumida
N. vespilloides
Wnt16
Wnt10
Wnt9
0
0
0
0
42
17

Supplement Figure S2.1 | Maximum likelihood tree of all analysed arthropod species. Protein substitution model VT, 1000 bootstrap replicates using RAxML.

Chapter 2

3 | Wnt gene expression during embryogenesis in *Bicyclus anynana*

3.1 | Background

In the previous chapter the Wnt repertoire in arthropod species was analysed to determine conservation and loss of Wnt genes. This provided new insights into Wnt repertoire evolution but for a more comprehensive understanding of evolutionary mechanisms it was necessary to analyse and compare their expression and potential function during development among arthropods. The function of most Wnt genes is well understood in the fruit fly *D. melanogaster* (Diptera) and to some extent in the flour beetle *T. castaneaum* (Coleoptera) but little is known about their roles in other insect orders such as Hemiptera, Hymenoptera and Lepidoptera. To address this, the Wnt gene expression was characterised, and thus their possible functionality in the sister group of Diptera and Coleoptera, the Lepidoptera. Here, a well-established model organism for developmental studies was used, *Bicyclus anynana* (Butler, 1879; Lepidoptera, Nymphalidae) (Figure 3.1).

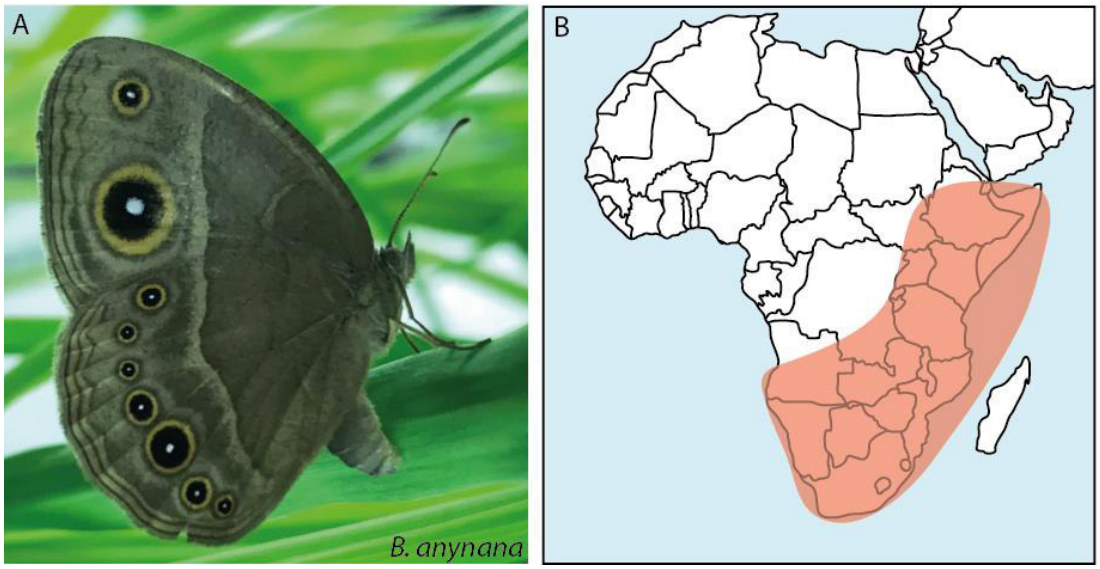

Figure 3.1 | The African butterfly *B. anynana* and its distribution. **(A)** Shown is a female specimen of *B. anynana* with the characteristic eyespots on its wings. Picture kindly provided by Dr. Casper Breuker **(B)** The distribution of *B. anynana* in Southeast Africa. This species can be found in several countries e.g. Kenya, Tanzania, Zambia, Malawi, Botswana and South Africa.

So far, analysis of Wnt gene expression was performed on developing wing discs from pupal stages but not during butterfly embryogenesis (Brakefield and French, 1999; Jiggins *et al*., 2017; Martin and Reed, 2014; Zhang *et al*., 2017). In this study, we aimed to understand the expression dynamics of all described Wnt genes in butterflies and compared this data with the published expression in *Drosophila* and *Tribolium* to

understand potential underlying conservation of expression domains or differences. Functional testing of all butterfly Wnts would be needed for further analysis and comparison to understand how function might be able to influence the evolutionary fate of Wnt genes in insects.

3.1.1 Embryogenesis in Lepidoptera

Lepidoptera were considered to have intermediate germ band development, because they showed characteristics of both, short and long germ band development and were therefore first described as "unclassifiable" (Carter *et al*., 2013; Krause, 1939; Krause and Krause, 1964; Sander, 1983). Short germ band development was characterized by the formation of a small, and therefore a short blastoderm, consistent of head and gnathal structures, which was followed by a growth zone that was adding segment after segment. Long germ band insects, such as *Drosophila* form larger blastoderms with more structures including head, thoracic and abdominal segments which were patterned simultaneously. Lepidoptera showed a short blastoderm first but increased rapidly in size before patterning takes place, therefore showing no typical characteristics of neither short nor long germ bands (Carter *et al*., 2013; Krause, 1939; Krause and Krause, 1964; Sander, 1983). While studying embryogenesis among several different insects, it had been shown that numerous variations of these classifications exist (summarised in Davis and Patel (2002)).

Among lepidopterans, embryogenesis had been described for *Bombyx mori* (Krause and Krause, 1964; Miya, 2003), *Manduca sexta* (Broadie *et al*., 1991; Dow *et al*., 1988), *Endoclyta signifier* (Ando and Tanaka, 1980) and *Eriocrania sp* (Kobayashi and Ando, 1990), which were all different moths species, however descriptions for butterflies were rare and incomplete (Masci and Monteiro, 2005). In the following part a brief overview of what is known about lepidopteran embryogenesis based on descriptions from the silk moth *B. mori* is given (Krause and Krause, 1964; Miya, 2003; Ueno, 1995).

The germ disc of *B. mori* was formed within the first hours after egg lay (AEL) and increases in size until it spanned two thirds of the egg surface. The germ disc elongated,

which could be seen as the transition from the germ disc to the germ band. The protocephalon (head structure) and the gnathal segments form around this stage. In the medial and posterior regions of the germ band, cells proliferated. During the next stage, the edges of the germ band rolled inwards and the determination of the embryonic layers (ectoderm and mesoderm) happened soon afterwards while the germ band elongated, narrowed, and started segment formation. Around three days AEL, the now fully patterned embryo became shorter and the abdominal appendages developed on the ventral side of the embryo (facing distally). The embryo started to reverse its position in the egg, a process called blastokinesis or embryo revolution (reviewed in Panfilio (2008)). Dorsal closure happened around four days AEL. After dorsal closure, internal development took place and the tissues and organs were formed. The embryonic development was completed around 10 days AEL and the first instar larva hatched from the egg.

For the purpose of the presented study, it was necessary to actually analyse the embryogenesis of butterflies and compare with previous knowledge from moths. This will help to stage the embryos used for Wnt expression and compare them to expression patterns from other insects at a similar developmental stage.

3.1.2 Wnt genes in lepidopteran development

In derived lepidopterans, the Ditrysia, Wnt gene expression during embryogenesis had only been studied for *Wnt1* in the moths *B. mori* and *M. sexta* (Broadie *et al*., 1991; Dow *et al*., 1988; Krause and Krause, 1964; Miya, 2003). *Wnt1* expression patterns appeared consistent with the conserved segment polarity role of this gene during arthropod embryogenesis (Dhawan and Gopinathan, 2003; Kraft and Jäckle, 1994; Nakao, 2010). Furthermore, *Wnt1* had subsequently been functionally tested in *B. mori* using CRISPR/Cas9 knockout strategy (Zhang *et al*., 2015). Those mutants that were analysed showed loss of *Wnt1* dependent segmentation defects and altered pigmentation when reaching adult hood (Zhang *et al*., 2015).

Seven Wnt genes from seven different subfamilies were previously described for the butterfly *Heliconius melpomene* (Martin *et al*., 2012) and their expression was shown in larval wing discs. Here, only expression for *Wnt1*, 6, 10 and A was detected during wing development (Martin and Reed, 2014). *Wnt1* and *WntA* function during

wing development had been studied in butterflies, while the function of all other Wnts in wing development or embryogenesis remained unresolved (Carroll *et al*., 1994; Macdonald *et al*., 2010; Martin and Reed, 2014). *WntA* for example, was a potential underlying main regulator of the so called symmetry systems in the wing colour patterning (Martin *et al*., 2012; Martin and Reed, 2014) and *Wnt1* which also was involved in wing colour patterning but also seems to play a role in wing margin determination (Macdonald *et al*., 2010). Several studies have shown, that Wnt signalling was very important in the development and potentially in the evolution of lepidopterans. Therefore, understanding the role of Wnts during embryogenesis would contribute to reveal mechanisms of evolution in lepidopterans and comparison with other insect species might help to imply an evolutionary role of Wnts in a broader context.

3.1.3 Aims

In the previous chapter, it was possible to confirm the presence of seven published Wnt genes in *Heliconius* but also an 8th Wnt gene was detected in *B. anynana*. Here, a Wnt gene from the *Wnt11* subfamily was found which was also present in both analysed moth species (see Chapter 1). Therefore, we propose, that a main core of at least eight Wnt genes was present in lepidopterans, whereas some subfamilies could be lost lineage specific. As part of the Wnt expression analysis in this Chapter it will be possible to confirm if a *Wnt11* was present and maybe even expressed during embryogenesis in *B. anynana*. Further, the embryonic development of the butterfly *B. anynana* will be analysed in detail, to be able to stage embryos from *in situ* experiments and compare expression patterns with known Wnt expression in other species, such as *Drosophila* and *Tribolium*.

This analysis will provide a first step into understanding the underlying mechanisms of Wnt gene evolution in insect species. Further functional testing of the Wnt genes during development will be needed, but this analysis will provide the necessary background for these future studies.

3.3 | Methods

Animal husbandry

Bicyclus anynana stocks were kept in netted cages under controlled temperature, light and humidity (26°C; RH 70%; LD: 12:12 with dawn and dusk transition times). A stock for the current study was established with eggs from a large outbred stock kindly provided by Oskar Brattstrom (University of Cambridge). A fresh potted host plant (*Brachypodium sylvaticum*) was provided for egg deposition. Eggs for the embryonic staging were collected for every hour starting at 1 h AEL and ending at 51 h. Embryos from these collections were also used for *in situ* hybridisations and RNA extractions. Embryos and eggs were fixed according to Brakefield *et al*. (2009) and stored in 100% methanol at -20°C.

In situ *hybridisation*

For whole mount *in situ* hybridisation, the published protocol for *Pararge aegeria* (Ferguson *et al*., 2014) was used with minor modifications. Ribonucleotide probes were generated from cDNA reverse transcribed RNA of mixed embryonic stages (0-72h) (See Primer list and size of probes in Supplement Table S2.1). RNA was extracted using QIAzol reagent (Quiagen) and reverse transcribed using Quantitect Reverse transcription kit (Quiagen) into cDNA. Embryos were rehydrated from 100% methanol to 100% PBS-T (137 mM NaCl, 2.7 mM KCl, 4.3 mM Na_2HPO_4 $2H_2O$ and 1.47 mM KH_2PO_4 plus 0.1% Tween20), digested with Proteinase K and briefly fixed for 20 minutes in 4% formaldehyde. Afterwards, embryos were hybridised at 56°C overnight with the probe (Hybridisation buffer with 25 ml formamide, 12.5 ml 20x SSC pH 7.0, 1 ml salmon sperm (10 mg/ml), 250 µl tRNA (20 mg/ml), 25 µl heparin (100 mg/ml) and 0.1% Tween 20, adjust pH 6.5 with 1M HCl). The next day embryos were brought back to PBS-T and incubated with the Anti-Fab AP Fragment antibody (Roche) in 1x blocking reagent (Roche). After washing in PBS-T overnight, embryos were stained using NBT/BCIP (Roche) in the AP staining buffer (100 mM NaCl, 50 mM $MgCl_2$, 100 mM Tris HCl pH 9.5 and 0.1% Tween 20). Staining was stopped by several washes with PBS-T and additionally stained with 4',6-diamidino-2-phenylindole (DAPI) for 30 minutes. Embryos were kept in PBS or mounted in 80% glycerol. All images were taken using an Axio Zoom.V16 microscope with an Axiocam 506 colour camera (Zeiss, Germany).

3.4 | Results and discussion

3.4.1 *Bicyclus anynana* embryogenesis

The descriptions of the embryonic stages and morphology in the following section are based on (Kobayashi and Ando, 1990; Krause and Krause, 1964; Miya, 2003). The determination of the completion rate of development is based on Dorn *et al*. (1987).

4-8 h AEL (0-10% development completed)

The freshly laid egg was syncytial with the energids distributed throughout the egg and no clear structures detectable (4 h AEL; Figure 3.2 A). Subsequently, the energids started to move to the egg surface where they cellularised and formed the blastoderm (5 h AEL; Figure 3.2 B). The blastoderm will form the germ disc and the remaining, so called extraembryonic blastoderm will form later the serosal tissue. The early development was similar to the previously described developmental course in *B. mori* (Kobayashi and Ando, 1990; Krause and Krause, 1964; Miya, 2003).

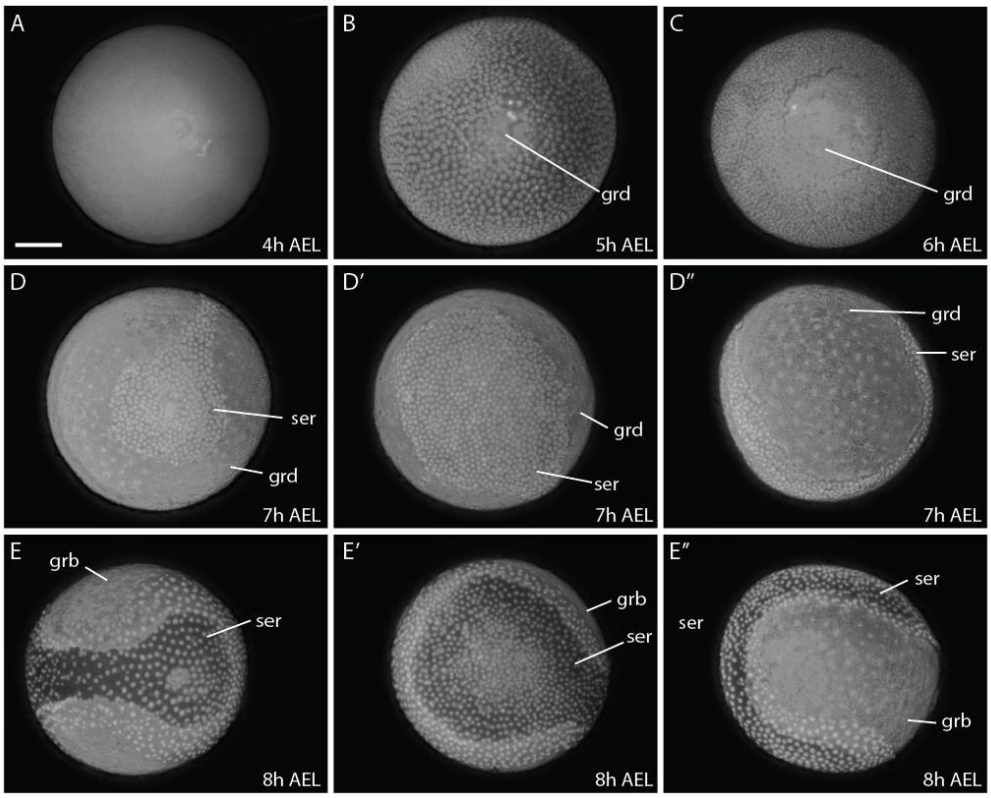

Figure 3.2 | Early developmental stages of *B. anynana* from 4 to 8 hours. The germ disc starts to form around 5 h AEL **(A and B)**, expands at 6 h AEL **(C)** and starts forming the germ band at around 8 h AEL **(D and E)**. See detailed descriptions in the main text. All eggs are stained with DAPI. AEL: after egg lay; grd: germ disc; grb: germ band; ser: serosa. All pictures to the same scale. Scale 400 µm.

The germ disc was enlarged around 6 to 7 h AEL and covered more than two thirds of the egg surface (Figure 3.2 C-D''). From here, the germ disc elongated and transformed into the germ band (8 h AEL; Figure 3.2 E-E''). Less of the egg surface was now covered by the embryonic tissue and it could be seen that the serosa was formed on the remaining surface and started to overgrow the embryonic tissue. Later, the serosa will envelope the whole egg (data not shown).

9-14h AEL (10-15 % development completed)

At 9 to 10 h AEL, the margins of the germ band started curling inwards (Figure 3.3 A-B''). This process indicated the start of the formation of the germ layers and the ectoderm and mesoderm started differentiating (Krause and Krause, 1964). The patterning of the germ band started at the anterior where at first, the protocephalon became visible. The primitive grove invaginated along the midline from anterior to posterior - the grove was deep at the anterior and it was shallower at the posterior end. Around this time, the first gnathal segments were detectable (11 h AEL; Figure 3.3 C-C''). The stomodeum, an invagination between the brain and the following gnathal segments became visible and will form the future mouth region (Figure 3.3 C'').

Within the next three hours all gnathal and thoracic segments were determined (12-14 h AEL; Figure 3.3 D-E'') and thus the protocephalon was followed by the mandibular, maxillary and labial segments. The primitive groove developed into the neurogenic furrow (12 h AEL; Figure 3.3 D-D''), while the terminal region, the telson, differentiated and submerged into the yolk (14 h AEL; Figure 3.3 E-E''). At 14 h AEL, tissue for the abdominal segments started formation as well as a terminal segment, the telson. This tissue was still not completely differentiated, and no separated segments were visible yet.

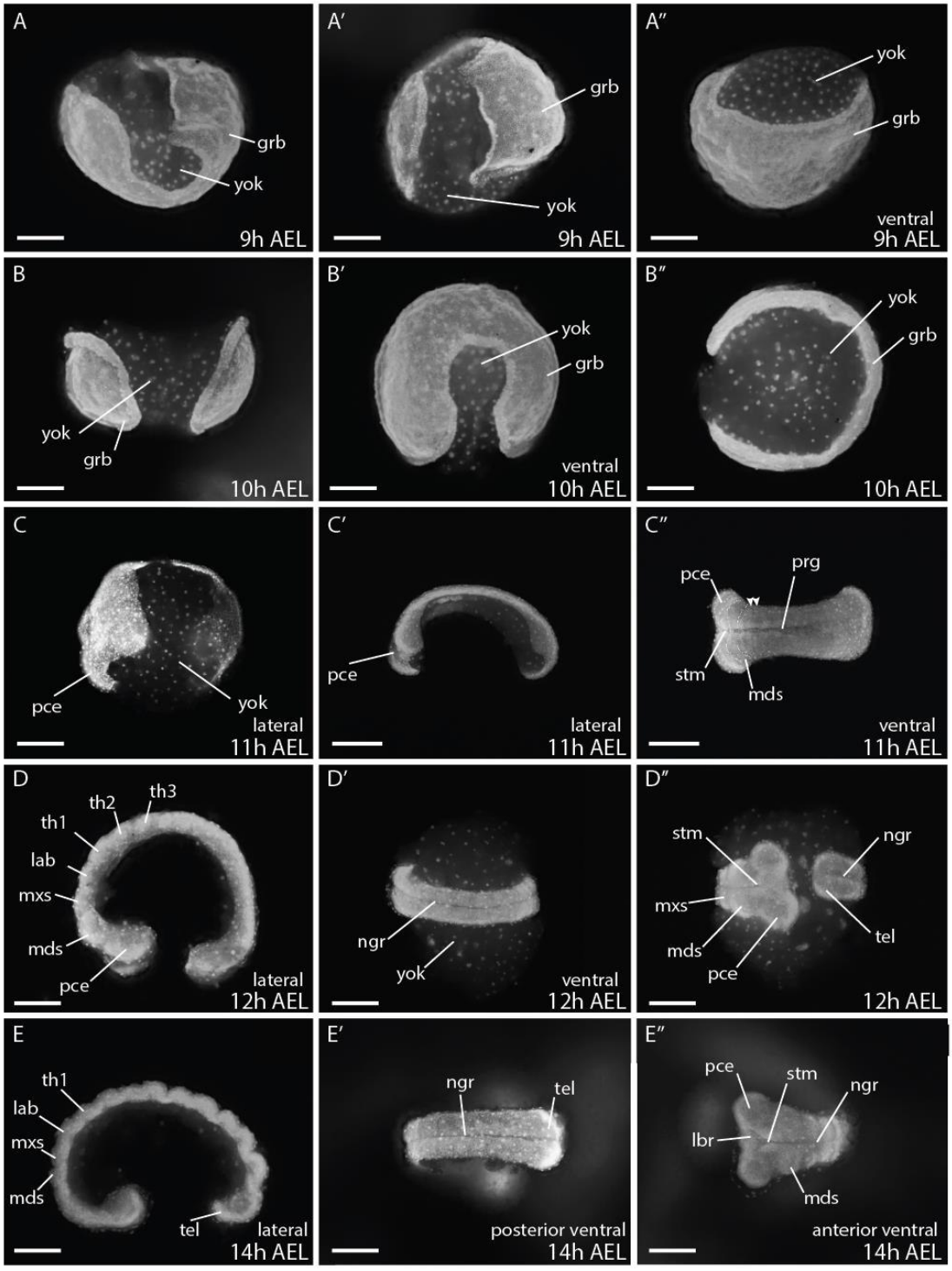

Figure 3.3 | Embryonic stages of *B. anynana* from 9 to 14 h AEL. During this time the germ band develops into a basic patterned embryo with all gnathal, thoracic and abdominal segments as well as a defined terminal segment, the telson. Detailed description in the text. AEL: after egg lay; grb: germ band; yok: yolk; pce: protocephalon; pco: protocorm; prg: primitive grove; stm: stomodeum; mds: mandibular segment; mxs: maxillary segment; lab: labial segment; th1-3: thoracic segment 1-3; ngr: neurogenic furrow; tel: telson; lbr: labrum. Orientation of pictures is indicated if possible. Anterior is always orientated towards left. Scale 400 µm.

16-28 h AEL (20-30% development completed)

The differentiation of the abdominal segments occurred rapidly between 14 h AEL (Figure 3.3 E-E'') and 18 h AEL (Figure 3.4 A-B''). At 20 h AEL, all ten abdominal segments were formed and therewith the whole body of *B. anynana* was determined along the anterior-posterior axis (Figure 3.4 C). Further differentiation and outgrowth of the gnathal segments started around 18 h AEL where mandibular and maxillary segments became pronounced, the head lobes were enlarging, the labrum and antennal rudiments became visible (Figure 3.4 A-C'').

Between 24 to 28 h AEL, head structures continued to differentiate, and the prothoracic appendages elongated while the abdominal proleg buds became visible (Figure 3.4 D-F''). Patterning of the prothoracic legs was accomplished around 28 h AEL (Figure 3.4 E-F''). At this stage the telson was still buried in the yolk and not fully extended (Figure 3.4 F-F'').

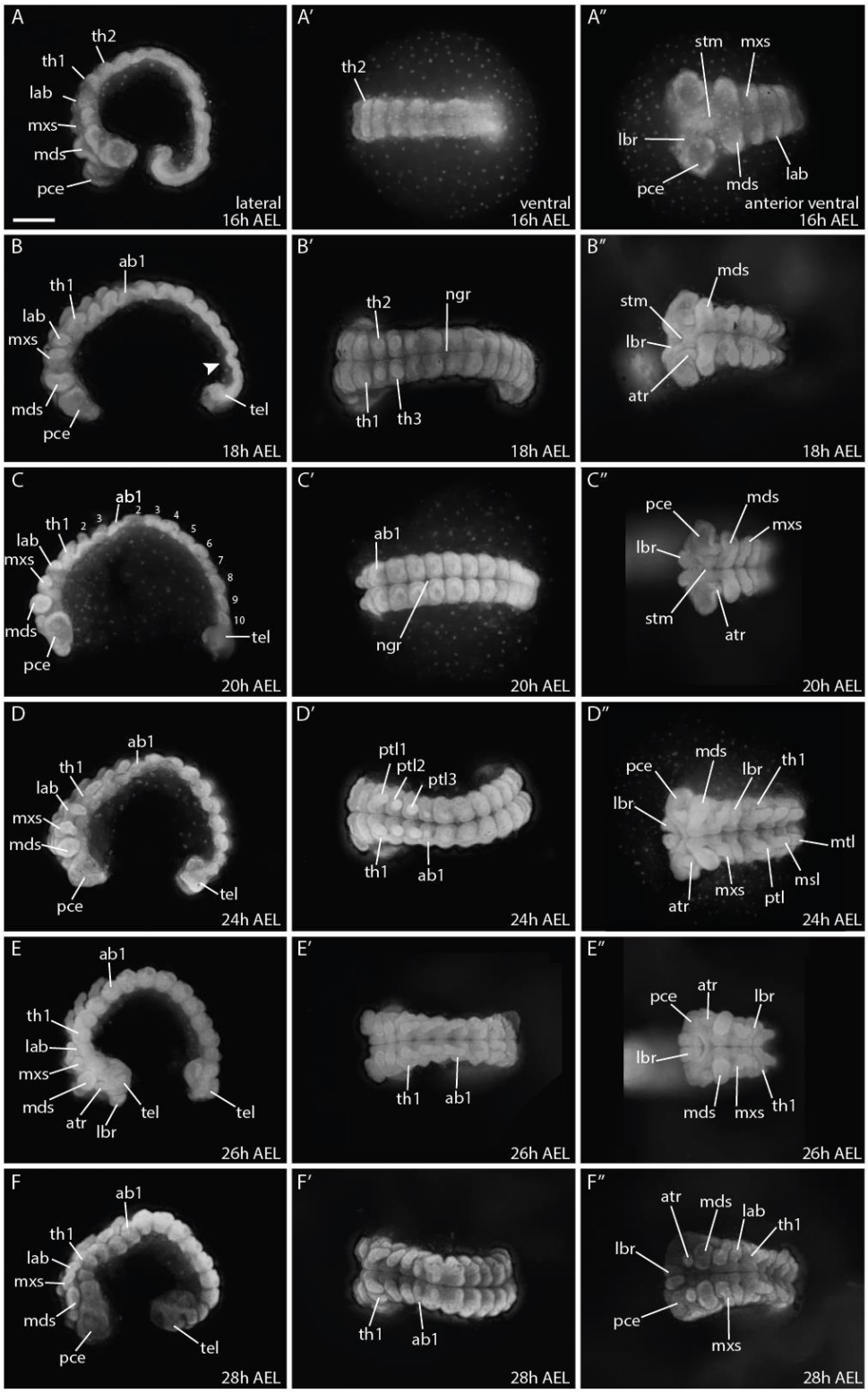

Figure 3.4 | Embryonic development from 16 to 28 hours in *B. anynana*. Detailed description in the text. AEL: after egg lay; ab1: abdominal segment 1; atr: antennal rudiment; ptl: prothoracic leg 1-3; pce: protocephalon; pco: protocorm; stm: stomodeum; mds: mandibular segment; mxs: maxillary segment; lab: labial segment; th1: thoracic segment; tel: telson; lbr: labrum. All columns are orientated in the same way, indicated in the top row. Anterior is always to the left and the ventral side is to the top. All pictures are to the same scale. Scale bar: 400 µm.

30-51 h AEL (35-50 % development completed)

Between 30 and 36 h AEL the embryo became compressed and thickened. The head structures continued to differentiate and became integrated in the protocephalon (Figure 3.5 A-B''). Around 42 h AEL, the embryonic reversion (blastokinesis) started from the posterior end of the embryo. During this process the whole embryo rotated around its own axis and ended up with the ventral side pointing proximal at around 51 h AEL (Figure 3.5 C-F''). Figure 3.5 D showed an embryo with the characteristic S-shape of this movement. After the full rotation of the embryo, the dorsal side was facing distally. However, the dorsal opening was not yet closed, and the embryo was still incorporated with the yolk via this opening (around 44 h AEL; arrowheads) (Krause, 1939). At 48 h AEL, the dorsal opening became smaller (Figure 3.5 E) and only a small amount of yolk remained attached to the embryo (Figure 3.5 E'; asterisks). Full dorsal closure happened around 51 h AEL (Figure 3.5 F-F'').

At around 48h AEL, and after blastokinesis, the more angled head shape had developed including all gnathal appendages. Subsequently, the embryo was growing and developing internal organs. Since this whole staging was performed to analyse Wnt gene expression during embryogenesis, this staging was not extended beyond 50% of developmental time (51 h AEL) (Broadie *et al*., 1991; Dorn *et al*., 1987).

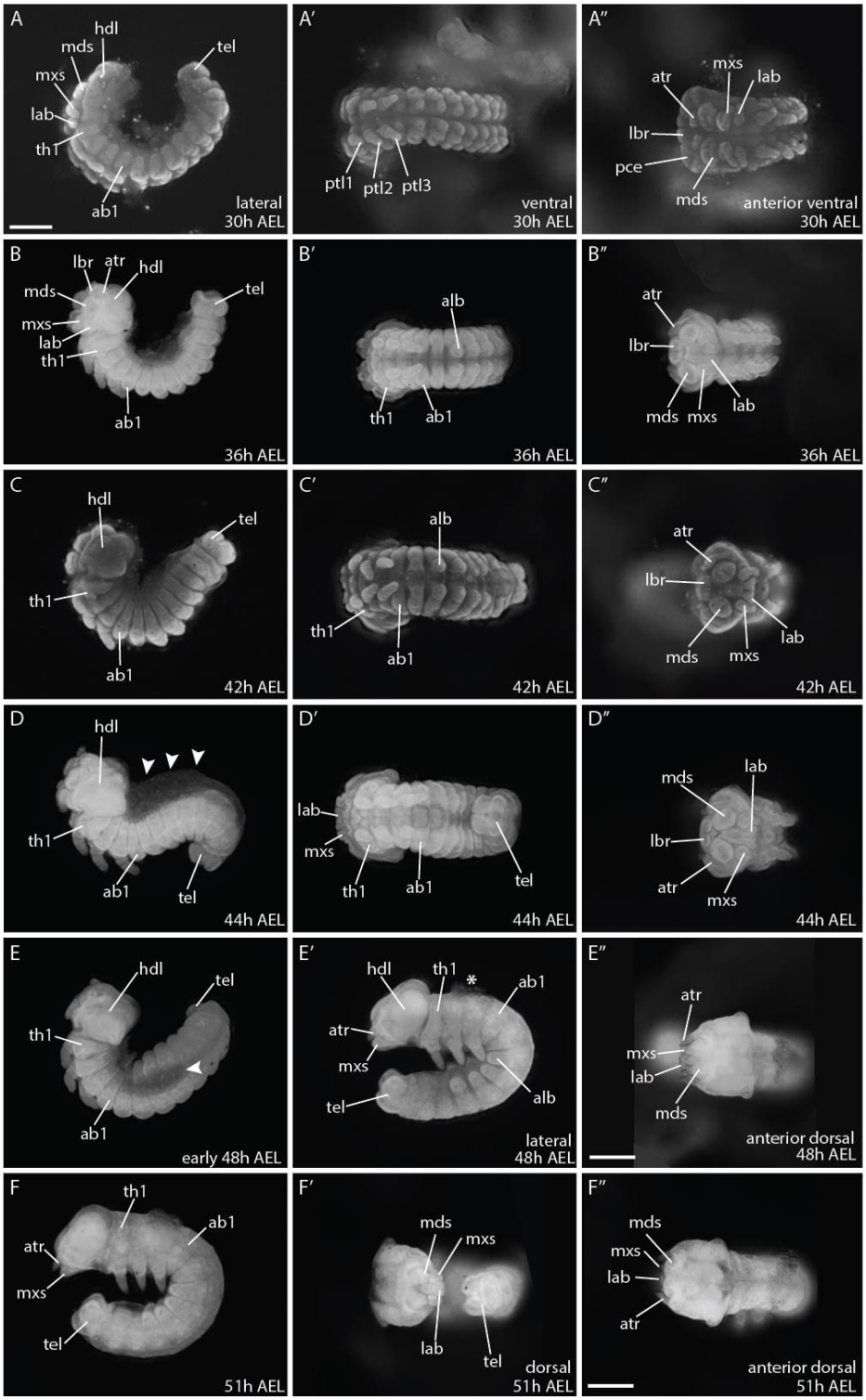

Figure 3.5 | Developmental stages of *B. anynana* from 30 to 51 hours. See detailed description in text. AEL: after egg lay; ab1: abdominal segment 1; atr: antennal rudiment; ptl: protoracic leg 1-3; pce: protocephalon; pco: protocorm; prg: primitive grove; stm: stomodeum; mds: mandibular segment; mxs: maxillary segment; lab: labial segment; th1: thoracic segment; tel: telson; lbr: labrum; alb: abdominal limb bud; hdl: head lobe. All pictures are orientated with anterior to the left and the dorsal side to the top, indicated also in the top row for each column if not other stated. All pictures are to the same scale indicated in A (scale bar = 400 µm.), except E'' and F'' which have individual scale bars, also 400 µm.

Overall, the embryonic development of *B. anynana* proceeded similar to previously described lepidopteran species, such as *B. mori* or *M. sexta* (Broadie *et al*., 1991; Krause, 1939; Krause and Krause, 1964). To study the expression of Wnt genes (*Wnt1, 5, 6, 7, 9, 10, 11* and *A*) I focussed on 9 to 28 hours AEL because this is the period during which the segments were formed and patterned along the axes. The exact embryonic staging allowed a comparison of Wnt gene expression in the complementary stages in other insect species (e.g. (Bolognesi *et al*., 2008; Martin and Kimelman, 2012; Oberhofer *et al*., 2014).

3.4.2 Expression of Wnt genes during butterfly embryogenesis

Wnt1/wingless

In situ hybridisations in *B. anynana* showed expression of *wg* in very thin and faint stripes at the anterior margin of the germ disc at 9 h AEL (Figure 3.6 A and A' (DAPI staining and indication of morphology); see arrowheads). This expression was the earliest observed in all experiments. As soon as the germ band was formed and head lobes, gnathal and thoracic segments were visible, segmental stripe expression was observed in all formed segments (indicated by an arrowhead) and in the head lobes (asterisks) (Figure 3.6 B; 10 h AEL). The previously described expression patterns in moths were similar to the segmental stripes detected in the butterfly *B. anynana*. In the moth species *B. mori* and *M. sexta* (Dhawan and Gopinathan, 2003; Kraft and Jäckle, 1994; Nakao, 2010; Zhang *et al*., 2015), expression was described early in embryogenesis in medial stripes, at the anterior and posterior ends of the embryo and was seen in stripes concomitant with the formation of the first segments (gnathal and thoracic) (Kraft and Jäckle, 1994; Nakao, 2010). Two broader domains were observed in the anterior head lobes, which were also observed previously for the moth species (Figure 3.6 B and C; asterisks). At 16 h AEL, when all segments were formed, expression in all anterior compartments of the segments was observed, which was consistent with the segment polarity role of *wg* in *B. mori, M. sexta, D. melanogaster* and *T. castaneum* (Figure 3.6 E; indicating expression in mandibular segment with arrowhead; also start of thoracis and abdominal segments were marked) (Bolognesi *et al*., 2008; Kraft and Jäckle, 1994; Nakao, 2010; Nusslein-Volhard *et al*., 1984).

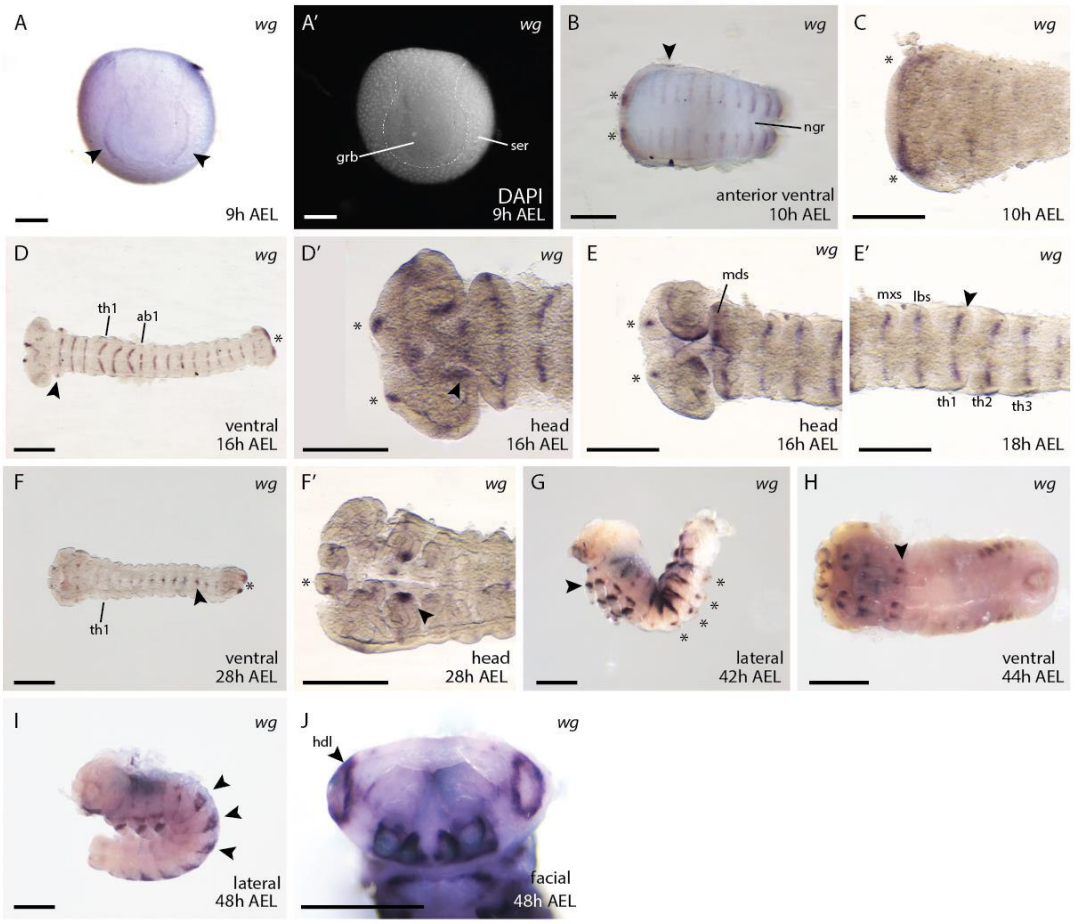

Figure 3.6 | *Wnt1/wg* expression during embryogenesis in *B. anynana*. **(A and A')** Early expression of *wg* at the anterior rim of the germ disc. **(B)** Expression in segmental stripes at 10 h AEL. **(C)** Higher magnification of the head region around 10 h AEL. **(D)** Segmental expression of *wg* at 16 h AEL. **(D')** Higher magnification of 16h AEL. **(E)** Expression in the head at a similar stage around 16 h AEL. **(E')** Higher magnification of the segmental stripes in the anterior compartment of the forming segments. **(F)** Expression at 28 h AEL **(F')** Expression in the distal parts of the antennae (asterisks) and the mandibular segments (arrowhead). **(G)** *wg* expression at 42 h AEL. **(H)** Expression in two domains on the thoracic legs (arrowhead). **(I)** Expression pattern around 48 h AEL. **(J)** Anterior view showing expression in the head lobes, mandibular, maxillary and labial segments. All pictures are orientated with anterior to the left if not otherwise stated. H: hour; AEL: after egg lay; grb: germ band; hdl: head lobe; ser: serosa; ngr: neurogenic furrow; lbs: labial segments; th1-3: thoracic segments 1-3; ab1-3: abdominal segments 1-3; mds: mandibular segments; mxs: maxillary segments. Scale bar: 400 µm.

Expression in the embryonic head was observed in the most anterior part of the head lobes (asterisks), and around the stomodeum (Figure 3.6 D-E'') as well as two distinct dots were observed in the telson (Figure 3.6 D, asterisk). During subsequent development the expression of *wg* in the segments was reduced and became concentrated on the neuronal furrow along the A-P axis (Figure 3.6 F, asterisk). Strong

spots of expression could be seen in the tips of the mandibular segments (Figure 3.6 F'; arrowhead) as well as in the distal parts of the antennal rudiments (Figure 3.6 F'; arrowhead). During very late developmental stages around 42 to 48 h AEL, *wg* could be detected in two separate domains in the thoracic legs (Figure 3.6 G and H; arrowheads), as well as dot-like expression in the abdominal limb buds (Figure 3.6 G; asterisks). Expression could also be seen on the dorsal side in stripes (Figure 3.6 I, arrowheads) and further analyses would be necessary to understand exactly in which tissue this expression was located. At 48 h AEL, expression in the head lobes (arrowhead), maxillary lobes and the labium was observed (Figure 3.6 I'). Overall, the newly detected expression of *wg* during *B. anynana* embryogenesis was as expected and was consistent with *wg* expression in moths and other arthropods at similar developmental stages: *wg* had an early role of determining the body axis and the segment boundaries, while it also had a later function where it was involved in patterning the head and appendages.

Wnt5* and *Wnt6

No embryonic expression was observed for *Wnt5* or *Wnt6* by means of *in situ* hybridisation in *B. anynana* embryos (see Supplement Figure S3.1). *Wnt5* was expressed in the nervous system in other arthropods such as *Drosophila* (Fradkin *et al*., 1995; Fradkin *et al*., 2004) and *Tribolium* (Bolognesi *et al*., 2008). Therefore, it could be possible, that *Wnt5* was expressed during development but not at the stages which were analysed here. It was possible to extract Wnt5 sequence from a pool extracted RNA from different embryonic and larval stages, therefore it might be expressed at a later time point, but not during early embryogenesis in *B. anynana*.

Wnt6 was expressed in a *wg* pattern in *Tribolium* which was not observed here (Bolognesi *et al.* 2008) but interestingly, it was also not expressed during embryonic stages in *D. melanogaster* (Janson *et al*., 2001). Here, only later in larval tissues, expression of *Wnt6* was overlapping with *wg*, which could also be seen in butterfly wing discs (Martin *et al*., 2012; Martin and Reed, 2014). As well as for *Wnt5*, it was possible to extract *Wnt6* from an RNA pool of embryonic and larval tissue and therefore a later role in development was assumed. For both genes, different *in situ* probes were tested when possible, but none of the additional probes gave any signal (see Supplement Table S3.1).

Wnt7

In *B. anynana* embryos, *Wnt7* expression was detected from around 16 h AEL in each of the segments in lateral "dots" (Figure 3.7 A-C; asterisks). This included the three thoracis (th1-3) and all ten abdominal (ab1-10) segments (Figure 3.7 B). No expression could be seen in the maxillary, mandibular or labial segments but faint expression was detected in the head lobes of the embryo (Figure 3.7 B and C). In *Drosophila* and *Tribolium*, *Wnt7* was expressed in mesodermal cells (Bolognesi *et al*., 2008; Kozopas *et al*., 1998) and in *Tribolium* also in the CNS (Bolognesi *et al*., 2008). It could be possible that the *Wnt7* "dots" were corresponding to the nervous system nodes in each developing segment in butterflies.

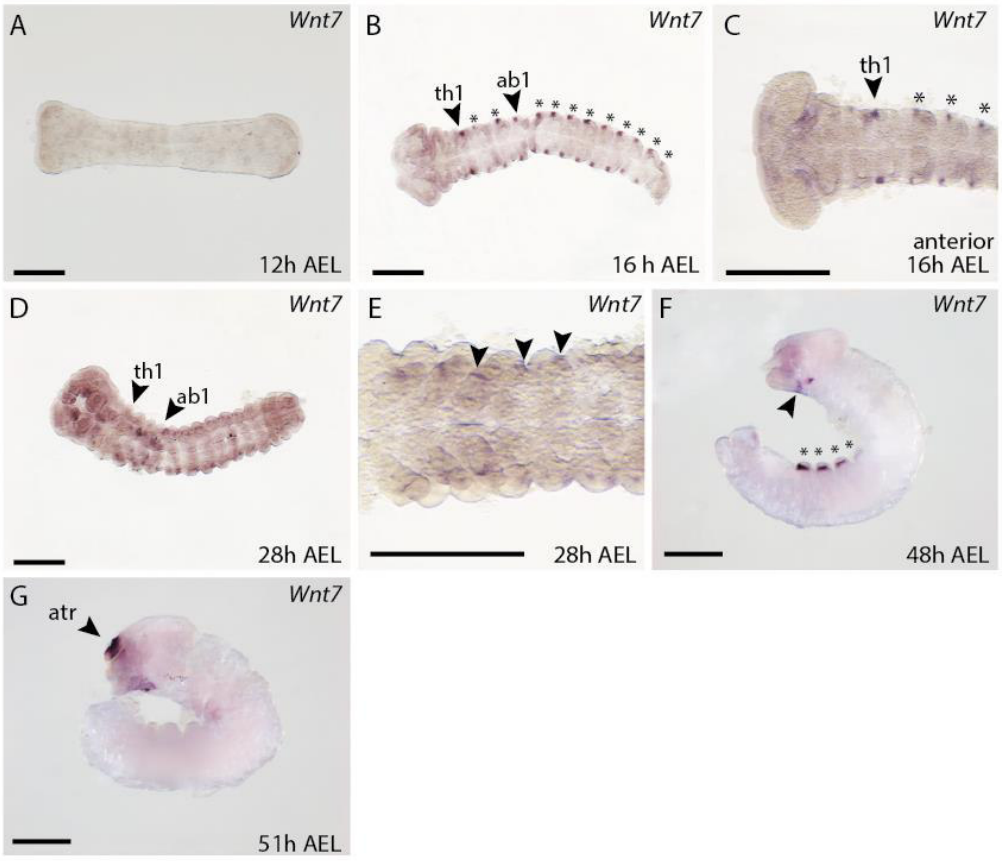

Figure 3.7 | Expression of *Wnt7* during development in *B. anynana*. **(A)** No expression was detected at around 12 h AEL. **(B)** The first expression of *Wnt7* occurs around 16 h AEL. **(C)** Close up of the anterior head region. **(D)** Around 28 h AEL the expression becomes faint but is still present in the periphery of each segment. **(E)** Close up of the ventral abdominal part of the embryo around 28 h AEL: Lateral dot-like expression can be observed (arrowheads). **(F)** Expression around 48 h AEL. **(G)** Staining in the antennal region for *Wnt7* can be seen. H: hours; AEL: after egg lay; th1-3: thoracic segment 1-3; ab1: abdominal segment 1; atr: antennal rudiment. All pictures are orientated with anterior to the left. Scale bar: 400 µm.

Faint expression at 28 h AEL could be seen on both sides in each of the segments (Figure 3.7 D and E; see arrowheads and indication of thoracis and abdominal segments in D). Overall, it seemed that the intensity of the expression was reduced (Figure 3.7 D). Just after blastokinesis, a "ring" shaped expression domain was present medially in four of the abdominal limb buds and some expression could be observed in the labial and maxillary segments (Figure 3.7 F; asterisks and arrowhead). Later the only observed expression was detected in the antennal rudiments (Figure 3.7 G arrowhead). While performing these experiments, I often observed that a very thin membrane (probably the forming embryonic membrane) covered all appendages, starting formation around 51 h AEL. This membrane seemed to be acceptable to the staining procedure of *in situ* hybridisations. Staining of this membrane was observed in all embryos from a sense staining as well when no *in situ* probe was used during the hybridisation step (data not shown). This indicates, that this staining on the head structures at these late stages has to be regarded carefully because it might be a staining relict and no true expression of the analysed Wnt genes.

Wnt9

No embryonic expression of *Wnt9* was detected by performing an *in situ* in *B. anynana* which was confirmed using different probes (Supplement Figure S3.1). This was consistent with *Tribolium*, although later expression in the gut region was described in this beetle (Bolognesi *et al*., 2008). In *Drosophila*, expression of *Wnt9* had been observed in the CNS and in the gut of larval stages (Graba *et al*., 1995). Here again, *Wnt9* was extracted from a pooled RNA sample consisting of embryonic and larval tissue. This confirms the presence of the gene but also indicates, that expression during embryogenesis might not occur but was possible in later stages. It could be possible that *Wnt9* in *B. anynana* was expressed in the developing gut during larval stage which was not analysed in the present study.

Wnt10

Expression of *B. anynana Wnt10* became visible around 16 h AEL (Figure 3.8 A - B') in segmental stripes. The stripes appeared in the middle of each segment, along the neurogenic furrow. Distinct expression was also observed in the embryonic head region (Figure 3.8 Band B', asterisks), where antennal rudiments, head lobes, mandibular and

maxillary segments could be seen (Figure 3.8 B', asterisks and indications of mandibular and maxillary segments with arrowheads). Later, at 20 to 26 h AEL, the expression in all segments from the first thoracic to the last abdominal segment, continued to concentrate along the neurogenic furrow (Figure 3.8 C and D; morphological indication with arrowheads). Later, this expression was only dominant in the last six abdominal segments (Figure 3.8 E', arrowhead). Expression in the head segments became fainter while distinct expression still was detectable in the mandibular, maxillary and labial lobes at 28 h AEL (Figure 3.8 E). Two discreet domains were observed during all stages in the telson (Figure 3.8 B-E, asterisk). Very late expression was only observed in the mandibular/antennal regions on the head (Figure 3.8 F, arrowhead). As already described for *Wnt7*, this very late staining in the head regions might be artefacts from the staining method used due to a small membrane around these appendages at this stage which was able to accumulate signal.

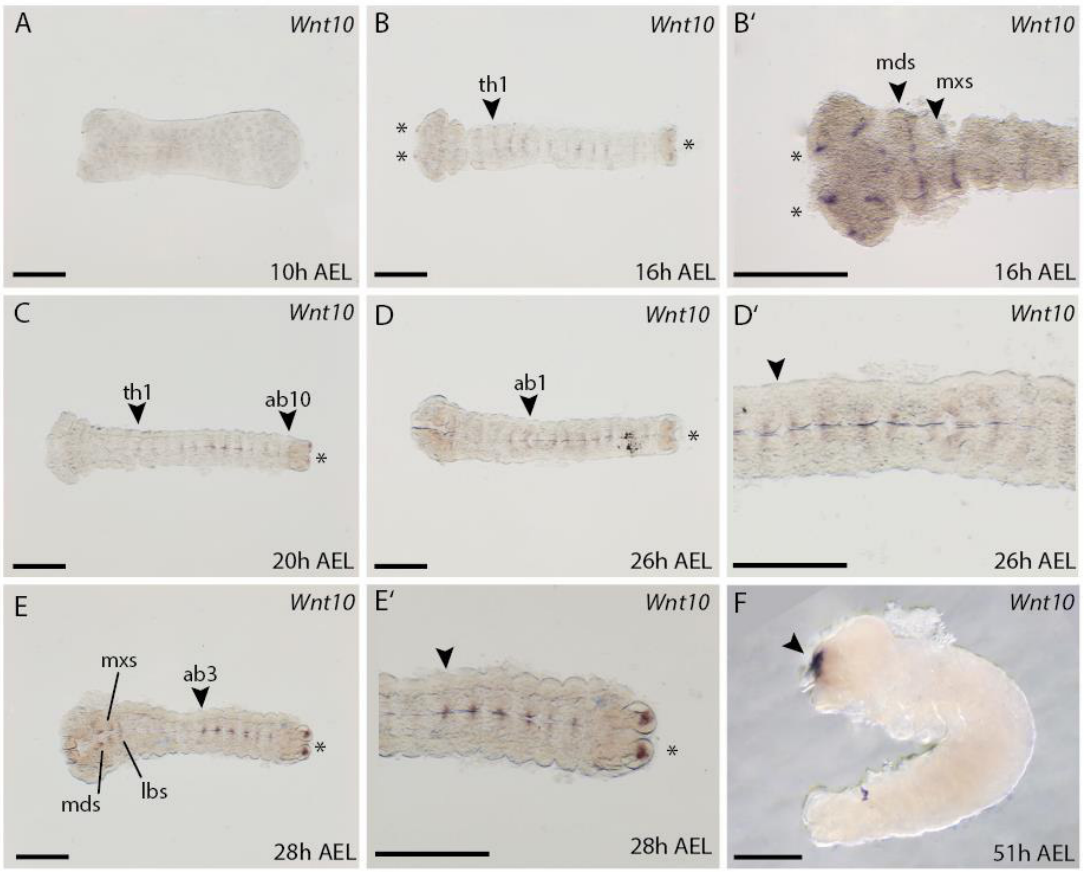

Figure 3.8 | *Wnt10* expression during *B. anynana* embryogenesis. **(A)** No expression of *Wnt10* was seen at 10 h AEL. **(B)** Expression around 16 h AEL. **(B')** Higher magnification of the head region. **(C, D and D')** Expression around 20 to 26 h AEL becomes more restricted on either side of the neurogenic furrow. **(E and E')** *Wnt10* expression at 28 h AEL. **(F)** Expression around 51 h AEL. H: hour; AEL: after egg lay; th1: thoracic segment 1; ab1: abdominal segment 1; mds: mandibular segment; mxs: maxillary segment; lbs: labial segment. Scale bar: 400µm.

The expression in the neurogenic furrow and the head region indicated that *Wnt10* might be involved in patterning or differentiating the nervous system. Expression of *Wnt10* in the developing CNS was also known from *Drosophila* and *Tribolium* (Bolognesi *et al*., 2008; Janson *et al*., 2001). Expression of *Wnt10* in the gut, as described for *Drosophila,* was not detected here (Janson *et al*., 2001), but to investigate this further, later stages could be analysed in the future. The observed expression in the mandibular segments of *B. anynana* has also been described for *Tribolium.* Additionally, *Wnt10* expression in stripes in all segments has been seen for *Tribolium* (Bolognesi *et al*., 2008). The similar expression patterns between *B. anynana* and *T. castaneum* could indicate that a similar function potentially could be conserved between these two species.

Wnt11

Expression of *B. anynana Wnt11* was only observed during very late stages of embryogenesis (Figure 3.9). Around 48 h AEL expression could be seen in the proximal region of the mandibular segments as well as in the antennal regions (Figure 3.9 A and B, arrowheads). Later, the expression in the head region (arrowhead) increased and was now found in the mandibles, maxillae and labium as well as in the antennal rudiments (asterisks) (Figure 3.9 C and D). Expression was also observed in the distal tips of the thoracic legs at this stage, (Figure 3.9 C, asterisks) which was similar to staining described for *Tribolium* at a similar developmental stage (Bolognesi *et al*., 2008). Interestingly, no other *Wnt11* was found so far in butterflies, but *Wnt11* was found in moths and closely related beetles (see Chapter 1). Taking this data together, a *Wnt11* could be present in several butterfly species but more phylogenetic analysis would be needed for understanding these dynamics.

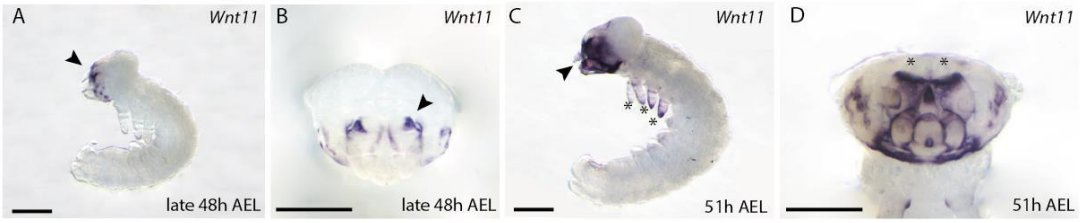

Figure 3.9 | *Wnt11* expression during late embryogenesis in *B. anynana*. **(A and B)** Around 48 h AEL expression can only be observed in the head for *Wnt11* (arrowhead). **(C and D)** At 51 h AEL the expression in the head increases (arrowheads). H: hour; AEL: after egg lay. Scale bar: 400 µm.

WntA

The expression of *WntA* in *B. anynana* was similar to *Wnt1*, which, rather interestingly, was also observed for expression during wing development (Martin and Reed, 2014). *WntA* was observed as early as 10 h AEL and appears in segmental stripes in the gnathal and thoracic segments (Figure 3.10 A and B, arrowhead). In addition, two distinct domains were detectable in the forming head lobes, similar to *Wnt1* expression (Figure 3.10 A and B; asterisks). It must be noted that the stripes were interrupted at the primitive groove (later forming the neurogenic furrow) and did not cross the whole segments. Around 16 h AEL when all segments were formed, *WntA* expression could be seen in the anterior part of all gnathal, thoracic and abdominal segments (Figure 3.10 C; morphology indicated by arrowheads) which very likely might be overlap with *wg*

expression at this stage. To test this, for example double *in situs* would be helpful. Between 20 to 26 h AEL; the expression concentrated at the midline and could now be detected in "dots" along the neurogenic furrow (Figure 3.10 D and E, arrowheads).

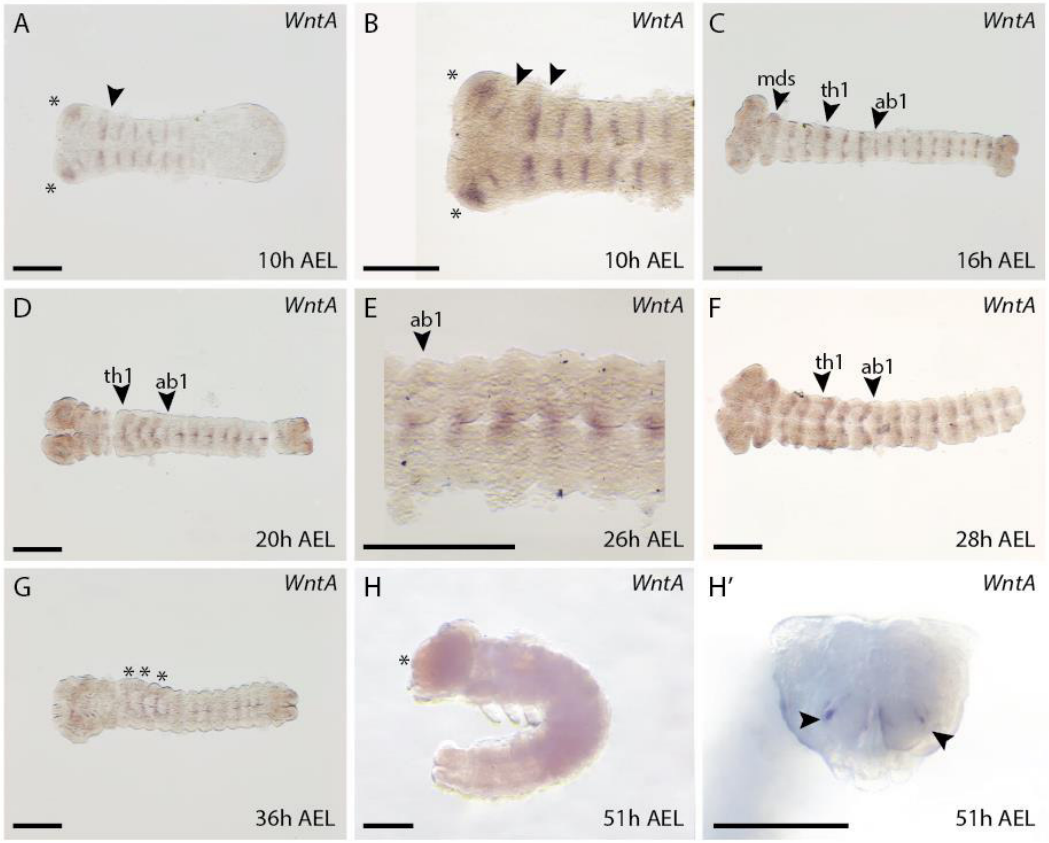

Figure 3.10 | Expression of *WntA* during the development of *B. anynana*. **(A)** Expression in segmental stripes at 10 h AEL. **(B)** Higher magnification of the expression at 10 h AEL. **(C)** Expression around 16 h AEL. **(D)** Expression of *WntA* is concentrated along the neurogenic furrow from 20 to **(E)** 26 h AEL. **(F and G)** Expression continues to decrease and concentrate at the neurogenic furrow around 28 to 36 h AEL. **(H)** No expression can be seen along the body at around 51 h AEL. **(H')** Higher magnification of head at 51 h AEL. h: hours; AEL: after egg lay; th1: thoracic segment 1; ab1: abdominal segment 1; mds: mandibular segment. Scale bar: 400 µm.

No clear expression was observed in the head region of the embryo, in contrast to *Wnt1* in *B. anynana*. Around 28 and 36 h AEL, expression decreases but was concentrated at the ventral side of the thoracic limbs (asterisks in G) as well as in very small domains along the neurogenic furrow (Figure 3.10 F and G). In very late embryonic stages, *WntA* expression could only be detected in the head region on the lateral-proximal side of the mandibles (Figure 3.10 H and H'). As previously mentioned for *Wnt7* and *Wnt10*, it might be non-specific staining in this tissue. The observed expression of *WntA* was similar to the previously described expression of *WntA* in *Tribolium* which was

also present in segmental stripes, concentrated during development along the midline (Bolognesi *et al*., 2008).

Overall, expression for five Wnt genes could be observed during embryogenesis leaving three Wnt genes which were potentially expressed at later stages. All embryonically expressed butterfly Wnts were similar in their expression pattern to *Tribolium* (*Wnt1, Wnt7, Wnt10, Wnt11* and *WntA*) (Bolognesi *et al*., 2008). Only expression of *Wnt1* and potentially *Wnt7* were similar to those described from *Drosophila* at comparative stages. These results make a further comparison of the Wnt function between Coleoptera and Lepidoptera very interesting. It seems, that these two sister groups could have maintained a similar function of their Wnt genes.

3.5 | Conclusions and future directions

The early embryonic development of *B. anynana* was very similar to described patterns in other lepidopterans e.g. *M. sexta* and *B. mori* (Broadie *et al*., 1991; Kobayashi and Ando, 1990; Krause and Krause, 1964) and clearly, early development seems to be quite conserved in the lepidopteran order. However, it would be interesting to analyse the later development, e.g. of internal organs further, to achieve a better understanding of the patterning mechanisms during larval development. This staging will be useful for many other experiments which could be done in the future, by providing an accurate referencing for developmental stages.

The analysis of the Wnt expression evidenced an involvement of *Wnt1, 7, 10, 11* and *A* during early embryogenesis (see summary of expression pattern Figure 3.11), while no expression was observed for *Wnt5, 6* and *9*. During the course of the experiments, it was made sure that no staining is present in embryonic stages of any of these genes but later expression in larval tissues seemed to be likely. For *Wnt6*, expression was shown in wing discs, where it overlaps with *Wnt1* expression which was a first hint that this assumption might be right (Martin and Reed, 2014).

The early segmental stripe expression of *wg, Wnt10* and *WntA* (Figure 3.11) might indicate a role in forming the segment polarity during butterfly development. The same pattern had been seen for *wg* in the moth species *B. mori* and *M. sexta* (Dhawan and Gopinathan, 2003; Kraft and Jäckle, 1994; Nakao, 2010) where it was also shown that a role in segmentation was true for *Wnt1*. The function of the other Wnts had to be tested in this context. Especially understanding the relationship between *Wnt1* and *WntA*, which was very close in wing pattern development would be very interesting. It was very likely, that a conserved role in segmentation was present in butterflies, beetles and flies, which were all closely related sister groups (see Chapter 1) (Bolognesi *et al*. (2008) and Nusslein-Volhard *et al*. (1984)). If the function of *Wnt1* is conserved in these insects, this could also influence the evolution of *Wnt1* – it is very likely that a gene with such a crucial function will be conserved. And this was exactly what was seen in all arthropods (see Chapter 1), where *Wnt1* was highly conserved in all analysed species. It would of course be necessary to analyse the function of *Wnt1* in many more species to see if this correlation is correct.

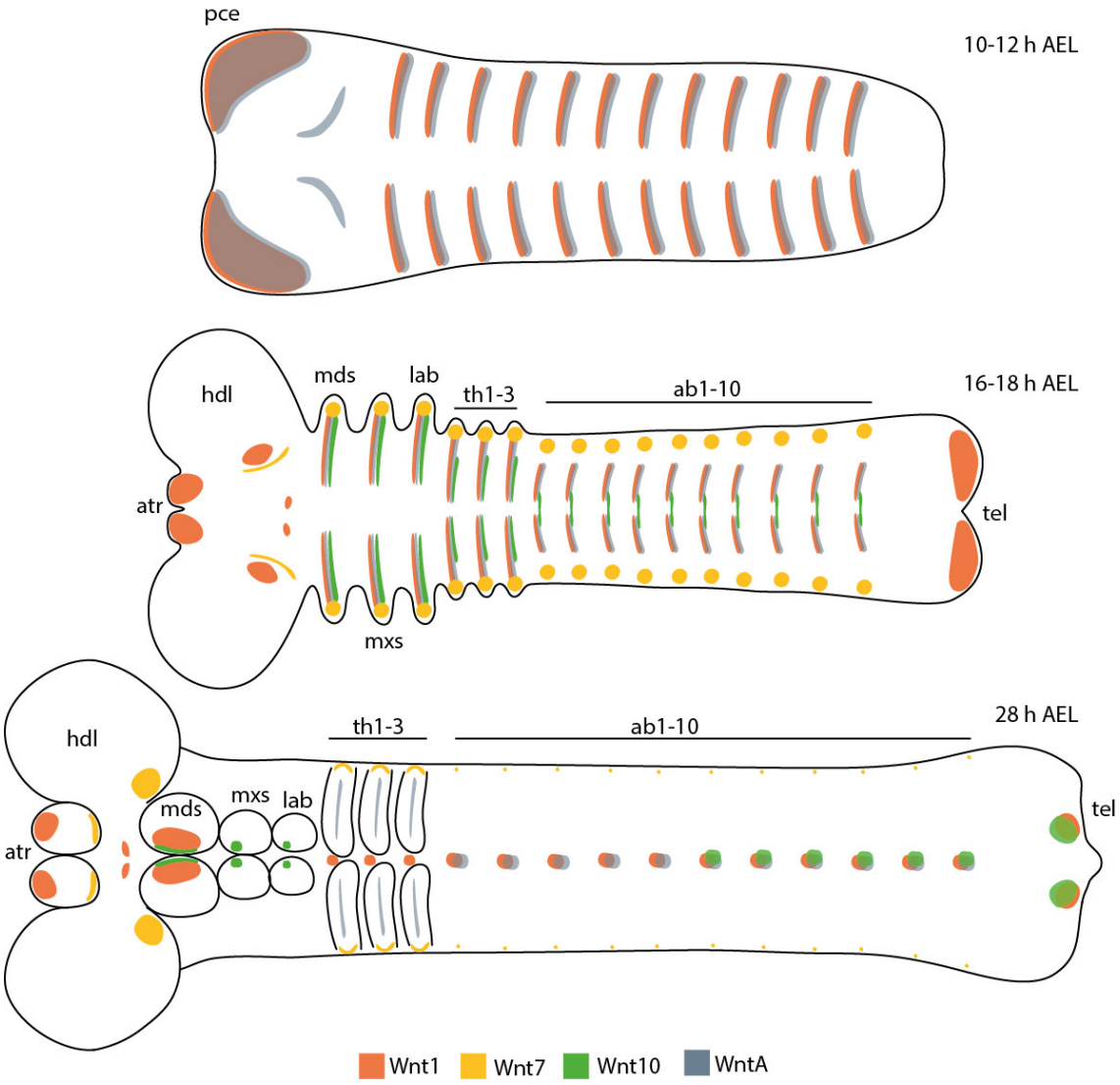

Figure 3.11 | Schematic summary of the Wnt expression pattern in early embryogenesis of *B. anynana*. Indicated is the morphological outline of the embryo at different developmental times (10-12 h AEL; 16-18 h AEL and 28 h AEL). The expression of *Wnt1* in orange, *Wnt7* in yellow, *Wnt10* in green and *WntA* in blue are indicated. pce: protocephalon; atr: antennal rudiments; mds: mandibular segments; mxs: maxillary segments; lab: labial segments; hdl: head lobes; th1-3: thoracic segments; ab1-10: abdominal segments; tel: telson; h: hours; AEL: After egg lay.

Revealing Wnt gene expression patterns during early embryogenesis and body patterning in lepidoptera will form a foundation for further functional analysis. It would be interesting to knock out Wnt genes using CRISPR/Cas9, which was recently established for several butterfly and moth species (Livraghi *et al.*, 2018; Matsuoka and Monteiro, 2018; Prakash and Monteiro, 2018a). The data provided from this study will help to interpret and anticipate future loss of function phenotypes from these knockout experiments.

Overall, analysing the expression and function of Wnt genes in several closely related species will increase the insight into the underlying evolutionary mechanisms of Wnt genes. As a start, butterflies could provide a great model for studying Wnt function and compare this knowledge to several other insect species, in particular beetles which seem to have similar functions, and analyse a potential conserved functional role of Wnts in evolution.

In the following chapter of this thesis, the focus will be on the exact function of a Wnt gene in *Drosophila melanogaster*. From the analysis in this Chapter it was shown how important the understanding of Wnt function could be not only for the development of one species but also for understanding evolution and development in a larger context. If I would like to compare the function of all Wnt subfamilies between several species, it is necessary to understand the function in each individual species first. Therefore, it was decided in the last part of this thesis to analyse one of the less well studied Wnt genes in *Drosophila. Wnt6* is part of the ancestral Wnt cluster, highly conserved in arthropods (Chapter 1) as well as similarly expressed as *wg* in several species such as *Drosophila* and *Tribolium* (Janson *et al*., 2001; Bolognesi *et al*., 2008) and forms therefore a nice candidate for phylogenetic functional comparisons.

3.6 | Supplement

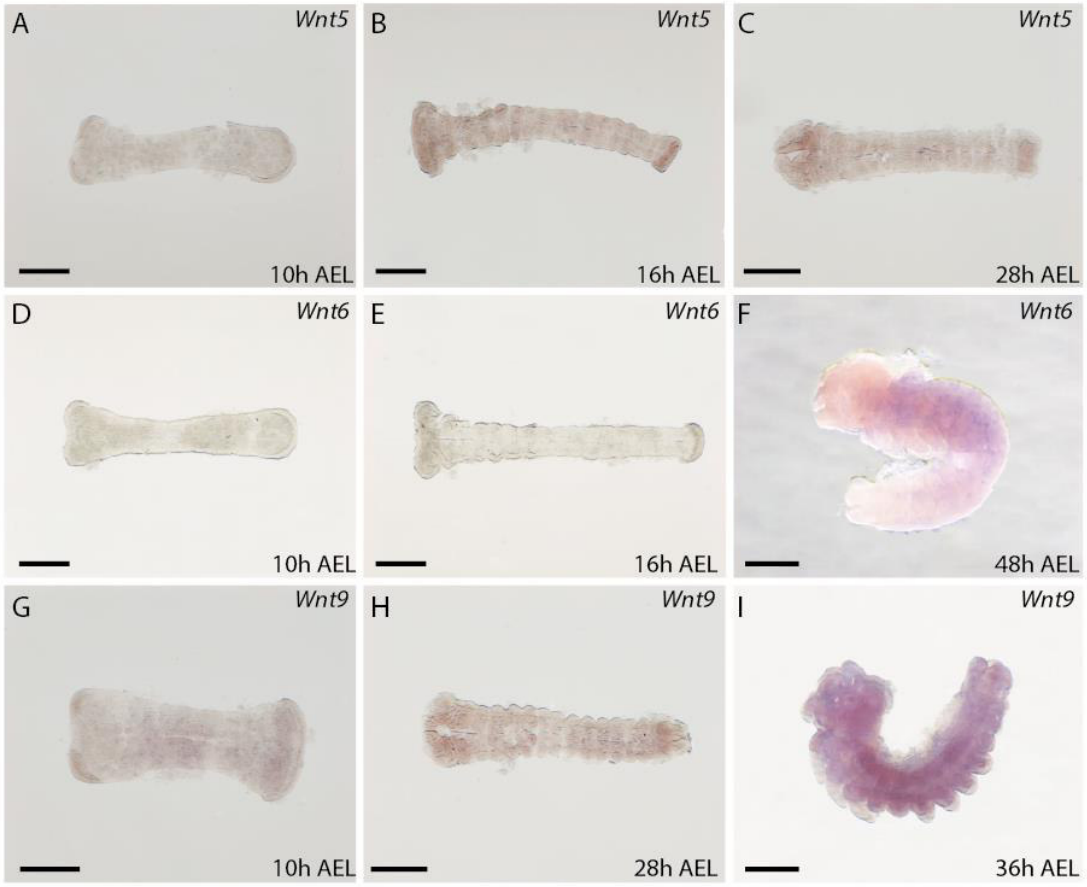

Supplement Figure S3.1 | Embryos stained with *Wnt5*, *Wnt6* and *Wnt9* probes. No expression was observed in the stages assayed**. (A-C)** Embryos stained for *Wnt5*. **(D-F)** Embryos stained for *Wnt6*. **(G-I)** Embryos stained for *Wnt9*. H: hours; AEL: after egg lay. Scale bar: 400µm.

Supplement Table S3.1 | Primer sequences for all Wnt probes used in this study. Capital letters show the gene specific sequence, small letters are T7 overhangs used for the cloning method of the probes.

Gene	Forward 5'-3'	Reverse 5'-3'	Probe in bp
Wnt1/wg	ggccgcggGAGTGCAAGTGCCACGGTATGT	cccggggcACCTCGCAGCACCAGTG GAACGTGCAGT	455
Wnt5	ggccgcggCGACACAAGGACCACATGC	cccggggcACATTAGTGAGCACCCGTCA	768
Wnt6	ggccgcggACAAGAGAGACGGGGTTTGT	cccggggcGCACGTTTGTATGTCTCGCT	765
Wnt7	ggccgcggGGGCAGCACAATCAGAAACT	cccggggcACCAGCGTTTTGTCTTGACC	696
Wnt9	ggccgcggGGCTTCTACACCACCAGCTA	cccggggcCACCAGCTTCTTCTTCACGG	750
Wnt10	ggccgcggCAAGAGACAACATGCTGCCA	cccggggcTCGTAACACTGAAGGGCTGT	719
Wnt11	ggccgcggCATGCCCCACAAGAACTACG	cccggggcCAGCCTGGTCTTGGTCCTC	726
WntA	ggccgcggTGCACAAAGAAAGCTGCCAT	cccggggcAGATCGGTTTTGTTCGGTTTCT	702

Chapter 3

4 | Investigating the functional role of *Wnt6* in *Drosophila melanogaster*

4.1 | Background

Since the 1980s *Drosophila melanogaster* had been widely used to understand the Wnt signalling pathway and all its components. *Drosophila* contains seven Wnt ligands, and while *wingless* (*wg*), the first Wnt ligand to be identified, had been intensively studied, the exact functions and interactions of other ligands remains unclear, in particular, *Wnt6* and *Wnt10*. In this part of the study, the focus was on understanding the function of *Wnt6* which is the most similar Wnt ligand to *wg* in *Drosophila*. The two genes share an overlapping expression pattern, high protein sequence similarity as well as a close genomic location (see Chapter 1). Recently a publication showed involvement of *Wnt6* in maxillary palp development (Doumpas *et al*., 2013). Here, I further studied the role of *Wnt6* in maxillary palp development. Maxillary palps (MP) were important sensory organs on the fly head and were responsible for olfactory perception. The underlying developmental pathway of maxillary palps was partially understood and included an important role of *wg*, however, the position, interactions and role of *Wnt6* in this pathway remain unclear.

4.1.1 The *Wnt6* gene in *D. melanogaster*

Drosophila Wnt6 has four exons, three introns and encodes a protein of 421 amino acids. This protein sequence includes a N-terminal signal peptide from amino acid 1-22, which is needed for proper secretion (Figure 4.1 A). The secretion depends on lipid modification of a serine residue by Porcupine that enables *Wnt6* to interact with the transmembrane protein Wntless, which in turn then facilitates the transport into the extracellular matrix (Herr and Basler, 2012) (see Introduction).

Expression of *Wnt6* could be detected only from the 3rd instar larval stage onwards and overlaps with *wg* expression in all imaginal discs (Figure 4.1 B-D) (Doumpas *et al*., 2013; Janson *et al*., 2001). Here, *Wnt6* was expressed in a stripe at the dorsal-ventral boundary (asterisks), the hinge and the notum in the wing disc (Figure 4.1 B), in the anterior/dorsal domain in the antennal region of the eye antennal disc (arrowhead, Figure 4.1 C), as well as in a ventral anterior domain in the leg discs (arrowhead, Figure

4.1 D) (Janson *et al*., 2001). No expression could be seen in the maxillary palp field on the ventral side of the antennal disc at this stage.

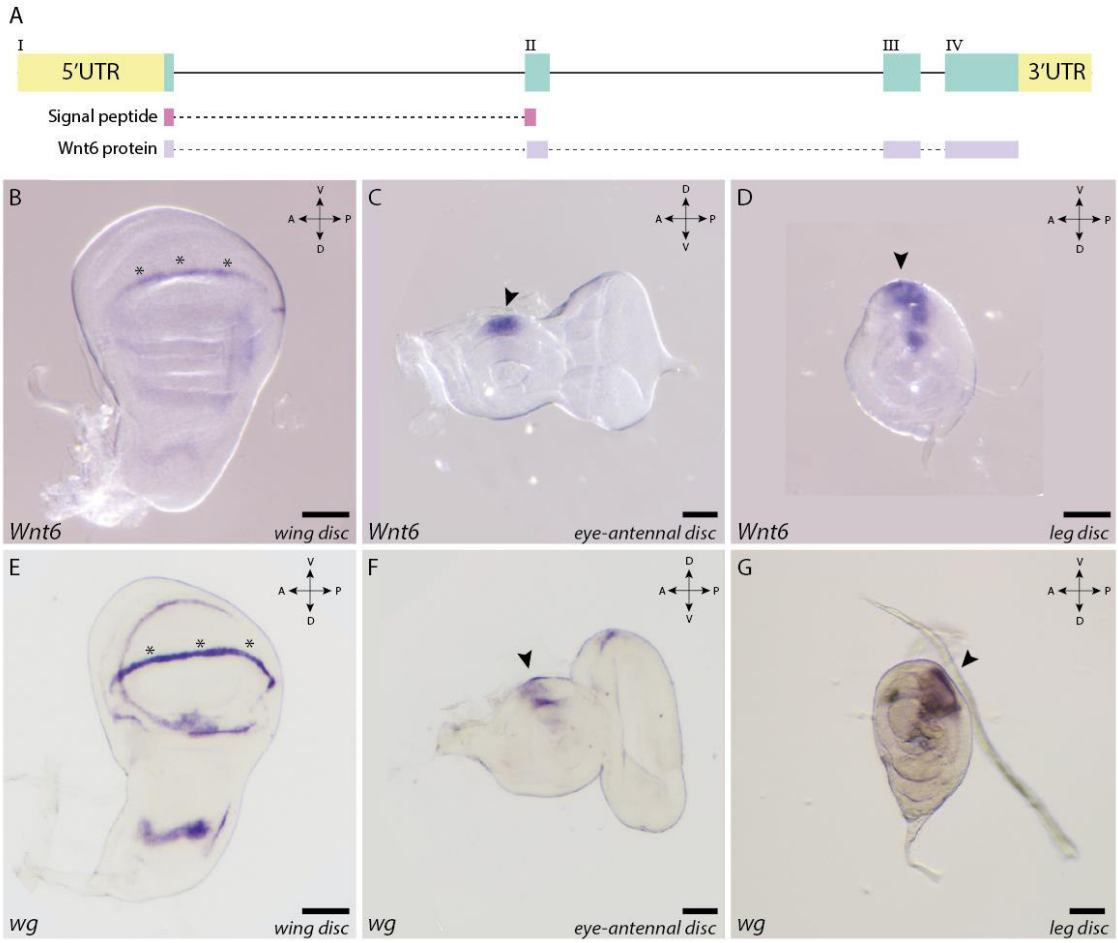

Figure 4.1 | *Wnt6* structure and expression in imaginal discs of 3rd instar larvae of *D. melanogaster*. **(A)** Genomic structure of the *Wnt6* locus. Four exons (green) are interspaced by three intronic sequences (black line). The first 22 amino acids of the coding sequence are the signal peptide (pink) and the processed coding region *Wnt6* (purple). **(B-D)** *In situ* hybridisations showing *Wnt6* expression in 3rd instar imaginal discs. **(B)** In the wing disc**, (C)** the eye-antennal disc and **(D)** the 2nd leg disc. **(E-G)** Expression pattern of *wg* in 3rd instar imaginal discs. Observed expression in the wing **(F),** eye-antennal **(G)** and 2nd leg disc **(H).** kb: kilobases; UTR: untranslated region; A: anterior; P: posterior; D: dorsal; V: ventral. Orientation of disc indicated by coordinate cross. Scale 400 µm.

A previous study showed that both *Wnt6* and *wg* seem to be involved in early cell regeneration and damage response in imaginal discs (Smith-Bolton *et al*., 2009), although the exact function of *Wnt6* in these processes remained unclear. Interestingly, an enhancer (BRV118) was identified between *wg* and *Wnt6* that promoted damage related activation of *wg* and *Wnt6* expression and ablation of this enhancer decreased the expression of both Wnt genes (Harris *et al*., 2016). A second function of *Wnt6* in

Drosophila was shown in a study published in 2013, where the deletion of the first exon of *Wnt6* suggested that this ligand was required for development of the MP (Doumpas *et al*., 2013). Additionally, a very recent publication found evidence for the involvement of *Wnt6* in the maintenance of escort cells in *Drosophila* oocytes (Wang and Page-McCaw, 2018).

4.1.2 The developmental regulation of maxillary palps

The successful development of maxillary palps (MP) required a distinct genetic regulation which was in parts similar to antennal development. MP originate from the maxillary palp field (Haynie and Bryant, 1986; Lebreton *et al*., 2008) in the imaginal eye-antennal disc (Figure 4.2 A), which gave rise to the adult eye, antennae several other head structures as well as the MP. The MPF is positioned ventrally to the antennal field on the anterior side of the imaginal disc (Figure 4.2 A) (Haynie and Bryant, 1986; Held Jr, 2002). The separation between the antennal and maxillary field occurred during the 2nd instar (L2) whereas the differentiation of the organs happened during the 3rd instar (L3) and later (Lebreton *et al*., 2008).

During antennal development *engrailed* (*en)* activated hedgehog which triggered the expression of *wingless* (*wg)* and *decapentaplegic* (*dpp)* from L2 onwards. These two genes activated *distalless* (*dll)* which could activate *homothorax* (*hth)*. *Dll* and *hth* together activated the expression of *spineless (ss),* which stimulates the expression of the *distal antennae related gene (dan)* for differentiation of antennae (Figure 4.2 B) (summarized by Lebreton *et al.* 2008).

The MPF is early on defined by expression of *deformed* (*dfd*) (Merrill *et al*., 1987) and *proboscipedia* (*pb*) in L2 (Pultz *et al*., 1988) and both genes were not present during antennal development. *pb* is generally involved in the patterning of the proboscis (Abzhanov *et al*., 2001) and specifically responsible for the formation of the proximal-distal axis of the MP (Percival-Smith *et al*., 2017). Ectopic expression of *pb* in the eye-antennal disc lead to homeotic transformation of antennae to MP or legs (Benassayag *et al*., 2003; Cribbs *et al*., 1995; Held Jr, 2002; Kaufman, 1978). Still, it remained unclear how *pb* is influencing the axis formation in MP (Percival-Smith *et al*., 2017).

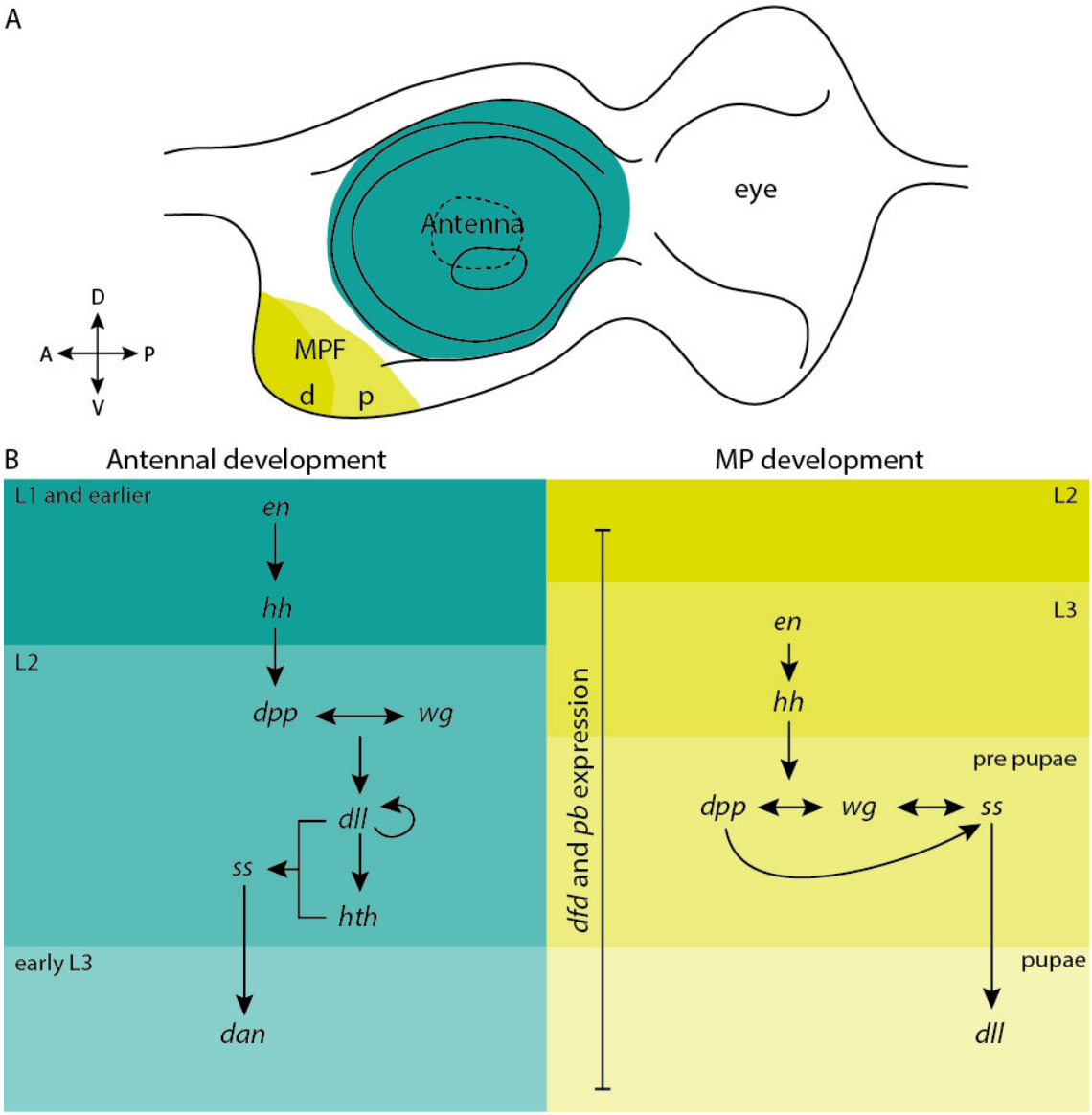

Figure 4.2 | Developmental pathways of antennal and maxillary palp development. **(A)** Schematic drawing of an eye-antennal disc with the antennal field indicated in blue and the maxillary palp field (Waterhouse *et al.*) in yellow at the anterior ventral side of the disc. In the MPF, the distal (d) and proximal (p) region of the adult MP are indicated. The cross indicates the orientation of the disc. **(B)** Developmental pathways of antennae and maxillary palp development. A: anterior; P: posterior; D: dorsal; V: ventral; p: proximal; d: distal; MPF: Maxillary palp field; MP: maxillary palp. L1: first instar larval stage; L2: 2nd instar larval stage; L3: 3rd instar larval stage. Based on Haynie & Bryant, 1978; Held Jr, 2002; Lebreton *et al.* 2008.

dfd is also expressed from early stages on in the MPF, whereas its exact function or regulation during MP development remained unclear (Diederich *et al.*, 1991). One potential gene involved in the regulation of *dfd* is *hth.* An interaction between these two genes was described in the central nervous system (CNS) where *hth* regulates the expression of *dfd* (Kumar *et al.*, 2015). However, this has not yet been observed for the

MPs. Loss of *dfd* lead to complete loss of MP which implies that *dfd* is an important factor in the underlying developmental pathway (Merrill *et al*., 1987).

During the development of the MP, *hh* and *en* appeared in the MPF during L3, while no expression of *wg* and *dpp* could be seen before prepupal stages. Compared to antennal development, expression of all four genes was observed later during development. *en* and *hh* were co-expressed with *dfd* during L3 (Lebreton *et al*., 2008) but the exact interactions remain unresolved (Figure 4.2 B).

It was shown by Lebreton *et al*. (2008) that late expression of *wg* during the prepupal stage was crucial for MP development and dependent on *hh* activation (Figure 4.2). Earlier expression of *wg* in L2 or L3 lead to development of ectopic antennae from the MPF (Lebreton *et al*., 2008). *dpp* expression also depends on *hh* activation and together with *wg* it could activate the expression of *spineless (ss)* which was important in antennae and legs to define the distal regions of these appendages. It seems that *ss* had a similar role in MP development and its loss lead to truncated MP (Duncan *et al*., 1998), while ectopic expression of *ss* increased expression of *dll* and *hth* which triggers development of distal antennae parts from the MPF (Figure 4.2 B) (Duncan *et al*., 1998; Emmons *et al*., 2007). In the MPF, *wg* and *ss* seemed to depend on each other due to a regulatory feedback loop (Lebreton *et al*., 2008). In contrast to antennal development, where *dll* activated *ss* (Emmons *et al*., 2007), in the MPF, *ss* appeared to activate *dll* expression (Figure 4.2 B) (Cohen and Jürgens, 1989; Emmons *et al*., 2007; Lebreton *et al*., 2008).

While the overall interactions and regulations of the developmental pathway in MPs remains partially unresolved, very late *wg* expression is clearly important to determine MP fate. *Wnt6* could play a role in several parts of this developmental process, but no direct interaction of *Wnt6* with any of the above-mentioned genes is so far known and further study of *Wnt6* and *wg* during MP development is needed.

4.1.3 Aims

As mentioned in the conclusions of Chapter 2, a detailed analysis of the function of Wnt genes is needed for a phylogenetic comparison of Wnt function to understand the evolution of Wnt genes. Here, the focus was on *Drosophila*, which is a very well-studied

model organisms regarding Wnt genes and the Wnt signalling. Still, some Wnts were less studied and a clear idea about their function was missing. This is particularly the case for *Wnt6* and *Wnt10*, both genes are part of the ancestral Wnt cluster, whereas *Wnt6* is also very similar to *wg* sequence and highly conserved throughout arthropods (see Chapter 1). Therefore, *Wnt6* will be in the focus of this part of the study and the exact functional role during MP development will be analysed. Where is it involved in the developmental pathway – which genes does it interact with? Does *Wnt6* play a distinct role, independently of *wg*? To answer some of these questions, I will use the UAS/Gal4 system to ectopically express wildtype *Wnt6* under the control of several different driver lines with a known role in the developmental pathway, such as *dpp* and *hth*. Additionally, I followed up the published rescue experiment from Doumpas *et al*. (2013), where the authors used *elav*-Gal4, driving expression in the nervous system, which lead to a rescue of MPs in *Wnt6* knockout flies.

Further, a new *Wnt6* knockout line will be created using CRISPR/Cas9 for homologous recombination. Creating a new *Wnt6* knockout line will allow to compare both knockout lines and independently confirm the loss of *Wnt6* phenotype seen by Doumpas *et al.* (2013). Finally, a small nuclear tag will be introduced in the N-terminal region of *Wnt6* to be able to better analyse the protein location of *Wnt6* because no specific antibody was available for *Wnt6*.

4.3 | Material and Methods

Fly husbandry and fly genetics

All fly stocks were kept at 25°C under a controlled 12/12 dark/light cycle. Flies were reared on fly food containing a mix of maize flour, yeast, sugar and preservatives. The *Wnt6* knockout line (*Wnt6*{KOd}) and a UAS-*Wnt6* stock were kindly provided by Aurelio Teleman (University of Heidelberg, Germany). The following stocks were obtained from the Bloomington *Drosophila* Stock centre (Indiana University, Bloomington: *elav*-Gal4 (BDSC#8760), *dpp*-Gal4 (BDSC#67066), *hth*-Gal4 (BDSC#62588)). *Drosophila melanogaster* flies of the w^{1118} strain were obtained from the lab collection, as well as a single balancer strain on the second chromosome (w-; *sp/CyO*) and a double balancer on the second and third chromosome (w-; *if/CyO;MKRS/TM6b*). The MP phenotype was only detectable in flies homozygous for the *Wnt6*{KOd} knockout on the 2nd chromosome. Therefore, for all UAS/Gal4 rescue experiments, the UAS-*Wnt6* and all Gal4 lines had to be crossed into the *Wnt6*{KOd} line first and also needed to be on the first or thired chromosome. The deficiency line BDSC#9703 was used for crosses with *Wnt6*{KOd} and *Wnt6*{KOmche} as well as the FlyLight lines GMR25A04 (BDSC#45137) and GMR25A05 (BDSC#45138) for putative enhancer testing. For full genotypes, crosses and sources see Supplement.

Dissections, measurements and statistics

Three days after eclosion, female and male flies were collected and stored in 70% ethanol. The second pair of legs and wings were dissected and mounted in Euparal (ALS Hindolveston, Norfolk). Slides were dried overnight at 65°C and imaged using the Axio zoom.V16 microscope with the Axiocam 506 color camera (Zeiss, Germany).

For dissection of the MP, the proboscis, including the palatal plate, were dissected off the fly head. The MP, which are attached to the more proximal part of the proboscis, were then removed and transferred into a droplet of Hoyer's medium (Hoyer's medium and lactic acid 1:1 mixture) and positioned on 8-well slides (Hendley, UK). Each individual MP was imaged using an Axioplan microscope (Zeiss, Germany).

Palps, legs and wings were measured using ImageJ 1.48v (Schneider *et al*., 2012) and analysed using R version 3.2.0 (R core Team, 2013).

Measurements for the 2nd leg tibia for all lines served as a proxy for the body size of the flies (Supplement Figure S4.5 and S4.6). Unless stated otherwise, all lines showed a very similar body size. Wing length was measured across the wing from the branching of the longitudinal vein 2 and 3 until the end of longitudinal vein 3. All maxillary palp data was analysed for normal distribution using a Shapiro-Wilk test. Only data for the following lines were probably not normally distributed: UAS-*Wnt6*_f, *Wnt6KOd*;*elav*>*Wnt6*_m, *Wnt6KOd*;*hth*>*Wnt6*_f and *Wnt6KOd*/*Wnt6KOmche*_m. Data deviating from normal distribution was additionally analysed using a q-q plot (Figure S4.7). Deviation from the normal distribution were mainly caused by outliers. An ANOVA followed by a Tukey HSD test was performed to test significant differences between MP, legs or wings. Here, differences between female lines or male lines were always analysed separately. The significant threshold was set at <0.05. The F-value obtained from this analysis indicates how far the measured data is scattered from the mean. A large dispersion of the data was indicated by high F-values, whereas no dispersion was present when F=1. Plots were created using the ggplot2 package in R (Wickham, 2009).

Cloning the CRISPR construct for the Wnt6*{KO}*

A CRISPR/Cas9 approach based on homologous recombination was used to insert a 1.5 kb fragment into the coding sequence of *Wnt6,* and therefore, disrupting the correct reading frame (Figure 4.3 A and B). The *guide*RNA (gRNA) was designed using the flyCRISPR website prediction tool (Gratz *et al*., 2014; Iseli *et al*., 2007). The candidate gRNA (GACTGGATTCGGCTGGTAAG) was then tested for its efficiency using the prediction tool from the Harvard medical website (http://www.flyrnai.org/evaluateCrispr/). The predicted value was at 8.6, which predicts very good efficiency. This gRNA was then cloned into the pCFD3 vector using the protocol provided by the flyCRISPR website (http://flycrispr.molbio.wisc.edu/tools). The final vector was confirmed by sequencing (Eurofins).

The homologous recombination plasmid was created using 1 kb genomic DNA upstream (5'HR) and downstream (3'HR) of the gRNA cut-site. Note that the full gRNA sequence was excluded from these sequences to prevent any re-cutting events after homologous recombination. Both homology arms were cloned into the final vector pTV3 (Baena-Lopez *et al*., 2013) kindly provided by Cyrille Alexandre (Francis Crick Institute, London). This vector includes two multiple cloning sites (MCS) interspaced by an attP site and a pax_mCherry marker, flanked by loxP sites. The homology arms were amplified using a PCR One taq Master Mix (conditions according to manufactures instructions; NEB) and cleaned up via a gel purification (Gel and PCR Clean up Kit from Macherey-Nagel). The PCR product was than sub-cloned into a pCR4 vector using the TOPO-TA Cloning kit (Invitrogen). For the insertion of the 5' homology arm (5'HR) into the final vector, the plasmid pTV3 and the TOPO-5'HR were digested using the restriction enzymes *Nhe*I-HF and *Kpn*I-HF (NEB). Both digested products were gel purified and ligated overnight (T4 Ligase, Promega). This procedure was repeated for insertion of the 3' HR, digested with *Aat*II and *Age*I-HF (NEB). The sequence of the final vector pTV3-Wnt6KO-5'HR-3'HR was confirmed via PCR and sequencing (Eurofins). All used primer sequences can be found in Supplement Table S3.2.

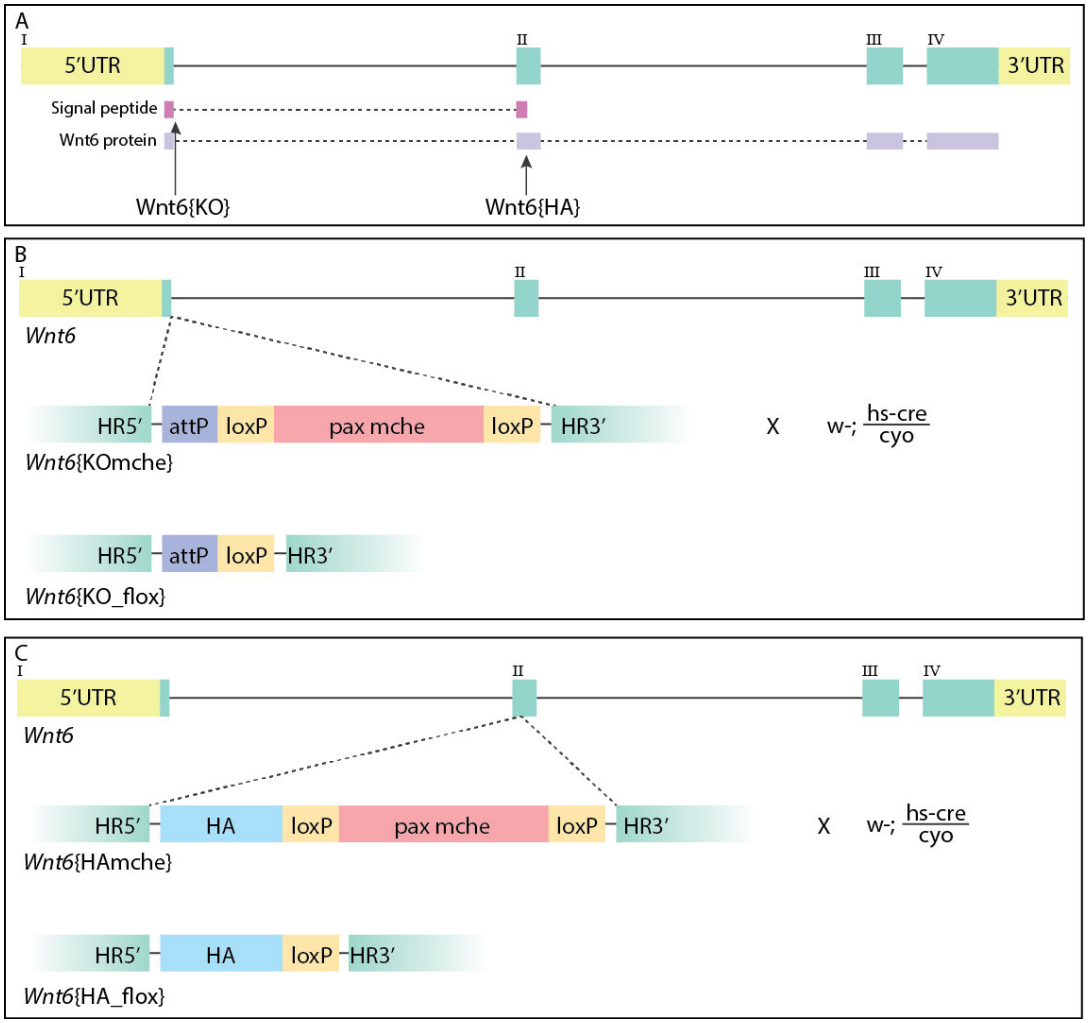

Figure 4.3 | Methodological overview about the CRISPR strategy for the *Wnt6*{KOmche} and the *Wnt6*{HA} fly lines. **(A)** Overview of the genomic structure of *Wnt6*. Shown are the four exons, UTRs and the signal peptide. Indicated are the positions of the CRISPR targeted sites for the *Wnt6*{KOmche} and the *Wnt6*{HA}. **(B)** The strategy for generating the *Wnt6*{KOmche} by inserting a 1.5 kb long sequence including an attP recombination site as well as a pax mChery fluorescent marker flanked by loxP sites. **(C)** CRISPR strategy for the insertion of the HA tag. UTR: untranslated region; HR: Homology arm; KO: knockout; w: white; hs-cre: heatshock activated cre recombinase.

The gRNA plasmid pCFD3-gRNA-Wnt6KO and the pTV3-Wnt6KO-5'HR-3'HR were amplified by Miniprep (EZNA isolation kit plasmid MINI I, VWR) and sent to BestGene (Chino Hills, USA) for microinjections into a *D. melanogaster* stock containing an endogenous *nanos-cas9* on the third chromosome (CAS-003). The final transgenic fly line *Wnt6*{KOmche} was then made homozygous (Figure 4.3 B and S4.2). Using a heat shock-cre recombination system the fluorescent marker pax_mCherry was subsequently 'floxed out' to obtain the fly line *Wnt6*{KO_flox} (Figure S3.2).

Cloning the Wnt6 HA tag vector

The insertion site for the HA tag was designed to be exactly after the signal peptide and in frame with the following coding sequence (Figure 1.2 A and C). The signal peptide is needed for the secretion of Wnt ligands and is cut off during this procedure. The position of the signal peptide was characterised using SignalP 3.0 (Bendtsen *et al*., 2004). To prevent the removal of the HA tag from the protein together with the signal peptide, a gRNA site was identified as close to this site as possible, and precise recombination was assured using homology arms designed corresponding exactly to the end of the signal peptide and remaining *Wnt6* coding sequence. The gRNA (GCCCTCCGCCCTGAAAATAG) was designed and tested for efficiency (6.8) as described above. The final vector for homologous recombination was HAche929, which was kindly provided by Cyrille Alexandre (Francis Crick Institute, London). This plasmid contained two insertion sites interspaced with a 2xHA tag, loxP sites and a pax_mCherry marker (Figure 4.3). Both homology arms were inserted using the SLIC method (Li and Elledge, 2012). Here, the HAche929 vector 5' insertion site was cut open using the restriction enzyme *BsaI* (NEB). The 5'HR was PCR amplified using overhangs on primers, which are complementary to the cut sites on the vector. Using a T4 DNA Polymerase (NEB), complementary ends were annealed and the whole reaction mix was directly transformed using TOP10 cells. This procedure was repeated for the 3' homology arm with the restriction enzyme *Sap*I (NEB).

The gRNA vector and the homology repair plasmid were miniprepped and sent for microinjections to BestGene (Chino Hills, USA). Injected flies were balanced and later floxed using the Cre/LoxP recombination system (Figure 3.3 C and S3.2). The correct position of the HA insertion was confirmed by sequencing of the homozygous floxed stock, *Wnt6*{HA}-M1Mb-F (Eurofins) (Figure 3.12).

In situ *hybridisation*

Third instar larvae were inverted and fixed for 20 minutes in 4% formaldehyde in 1x PBS (137 mM NaCl, 2.7 mM KCl, 4.3 mM Na_2HPO_4 $2H_2O$ and 1.47 mM KH_2PO_4) and for 20 minutes in 4% formaldehyde in 1x PBS-T (PBS plus 0.1% Tween 20). Larvae were brought gradually to 100% methanol or directly used for *in situ* hybridisation. *In situ*

hybridisations were performed according to a protocol based on Tautz and Pfeifle (1989) with modifications. Inverted larvae were washed with PBS several times and transferred to 1:1 PBS-T/Hybridisation buffer A (25 ml Formamide, 12.5 ml 20x SSC pH 7.0, 1 ml salmon sperm (10 mg/ml), 250 µl tRNA (20 mg/ml), 25 µl Heparin (100 mg/ml) and 0.1% Tween 20, adjust pH 6.5 with 1M HCl) for 10 minutes at 56°C. Afterwards, samples were pre-hybridised with hybridisation buffer A for 30 minutes to 1 hour at 56°C , followed by adding the probe (See primer list Supplement Table S 3.1) to the solution in the appropriate concentration. Larvae were incubated overnight, at least 16 hours. The next day, the probe was washed off using hybridisation buffer B (25 ml Formamide, 12.5 ml 20x SSC and 0.1% Tween 20) and larvae were gradually brought back to PBS-T. Samples were incubated in 1x blocking reagent (Roche) and after 30 minutes the Anti-AP Fab fragments antibody (Roche) was added, followed by incubation for minimum 1 hour. Samples were washed several times with PBS-T and transferred into freshly mixed staining solution AP (100 mM NaCl, 50 mM $MgCl_2$, 100 mM Tris HCl pH 9.5 and 0.1% Tween 20). All samples were transferred to glass block wells and 4 µl of NBT/BCIP (Roche) in 600 µl of AP buffer was added. Staining was stopped by washing several times with PBS-T.

Larvae were either stored in 80% glycerol or discs were directly dissected and mounted on a Poly-L-Lysin slide (self-made) for imaging. Images were taken using the Axio zoom.V16 microscope with an Axiocam 506 colour camera (Zeiss, Germany).

Immunohistochemistry and confocal microscopy

Third instar larvae and prepupae were inverted/opened and fixed for 20 minutes in 4% formaldehyde in 1x PBS and washed several times with PBS - 0.2% Triton. For HA, the primary antibody, anti-HA High Affinity monoclonal rat antibody (Roche) in 1:100 and for *wg* 4D4 monoclonal mouse antibody (DSHB) (also 1:100) were used in 5% NDS. As secondary antibodies, Alexa Fluor 647 anti-mouse and Alexa Fluor 488 anti-rat (Invitrogen) were added 1:1000 in 5% NDS to the sample. All tissues were additionally stained with DAPI. Pictures were taken with the Confocal LSM 880 (Zeiss, Germany) and analysed using Fiji 2.0.0-rc-65/1.52b (Schindelin *et al*., 2012).

Developmental assays

For analysing the developmental timing from egg to pupae of the new *Wnt6* knockout lines, 30 eggs were collected from 1 to 2 hour egg lays and placed into a fly food vial. The vials were monitored throughout the following 145 hours twice a day and from 100 hours onwards every hour. The first appearance of pupae was noted for several *Wnt6* knockout lines and the control w^{1118}. Larval development was studied by collecting 100 eggs of several *Wnt6* knockout lines and a control and placing them on a fly food plate (5 cm diameter). Larvae were collected into 1.5 ml reaction tubes with PBS every 24 hours and heat shocked for 3 minutes at 65°C to make their bodies straight and imaging easier. Additionally, larvae were collected at all time points and fixed to measure the size of the imaginal discs. Pictures were taken using the Axio zoom.V16 with a Axiocam 506 color (Zeiss, Germany) and analysed using ImageJ 1.48v (Schneider *et al*., 2012), Fiji 2.0.0-rc-65/1.52b (Schindelin *et al*., 2012) and R version 3.2.0 (R core Team, 2013). For statistical testing a one-way ANOVA followed by a Tukey test were performed (see Statistics section above).

4.4 | Results and Discussion: The role of *Wnt6* in *Drosophila melanogaster*

4.4.1 | Analysing the *Wnt6*{KOd} function

Analysing the phenotype of the Wnt6{KOd} fly line

To better understand the function of *Wnt6*, the published *Wnt6* knockout line created by Doumpas *et al.* (2013), hereafter called *Wnt6*{KOd}, was re-analysed. To generate the *Wnt6*{KOd} line, the authors used the ends-out recombination method (Huang *et al*., 2008) to delete the whole first exon, which included mainly the 5'UTR and a very small section of the coding sequence (encoding part of the signal peptide), and replaced it with the mini-white marker under the control of an hsp70 promoter (Figure 4.4 A) (Doumpas *et al*., 2013).

First, the size of MP in *Wnt6*{KOd} homozygotes compared to controls were analysed. Here, MPs were dissected off the flies, flat mounted and area measurements were performed in the previous study (Figure 4.4 D; see Methods). No such measurements of MP were performed before. In contrast to the findings of Doumpas *et al.* (2013), it was found that the *Wnt6*{KOd} knockout flies did not completely lose the MP (Figure 4.4 B, C and D). However, their palps were significantly smaller (t-test $p<0.001$) and differed in shape compared to w^{1118} flies (Figure 4.4 B and C). The control MP have a bean-like shape, whereas the palps of *Wnt6*{KOd} flies were smaller and rounded (Figure 4.4 B and C). No significant differences were observed in the size of the 2nd leg tibia (Figure 4.4 F) or the male wing (Figure 4.4 E), indicating a similar body size for both fly lines. Only female wings of the *Wnt6*{KOd} line were slightly larger than the control line wings (Figure 4.4). It has to be noted, that these measurements on the wings were taken across the wing span, which did not take a different shape of the wing into account (see Methods). Therefore, it would be interesting to also measure the wing area or, using geometric morphometrics, measure the wing shape differences between the control and knockout fly lines.

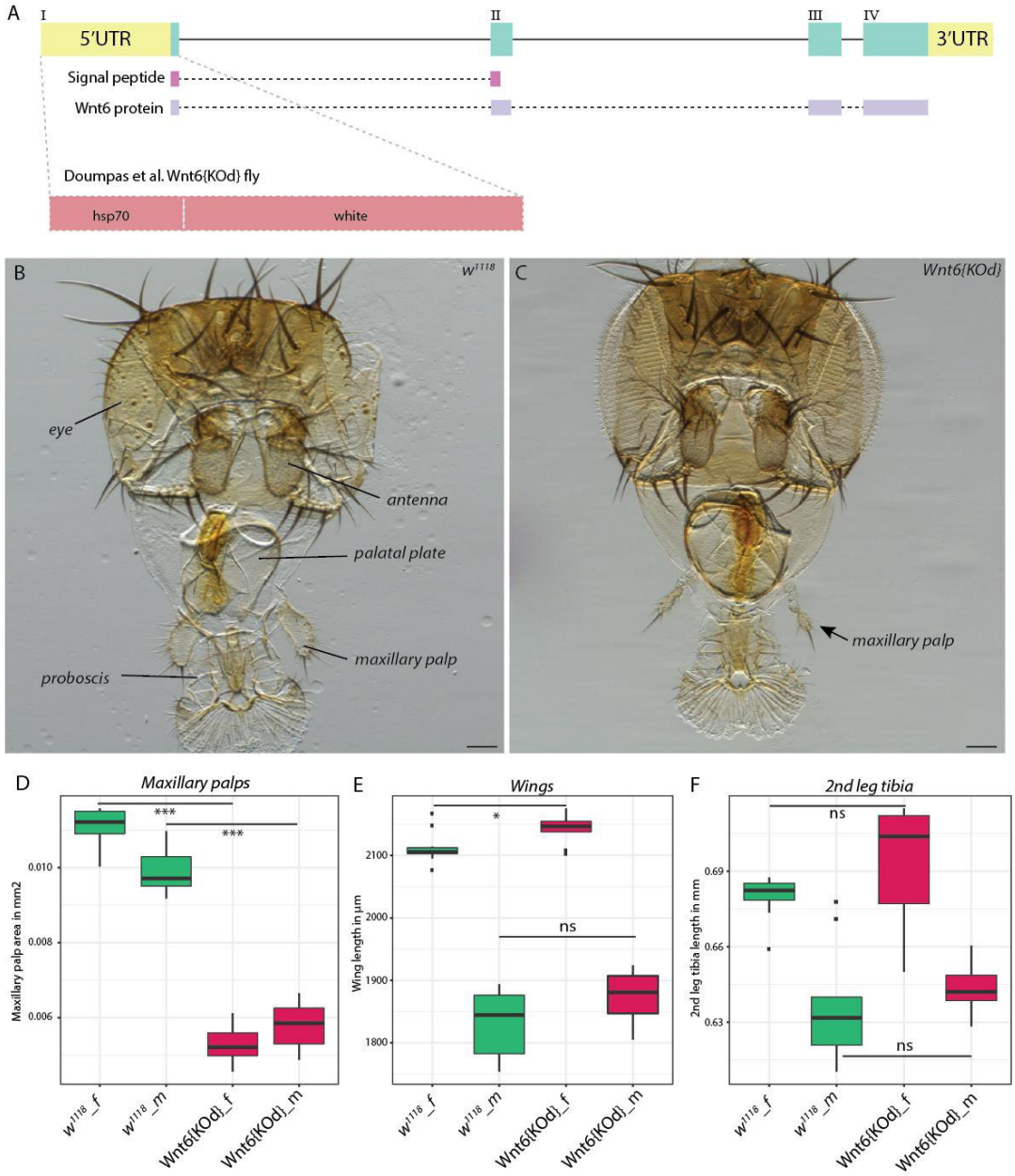

Figure 4.4 | Analysis of the *Wnt6*{KOd} fly line. **(A)** Genomic *Wnt6* locus showing the deletion of the first exon and replacement with the mini-white under control of the *hsp70* promoter. **(B)** Head mounts of a female from w^{1118} and **(C)** of a female from the *Wnt6*{KOd} line. **(D)** Measurements of the MP area in both analysed lines, **(E)** wing length and **(F)** the length of the 2nd leg tibia. All fly lines were collected at the same time and sample size for all lines and tissues n=10. Here, greater t-values indicating large differences between the two populations and show that the null hypothesis is incorrect, which means that the two tested populations are significantly different. f: female; m: male; *** p<0.001; * p<0.05; ns: non-significant. Scale bar 100 µm. Significances were tested using t-test ($t_{MPfemale}$=26.099; $p_{MPfemale}$<0.001; t_{MPmale}=16.127; p_{MPmale}<0.001; $t_{Legfemale}$= -1.8252; $p_{Legfemale}$= 0.09788; $t_{Legmale}$= -0.82434; $p_{legmale}$=0.428; $t_{Wingfemale}$= -2.7113; $p_{Wingfemale}$= 0.01455; $t_{Wingmale}$= -1.9408; $p_{Wingmale}$= 0.06941).

Overall, measuring the MP area revealed different results about MP loss as shown in the previous publication. A drastic decrease in MP size was observed whereas

small, malformed structures were still maintained. A potential effect on wing development needed to be further analysed by different wing size and shape measurements, such as wing area or geometric morphometrics. Further, an effect of the *Wnt6* knockout on the MPs was still present and further analysis regarding its function during the MP development was needed to understand its interactions during development.

Rescuing the Wnt6*{KOd} maxillary palp phenotype using the UAS/Gal4 system*

To test the role of *Wnt6* in MP development, the published rescue experiment was repeated first, where Doumpas *et al.* used the *elav*-Gal4 driver line together with an UAS-*Wnt6* line to rescue the *Wnt6*{KOd} phenotype (Doumpas *et al*., 2013). The authors showed that the ectopic expression of *Wnt6* under the control of *elav* was sufficient to rescue the loss of MPs. However, from the above-mentioned analysis, it was observed that the *Wnt6*{KOd} flies did not have a complete loss of MP. Therefore, it would be interesting to re-analyse the rescue experiment and determine the effect of *Wnt6* under the control of *elav* expression on the MP development.

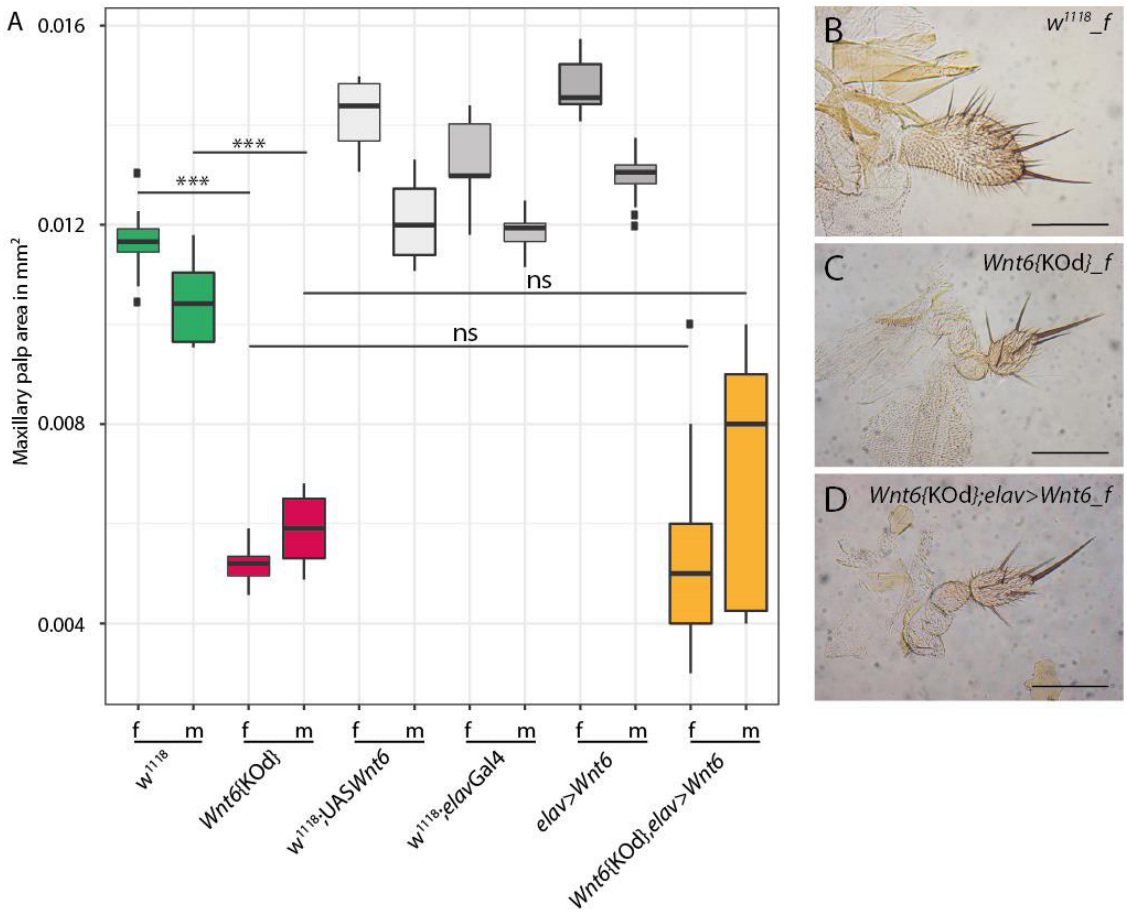

Figure 4.5 | Rescuing the MP development using *elav*-Gal4. **(A)** Shown are the measurements of MP areas for control MP (w^{1118}, green) and the *Wnt6*{KOd} (magenta), the control lines w^{1118};UAS-*Wnt6* and w^{1118};*elav*-Gal4 (grey), overexpression of *Wnt6* (dark grey) and the rescue cross *Wnt6*{KOd};*elav*-Gal4>UAS-*Wnt6* (yellow). **(B-D)** Microscopic pictures of dissected female MP. All samples were collected at a similar time. f: female; m: male; ns: non-significant; ***p<0.001. Scale bar 100 µm. Significances were tested using ANOVA (df=11; F-value=110.5) followed by a Tukey HSD test.

In contrast to previous findings (Doumpas *et al.* 2013), the overexpression of *Wnt6* under *elav* control in a *Wnt6* mutant background (*Wnt6*{KOd}) did not increase the size of the MP (Figure 4.5 A). Moreover, the shape of the MP did not change when *Wnt6* was ectopically expressed under the control of *elav* (Figure 4.5 B-E). The overexpression of *Wnt6* using *elav*-Gal4 in a wild-type background lead to no significant difference when compared to the control lines w^{1118};UAS-*Wnt6* and w^{1118};*elav*-Gal4 (all lines n=10). While both control lines and the overexpression cross were significantly different from the w^{1118} ($p<0.001$). It could be assumed, that the different genetic background of the UAS and Gal4 lines might cause these differences.

Note, that while *elav* was expressed in the nervous system as well as in the morphometric furrow in the eye imaginal disc (Robinow and White, 1988), it was not possible to detect expression of *elav* in the antennal field or MPF of the 3rd instar disc by *in situ* hybridisation (Supplement Figure S4.3). Thus, it could be concluded that *elav* was not expressed when MP were defined and therefore ectopic expression of *Wnt6* under the control of *elav* did not rescue the MP development, because ectopic *Wnt6* might not be present at the right time in the correct tissue. According to the pictures shown by Doumpas *et al.* the rescued palps look very much like the palps observed in the knockout line.

Since *elav* might not be an appropriate driver to rescue the *Wnt6* mutant phenotype, two other drivers of genes known to be involved in MP development were used: *homothorax* (*hth*) and *decapentaplegic* (*dpp*). First, *hth*-Gal4-driver together with UAS-*Wnt6* in the *Wnt6*{KOd} background was crossed. The expression of *hth* spread over the whole antennal part of the imaginal disc during L2 and L3, where expression could also be seen in the MPF (Supplement Figure S4.3). Still, no role in MP development was previously described for *hth*. Still, its expression in the MPF makes this gene an interesting candidate to test its involvement during MP development and use this driver line to ectopically express *Wnt6* in the MPF.

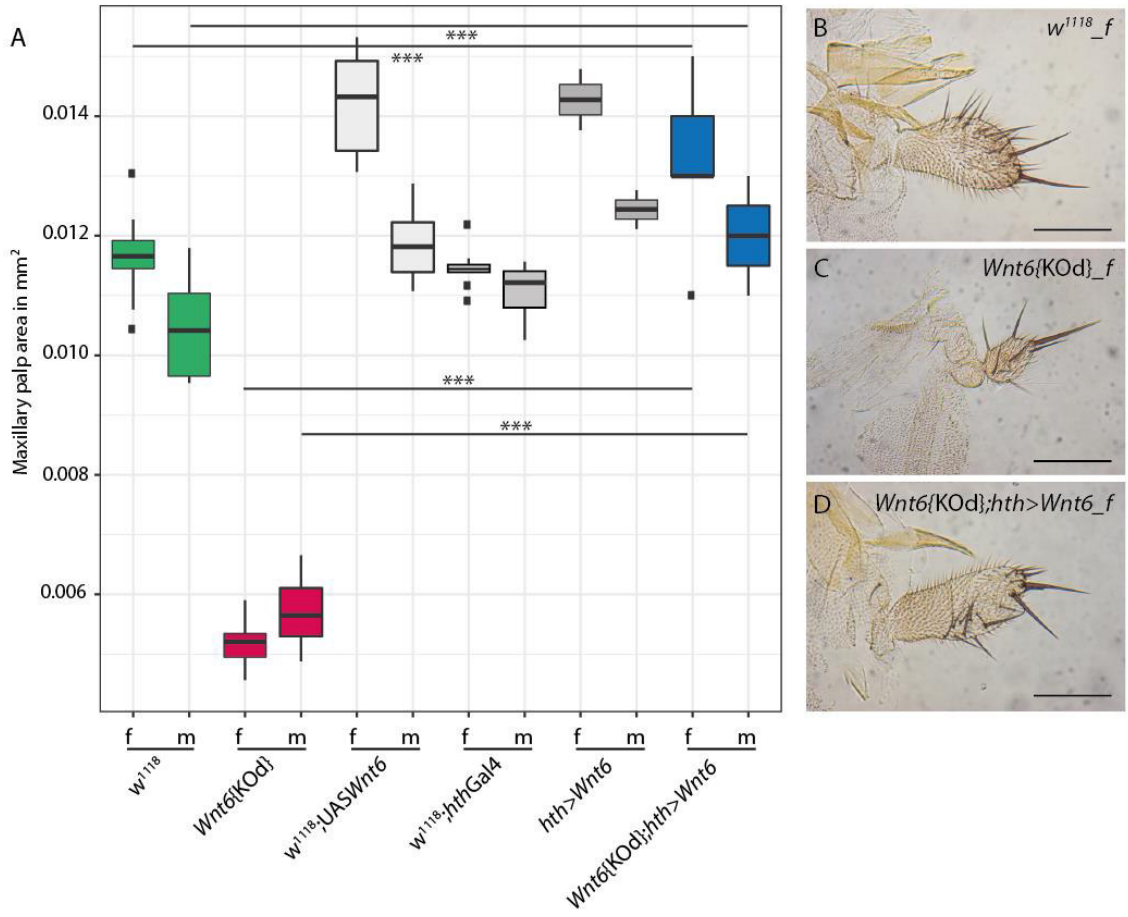

Figure 4.6 | Rescuing the MP phenotype of *Wnt6*{KOd} using *hth*-Gal4. **(A)** Measurements of the MP area in the control w^{1118} (green), the *Wnt6*{KOd} (magenta) the two control lines w^{1118};UAS-*Wnt6* and w^{1118};*hth*-Gal4 as well as the overexpression *hth*-Gal4>UAS-*Wnt6* (all grey) and the rescue cross (blue) are shown. **(B-D)** The dissected pictures of examples of all used lines. All samples were collected at a similar time. f: female; m: male; ns: non-significant; ***p<0.001. Scale bar 100 µm. Significances were tested using ANOVA (df=11; F-value=158.6) followed by a Tukey HSD test.

The *Wnt6*{KOd}; *hth*-Gal4>UAS-*Wnt6* progeny ($n_{females}$=11; n_{males}=11) showed a significant increase in the size of MP (F-value=158.6; p<0.001) and recovery of the wildtype shape of MP (Figure 4.6) when compared to *Wnt6*{KOd}. The F1 generation of the overexpression cross (both n=2), leading to ectopic expression of *Wnt6* under the control of *hth* in a wildtype background, also showed a significant increase in MP size compared to the w^{1118} (p<0.001). It had to be noted, that the control lines w^{1118};*hth*-Gal4 and w^{1118};UAS-*Wnt6* also had enlarged palps compared to the wildtype (all lines n=10). All of these lines, w^{1118};*hth*-Gal4, w^{1118};UAS-*Wnt6* and *hth*-Gal4>UAS-*Wnt6*, were not significantly different from each other except females from the overexpression and the w^{1118};*hth*-Gal4 control (p<0.001). Also, the difference of body size of all lines

between females and male was non-significant (Supplement Figure S4.5). The maxillary palps of males or females from w^{1118};*hth*-Gal4 were more similar to the size of w^{1118} MP, respectively. The MP of the overexpression progeny and the rescue flies were not significantly different.

Concluding from these results, using *hth*-Gal4 as driver was sufficient to ectopically express *Wnt6* in the right tissue and time to rescue the MP phenotype of the *Wnt6*{KOd} line. This confirms the assumption, that the *elav*-Gal4 line was not driving ectopic *Wnt6* expression at the right developmental time and in the correct tissue. Further, the *dpp*-Gal4 driver was used, where it is known that *dpp* was expressed in the MPF during development as well it had been shown that *dpp* was involved in MP development (Lebreton *et al*., 2008). Previous studies have shown, that ectopic expression of a thermosensitive *wg* mutant under the control of *dpp*-Gal4 lead to homeotic transformation of MP to antennae (Johnston and Schubiger, 1996). Also, massive malformations were observed in other head structures such as the eye and antennae as well as in legs and wings (Johnston and Schubiger, 1996). These results made the *dpp*-Gal4 driver an interesting candidate to test together with UAS-*Wnt6* to rescue the *Wnt6* knockout phenotype.

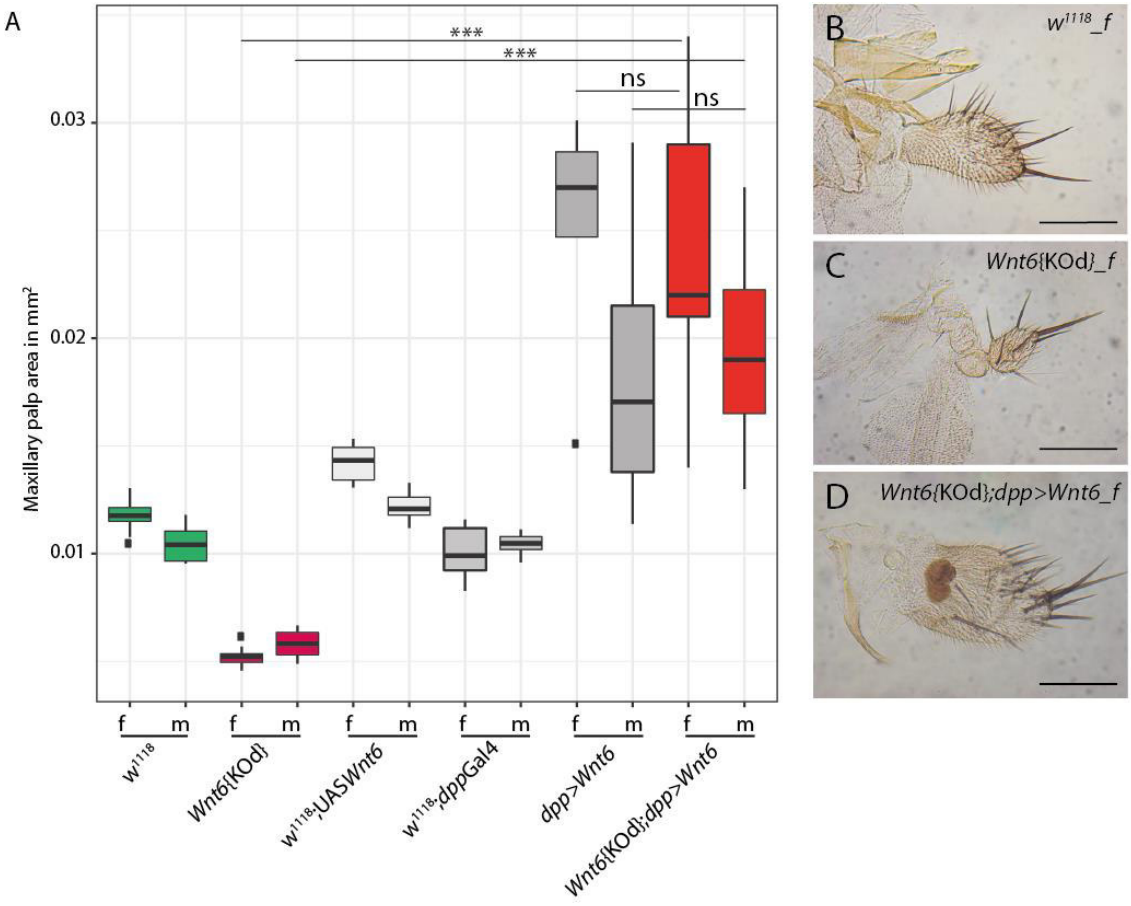

Figure 4.7 | Rescuing the MP phenotype of *Wnt6*{KOd} using *dpp*-Gal4. **(A)** MP areas of the control w^{1118} (green), the *Wnt6*{KOd} (magenta), the two control lines w^{1118};UAS-*Wnt6* and w^{1118};*dpp*-Gal4, the overexpression (*dpp*-Gal4>UAS-*Wnt6*) and the rescue *Wnt6*{KOd};*dpp*-Gal4>UAS-*Wnt6* (red). **(B-D)** Pictures of dissected female MP showing the w^{1118} and *Wnt6*{KOd} palps compared to the rescue palps. All samples were collected at a similar time. f: female; m: male; ns: non-significant; ***p<0.001. Scale bar 100 µm. Significances were tested using ANOVA (df=11; F-value=34.66) followed by a Tukey HSD test.

The ectopic expression of *Wnt6* under the control off *dpp*-Gal4 lead to overgrowth of MP, but also several other appendages, such as the antennae and legs, as well as caused malformed eyes (Figure S4.8). The MP were enlarged and truncated in *Wnt6*{KOd};*dpp*-Gal4>UAS-*Wnt6* ($n_{females}$=7; n_{males}=6) as well as in the overexpression in *dpp*-Gal4>UAS-*Wnt6* flies ($n_{females}$=5; n_{males}=10) compared to the control lines (all lines n=10) (Figure 4.8). In general, flies did not eclose from their pupal cases and had to be dissected out. *dpp* was one of the most important key factors in MP development, together with *wg* (Figure 4.2) and it was interesting that the ectopic expression of *Wnt6* under the control of the *dpp* regulatory regions had such a dramatic effect on MPs. However, while ectopic expression of *wg* lead to homeotic transformation of MP to

antennae it was not possible to see confidently the same effect for *Wnt6*. Therefore, it could be assumed that *Wnt6* did not have the same function during MP development as *wg* but potentially could interact with both key factors, *dpp* and *wg*.

Overall, the Gal4/UAS experiments have shown that *Wnt6* loss of function could not be rescued with the *elav*-Gal4 driver but with *hth*-Gal4 and *dpp*-Gal4. This implies that *Wnt6* was needed to be present from an early developmental time and also had to be ectopically expressed in the MPF to influence the development of MPs. It also could be confirmed, that *Wnt6* did have an influence on the MP size and shape whereas it remained unclear with which genes it was interacting. It would be great for future experiments to also dissect imaginal discs from pre-pupal stages of all above mentioned crosses and analyse expression of candidate genes from the MP developmental pathway using *in situ* hybridisations or immunohistochemistry. Using the MPF markers *deformed* or *proboscidia* could show variation in the MPF size due to loss of *Wnt6* or ectopic expression of *Wnt6* during larval development. Further, *wg* and *en* expression could be monitored in the context of loss or gain of *Wnt6* expression in the MPF.

4.4.2 | Creating a *Wnt6* knockout fly using CRISPR/Cas9 mediated homologous recombination

Given that the published *Wnt6* knockout generated by deleting the first exon did not appear to entirely remove the MP as previously reported (Doumpas *et al.* 2013) and the regulatory regions of Wnt genes were scattered through the cluster (Koshikawa *et al.* 2015). Also, it also has been shown, that regulatory elements could be located in exons and even quite a large proportion of regulatory elements could be found in coding sequences (Birnbaum *et al*., 2012; Ritter *et al*., 2012). It was decided to create a new *Wnt6* knockout line, with no deletion, and with the possibility to be further manipulated if required. The new *Wnt6* knockout line *Wnt6*{KOmche} or *Wnt6*{KO_flox} was created using CRISPR/Cas9 to insert a 1.5 kb long fragment in the coding sequence of *Wnt6* (see Methods) (Figure 4.3). This insertion was expected to lead to a disruption of the reading frame (Figure 4.8).

The success of the *Wnt6* knockout was tested using semi quantitative PCR (Figure 4.8 A), *in situ* hybridisation (Figure 4.8 B) and sequencing (Figure 4.8 C). The semi-quantitative PCR showed that *Wnt6* mRNA could not be detected in the *Wnt6*{KOmche} flies (Figure 4.8 A) compared to controls (asterisk, Figure 4.8 A), while no band was seen for the *Wnt6*{KOd}. However, in the *Wnt6*{KO_flox} line, a band of the expected size was detected (asterisk, Figure 4.8 A). In the floxed version of the CRISPR *Wnt6* knockout, the fluorescent marker was removed via the Cre/LoxP recombination system, which lead to a small remaining insertion of ~150 bp in the signal peptide of *Wnt6*. This insertion was still sufficient to create a frame shift, but it was possible to detect *Wnt6* mRNA in the *Wnt6*{KO_flox} line, whereas sequencing results have shown, that several stop codons (the first at position 28) in the mRNA would lead to a translation of a non-functional protein (Figure 4.8 C). However, due to the lack of any antibodies against *Wnt6* it was not possible to test if any protein was present.

In situ hybridisation was performed on the eye-antennal discs of the w^{1118} line, the *Wnt6*{KOmche} and the floxed version with probes for *wg* and *Wnt6*. Normal expression of *wg* and *Wnt6* was observed in the antennal and eye parts of the imaginal discs of w^{1118} (Figure 4.8 B) and normal expression of *wg* was detectable in all *Wnt6* knockout lines. However, consistent with the PCR result above, expression of *Wnt6* could only be observed faintly in *Wnt6*{KO_flox} line and no expression was detected in the *Wnt6*{KOmche} line (Figure 4.8).

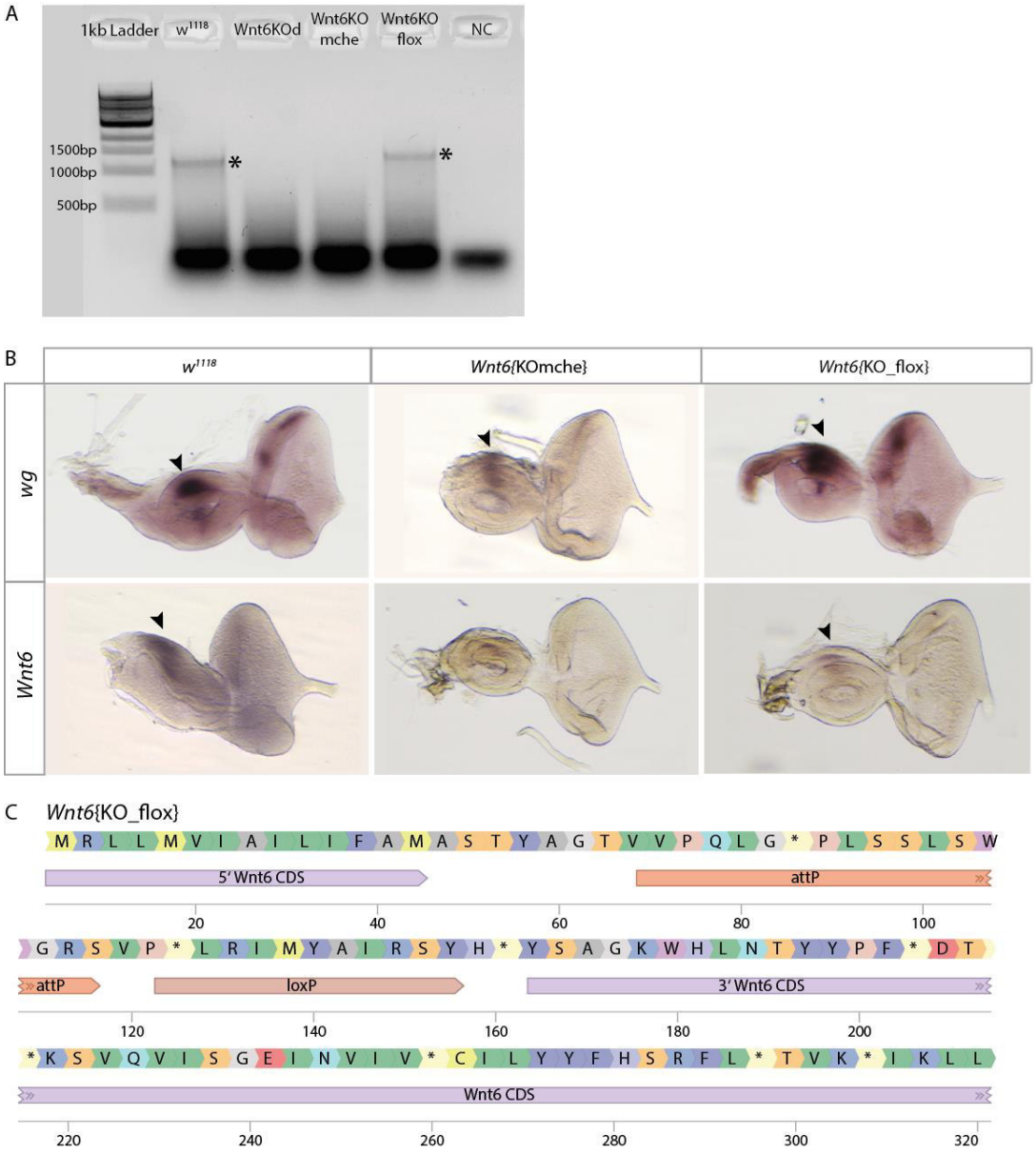

Figure 4.8 | Confirming the successful knockout of *Wnt6* in the *Wnt6*{KOmche} line. **(A)** Results of a semi-quantitative PCR showing the expected band for *Wnt6* transcripts at about 1.3 kb for w^{1118} (asterisk). **(B)** *In situ* hybridisations showing expression patterns of *wg* and *Wnt6* in the imaginal eye-antennal disc. **(C)** Sequence of *Wnt6* cDNA from the *Wnt6*{KO_flox} line. CDS: coding sequence; NC: negative control.

After confirming that the new *Wnt6* line likely lead to the loss of *Wnt6* function, the MP phenotype of the new line was analysed and compared to the control lines (all lines n=10). Surprisingly measurements of the MP revealed no significant reduction in MP size in the *Wnt6*{KOmche} line.

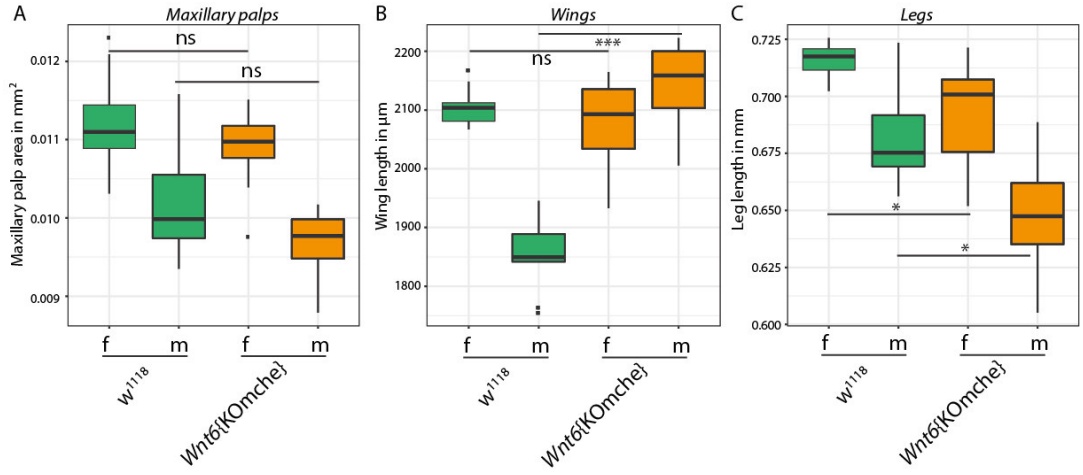

Figure 4.9 | Analysing the MP phenotype of the new CRISPR *Wnt6* knockout line. **(A)** Measurements of the MP area for w^{1118} (green), *Wnt6*{KOmche} (yellow) and *Wnt6*{KO_flox} (orange). **(B)** Wing length of the two *Wnt6* knockout lines and w^{1118}. **(C)** length of the 2nd leg tibia. ns: non-significant; *p<0.05; ***p<0.001. All fly lines were raised under controlled conditions and collected at the same time. Significances were tested using t-test, with great t-values indicating significant differences between tested populations ($t_{MPfemale}$= -1.3855, $p_{MPfemale}$= 0.1836; t_{MPmale}= -2.0263, p_{MPmale}= 0.06085; $t_{Wingfemale}$= -1.2933, $p_{Wingfemale}$= 0.2245; $t_{Wingmale}$= 8.3867, $p_{Wingmale}$<0.001; $t_{Legfemale}$= -2.7582, $p_{Legfemale}$= 0.02067; $t_{Legmale}$= -2.8709, $p_{Legmale}$= 0.01282).

No significant differences were observed in wing length between all analysed strains (all strains n=10) except that *w*^{1118} males had significantly shorter wings (p<0.001) than females which could be explained to a certain extent by the difference in body size between the sexes. Interestingly, this difference between females and male was lost in the knockout line which lead to non-significant different wing length between female and male flies. Note, that the wing length was taken across the wing from the branching of the longitudinal vein 2 and 3 until the end of longitudinal vein 3. Before it would be possible to find an explanation for this difference it would be necessary to remeasure these wings. Here, it would be important to measure the wing area or the wing shape. Both measurements could indicate if the increase in size might only be observed due to a difference in shape or if the wings were indeed larger than the control wings. The measurements of the 2nd leg tibia showed, that *Wnt6*{KOmche} males and females were significantly smaller (p<0.05) than males and females from the control line. It also showed that the difference between females and males from w^{1118}, i.e. males were smaller than females which was also observed for the *Wnt6* knockout line. This was an additional hint, that the measurements for the wings had to be further analysed before conclusions could be made.

Importantly, in comparison to the previously published *Wnt6*{KOd}, the newly designed CRISPR *Wnt6* knockout line did not show a decrease in MP size. This led to the question of how the two fly lines with *Wnt6* loss of function showed two different phenotypes.

4.4.3 Analysing the differences between the two *Wnt6* knockout lines

From the previous analysis, there were two confirmed *Wnt6* null mutants which did not show the same phenotype. The *Wnt6*{KOd} line was created by the ends-out recombination method, where the first exon was deleted and replaced with a mini-white marker (Figure 4.4). The new *Wnt6* knockout line *Wnt6*{KOmche} was generated using a CRISPR/Cas9 mediated knock-in of a fluorescent marker, but with no deletion of any endogenous sequence and it was confirmed with various tests that this was a true *Wnt6* knockout (Figure 4.3). So, it could be concluded that the only difference between the lines was the deletion of the first exon of *Wnt6* which included the 5'UTR and a small region encoding the signal peptide sequence (Figure 4.4). The question then arose if the deletion of the first exon was responsible for reducing MP size.

Analysis of the Wnt6*{KO} lines using deficiency lines*

To test whether the deletion of the first exon caused smaller MP or if an off-target effect was responsible, both *Wnt6* knockout lines were crossed to a deficiency line. The deficiency line Df(2L)BSC226 included a deletion on the left arm of the second chromosome from 7,249,632 to 7,366,119 (Figure 4.10 A), which removed the three Wnt genes D*Wnt4 (Wnt9)*, *wg* and *Wnt6* as well as a small region of the 5' end of *Wnt10*, and was therefore homozygous lethal.

When the *Wnt6*{KOd} line was crossed to Df(2L)BSC226, one chromosome had a full deletion of the *Wnt6* locus, whereas the other chromosome had only the deletion of the first exon. If the first exon was responsible for the MP phenotype it was expected to see a decrease in palp size, due to the homozygous deletion of the first exon sequence. If there were any off-target effects caused by the mutagenesis method, there should be no effect on MP size.

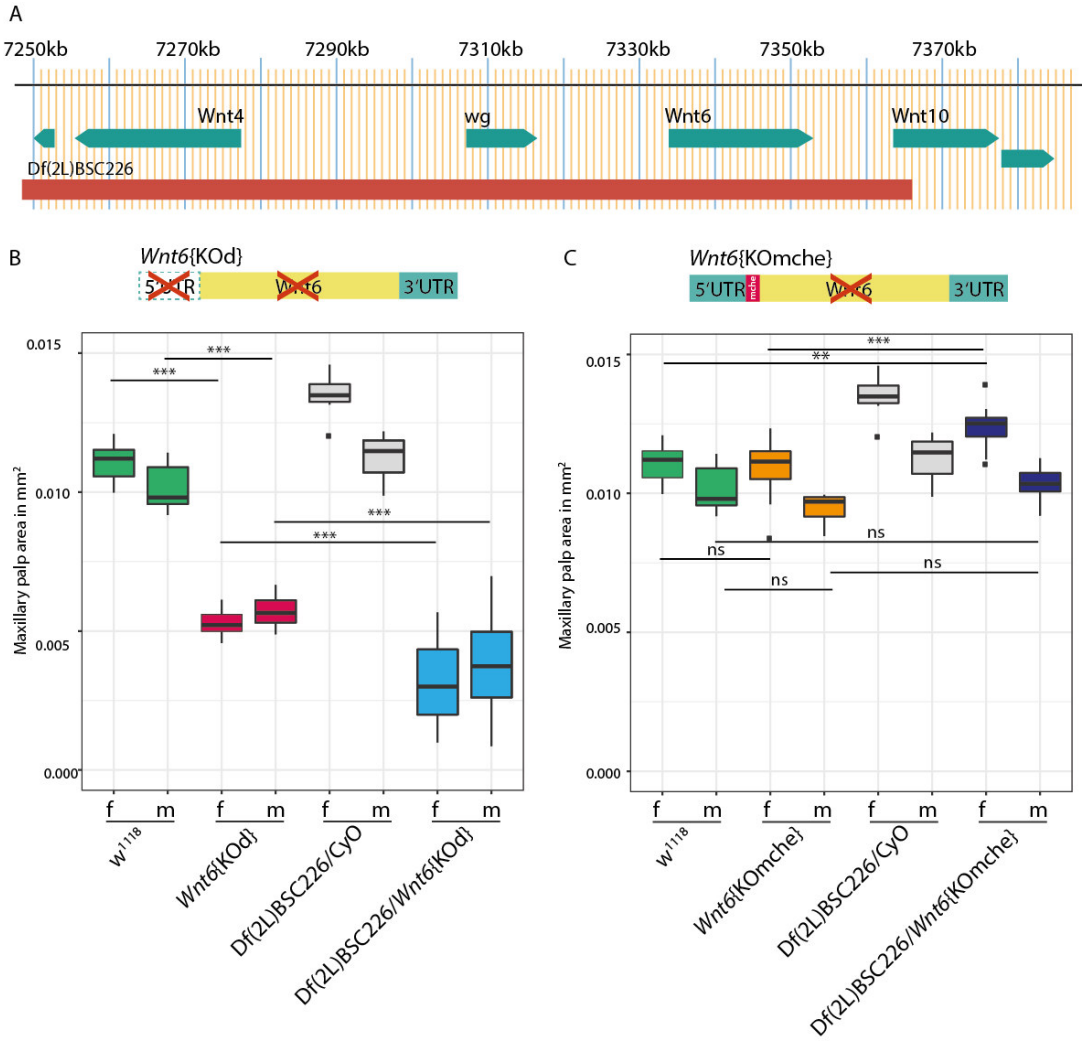

Figure 4.10 |Crosses of the two *Wnt6* knockout lines to the deficiency line Df(2L)BSC226. **(A)** Genomic location of the deficiency line Df(2L)BSC226 (marked in red). **(B)** Cross between the deficiency line and *Wnt6*{KOd}. **(C)** Cross between Df(2L)BSC226 and *Wnt6*{KOmche}. All fly lines were collected and dissected at the same time. The same controls were used for both plots. Genotypes of both *Wnt6* knockout lines are indicated with schematic drawings in (B) and (C). f: female; m: male; ns: non-significant; **p<0.01; ***p<0.001. Significances tested using ANOVA (df=7; F-value$_{Wnt6KOd}$=123.9; F-value$_{Wnt6KOmche}$=33.46) followed by a Tukey HSD test.

The Df(2L)BSC226/*Wnt6*{KOd} progeny (n_{female}=3; n_{male}=10) did have significantly smaller MP than any of the control lines (p<0.001) (all controls n=10). Interestingly, these MP were even smaller than the *Wnt6*{KOd} MP (Figure 4.10 B). The offspring of this cross now had not only a homozygous deletion of the first exon of *Wnt6* but, intriguingly, also a heterozygous loss of *wg*, which was an important factor in MP development and so the additional loss of one copy of *wg* could be responsible for the more severe truncation of MP in this genetic background. Additionally, maintaining the MP phenotype in this cross confirmed, that the MP phenotype in *Wnt6*{KOd} was not

caused by any off-target effect, but have arisen due to the deletion of the first exon of *Wnt6*.

Following this first cross, the new *Wnt6*{KOmche} line was also crossed to the deficiency line Df(2L)BSC226. The progeny from this cross will have the deficiency chromosome and one chromosome with the null mutation of *Wnt6* caused by the insertion, but with an intact first exon of *Wnt6* (Figure 4.10 C). Therefore, the offspring will be homozygous for the loss of *Wnt6* function but only heterozygous for the deletion of first exon of *Wnt6*. If loss of *Wnt6* protein itself was responsible for the smaller MP it was expected to observe this phenotype in this progeny. However, if the first exon deletion in the *Wnt6*{KOd} line was responsible for the smaller MP it would be expected to see normal MP in the progeny of this cross.

The F1 generation of Df(2L)BSC226/*Wnt6*{KOmche} (n_{female}=15; n_{male}=10) showed a very slight decrease in female palp size compared to Df(2L)BSC226/CyO ($p<0.01$) while male MP were not significantly different (all controls n=10) (Figure 4.10 C). However, it was unclear if this was caused by the loss of one of the *wg* alleles or due to the homozygous loss of *Wnt6* although the latter was very unlikely given the palp size of homozygous *Wnt6*{KOmche} flies. It was therefore concluded from this cross that the loss of *Wnt6* had no detectable effect on MP development in contrast to the effect of deletion of the first exon of *Wnt6* in the line *Wnt6*{KOd}.

Furthermore, the effects on MP size were tested when *Wnt6*{KOd} was crossed to *Wnt6*{KOmche}. Here, the resulting progeny was only missing the first exon on one chromosome while loss of *Wnt6* function was homozygous (Figure 4.11) and this experiment excluded any potential influence of the loss of the other Wnt genes in the deficiency line.

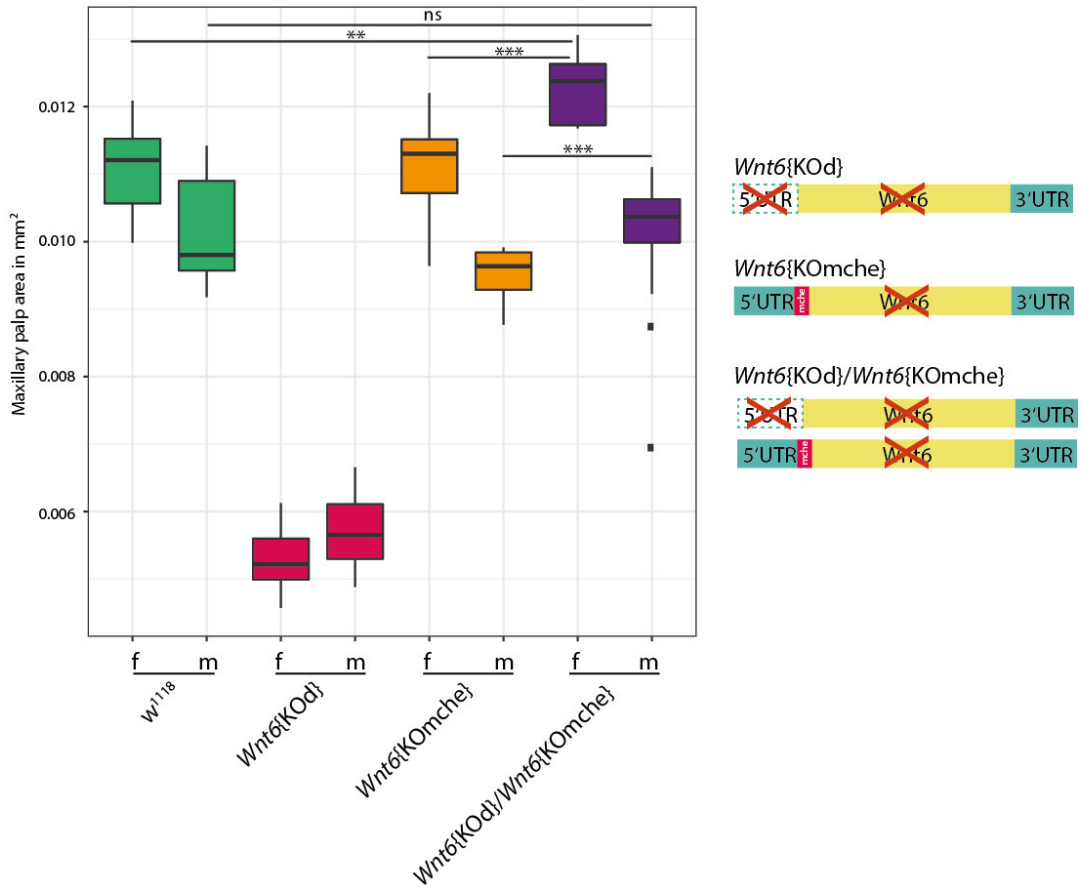

Figure 4.11 | Cross between both *Wnt6* knockout lines. Schematic drawings to the right indicate the genotype of both *Wnt6* knockout lines as well as from the cross of *Wnt6*{KOd}/*Wnt6*{KOmche}. Data for w^{1118}, *Wnt6*{KOd} ($n_{females}$=14) and *Wnt6*{KOmche} (n_{males}=13) were used from the previous crosses shown in Figure 3.10 which were performed at a similar time. All control lines n=10. f: female; m: male; ns: non-significant; **p<0.01; ***p<0.001. Significances tested using ANOVA (df=7; F-value=134.7) followed by a Tukey HSD test.

In *Wnt6*{KOd}/*Wnt6*{KOmche} flies (Figure 4.11) the MP were not reduced in size as observed for *Wnt6*{KOd}. Indeed, the data revealed that females from the *Wnt6*{KOd}/*Wnt6*{KOmche} cross showed a significant increase in MP size compared to the controls w^{1118} and *Wnt6*{KOmche} (p<0.01) Furthermore, females from *Wnt6*{KOmche} had enlarged MP compared to w^{1118}, although this difference was not significant.

These results suggested that loss of *Wnt6* function did not appear to result in smaller MP, but that the deletion of the first exon might instead be the cause of this phenotype. This would mean that *Wnt6* was not required for palp growth, but that the first exon of *Wnt6*, including the 5'UTR somehow regulated MP size independently of

Wnt6 protein function. However, it was difficult to reconcile these results with my previous results from the UAS/Gal4 crosses, where ectopic expression of *Wnt6* was partially sufficient to rescue MP size and suggested *Wnt6* generally contributes to growth, although given the effect of over expression of *Wnt6* on the legs this may be rather a general effect. These results also suggested that the first exon of *Wnt6* may contain regulatory elements that regulated gene(s) involved in MP development or that deletion of this region disrupted the function of other nearby enhancers used in MP development.

Given its crucial role in MP development and close genomic location to *Wnt6*, *wg* was one of the potential candidates to be able to interact with *Wnt6* or be regulated by enhancers hosted by *Wnt6*. Indeed it had already been suggested that *Wnt6* and *wg* could share regulatory elements (Harris *et al*., 2016). Another potential clue is that Doumpas *et al.* (2013) showed that Wg expression in the MPF was lost in their *Wnt6* knockout fly. At their time, this observation was explained due to a cross-reaction of the Wg antibody with Wnt6 protein in the developing MP (Doumpas *et al.* 2013). However, in light of my results the lack of Wg in the MPF could also mean that the deletion of the first exon of *Wnt6* disrupted Wg expression in MPF directly.

4.4.3 | Analysing the Wnt6 and Wg protein distribution in *Wnt6* knockout lines

To further investigate the potential effects of the deletion of the first exon of *Wnt6* on Wg localisation in the MPF, it was sought to better understand the expression of Wnt6 and Wg, in the developing MP. Since, no antibody was available for Wnt6, a 2xHA tag was introduced into the endogenous *Wnt6* locus after the signal peptide, using CRISPR/Cas9 (see Methods and Figure 4.3). The HA tag could then be detected by a HA antibody to reveal the location of the Wnt6 protein. Sequencing confirmed the correct in frame insertion of the HA tag with no disruption to the reading frame (Figure 4.12).

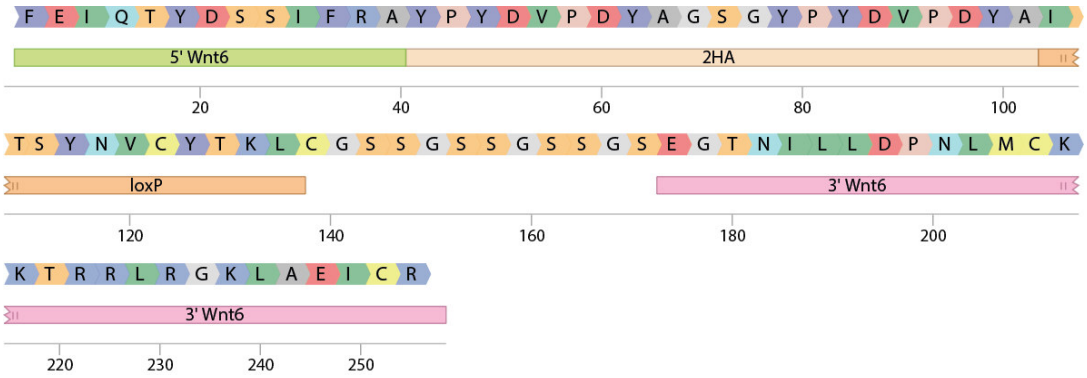

Figure 4.12 | Sequencing confirmation of the correct insertion of the HA tag into the *Wnt6* locus. Here, the sequencing result for the *Wnt6*{HA} fly line is shown. The HA tag was successfully inserted and there was no disruption of the reading frame. Some additional amino acids are also included which origin from the plasmid but do not influence the in-frame insertion.

Several tissues from 3rd instar larvae were dissected and stained with HA and Wg antibodies as well as DAPI to visualise the nuclei of all tissues. From these first staining, it could be concluded that it was possible to successfully tag the *Wnt6* locus with the HA-tag and detect Wnt6 protein in several tissues (Figure 4.13 and S4.4). Expression of Wg and Wnt6-HA in several larval tissues was presented in the Supplement (Figure S4.4). Here, the focus will be on the expression of Wnt6 and Wg in the antennal disc.

The antibody staining for Wg and Wnt6-HA revealed expression of both genes in the dorsal part of the antennal field of the pre-pupal eye-antennal disc (Figure 4.18). This expression was described previously for both genes based on mRNA *in situ* hybridisations (Janson *et al*., 2001). Additionally, expression could be seen for both proteins in the MPF (Figure 4.13, arrowhead). Therefore, the presence of both Wg (described previously by for example by Lebreton *et al.* (2008)) and Wnt6 in the MPF could be confirmed and was consistent with the assumption that they were involved in the development of MP.

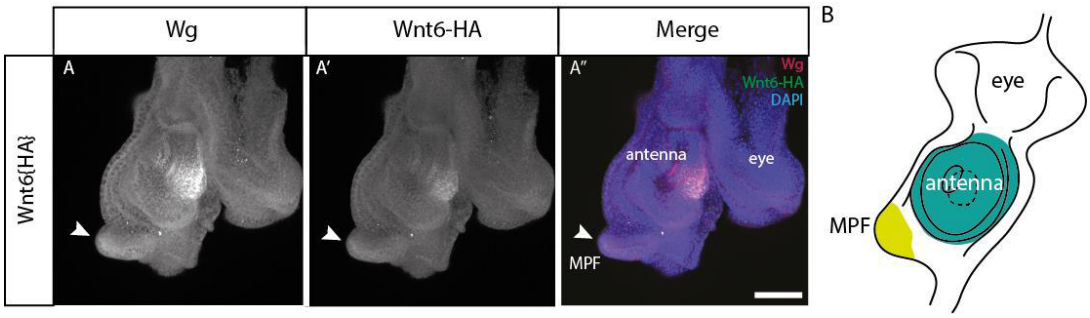

Figure 4.13 | Wg and Wnt6-HA protein localisation in the pre-pupal antennal disc. **(A-A'')** Shown is the antennal part of the eye-antennal disc which also includes the MPF at a pre-pupal or white pupae stage. Wg and Wnt6-HA expression can be detected in the antennal field but also in the MPF. **(B)** Schematic drawing of an eye-antennal disc which indicates disc orientation in all shown pictures. Scale bar: 100 µm.

Is the first exon of Wnt6 *an active regulatory region during MP development?*

In a next step, it was tested whether the first exon showed regulatory activity in MPF development during prepupal stages when *wg* and *dpp* were expressed. Conveniently, the FlyLight enhancer collection was available, which contains genomic sequences predicted to have an enhancer function cloned upstream of a Gal4-driver (Pfeiffer *et al.* 2008). Two lines containing either the full first exon of *Wnt6* (GMR25A04) or part of the first exon (GMR25A05) were analysed in combination with UAS-GFP line as the reporter (Figure 4.14 A). The exact genomic locations of these Flylight lines were shown in Figure 4.14 A indicating the overlap with the first *Wnt6* exon.

The cross with GMR25A04 which contains the full first exon of *Wnt6*, showed a GFP signal in the MPF during early pupal stages (Figure 4.14 B-E'). Here, several stages during the pre-pupal phase were shown from early stages (Figure 4.14 B) to late stages where pupae started to become already slightly brown in colouration (Figure 4.14 E). The GFP signal from the GMR25A05 line was slightly weaker and not as clear as seen for GMR25A04 in the MPF (Figure 4.14 F-G') and could also be seen at the rim of the antennal part of the disc (Figure 4.14 G-G').

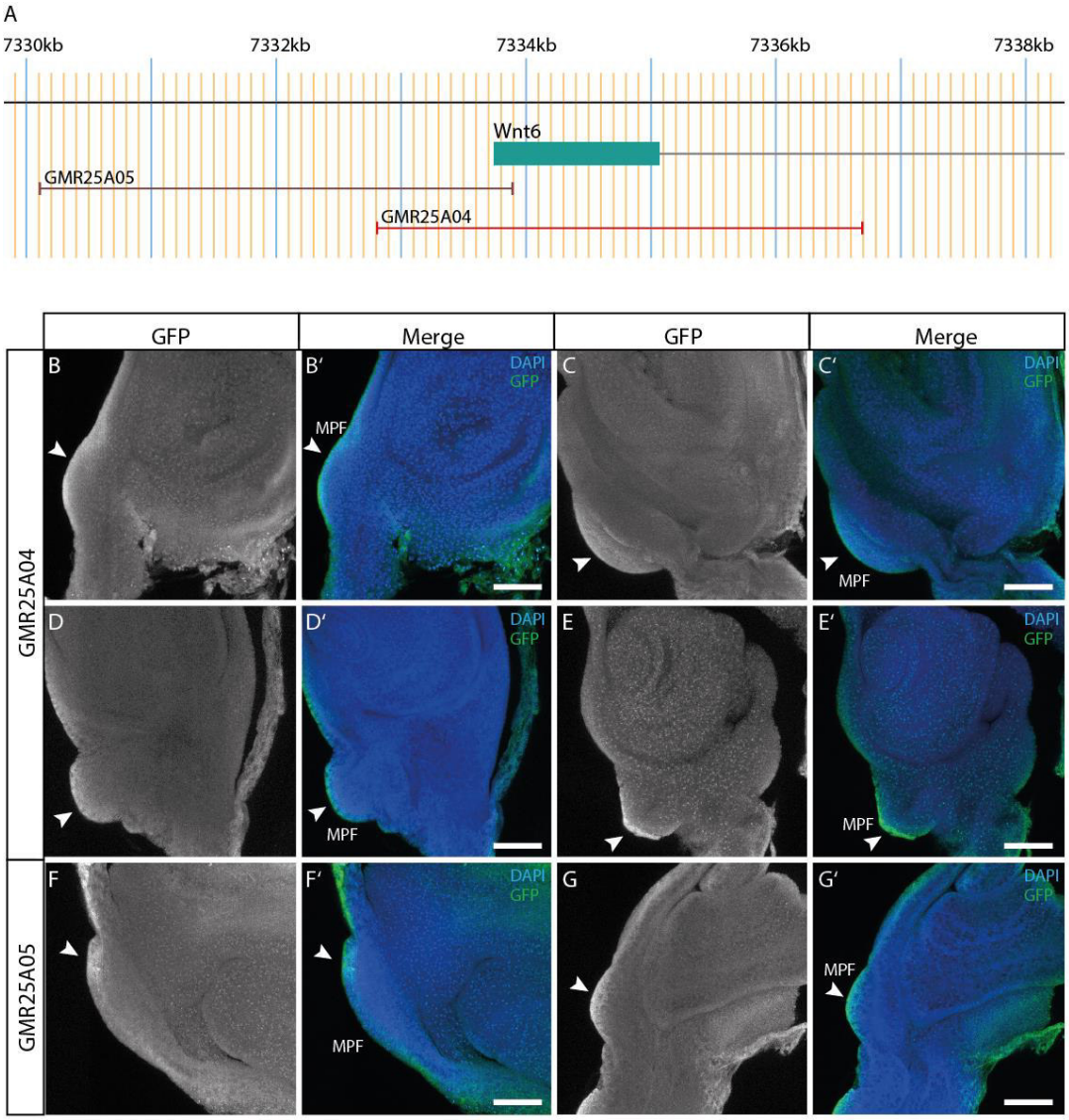

Figure 4.14 | Analysing the potential enhancer activity of the first exon of *Wnt6*. **(A)** Schematic overview of the genomic location of the FlyLight lines GMR25A04 and GMR25A05 with respect to the genomic *Wnt6* locus. **(B-E')** GFP expression of the GMR25A04 line in the pre-pupal antennal disc region. Early pre-pupal (B) and later pre-pupal stages are shown (E). **(F-G')** GFP expression in the line GMR25A05 in early pre-pupal antennal discs (F) and later stages (G). The location of the MPF is indicated in all merged pictures. Scale bar: 100 µm.

Overall, this experiment further suggested that the first exon of *Wnt6* might be active in the MPF and could drive the expression of a reporter. This GFP signal was also detectable around the same developmental stage where MP fate was determined by the very late *wg* expression (Lebreton *et al*., 2008). However, the genomic regions fused to the Gal4-drivers in the used lines were large and contain around 4 kb of genomic sequence. To further analyse which part of this region could actually be a potential enhancer for MP development, this region should be subdivided and analysed again.

This could be guided by analysing this region for conserved sequences throughout several species from the genus *Drosophila* since previous studies have been shown that potential enhancer sequences were conserved between closely related species (Basu *et al*., 2011; Pellegrini, 2012; Tagle *et al*., 1988). The so called "phylogenetic foot printing" could help to determine which regions were of interest by performing alignments and determine conserved regions between species (Basu *et al*., 2011; Pellegrini, 2012; Tagle *et al*., 1988).

Which gene in the developmental MP pathway is potentially affected by the potential regulatory function of the first exon?

Next, the loss of the first exon of *Wnt6* was studied which may influence the expression of other genes involved in the development of MP. It was previously shown by Doumpas *et al.* (2013) that expression of Wg changed in the MPF in their knockout line which contains a deletion of this part of *Wnt6*. They performed a Wg antibody staining on the *Wnt6*{KOd} line and compared the expression to a control line and observed a loss of Wg expression in the MPF. As mentioned above, the authors assumed that this was actually a loss of Wnt6 and not Wg, due to a cross reaction of the Wg antibody with the very similar *Wnt6* (Doumpas *et al.* 2013). If the cross-reaction was true, this would mean that any antibody staining done with the Wg antibody was non-specific to Wg and could detect also Wnt6, which would be a quite dramatic finding. To address this further the Wg antibody staining was repeated in the *Wnt6*{KOd} and *Wnt6*{KOmche}.

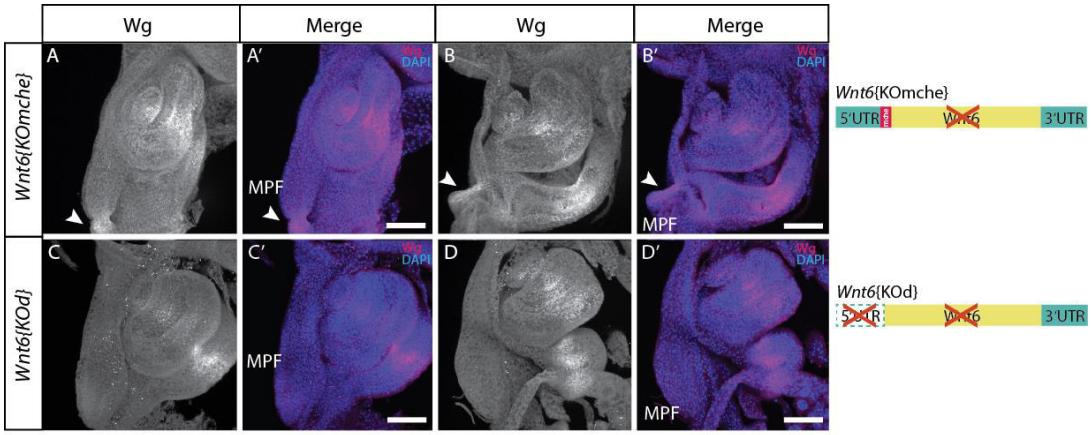

Figure 4.15 | Distribution of Wg protein in pre-pupal antennal discs in two *Wnt6* knockout lines. **(A-B')** Expression of Wg in the antennal disc of the newly created *Wnt6* knockout line using CRISPR (this study). Shown are two different stages during pre-pupal development. Early stages in (A-A') and later stages in (B-B'). **(C-D')** Wg expression in the antennal disc during pre-pupal stages. An early stage shown in (C) and a later one in (D). All pictures to the same magnification of 40x. Scale bar: 100 µm.

In all discs, the Wg expression in the dorsal part of the antennal disc could be seen, which indicated that the antibody staining worked in all cases and was detecting the expected expression of Wg (Figure 4.15). The antibody staining also revealed expression in the MPF during pre-pupal stages in the *Wnt6*{KOmche} line (Figure 3.15 A-B', arrowheads) while no Wg signal was observed in the MPF of the *Wnt6*{KOd} MPF (Figure 4.15 C-D'). It must be noted, that the development of the MPF in the *Wnt6*{KOd} line looked different compared to the controls and no protrusions were detected as seen for discs from the *Wnt6*{KOmche} line. This loss of the Wg signal in the *Wnt6*{KOd} line was consistent with the observations from Doumpas *et al.* (2013). However, Wg was present in the MPF in *Wnt6*{KOmche} discs, which could contradict the antibody cross-interaction explanation from Doumpas *et al.* (2013).

A possible explanation was, that the different mutations may be responsible for the different phenotypes observed in the two *Wnt6* knockout lines: loss of Wnt6 protein itself might not affected the late Wg expression in the MPF, normal development of MP occurred, and no reduced MP size was observed in adult flies (as seen for *Wnt6*{KOmche}). However, independently of the loss of Wnt6 protein, the deletion of the first exon of *Wnt6* might perturbed the late Wg expression needed in the MPF for correct development and resulted in a reduced MP size in adults (seen for *Wnt6*{KOd}).

Overall, my results indicated that loss of *Wnt6* alone probably didn't affect MP development while the first exon of the *Wnt6* locus did seem to have an effect. It was assumed that this region contained a regulatory element which could influence other gene(s) involved in the MP development. It also has been shown that regulatory enhancer elements could be present in coding sequences which could be possible in this present case (Birnbaum *et al.,* 2012; Ritter *et al.,* 2012). Indeed, from the last experiments (Figure 4.15), it was possible that the first exon of *Wnt6* influenced late *wg* expression in the MPF. Therefore, it would be very interesting in further experiments to show if the *wg* expression differs in these UAS/Gal4 crosses and therefore is influence by the different levels of *Wnt6*. However, it remained unclear how exactly this regulation worked and which exact sequence of the first exon had this activity.

Correlating the results from the knockout line *Wnt6*{KOmche} with the previous results from the UAS/Gal4 crosses, it could be assumed, that the loss of *Wnt6* did indeed not affect the MP development, but that the overexpression of *Wnt6* did overall affect the general growth of 'appendages' including the MP. This had been shown particularly clear for the *dpp*-Gal4>UAS-*Wnt6* cross, where malformations in several tissues occurred (Figure 4.7, Supplement Figure S4.8). In the light of the further analysis of the new *Wnt6* knockout line, the GAL4/UAS results also could show the influence of *Wnt6* on *wg* which would lead to a rescue of MP but also the massive malformations observed with the *dpp*-Gal4 driver. Therefore, it would be even more interesting if expression of wildtype *Wnt6* and *wg* would be analysed in all mentioned UAS/Gal4 crosses. The exact location and timing of expression for Wnt6 and wg could contribute the understand the MP development. Further experiments will be needed to analyse all these open questions including the staining for important factors such as *Wnt6*, *wg* and MPF markers (see section 4.5).

4.4.4 | Analysing the new *Wnt6*{KOmche} phenotype: developmental assays

Despite all previous experiments, it still remained unclear what *Wnt6* regulates during development in *D. melanogaster*. While performing the above experiments, it was

noticed that all of the *Wnt6* knockout lines appeared to develop more slowly than the control lines. Therefore, aspects of the developmental timing in all *Wnt6* knockout lines available were investigated.

Duration of larval development

First, the time needed for development until pupariation was measured for all knockout lines and a control fly line. Here, egg lays of 1 to 2 hours were set up and 30 eggs were collected into separate food vials. At least three replicates (R1-3) were collected for all analysed lines and the time to pupal formation recorded. The replicates of the analysed lines were not significantly different within each line (Figure 4.16 A), whereas all knockout lines, *Wnt6*{KOd}, *Wnt6*{KOmche} and *Wnt6*{KO_flox}, needed significantly more time to reach pupariation compared to the w^{1118} control (Figure 4.16 A and B). On average, the control larvae pupariated before 120 h AEL, whereas *Wnt6*{KOd} larvae pupariated between 120 h AEL and 130 h AEL, and both *Wnt6*{KOmche} and *Wnt6*{KO_flox} between 120 h AEL and 140 h AEL (Figure 4.16 A and B) i.e. all *Wnt6* knockout lines were delayed in their pupariation by 10 to 15 h.

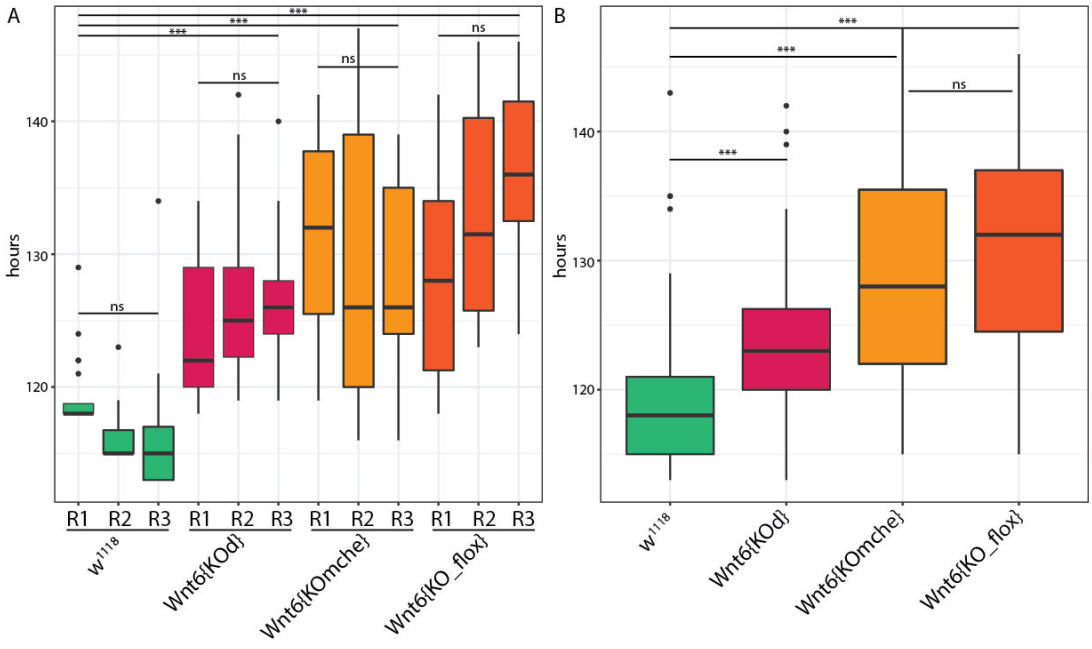

Figure 4.16 | Analysing the duration of larval development until pupariation. **(A)** The three replicates for the analysed lines are shown. All *Wnt6* knockout lines need significantly longer until larvae enter pupariation. **(B)** Summarized data for analysing the time needed until pupariation. ns: non-significant; ***p<0.001. Significances were tested using ANOVA (df=11; F-value=21.19) followed by a Tukey HSD test.

This led to the questions of why and when these larvae were delayed. Did embryos hatch from the eggs at a later time point? Did larvae grow more slowly and thus reach the critical mass later? Was the hormonal signal influenced which would lead to late pupariation?

Measuring larval size

From previous studies with reduced nutrition, it was known that starved larvae will pupariate later than well fed control lines. These flies also had smaller larvae, pupae and adults compared to a control line (Shingleton, 2010). Therefore, it would be interesting to understand if the delay in pupariation detected earlier was correlated to a reduced growth, and resulting therefore in smaller sized larvae, pupae and adult flies.

For these experiments, larvae from all above-mentioned fly lines were collected every 24 h AEL and the length of the larval body was measured (Figure 4.17). All lines reached the third instar larvae around 96 h AEL and no significant size differences were observed until then. Only around 120 h AEL, when pupariation should start, significant differences in size were observed. All *Wnt6* knockout lines had larger larval body length than the control line. It must be noted that the control larvae at 120 h were smaller compared to 96 h larvae of the same line. However, for w^{1118} pupariation had already happened for most of the larvae at 120 h AEL and only a few remaining larvae were measured for this timepoint. These remaining larvae might have reached the critical mass later, had smaller body size and will pupariate later then the majority of w^{1118} larvae. As already seen in the pupariation analysis (Figure 4.16) the exact timing of pupariation varies within each strain between several hours. The significant differences between w^{1118} and all *Wnt6* knockout lines at 120 h AEL could be explained by this variation. Also, no significant size differences were observed between all *Wnt6* knockout lines at 96 h or 120 h AEL (Figure 4.17). Still, it was possible to collect larvae for the *Wnt6* knockout lines *Wnt6*{KOmche} and *Wnt6*{KO_flox} which were significantly larger than the control w^{1118} at 96 h or 120 h AEL ($p<0.001$) (Figure 4.17).

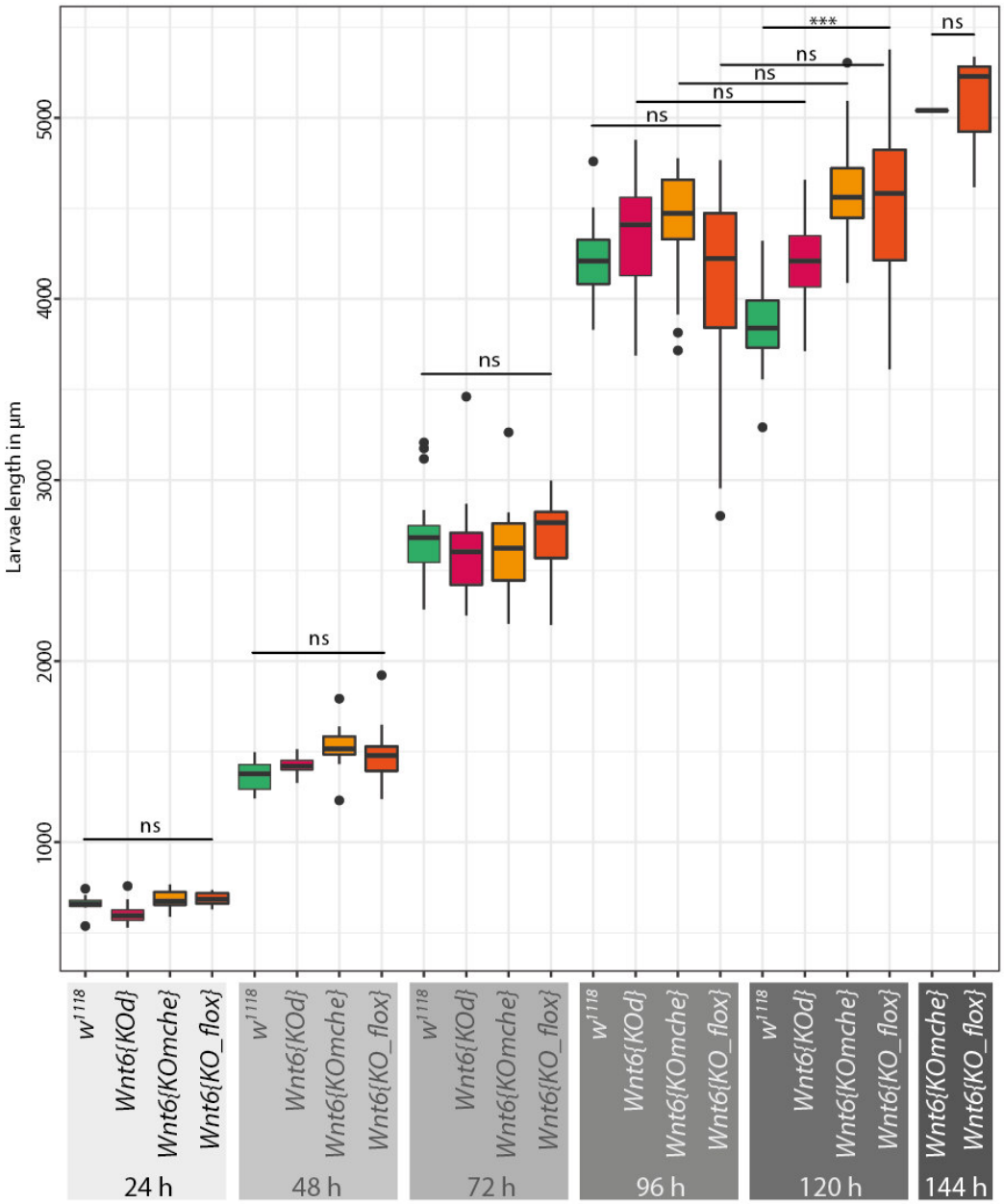

Figure 4.17 | Analysis of the larval length over time in control and *Wnt6* knockout lines. Larval length was measured every 24 h AEL. These measurements were taken for the control w^{1118}, *Wnt6*{KOd}, *Wnt6*{KOmche} and *Wnt6*{KO_flox} lines. AEL: after egg lay; h: hours; ns: non-significant; ***p<0.001. Significances were tested using ANOVA (df=26; F-value=644.8) followed by a Tukey HSD test.

During normal growth, larvae reached the critical mass when entering the third instar larval stage which would lead to an increased hormone production. One of the important hormones was ecdysone which is also involved in triggering the pupariation signal in late third instar larvae by a very high peak in its concentration. It was unclear which factors and components of this signal were influenced by the loss of *Wnt6* and several further experiments would be needed to analyse these observations.

4.5 | Conclusions and outlook

A potential regulatory role of the first exon of Wnt6*.*

In the first part of this chapter, a potential role of the first *Wnt6* exon in regulating maybe the late expression of *wg* during maxillary palp development was suggested. To analyse this assumption further, a more detailed examination of this region would be helpful. First, it could be interesting to repeat the cross with the FlyLight lines but use the same UAS-GFP line (BDSC#32185) that was used in the original publication and gives a quite specific signal (Pfeiffer *et al*., 2008). Also, an additional antibody staining for Wg could be performed on the same discs to indicate the expression of this gene in MPF. Second, it would be interesting to split this ~1.5 kb region up into smaller parts and test their activity with the UAS/Gal4 system in the MPF. The decision into which parts to split this region should be based on the so-called phylogenetic profiling (Basu *et al*., 2011; Pellegrini, 2012; Tagle *et al*., 1988). Here, with the help of an alignment of several *Wnt6* sequences from several *Drosophila* species, the regulatory region could be narrowed down.

Furthermore, the question remained if Wg might be the target of this putative enhancer in the first exon of *Wnt6*. Here, stains for *Wnt6* and wg as well as several of the MPF marker genes such as *dfd* and *pb* would be very informative about the expression dynamics in the MPF in all used UAS/Gal4 crosses. Especially visualising expression of *wg* in the context of the UAS/Gal4 crosses could indicate the potential influence of *Wnt6* on *wg* expression. Further, it was proposed to perform a rescue cross for the *Wnt6*{KOd} MP phenotype. This cross would include: (1) crossing a UAS-*wg* into the *Wnt6*{KOd} fly. (2) cross also the Gal4 FlyLight line GMR25A05 into the *Wnt6*{KOd} background and perform the final rescue cross where in the *Wnt6*{KOd} background the GMR25A05 construct (including the full first exon of *Wnt6*) would express UAS-*wg*. The presence of the GMR25A05 construct should facilitate as a rescue of the deleted site in the *Wnt6*{KOd} line and it is assumed that this region does activate Wg expression in the MPF, normal MPs could be seen in the adult F1 flies from this cross.

Wnt6 might be involved in regulating the signal to pupate

In the second part of this chapter it was observed, that in all *Wnt6* knockout lines the pupariation was delayed compared to a control. To understand if the delayed pupariation was correlated with an overgrowth of imaginal discs, proper measurements of the discs were needed. Here, it would be possible to dissect discs and dissociate the cells for counting (Bryant and Levinson, 1985; Bryant and Simpson, 1984). This method could also be combined with analysing if not only the number of cells was affected, but also if the size of the cells was different. Analysing the total weight of larvae, could also give a first clue about differences in size in the *Wnt6* knockout lines (Garelli *et al*., 2012). Additionally, the number of mitotic cells could be determined with a phosphor histone H3 (PH3) staining. An increased growth rate could also show larger number of mitotic cells (Martin and Morata, 2006).

Furthermore, it was previously proposed that the larval wing disc size was equal to the adult wing size. Therefore, measuring adult wings, including not only length but also area could also indicate an overgrowth of discs during larval development (Aegerter-Wilmsen *et al*., 2007). If the loss of *Wnt6* did have an effect on normal growth, it also could be possible to analyse the expression or levels of *dpp*, which is an important factor during growth (Aegerter-Wilmsen *et al*., 2007; Martin and Morata, 2006; Shingleton, 2010). In addition, if *Wnt6* did influence the pupariation signal itself and not the growth, it would be interesting to analyse the levels of hormones such as ecdysone and the juvenile hormone in the *Wnt6* knockout lines. The levels of these hormone could be determined by the haemolymph of the third instar larvae, around the time when pupariation would be expected (Borst *et al*., 1974; Riddiford *et al*., 2010; Shingleton, 2010; Yamanaka *et al*., 2013).

4.6 | Supplement

Supplement Table S4.1 | Stocklist of all used fly lines with their full genotypes, commercial stock numbers and sources. MH: Michaela Holzem; BDSC: Bloomington Drosophila Stock Centre

Stock	**Stock number**	**Genotype**	**Source**
DB	-	w-;if/cyo;MKRS/TM6b	Lab stock
Df(2L)BSC226	BDSC#9703	w[1118]; Df(2L)BSC226/CyO	Bloomington
dpp-Gal4III	BDSC#67066	w*; P{UAS-3xFLAG.dCas9.VPR} attP40, P{tubP-GAL80ts}10/CyO; P{GAL4-dpp.blk1}40C.6/TM6B, Tb1	Bloomington
elav-Gal4 III	BDSC#8760	w[*]; P{w[+mC]=GAL4-elav.L}3	Bloomington
GMR25A04	BDSC#45137	w[1118]; P{y[+t7.7] w[+mC]=GMR25A04-GAL4}attP2	Bloomington
GMR25A05	BDSC#45138	w[1118]; P{y[+t7.7] w[+mC]=GMR25A05-GAL4}attP2	Bloomington
hs-cre	-	w-;hs-cre w+/cyo;TM2/TM6B	Alberto Baena-Lopez
hth-Gal4 III	BDSC#62588	w^{1118}; PBac{IT.GAL4}hth0035-G4/TM6B, Tb1	Bloomington
if/cyo UAS-Wnt6	-	w-;if/cyo;UAS-Wnt6/UAS-Wnt6	MH
if/cyo;elav-Gal4	-	w-;if/cyo;elav-Gal4/(TM6b)	MH
nos int;if/cyo	-	Nos int;if/cyo;	MH
SB	-	w-;sp/cyo;	Lab stock
UAS-Wnt6 III	-	w-;;UAS-92/UAS-Wnt6	A. Teleman
w^{1118}	-	Wildtype *D. melanogaster*	Lab stock
Wnt6HA-M1Ma/(CyO)	-	w-;Wnt6HAmche/(CyO)	MH; BestGene
Wnt6HA-M1Mb	-	w-;Wnt6HAmche	MH; BestGene
Wnt6KOd stock	-	w-;Wnt6KO/Wnt6KO;	A. Teleman
Wnt6KOd;MKRS/TM6b	-	w-;Wnt6KO/Wnt6KO;MKRS/TM6b	MH
Wnt6KOd-elavGal4	-	w-;Wnt6KO/Wnt6KO;elav-Gal4/(TM6b)	MH
Wnt6KOd-UAS Wnt6	-	w-;Wnt6KO/Wnt6KO;UAS-Wnt6/(TM6b)	MH
Wnt6KO-F3	-	w-;Wnt6KOmche/Wnt6KOmche	MH; BestGene
Wnt6KO-F3-F (floxed)		w-;Wnt6KO/Wnt6KO	MH
Wnt6KO-M4	-	w-;Wnt6KOmche/Wnt6KOmche	MH; BestGene
Wnt6KO-M4-F (floxed)		w-;Wnt6KO/Wnt6KO	MH

Supplement Table S4.2 | Primer list. All used primer in this study are shown with their optional 5' overhangs, their sequence from 5' to 3' as well as the Primer number. The primer number refers to my personal primer list available to the McGregor lab members.

Name	**Primer No.**	**5'-3' overhang**	**5'-3'**
GT Wnt6 cDNA F	98		ATGCGTTTGCTCATGGTAATTGCAA
GT Wnt6 cDNA R	99		TCAGAGGCAGGTGTTGACCG
dfd ISH F	480	ggccgcgg	TGCGGTGTGATGATATGGGA
dfd ISH R	481	cccggggc	CGGATAAGAGCTGGTCGTCT
HA seq R	117		CGCGCATTAAGATTTTCCTCATG
KOmcheseqF	105		GCACACGTCAACGGTATTCA
hth ISH F	294	ggccgcgg	CATGTACGATCCACACGCC
hth ISH R	295	cccggggc	CAGTGGACCGGGAGTACTAC
dpp ISH F	296	ggccgcgg	AGAGATTCATCGCCGCCATA
dpp ISH R	297	cccggggc	TTGGGGATGTTGACCGAGTC
elav ISH F	237	ggccgcgg	CGCAGGTCTACATCGATCCT
elav ISH R	238	cccggggc	TCGTTGTGGGATCCTTGACA
gRNA Wnt6KO F	201	GTC	GACTGGATTCGGCTGGTAAG
gRNA Wnt6KO R	202	AAAC	CTTACCAGCCGAATCCAGTC
gRNA Wnt6HA F	203	GTC	GCCCTCCGCCCTGAAAATAG
gRNA Wnt6HA R	204	AAAC	CTATTTTCAGGGCGGAGGGC
wg ISH fwd	165	ggccgcgg	CTCCCGGGAATTCGTCGATA
wg ISH rev	166	cccggggc	TTTTGGTCCGACACAGCTTG
Wnt6 ISH fwd	167	ggccgcgg	GATGCTGCGACAACAAATGC
Wnt6 ISH rev	168	cccggggc	CACTTTTCGCAGGTCACCTC
Wnt6KO HR5´F	86	GTTAACCGGAATTC	CCTCGAATGTGTGCGTCTTG
Wnt6KO HR5' R	87	GTTAACCGGCTAGC	CATTGCGAATATTAAAATTGCA ATTACCAT
Wnt6KO HR3' F	88	GTTAACCGACTAGT	ATTCGGCTGGTAAGTGGCATT TAAATAC
Wnt6KO HR3' R	89	GTTAACCGTTAATTAA	ACTTGTGTGTTAGAAGGAAGCCCC
Wnt6HA HR5´F	78	CCCGGGCTAATTATG GGGTGTCGCCCTTCG	ACGTTCACACATACTTGCT CCCACCAATAT
Wnt6HA HR5' R	79	TCCTGCATAGTCAGG GACGTCGTAGGGATA	CGCCCTGAAAATAGAGGAA TCATAGGTTTG
Wnt6HA HR3' F	125	AGTTCGGGGTCCAGCGGT TCTTCAGGCAGT	GAGGGCACCAACATCCTTCT
Wnt6HA HR3' R	126	GTCGCCCTTGAACTC GATTGACgctcttcG	GGCTCATTTCAGGCGCTATT

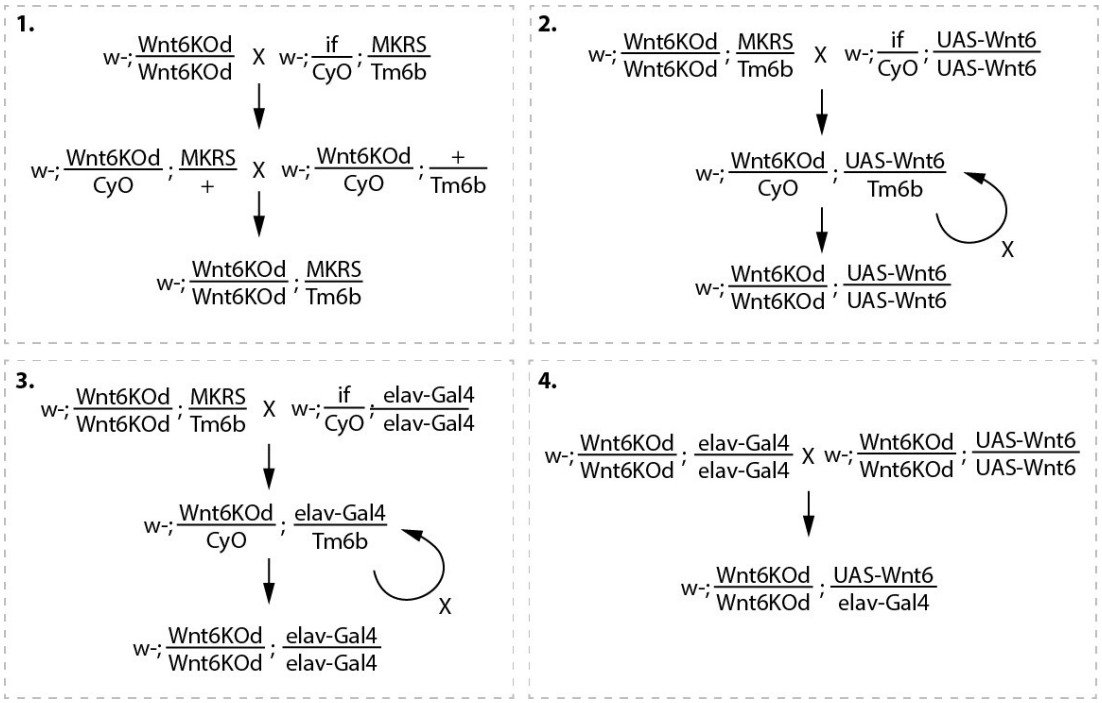

Supplement Figure S4.1 | Crosses for rescuing the *Wnt6*{KOd} phenotype using the UAS/Gal4 system. (1.) Balancing the third chromosome of the *Wnt6*{KOd} fly line. (2.) Crossing UAS-*Wnt6* into the balanced *Wnt6*{KOd} line. (3.) Crossing *elav*-Gal4 into the *Wnt6*{KOd}. (4.) Final UAS/Gal4 cross example for *elav*-Gal4 and UAS-*Wnt6*.

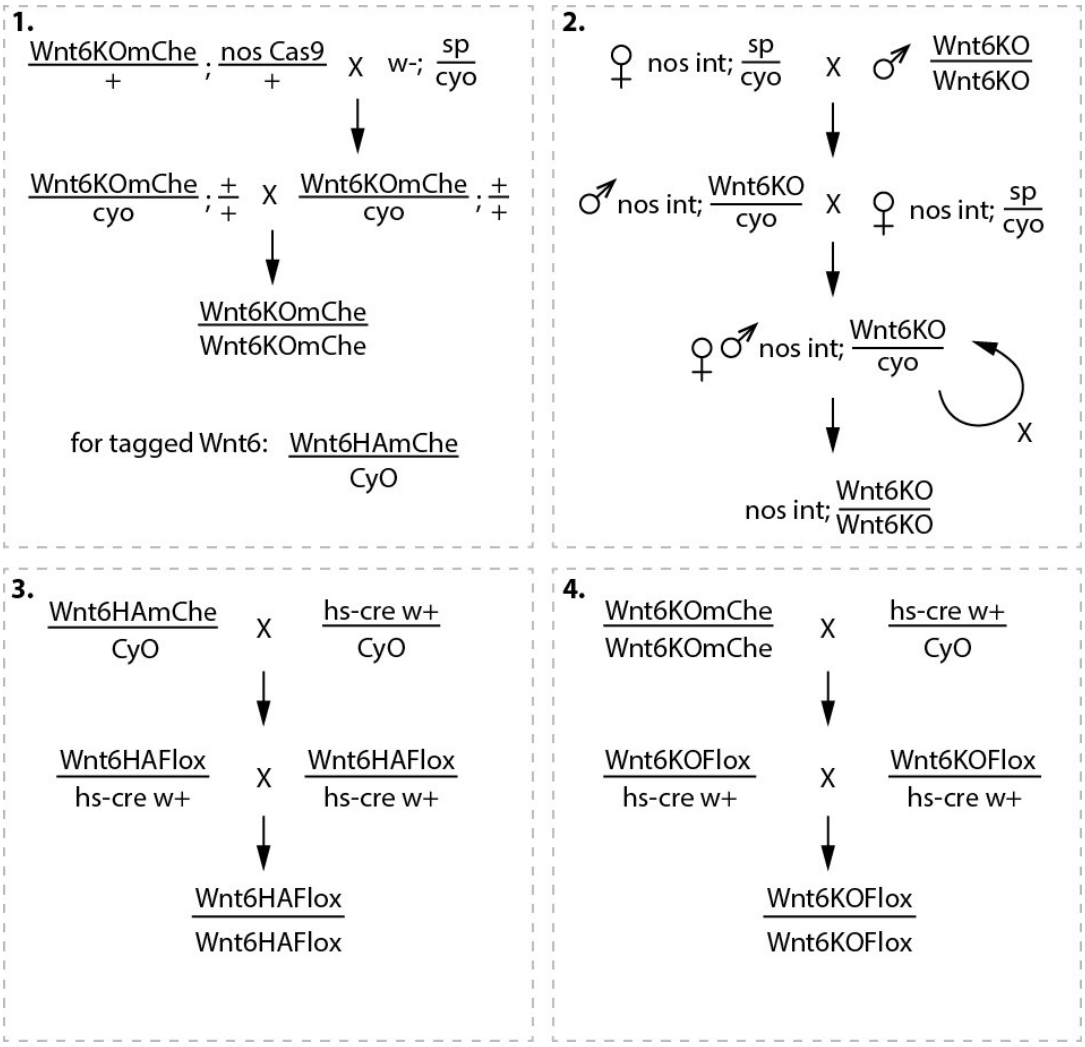

Supplement Figure S4.2 | Balancing and 'floxing' crosses of the CRISPR generated *Wnt6KO* and HA tag flies. (1.) Crossing scheme for the F1 generation of the transgenic *Wnt6* knockout created by CRSIPR/Cas9. The same crossing scheme was performed for the tagged *Wnt6* flies. (2.) Crossing the nanos-integrase into the newly created *Wnt6* knockout line for further recombination experiments. (3.) Floxing the mCherry marker cassette out of the HA tagged *Wnt6* line or the newly created *Wnt6*{KOmche} strain (4.).

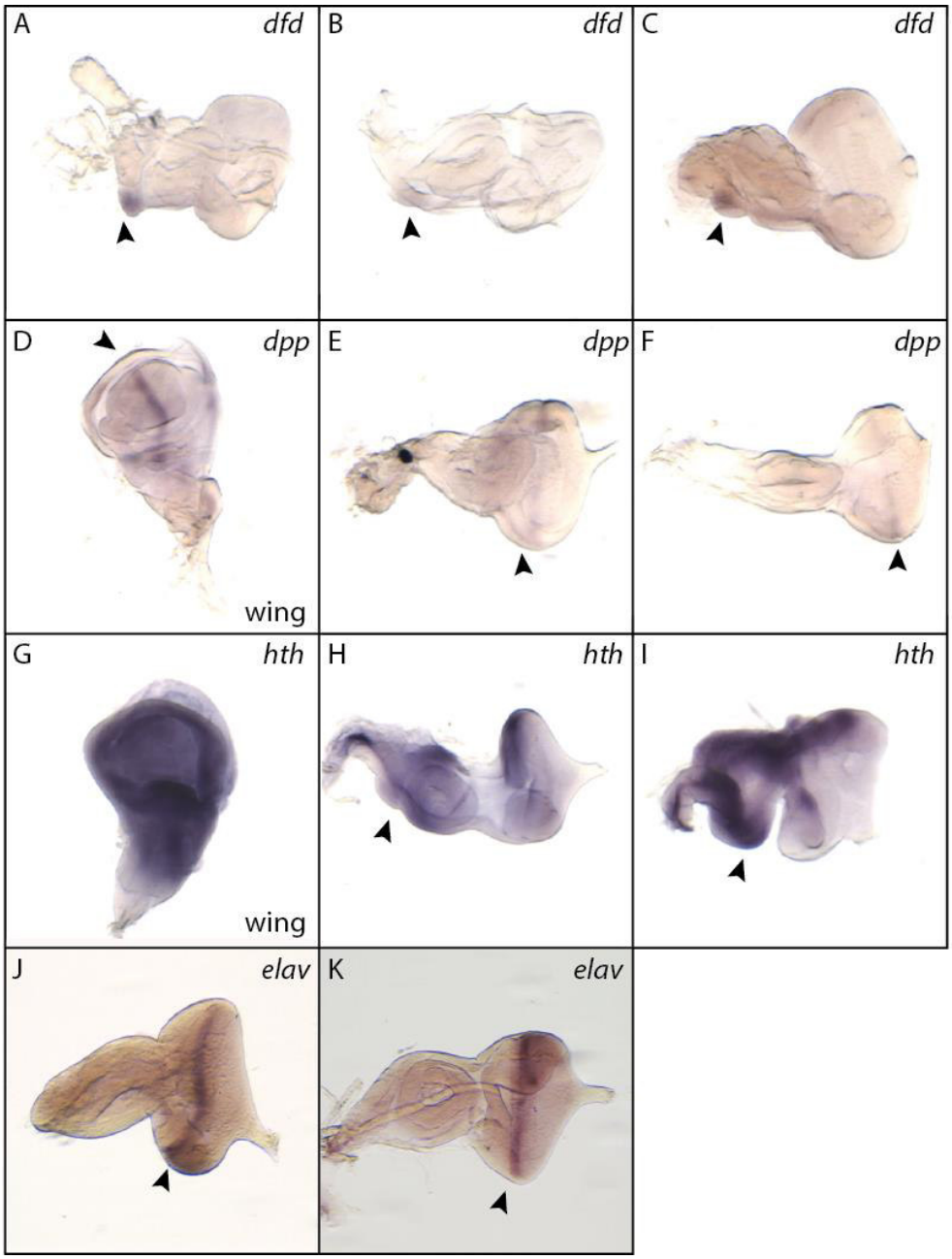

Supplement Figure S4.3 | *In situ* hybridisations of 3rd instar larval discs for *dfd*, *dpp*, *hth* and *elav*. **(A-C)** Several imaginal eye-antennal discs stained for the expression of *dfd*. Expression can be observed in the MPF indicated by an arrow. **(D-F)** Expression pattern of *dpp* in the wing and eye-antennal disc indicated by black arrow heads. **(G-I)** *hth* is expressed in the wing disc ubiquitously. Expression in the wing disc is broadly distributed as well. Here, expression in the MPF can be observed. **(J and K)** expression pattern of *elav* in the imaginal antennal-eye disc.

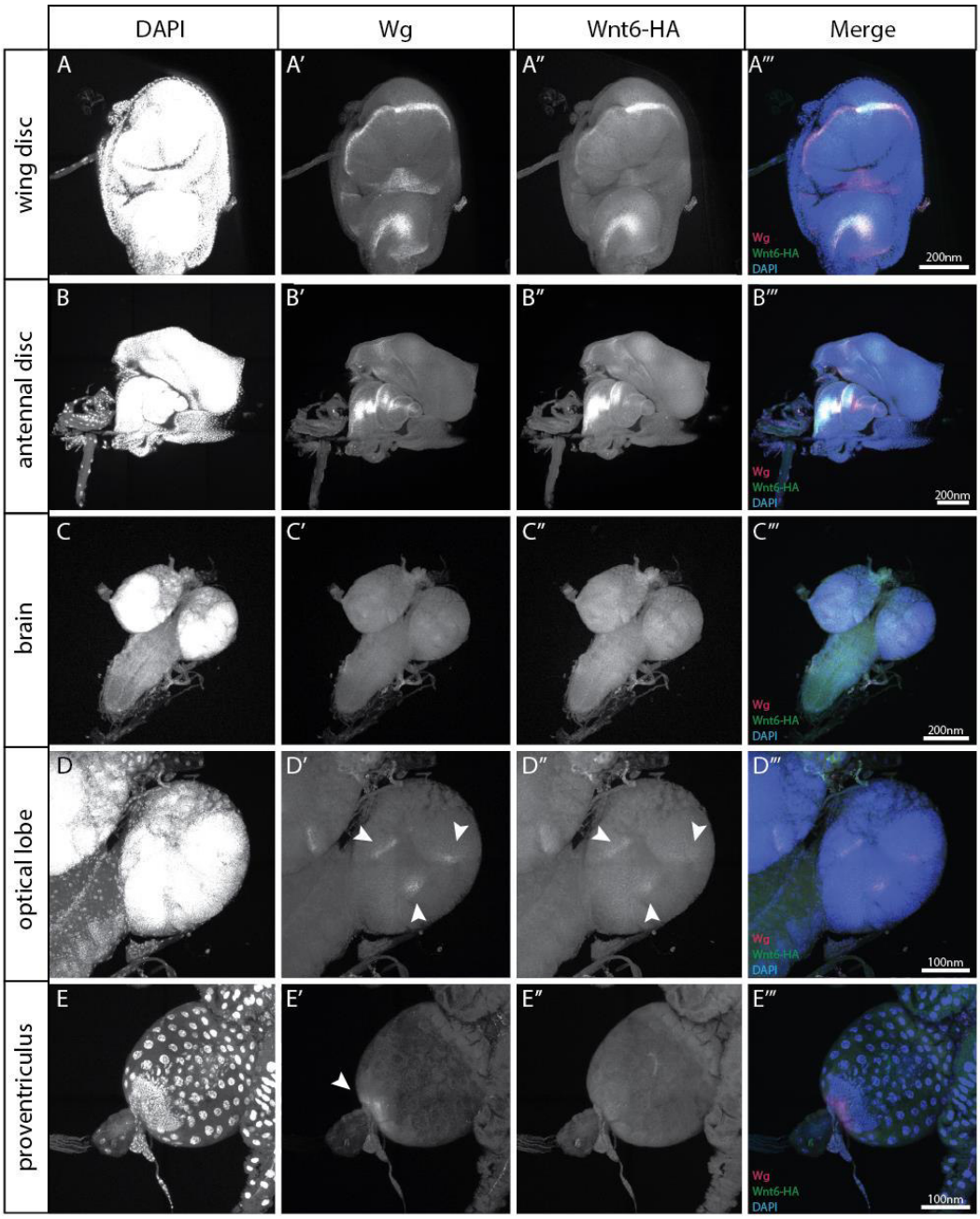

Supplement Figure S4.4 | Antibody staining's of Wnt6-HA together with Wg protein localisation in different 3rd instar larval tissues. **(A-A''')** expression of Wnt6 and Wg in the 3rd instar wing disc. **(B-B''')** Expression in the imaginal eye-antennal disc of Wg and Wnt6. **(C-C''')** Wg and Wnt6 expression in the 3rd instar larval brain. **(D-D''')** Close up of the expression in the optical lobe of a 3rd instar larval brain. **(E-E''')** Expression of Wg in the imaginal ring of the proventriculus in a 3rd instar larvae. All pictures are taken at 40x magnification, whereas the wing disc, eye imaginal disc and the brain are 2x2 tile scans.

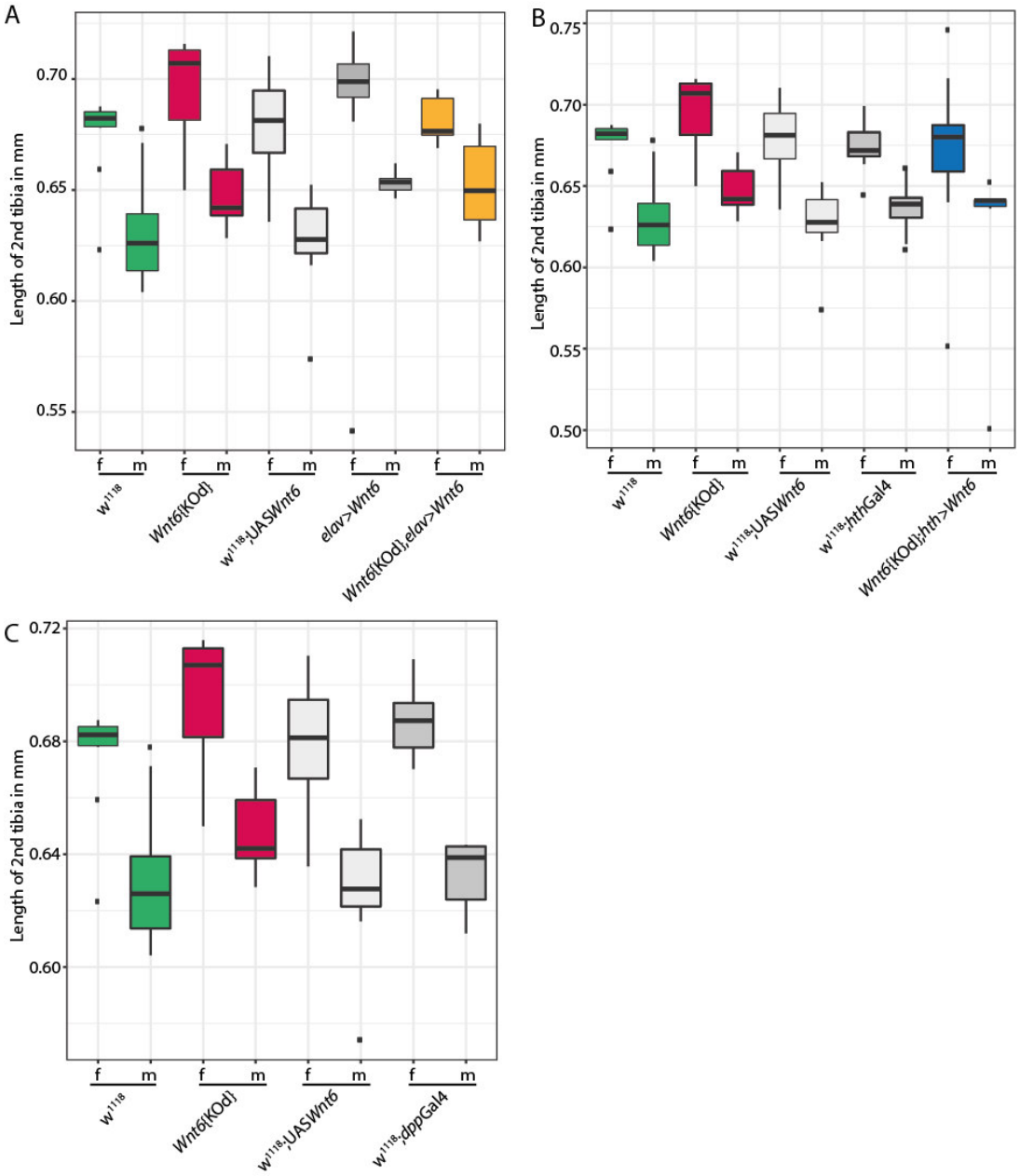

Supplement Figure S4.5 | Measurements of the 2nd leg tibia length for the lines from the UAS/Gal4 crosses. **(A)** Leg measurements for the *elav*-Gal4 crosses. **(B)** Tibia length of the *hth*-Gal4 cross and **(C)** measurements for the *dpp*-Gal4 crosses. Leg data is missing for w^{1118}; *elav*-Gal4 and the overexpression *hth*-Gal4>UAS-*Wnt6*. All female legs or male legs are **not** significantly different to each other. Significances were tested using ANOVA (df_{elav}=9; df_{hth}=9; df_{dpp}=7; F-$value_{elav}$=9.845; F-$value_{hth}$=9.338; F-$value_{dpp}$=22) followed by a Tukey HSD test.

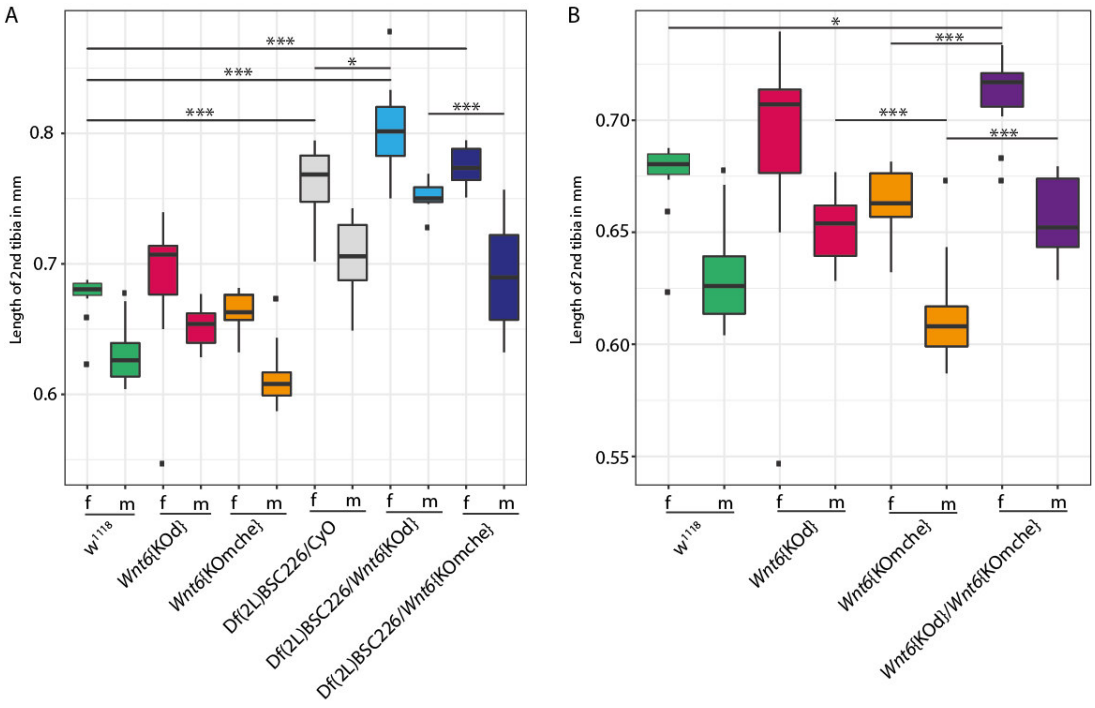

Supplement Figure S4.6 | Leg measurements of the deficiency line crosses and the cross between both *Wnt6* knockout lines. **(A)** Measurements of the 2nd leg tibia in all lines used for the deficiency crosses. **(B)** Leg measurements for the cross between both *Wnt6* knockout lines. ***p<0.001; **p<0.01; *p<0.05; f: female; m: male. Significances were tested using ANOVA (df_A=11; df_B=7; F-$value_A$=54.16; F-$value_B$=18.02) followed by a Tukey HSD test.

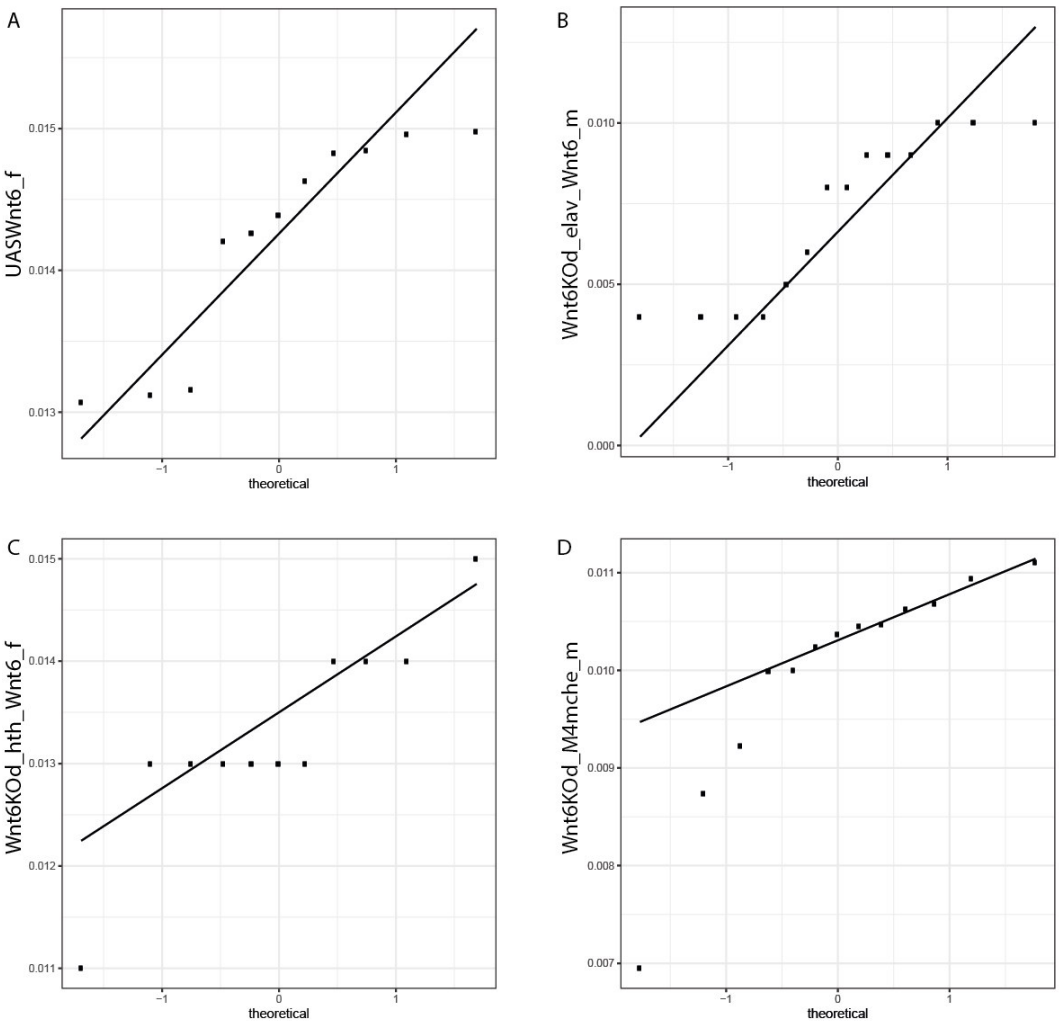

Supplement Figure S4.7 | q-q plots for non-normally distributed strains. Only data from non-normally distributed lines were additionally analysed with q-q plots. **(A)** UAS-*Wnt6* female distribution, **(B)** *Wnt6*{KOd}; *elav*-Gal4/UAS-*Wnt6* male distribution, **(C)** *Wnt6*{KOd}; *hth*-Gal4/UAS-*Wnt6* female distribution and **(D)** *Wnt6*{KOd}/*Wnt6*{KOmche} male distribution.

Supplement Figure S4.8 | 2nd leg pair of the *Wnt6*{KOd};*dpp>Wnt6* cross. **(A)** control 2nd leg pair of the w^{1118} line. **(B and C)** Malformed legs of the rescue cross using the *dpp*-Gal4 driver for ectopic *Wnt6* expression in the *Wnt6* knockout background.

5 | General Discussion

In this thesis, the evolution and function of Wnt genes from a broad scale survey of Wnt repertoires in arthropods down to assaying Wnt expression in a butterfly and investigating Wnt functionality in *Drosophila* were analysed. The importance of Wnt ligands in development and disease made an understanding of their function, but also the origin of these ligands interesting. Wnts were present in all metazoans and some subfamilies were very well conserved. These facts made it not only possible to study Wnt signalling dynamics in several model organisms and compare findings between several species but also made the underlying evolutionary mechanisms of Wnt gene evolution important to study.

Chapter 1

In the first chapter, a literature review showed the diversity of the Wnt gene repertoire in all metazoans and further a more detailed insight was gained with analysis of Wnt genes in arthropods. With this data it was possible to reveal evolutionary dynamics such as losses, conservation and duplications of Wnt genes. Here, it was shown that *Wnt3* was lost in all Ecdysozoa (Janssen *et al*., 2010), *Wnt2* and *Wnt4* were lost in all insects, as well as losses of *Wnt16* in all insects except hemipterans, loss of *Wnt8* and *Wnt9* in Hymenoptera and a loss of *Wnt8* in Lepidoptera. A loss of *Wnt10* in all chelicerates was also very likely, while this subphylum was the only one showing duplications of Wnt genes in all analysed arthropods. The duplications in chelicerates might be the result of one (Arachnida) or more (Xiphosura) whole genome duplications (Kenny *et al*., 2016; Schwager *et al*., 2017).

This analysis showed a broad overview about Wnt gene repertoires throughout the arthropod phylogeny, whereas questions about the underlying mechanisms behind the conservation or loss of Wnt genes remain unanswered. Here, it would be necessary to study the role of Wnts in several organisms to understand if for example the function is involved in these dynamics.

Chapter 2

Following this thought, the known functions of Wnt genes in arthropods were analysed and it was shown, that in very few species functional information were available for the whole Wnt repertoire. Here, the fruit fly *Drosophila* and the flour beetle *Tribolium* were well studied and therefore an interesting candidate species to

understand if Wnt function could be conserved and thus leading to conservation of that Wnt ligand. A sister group of both species were the Lepidoptera, which were phylogenetically positioned between flies and beetles and where very little was known about function of butterfly Wnt genes. In Chapter 2, the expression of all lepidopteran Wnt genes were analysed and compared with *Drosophila* and *Tribolium* expression during similar stages in embryogenesis. It was possible to show, that overall five Wnt genes (*Wnt1, 7, 10, 11* and *A*) were expressed during early embryogenesis, whereas four Wnt genes were involved in patterning the embryonic tissues (*Wnt1, 7, 10* and *A*). Comparing the expression to *Tribolum*, it was shown that most of the pattern were observed in similar tissues and therefore it will be interesting to also analyse the function of these Wnt genes in butterflies and repeat the comparison to *Tribolium*. The similarities were less pronounced when comparing butterflies to *Drosophila* expression, also due to differences in the Wnt gene repertoires of butterflies and flies. Only *Wnt1* was expressed in the same segmental stripe pattern, which indicated a strong potential functional conservation of *Wnt1* in all three insect groups.

This analysis revealed first insight into understanding the evolutionary constraints on Wnt ligands and that indeed the function of a particular Wnt gene could influence their conservation throughout phylogeny. Still, several questions remained unanswered and more studies regarding the function of Wnts in more species will be needed to complete the picture of Wnt evolution.

Chapter 3

When analysing the Wnt gene functions in *Drosophila* for Chapter 2, it was noticed that even in a well-studied model organism such as *Drosophila*, not all Wnt functions were completely understood. Here, especially the function of *Wnt6* and *Wnt10* were less described. In the following Chapter 3, a more detailed functional analysis of *Wnt6* was performed. *Wnt6* was chosen due to its close location to *Wnt1* (shown in Chapter 1) and their sequence similarities as well as overlapping expression in *Drosophila*. It was shown, that the function of *Wnt1* was potentially conserved in insects and in nearly all insects, the *Wnt1*-6 cluster was maintained (see Figure 2.8). It would be interesting to analyse the function of *Wnt6,* which was also conserved, and

this could influence its presence in all insects or maybe it was only maintained due to its close location to *Wnt1*.

In Chapter 3 the function of *Wnt6* was analysed in detail, where it was possible to show that the first exon of *Wnt6* might contain a putative regulatory element which might be able to influence *wg* signalling in the context of the maxillary palp developmental pathway. This indicates, that not only the location and function could influence the conservation of Wnt genes, but also regulatory dependencies between Wnts in the ancestral Wnt cluster (Koshikawa *et al.,* 2014). Interestingly, it was also possible to indicate a potential *Wnt6* function in regulating the timing of pupariation. Several further experiments were already proposed in the conclusions of the above-mentioned chapters, whereas here I would like to point out ideas and suggestions regarding broader questions in the Wnt field.

Future Wnt ideas

The tools generated for understanding the role of *Wnt6* during maxillary palp development could be used to analyse *Wnt6* loss or localisation of the *Wnt6* protein in the context of the other two proposed *Wnt6* functions in *Drosophila*. Here, an involvement of *Wnt6* in regeneration (Smith-Bolton *et al*., 2009) or the oogenesis (Wang and Page-McCaw, 2018) was proposed. With the *Wnt6*{HA} line it would be possible for the first time to analyse where Wnt6 protein is expressed during damage response and wound healing (Smith-Bolton *et al*., 2009). Additionally, the loss of function mutant of *Wnt6* could be used to analyse if a decrease in regeneration could be seen in these flies compared to a control line. Similar approaches would be possible for understanding the role of *Wnt6* in oogenesis. Here, *Wnt6* was involved in maintaining the escort cells which are important for correct development of the germline stem cells (Wang and Page-McCaw, 2018). It would be interesting to analyse the location of *Wnt6* in the escort cells with the *Wnt6*{HA} but also if it would be possible to see a negative effect on the germline stem cells in the *Wnt6*{KOmche} line.

The thirteen Wnt subfamilies have been subject to many losses and/or duplication leading very variable repertoires of Wnt genes, ranging from 5 to 29 Wnt genes, in metazoan lineages (see Figure 1.1). Additionally, several Frizzled receptors were present in different metazoans, which often could be bound by several Wnt ligands

and activate the same downstream signalling pathway. For example, in *Drosophila wg* and *Wnt7* could bind three of the four Fz receptors (Fz, Fz2 and Fz3) (Bhanot *et al*., 1996; Mulligan *et al*., 2012; Piddini *et al*., 2005; Wu and Nusse, 2002) and *Wnt7* can bind Fz, Fz2 and Fz4 (Wu and Nusse, 2002). *Wnt5* can bind Fz and Fz2 but not Fz3 (Srahna *et al*., 2006) while no information about Fz binding is known for *Wnt6* and *Wnt10*. *Drosophila* is therefore a good example to show the complexity of Wnt-Fz binding dynamics, where several Wnts could bind to the same receptor and trigger the same pathway. But how could it still be possible to distinguish between which Wnt ligands have bound to the Fz and create a Wnt specific target gene outcome?

One idea would be, that there is a way where the Wnt ligand itself could be involved in influencing specificity of the target gene expression. In the 1990s, a nice study was performed on the *wingless* gene in *Drosophila*, where several modifications and truncations of this sequence were functionally analysed to determine which of the ligand regions were important for signalling (Hays *et al*., 1997). In a different study, it was shown that *Drosophila* Wnt ligands, such as *Wnt7* and *wg* could work together to form the embryonic tracheal system. Here, the functional specific outcome was influenced by the combined activity of the two Wnts (Llimargas and Lawrence, 2001). Additionally, the crystal structure was revealed by Janda *et al*. (2012) which implied potential interaction and functional important binding sites. But rarely, all of this data was taken together and analysed in detail for understanding which Wnt ligand regions were necessary for the correct context dependent specificity.

During this study, I started working on these questions, but due to several experimental difficulties it was not possible to produce sufficient data to answer them. Here, a fly line with a Wnt loss of function mutation was used and it was planned to rescue this loss by introducing a different Wnt coding sequence. For this purpose, the *wg* knockout line (wg^{KO}) created by Cyrille Alexandre was analysed (Francis Crick Institute, London). This line had an attP landing site insertion in the first exon of *wg* which was used to insert a membrane tethered *wg* (NRT-*wg*) variant and analyse the long-range signalling of *wg* (Alexandre *et al*., 2014). The attP/B recombination system allowed to introduce any sequence into a specific locus and in my case, it was decided to insert different Wnt coding sequences into the *wg* locus to test if a rescue of the Wg function was possible. As previously shown, *wg* and *Wnt6* were very similar Wnt ligands

and it was decided to first introduce the *Wnt6* coding sequence into the genomic *wg* location. If the Wnt ligand sequence itself is involved in triggering the specific outcome of the Wnt signalling, it was expected that *Wnt6* could not rescue the Wg function in the wg^{KO} fly. Additionally, it was proposed to test if another *wg* sequence would be able to rescue the *wg* knockout in this fly line. For this purpose, a *wg* from a species, where *wg* has a completely different function than in *Drosophila* was chosen, but the two *wg* sequences were still very similar. The *wg* gene from the spider *P. tepidariorum* was a good candidate, because *wg* did not have a segment polarity role in this species as seen in *Drosophila* (Janssen *et al*., 2010). If the sequence of the Wnt ligand was important in specificity, it could be possible that the spider *wg* was able to rescue the *wg* function due to the high sequence similarity of these two ligands.

To ultimately test Wnt ligand functionality and specificity, it would be desirable to generate and test a synthetic Wnt ligand. With this long-term aim in mind, it was started to try to map the specificity of *wg* and in *Drosophila* by designing chimeric ligands which could be applied in the future to study Wnt ligands more generally. During the design of these ligands, it was observed that both Wnt ligands have a disordered region, which is unique to each ligand. The disordered regions occurred not only in these two ligands, but in all *Drosophila* Wnts. It has been shown recently that disordered regions could be involved in actual signalling regulation. Here, a protein called RECK bound the Wg disordered region and facilitated binding to the Fz receptor (Eubelen *et al*., 2018). In general, it would be very interesting to analyse these disordered regions regarding their binding sites and potential functional role further.

The information about the disordered regions were included in the design of four versions *wg/Wnt6* chimeric ligands which contained (A) the 5’ region of *wg* and 3’ region of *Wnt6* including the disordered region of *Wnt6*; (B) the 5’ part of *Wnt6* and the 3’ region of *wg* including the disordered region of *wg*; (C) 5’ region of *Wnt6* and 3’ of *wg* including the disordered regions of both genes and (D) 5’ and 3’ region of *Wnt6* with an insertion of *wg* sequence, excluding the disordered regions (Figure 5.1).

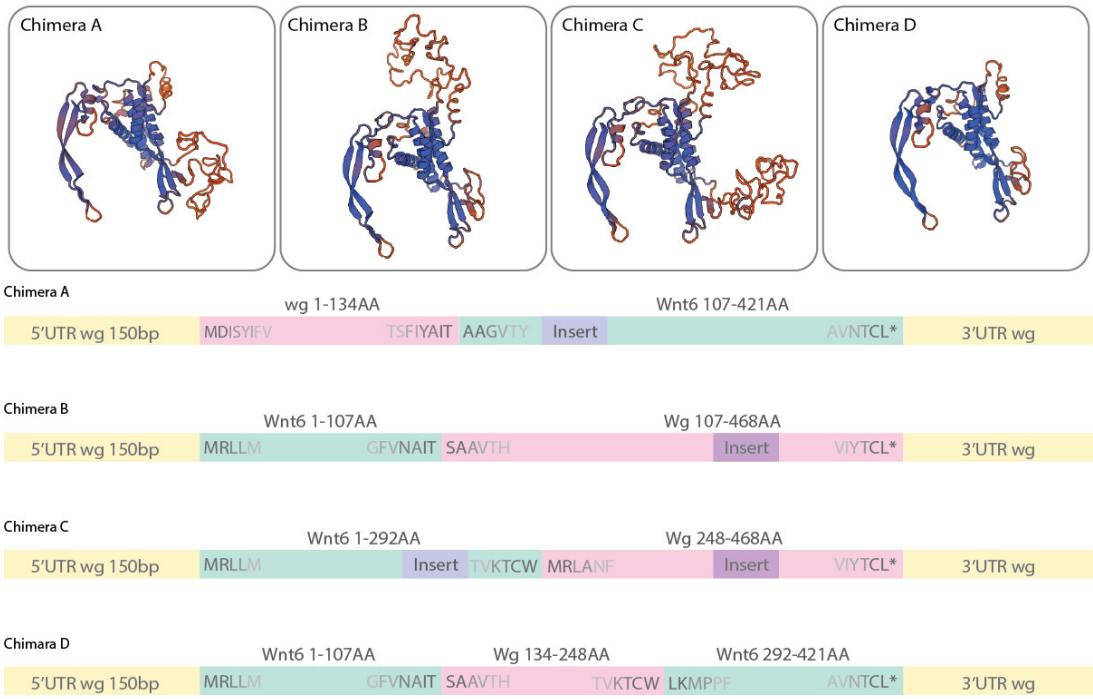

Figure 5.1 | The design of chimeric Wnt genes. Shown are the modelled ribbon structures of all four artificial Wnt genes in the top row. Below, the protein sequences are shown for all four chimeric genes. All artificial Wnts include the 5' and 3' UTR of the wg locus. Ribbon structures modelled in SWISS-MODEL (Waterhouse *et al.*, 2018).

However, these fragments needed to be brought into the wg^{KO} fly line and tested for their functional rescue capability. Each variant could indicate different parts of the Wnt ligand sequence which was important for functional specificity. For example, if Chimera A would be able to rescue the Wg function, this would indicate that the 5' region of *wg* is important for specific target gene expression. This region could then be further tested. In a second example it could also be possible that only the Chimeras B and C are rescuing the Wg function which would indicate that the 3' region including the disordered region of *wg* would be of importance.

Following up these preliminary ideas and designs, this work could contribute highly to the understanding of Wnt gene specificity. This basic work in *Drosophila* could influence the overall understanding of Wnt regulation in metazoans and would also impact our understanding of Wnt mis-regulation, e.g. in tumorgenesis and cancer (e.g. Nusse and Clevers (2017); Zhan *et al*. (2017)). Understanding the regulation and specificity of Wnts could also lead to find new ways to influence these mechanisms, which would be interesting for drug development and treatments. Additionally, this

study also could help to elucidate why so many Wnt ligands are conserved and how their regulation might influence their evolution.

Acknowledgements

Hereby I would like to thank Prof. Alistair P. McGregor for giving me the possibility to do my PhD studies in his laboratory. I always felt supported and encouraged to do my best and more, to become an enthusiastic scientist. I have learned so much during the three year in the McGregor Lab and I really enjoyed my time at Oxford Brookes University. I also would like to thank my PhD examiners Dr. Casper Breuker and Dr. Steffen Scholpp for kindly agreeing to review my thesis.

A huge thank you has to go to Dr. Claudia Mendes and Dr. Pedro Gaspar for their patience to answer my questions, the support of my ideas and to stand with help and advice at any time of day or night by my side. I'm going to take a lot of what I have learned from you two, personally and scientifically with me to my next assignments. I also would like to thanks Dr. Jonathan Lees for listening and helping me to think and talk about new 'Wnt' ideas.

In the everyday work in the laboratory, I was supported in particular by the technical assistants Christine Ashton and Madeleine Lindsey. They have always received me friendly and helpful, with an incomparable patience for any problems and 'urgent' orders.

I would also like to thank my parents, Martin and Peter Holzem, and my sister Dr. Christina Holzem for always having my back – whenever or whatever happened. They have travelled with me from Weimar, to Jena and Konstanz – and finally to Oxford, while always being there for me with their unconditional love and support.

I would not have made it through my PhD without the seemingly infinite support, love and understanding of my partner Jan Gerwin. I would not be the person I am without you. Thank you so much!

I will never forget the support by my all of my friends, especially Nora Braak – thanks for all the chats with Chai Latte, the knitting, living together and our excursions! My PhD without you would not have been the same. We only had a year, but it was great to have you, Franziska Franke and her little family, as friends and support during my PhD. I am already missing our Wednesday cooking evenings. I also would like to thank Fabiola

Ceroni for discussions and going through “the list” with me during my last months in Oxford.

Thank you so much, McGregor Lab for great three years with lots of science, Journal Pub and conferences!

References

2008. The genome of a lepidopteran model insect, the silkworm *Bombyx mori.* Insect biochemistry and molecular biology 38, 1036-1045.

Abascal, F., Zardoya, R., Posada, D., 2005. ProtTest: Selection of best-fit models of protein evolution. Bioinformatics 21, 2104-2105.

Abzhanov, A., Holtzman, S., Kaufman, T.C., 2001. The *Drosophila* proboscis is specified by two Hox genes, proboscipedia and Sex combs reduced, via repression of leg and antennal appendage genes. Development 128, 2803-2814.

Adams, M.D., *et al*. 2000. The genome sequence of *Drosophila melanogaster*. Science (New York, N.Y.) 287, 2185-2195.

Adamska, M., Degnan, B.M., Green, K., Zwafink, C., 2011. What sponges can tell us about the evolution of developmental processes. Zoology 114, 1-10.

Adamska, M., Degnan, S.M., Green, K.M., Adamski, M., Craigie, A., Larroux, C., Degnan, B.M., 2007. Wnt and TGF-beta expression in the sponge *Amphimedon queenslandica* and the origin of metazoan embryonic patterning. PloS one 2, e1031.

Adamska, M., Larroux, C., Adamski, M., Green, K., Lovas, E., Koop, D., Richards, G.S., Zwafink, C., Degnan, B.M., 2010. Structure and expression of conserved Wnt pathway components in the demosponge *Amphimedon queenslandica*. Evolution & development 12, 494-518.

Aegerter-Wilmsen, T., Aegerter, C.M., Hafen, E., Basler, K., 2007. Model for the regulation of size in the wing imaginal disc of *Drosophila*. Mech Dev 124, 318-326.

Alexandre, C., Baena-Lopez, A., Vincent, J.P., 2014. Patterning and growth control by membrane-tethered *Wingless*. Nature 505, 180-185.

Amano, M., Nakayama, M., Kaibuchi, K., 2010. Rho-kinase/ROCK: A key regulator of the cytoskeleton and cell polarity. Cytoskeleton (Hoboken, N.J.) 67, 545-554.

Ando, H., Tanaka, M., 1980. Early embryonic development of the primitive moths, Endoclyta signifer walker and *E. excrescens* butler (Lepidoptera : Hepialidae). International Journal of Insect Morphology and Embryology 9, 67-77.

Aulehla, A., Wehrle, C., Brand-Saberi, B., Kemler, R., Gossler, A., Kanzler, B., Herrmann, B.G., 2003. Wnt3a plays a major role in the segmentation clock controlling somitogenesis. Developmental cell 4, 395-406.

Aulehla, A., Wiegraebe, W., Baubet, V., Wahl, M.B., Deng, C., Taketo, M., Lewandoski, M., Pourquie, O., 2008. A beta-catenin gradient links the clock and wavefront systems in mouse embryo segmentation. Nature cell biology 10, 186-193.

Baena-Lopez, L.A., Alexandre, C., Mitchell, A., Pasakarnis, L., Vincent, J.P., 2013. Accelerated homologous recombination and subsequent genome modification in *Drosophila*. Development 140, 4818-4825.

Banziger, C., Soldini, D., Schutt, C., Zipperlen, P., Hausmann, G., Basler, K., 2006. Wntless, a conserved membrane protein dedicated to the secretion of Wnt proteins from signaling cells. Cell 125, 509-522.

Bartscherer, K., Boutros, M., 2008. Regulation of Wnt protein secretion and its role in gradient formation. EMBO reports 9, 977-982.

Bartscherer, K., Pelte, N., Ingelfinger, D., Boutros, M., 2006. Secretion of Wnt ligands requires Evi, a conserved transmembrane protein. Cell 125, 523-533.

Basu, M.K., Selengut, J.D., Haft, D.H., 2011. ProPhylo: partial phylogenetic profiling to guide protein family construction and assignment of biological process. BMC bioinformatics 12, 434.

Beaven, R., Denholm, B., 2018. Release and spread of Wingless is required to pattern the proximo-distal axis of *Drosophila* renal tubules. eLife 7.
Benassayag, C., Plaza, S., Callaerts, P., Clements, J., Romeo, Y., Gehring, W.J., Cribbs, D.L., 2003. Evidence for a direct functional antagonism of the selector genes proboscipedia and eyeless in *Drosophila* head development. Development 130, 575.
Bendtsen, J.D., Nielsen, H., von Heijne, G., Brunak, S., 2004. Improved prediction of signal peptides: SignalP 3.0. J Mol Biol 340, 783-795.
Bhanot, P., Brink, M., Samos, C.H., Hsieh, J.C., Wang, Y., Macke, J.P., Andrew, D., Nathans, J., Nusse, R., 1996. A new member of the frizzled family from *Drosophila* functions as a Wingless receptor. Nature 382, 225-230.
Bolognesi, R., Beermann, A., Farzana, L., Wittkopp, N., Lutz, R., Balavoine, G., Brown, S.J., Schroder, R., 2008. *Tribolium* Wnts: evidence for a larger repertoire in insects with overlapping expression patterns that suggest multiple redundant functions in embryogenesis. Development genes and evolution 218, 193-202.
Boothby, T.C., Tenlen, J.R., Smith, F.W., Wang, J.R., Patanella, K.A., Nishimura, E.O., Tintori, S.C., Li, Q., Jones, C.D., Yandell, M., Messina, D.N., 2015. Evidence for extensive horizontal gene transfer from the draft genome of a tardigrade. 112, 15976-15981.
Borst, D.W., Bollenbacher, W.E., O'Connor, J.D., King, D.S., Fristrom, J.W., 1974. Ecdysone levels during metamorphosis of *Drosophila melanogaster*. Developmental biology 39, 308-316.
Brakefield, P.M., Beldade, P., Zwaan, B.J., 2009. *In situ* hybridization of embryos and larval and pupal wings from the African butterfly *Bicyclus anynana*. Cold Spring Harb Protoc 2009, pdb.prot5208.
Brakefield, P.M., French, V., 1999. Butterfly wings: the evolution of development of colour patterns. BioEssays : news and reviews in molecular, cellular and developmental biology 21, 391-401.
Broadie, K.S., Bate, M., Tublitz, N.J., 1991. Quantitative staging of embryonic development of the tobacco hawkmoth, *Manduca sexta*. Roux's archives of developmental biology 199, 327-334.
Bryant, P.J., Levinson, P., 1985. Intrinsic growth control in the imaginal primordia of *Drosophila*, and the autonomous action of a lethal mutation causing overgrowth. Developmental biology 107, 355-363.
Bryant, P.J., Simpson, P., 1984. Intrinsic and extrinsic control of growth in developing organs. The Quarterly review of biology 59, 387-415.
Cabrera, C.V., Alonso, M.C., Johnston, P., Phillips, R.G., Lawrence, P.A., 1987. Phenocopies induced with antisense RNA identify the *wingless* gene. Cell 50, 659-663.
Carroll, S.B., Gates, J., Keys, D.N., Paddock, S.W., Panganiban, G.E., Selegue, J.E., Williams, J.A., 1994. Pattern formation and eyespot determination in butterfly wings. Science (New York, N.Y.) 265, 109-114.
Carter, J.M., Baker, S.C., Pink, R., Carter, D.R., Collins, A., Tomlin, J., Gibbs, M., Breuker, C.J., 2013. Unscrambling butterfly oogenesis. BMC genomics 14, 283.
Cavallo, R.A., Cox, R.T., Moline, M.M., Roose, J., Polevoy, G.A., Clevers, H., Peifer, M., Bejsovec, A., 1998. *Drosophila* Tcf and Groucho interact to repress Wingless signalling activity. Nature 395, 604-608.
Challis, R.J., Kumar, S., Dasmahapatra, K.K.K., Jiggins, C.D., Blaxter, M., 2016.
Chaudhary, V., Boutros, M., 2018. Evidence of functional long-range Wnt/Wg in the developing *Drosophila* wing epithelium. bioRxiv.

Cho, S.J., Valles, Y., Giani, V.C., Jr., Seaver, E.C., Weisblat, D.A., 2010. Evolutionary dynamics of the wnt gene family: a lophotrochozoan perspective. Molecular biology and evolution 27, 1645-1658.
Cohen, S.M., Jürgens, G., 1989. Proximal-distal pattern formation in*Drosophila*: graded requirement forDistal-less gene activity during limb development. Roux's archives of developmental biology 198, 157-169.
Constantinou, S.J., Pace, R.M., Stangl, A.J., Nagy, L.M., Williams, T.A., 2016. Wnt repertoire and developmental expression patterns in the crustacean *Thamnocephalus platyurus*. Evolution & development 18, 324-341.
Coudreuse, D.Y., Roel, G., Betist, M.C., Destree, O., Korswagen, H.C., 2006. Wnt gradient formation requires retromer function in Wnt-producing cells. Science (New York, N.Y.) 312, 921-924.
Cribbs, D.L., Benassayag, C., Randazzo, F.M., Kaufman, T.C., 1995. Levels of homeotic protein function can determine developmental identity: evidence from low-level expression of the *Drosophila* homeotic gene proboscipedia under Hsp70 control. The EMBO journal 14, 767-778.
Croce, J.C., McClay, D.R., 2008. Evolution of the Wnt pathways. Methods in molecular biology 469, 3-18.
Croce, J.C., Wu, S.Y., Byrum, C., Xu, R., Duloquin, L., Wikramanayake, A.H., Gache, C., McClay, D.R., 2006. A genome-wide survey of the evolutionarily conserved Wnt pathways in the sea urchin *Strongylocentrotus purpuratus.* Developmental biology 300, 121-131.
Damen, W.G., 2002. Parasegmental organization of the spider embryo implies that the parasegment is an evolutionary conserved entity in arthropod embryogenesis. Development 129, 1239-1250.
Davis, G.K., Patel, N.H., 2002. Short, long, and beyond: molecular and embryological approaches to insect segmentation. Annual review of entomology 47, 669-699.
Dayhoff, M.O., Schwartz, R.M., Orcutt, B.C., 1978. A model of evolutionary change in proteins. Atlas of protein sequence and structure, 345-352.
Dearden, P.K., Wilson, M.J., Sablan, L., Osborne, P.W., Havler, M., McNaughton, E., Kimura, K., Milshina, N.V., Hasselmann, M., Gempe, T., Schioett, M., Brown, S.J., Elsik, C.G., Holland, P.W., Kadowaki, T., Beye, M., 2006. Patterns of conservation and change in honey bee developmental genes. Genome research 16, 1376-1384.
Dehal, P., Boore, J.L., 2005. Two rounds of whole genome duplication in the ancestral vertebrate. PLoS biology 3, e314.
Dhawan, S., Gopinathan, K.P., 2003. Expression profiling of homeobox genes in silk gland development in the mulberry silkworm *Bombyx mori*. Development genes and evolution 213, 523-533.
Diederich, R.J., Pattatucci, A.M., Kaufman, T.C., 1991. Developmental and evolutionary implications of labial, Deformed and engrailed expression in the *Drosophila* head. Development 113, 273.
Dorn, A., Bishoff, S.T., Gilbert, L.I., 1987. An Incremental Analysis of the Embryonic Development of the Tobacco Hornworm, *Manduca sexta*. International Journal of Invertebrate Reproduction and Development 11, 137-157.
Doumpas, N., Jekely, G., Teleman, A.A., 2013. *Wnt6* is required for maxillary palp formation in *Drosophila*. BMC biology 11, 104.

Dow, R.C., Carlson, S.D., Goodman, W.G., 1988. A scanning electron microscope study of the developing embryo of *Manduca sexta* (L.) (Lepidoptera : Sphingidae). International Journal of Insect Morphology and Embryology 17, 231-242.
Duncan, D.M., Burgess, E.A., Duncan, I., 1998. Control of distal antennal identity and tarsal development in *Drosophila* by spineless-aristapedia, a homolog of the mammalian dioxin receptor. Genes & development 12, 1290-1303.
Emmons, R.B., Duncan, D., Duncan, I., 2007. Regulation of the *Drosophila* distal antennal determinant spineless. Developmental biology 302, 412-426.
Eubelen, M., Bostaille, N., Cabochette, P., Gauquier, A., Tebabi, P., Dumitru, A.C., Koehler, M., Gut, P., Alsteens, D., Stainier, D.Y.R., Garcia-Pino, A., Vanhollebeke, B., 2018. A molecular mechanism for Wnt ligand-specific signaling. Science (New York, N.Y.), eaat1178.
Ferguson, L., Marlétaz, F., Carter, J.-M., Taylor, W.R., Gibbs, M., Breuker, C.J., Holland, P.W.H., 2014. Ancient Expansion of the Hox Cluster in Lepidoptera Generated Four Homeobox Genes Implicated in Extra-Embryonic Tissue Formation. PLoS genetics 10, e1004698.
Forrester, W.C., Kim, C., Garriga, G., 2004. The *Caenorhabditis elegans* Ror RTK CAM-1 inhibits EGL-20/Wnt signaling in cell migration. Genetics 168, 1951-1962.
Fradkin, L.G., Noordermeer, J.N., Nusse, R., 1995. The *Drosophila* Wnt protein DWnt-3 is a secreted glycoprotein localized on the axon tracts of the embryonic CNS. Developmental biology 168, 202-213.
Fradkin, L.G., van Schie, M., Wouda, R.R., de Jong, A., Kamphorst, J.T., Radjkoemar-Bansraj, M., Noordermeer, J.N., 2004. The *Drosophila* Wnt5 protein mediates selective axon fasciculation in the embryonic central nervous system. Developmental biology 272, 362-375.
Gao, B., Song, H., Bishop, K., Elliot, G., Garrett, L., English, M.A., Andre, P., Robinson, J., Sood, R., Minami, Y., Economides, A.N., Yang, Y., 2011. Wnt Signaling Gradients Establish Planar Cell Polarity by Inducing Vangl2 Phosphorylation through Ror2. Developmental cell 20, 163-176.
Garelli, A., Gontijo, A.M., Miguela, V., Caparros, E., Dominguez, M., 2012. Imaginal discs secrete insulin-like peptide 8 to mediate plasticity of growth and maturation. Science (New York, N.Y.) 336, 579-582.
Garriock, R.J., Warkman, A.S., Meadows, S.M., D'Agostino, S., Krieg, P.A., 2007. Census of vertebrate Wnt genes: isolation and developmental expression of *Xenopus Wnt2, Wnt3, Wnt9a, Wnt9b, Wnt10a,* and *Wnt16*. Developmental dynamics : an official publication of the American Association of Anatomists 236, 1249-1258.
Geib, S.M., Liang, G.H., Murphy, T.D., Sim, S.B., 2017. Whole Genome Sequencing of the Braconid Parasitoid Wasp *Fopius arisanus*, an Important Biocontrol Agent of Pest Tepritid Fruit Flies. G3: Genes|Genomes|Genetics 7, 2407-2411.
Goodman, R.M., Thombre, S., Firtina, Z., Gray, D., Betts, D., Roebuck, J., Spana, E.P., Selva, E.M., 2006. Sprinter: a novel transmembrane protein required for Wg secretion and signaling. Development 133, 4901-4911.
Gouy, M., Guindon, S., Gascuel, O., 2010. SeaView version 4: A multiplatform graphical user interface for sequence alignment and phylogenetic tree building. Molecular biology and evolution 27, 221-224.
Graba, Y., Gieseler, K., Aragnol, D., Laurenti, P., Mariol, M.C., Berenger, H., Sagnier, T., Pradel, J., 1995. DWnt-4, a novel *Drosophila* Wnt gene acts downstream of homeotic complex genes in the visceral mesoderm. Development 121, 209-218.

Gratz, S.J., Ukken, F.P., Rubinstein, C.D., Thiede, G., Donohue, L.K., Cummings, A.M., O'Connor-Giles, K.M., 2014. Highly specific and efficient CRISPR/Cas9-catalyzed homology-directed repair in *Drosophila*. Genetics 196, 961-971.
Greco, V., Hannus, M., Eaton, S., 2001. Argosomes: a potential vehicle for the spread of morphogens through epithelia. Cell 106, 633-645.
Green, J.L., Inoue, T., Sternberg, P.W., 2007. The *C. elegans* ROR receptor tyrosine kinase, CAM-1, non-autonomously inhibits the Wnt pathway. Development 134, 4053-4062.
Gross, J.C., Chaudhary, V., Bartscherer, K., Boutros, M., 2012. Active Wnt proteins are secreted on exosomes. Nature cell biology 14, 1036.
Guder, C., Philipp, I., Lengfeld, T., Watanabe, H., Hobmayer, B., Holstein, T.W., 2006. The Wnt code: cnidarians signal the way. Oncogene 25, 7450-7460.
Harris, R.E., Setiawan, L., Saul, J., Hariharan, I.K., 2016. Localized epigenetic silencing of a damage-activated WNT enhancer limits regeneration in mature *Drosophila* imaginal discs. eLife 5.
Hayden, L., Arthur, W., 2014. The centipede *Strigamia maritima* possesses a large complement of Wnt genes with diverse expression patterns. Evolution & development 16, 127-138.
Haynie, J.L., Bryant, P.J., 1986. Development of the eye-antenna imaginal disc and morphogenesis of the adult head in *Drosophila melanogaster*. The Journal of experimental zoology 237, 293-308.
Hays, R., Gibori, G.B., Bejsovec, A., 1997. Wingless signaling generates pattern through two distinct mechanisms. Development 124, 3727-3736.
Held Jr, L.I., 2002. Imaginal Discs: The Genetic and Cellular Logic of Pattern Formation. Cambridge University Press, Cambridge.
Hensel, K., Lotan, T., Sanders, S.M., Cartwright, P., Frank, U., 2014. Lineage-specific evolution of cnidarian Wnt ligands. Evolution & development 16, 259-269.
Herman, M.A., Vassilieva, L.L., Horvitz, H.R., Shaw, J.E., Herman, R.K., 1995. The *C. elegans* gene lin-44, which controls the polarity of certain asymmetric cell divisions, encodes a Wnt protein and acts cell nonautonomously. Cell 83, 101-110.
Herr, P., Basler, K., 2012. Porcupine-mediated lipidation is required for Wnt recognition by Wls. Developmental biology 361, 392-402.
Hino, K., Satou, Y., Yagi, K., Satoh, N., 2003. A genomewide survey of developmentally relevant genes in *Ciona intestinalis*. VI. Genes for Wnt, TGFbeta, Hedgehog and JAK/STAT signaling pathways. Development genes and evolution 213, 264-272.
Hoffmans, R., Stadeli, R., Basler, K., 2005. *Pygopus* and *legless* provide essential transcriptional coactivator functions to armadillo/beta-catenin. Current biology : CB 15, 1207-1211.
Hogvall, M., Schonauer, A., Budd, G.E., McGregor, A.P., Posnien, N., Janssen, R., 2014. Analysis of the Wnt gene repertoire in an onychophoran provides new insights into the evolution of segmentation. EvoDevo 5, 14.
Holland, P.W., Garcia-Fernandez, J., Williams, N.A., Sidow, A., 1994. Gene duplications and the origins of vertebrate development. Development (Cambridge, England). Supplement, 125-133.
Holstein, T.W., 2012. The Evolution of the Wnt Pathway. Cold Spring Harbor perspectives in biology 4.
Holt, R.A., *et al*. 2002. The genome sequence of the malaria mosquito *Anopheles gambiae*. Science (New York, N.Y.) 298, 129-149.
Huang, J., Zhou, W., Watson, A.M., Jan, Y.-N., Hong, Y., 2008. Efficient Ends-Out Gene Targeting In *Drosophila*. Genetics 180, 703.

Inoue, T., Oz, H.S., Wiland, D., Gharib, S., Deshpande, R., Hill, R.J., Katz, W.S., Sternberg, P.W., 2004. *C. elegans* LIN-18 is a Ryk ortholog and functions in parallel to LIN-17/Frizzled in Wnt signaling. Cell 118, 795-806.
Iseli, C., Ambrosini, G., Bucher, P., Jongeneel, C.V., 2007. Indexing Strategies for Rapid Searches of Short Words in Genome Sequences. PloS one 2, e579.
Jaillon, O., *et al*. 2004. Genome duplication in the teleost fish *Tetraodon nigroviridis* reveals the early vertebrate proto-karyotype. Nature 431, 946.
Janda, C.Y., Waghray, D., Levin, A.M., Thomas, C., Garcia, K.C., 2012. Structural basis of Wnt recognition by Frizzled. Science (New York, N.Y.) 337, 59-64.
Janson, K., Cohen, E.D., Wilder, E.L., 2001. Expression of *DWnt6, DWnt10,* and *DFz4* during *Drosophila* development. Mechanisms of Development 103, 117-120.
Janssen, R., Le Gouar, M., Pechmann, M., Poulin, F., Bolognesi, R., Schwager, E.E., Hopfen, C., Colbourne, J.K., Budd, G.E., Brown, S.J., Prpic, N.M., Kosiol, C., Vervoort, M., Damen, W.G., Balavoine, G., McGregor, A.P., 2010. Conservation, loss, and redeployment of Wnt ligands in protostomes: implications for understanding the evolution of segment formation. BMC evolutionary biology 10, 374.
Janssen, R., Posnien, N., 2014. Identification and embryonic expression of *Wnt2, Wnt4, Wnt5* and *Wnt9* in the millipede *Glomeris marginata* (Myriapoda: Diplopoda). Gene expression patterns : GEP 14, 55-61.
Jenny, F.H., Basler, K., 2014. Powerful *Drosophila* screens that paved the wingless pathway. Fly 8, 218-225.
Jiggins, C.D., Wallbank, R.W., Hanly, J.J., 2017. Waiting in the wings: what can we learn about gene co-option from the diversification of butterfly wing patterns? Philosophical transactions of the Royal Society of London. Series B, Biological sciences 372.
Johnston, L.A., Schubiger, G., 1996. Ectopic expression of wingless in imaginal discs interferes with decapentaplegic expression and alters cell determination. Development 122, 3519.
Kadowaki, T., Wilder, E., Klingensmith, J., Zachary, K., Perrimon, N., 1996. The segment polarity gene porcupine encodes a putative multitransmembrane protein involved in Wingless processing. Genes & development 10, 3116-3128.
Kao, D., Lai, A.G., Stamataki, E., Rosic, S., Konstantinides, N., Jarvis, E., Di Donfrancesco, A., Pouchkina-Stancheva, N., Semon, M., Grillo, M., Bruce, H., Kumar, S., Siwanowicz, I., Le, A., Lemire, A., Eisen, M.B., Extavour, C., Browne, W.E., Wolff, C., Averof, M., Patel, N.H., Sarkies, P., Pavlopoulos, A., Aboobaker, A., 2016. The genome of the crustacean *Parhyale hawaiensis*, a model for animal development, regeneration, immunity and lignocellulose digestion. eLife 5.
Kaufman, T.C., 1978. Cytogenetic Analysis of Chromosome 3 in *DROSOPHILA MELANOGASTER*: Isolation and Characterization of Four New Alleles of the Proboscipedia (pb) Locus. Genetics 90, 579-596.
Kenny, N.J., Chan, K.W., Nong, W., Qu, Z., Maeso, I., Yip, H.Y., Chan, T.F., Kwan, H.S., Holland, P.W., Chu, K.H., Hui, J.H., 2016. Ancestral whole-genome duplication in the marine chelicerate horseshoe crabs. Heredity 116, 190-199.
Kiecker, C., Niehrs, C., 2001. A morphogen gradient of Wnt/beta-catenin signalling regulates anteroposterior neural patterning in Xenopus. Development 128, 4189-4201.
Kikuchi, A., Yamamoto, H., Kishida, S., 2007. Multiplicity of the interactions of Wnt proteins and their receptors. Cellular signalling 19, 659-671.
Kikuchi, A., Yamamoto, H., Sato, A., 2009. Selective activation mechanisms of Wnt signaling pathways. Trends in cell biology 19, 119-129.

Kim, H.S., Murphy, T., Xia, J., Caragea, D., Park, Y., Beeman, R.W., Lorenzen, M.D., Butcher, S., Manak, J.R., Brown, S.J., 2010. BeetleBase in 2010: revisions to provide comprehensive genomic information for Tribolium castaneum. Nucleic acids research 38, D437-442.
Kobayashi, Y., Ando, H., 1990. Early embryonic development and external features of developing embryos of the caddisfly, *Nemotaulius admorsus* (trichoptera: Limnephilidae). Journal of Morphology 203, 69-85.
Korkut, C., Ataman, B., Ramachandran, P., Ashley, J., Barria, R., Gherbesi, N., Budnik, V., 2009. Trans-synaptic transmission of vesicular Wnt signals through Evi/Wntless. Cell 139, 393-404.
Koshikawa, S., Giorgianni, M.W., Vaccaro, K., Kassner, V.A., Yoder, J.H., Werner, T., Carroll, S.B., 2015. Gain of cis-regulatory activities underlies novel domains of wingless gene expression in *Drosophila*. Proceedings of the National Academy of Sciences of the United States of America 112, 7524-7529.
Kozopas, K.M., Samos, C.H., Nusse, R., 1998. DWnt-2, a *Drosophila* Wnt gene required for the development of the male reproductive tract, specifies a sexually dimorphic cell fate. Genes & development 12, 1155-1165.
Kraft, R., Jäckle, H., 1994. *Drosophila* mode of metamerization in the embryogenesis of the lepidopteran insect Manduca sexta. Proceedings of the National Academy of Sciences of the United States of America 91, 6634-6638.
Kramps, T., Peter, O., Brunner, E., Nellen, D., Froesch, B., Chatterjee, S., Murone, M., Zullig, S., Basler, K., 2002. Wnt/wingless signaling requires BCL9/legless-mediated recruitment of pygopus to the nuclear beta-catenin-TCF complex. Cell 109, 47-60.
Krause, G., 1939. Die Eitypen der Insekten. Biologisches Zentralblatt 59.
Krause, G., Krause, J., 1964. Schichtenbau und Segmentierung junger Keimanlagen von *Bombyx mori* L. (Lepidoptera) in vitro ohne Dottersystem. Wilhelm Roux' Archiv für Entwicklungsmechanik der Organismen 155, 451-510.
Kumar, R., Chotaliya, M., Vuppala, S., Auradkar, A., Palasamudrum, K., Joshi, R., 2015. Role of Homothorax in region specific regulation of *Deformed* in embryonic neuroblasts. Mechanisms of Development 138, 190-197.
Kusserow, A., Pang, K., Sturm, C., Hrouda, M., Lentfer, J., Schmidt, H.A., Technau, U., von Haeseler, A., Hobmayer, B., Martindale, M.Q., Holstein, T.W., 2005. Unexpected complexity of the Wnt gene family in a sea anemone. Nature 433, 156-160.
Langton, P.F., Kakugawa, S., Vincent, J.P., 2016. Making, Exporting, and Modulating Wnts. Trends in cell biology 26, 756-765.
Lapebie, P., Borchiellini, C., Houliston, E., 2011. Dissecting the PCP pathway: one or more pathways?: Does a separate Wnt-Fz-Rho pathway drive morphogenesis? BioEssays : news and reviews in molecular, cellular and developmental biology 33, 759-768.
Larkin, M.A., Blackshields, G., Brown, N.P., Chenna, R., McGettigan, P.A., McWilliam, H., Valentin, F., Wallace, I.M., Wilm, A., Lopez, R., Thompson, J.D., Gibson, T.J., Higgins, D.G., 2007. Clustal W and Clustal X version 2.0. Bioinformatics 23, 2947-2948.
Lebreton, G., Faucher, C., Cribbs, D.L., Benassayag, C., 2008. Timing of Wingless signalling distinguishes maxillary and antennal identities in *Drosophila melanogaster* Development 135, 2301.
Lengfeld, T., Watanabe, H., Simakov, O., Lindgens, D., Gee, L., Law, L., Schmidt, H.A., Ozbek, S., Bode, H., Holstein, T.W., 2009. Multiple Wnts are involved in Hydra organizer formation and regeneration. Developmental biology 330, 186-199.

Li, M.Z., Elledge, S.J., 2012. SLIC: a method for sequence- and ligation-independent cloning. Methods in molecular biology 852, 51-59.
Liu, Q., Onal, P., Datta, R.R., Rogers, J.M., Schmidt-Ott, U., Bulyk, M.L., Small, S., Thornton, J.W., 2018. Ancient mechanisms for the evolution of the bicoid homeodomain's function in fly development. eLife 7, e34594.
Livraghi, L., Vodă, R., Evans, L.C., Gibbs, M., Dincă, V., Holland, P.W.H., Shreeve, T.G., Vila, R., Dapporto, L., Breuker, C.J., 2018. Historical and current patterns of gene flow in the butterfly *Pararge aegeria.* Journal of Biogeography 45, 1628-1639.
Llimargas, M., Lawrence, P.A., 2001. Seven Wnt homologues in *Drosophila*: a case study of the developing tracheae. Proc Natl Acad Sci U S A 98, 14487-14492.
Logan, C.Y., Nusse, R., 2004. The Wnt signaling pathway in development and disease. Annual review of cell and developmental biology 20, 781-810.
MacDonald, B.T., Tamai, K., He, X., 2009. Wnt/β-Catenin Signaling: Components, Mechanisms, and Diseases. Developmental cell 17, 9-26.
Macdonald, W.P., Martin, A., Reed, R.D., 2010. Butterfly wings shaped by a molecular cookie cutter: evolutionary radiation of lepidopteran wing shapes associated with a derived Cut/wingless wing margin boundary system. Evolution & development 12, 296-304.
Maloof, J.N., Whangbo, J., Harris, J.M., Jongeward, G.D., Kenyon, C., 1999. A Wnt signaling pathway controls hox gene expression and neuroblast migration in *C. elegans.* Development 126, 37-49.
Martin, A., Papa, R., Nadeau, N.J., Hill, R.I., Counterman, B.A., Halder, G., Jiggins, C.D., Kronforst, M.R., Long, A.D., McMillan, W.O., Reed, R.D., 2012. Diversification of complex butterfly wing patterns by repeated regulatory evolution of a Wnt ligand. Proceedings of the National Academy of Sciences of the United States of America 109, 12632-12637.
Martin, A., Reed, R.D., 2014. Wnt signaling underlies evolution and development of the butterfly wing pattern symmetry systems. Developmental biology 395, 367-378.
Martin, B.L., Kimelman, D., 2012. Canonical Wnt signaling dynamically controls multiple stem cell fate decisions during vertebrate body formation. Developmental cell 22, 223-232.
Martin, F.A., Morata, G., 2006. Compartments and the control of growth in the *Drosophila* wing imaginal disc. Development 133, 4421-4426.
Masci, J., Monteiro, A., 2005. Visualization of early embryos of the butterfly *Bicyclus anynana.* Zygote (Cambridge, England) 13, 139-144.
Matsuoka, Y., Monteiro, A., 2018. Melanin Pathway Genes Regulate Color and Morphology of Butterfly Wing Scales. Cell Rep 24, 56-65.
McMahon, A.P., Moon, R.T., 1989. Ectopic expression of the proto-oncogene int-1 in *Xenopus* embryos leads to duplication of the embryonic axis. Cell 58, 1075-1084.
Merrill, V.K., Turner, F.R., Kaufman, T.C., 1987. A genetic and developmental analysis of mutations in the Deformed locus in *Drosophila melanogaster*. Developmental biology 122, 379-395.
Miller, J.R., 2002. The Wnts. Genome Biol 3, Reviews3001.
Miya, K., 2003. The early embryonic development of *B. mori* - an ultrastructual point of view. Gendaitosho 1, 1-209.
Moti, N., Yu, J., Boncompain, G., Perez, F., Virshup, D.M., 2019. Wnt traffic from endoplasmic reticulum to filopodia. PloS one 14, e0212711.
Muller, T., Vingron, M., 2000. Modeling amino acid replacement. Journal of computational biology : a journal of computational molecular cell biology 7, 761-776.

Mulligan, K.A., Fuerer, C., Ching, W., Fish, M., Willert, K., Nusse, R., 2012. Secreted Wingless-interacting molecule (Swim) promotes long-range signaling by maintaining Wingless solubility. Proceedings of the National Academy of Sciences of the United States of America 109, 370-377.
Murat, S., Hopfen, C., McGregor, A.P., 2010. The function and evolution of Wnt genes in arthropods. Arthropod structure & development 39, 446-452.
Nakao, H., 2010. Characterization of *Bombyx* embryo segmentation process: expression profiles of *engrailed, even-skipped, caudal,* and *wnt1/wingless* homologues. Journal of Experimental Zoology Part B: Molecular and Developmental Evolution 314B, 224-231.
Neumann, C., Cohen, S., 1997. Morphogens and pattern formation. BioEssays : news and reviews in molecular, cellular and developmental biology 19, 721-729.
Niehrs, C., 2012. The complex world of WNT receptor signalling. Nature reviews. Molecular cell biology 13, 767-779.
Nossa, C.W., Havlak, P., Yue, J.X., Lv, J., Vincent, K.Y., Brockmann, H.J., Putnam, N.H., 2014. Joint assembly and genetic mapping of the Atlantic horseshoe crab genome reveals ancient whole genome duplication. GigaScience 3, 9.
Nusse, R., 2001. An ancient cluster of Wnt paralogues. Trends in genetics : TIG 17, 443.
Nusse, R., 2003. Wnts and Hedgehogs: lipid-modified proteins and similarities in signaling mechanisms at the cell surface. Development 130, 5297-5305.
Nusse, R., Brown, A., Papkoff, J., Scambler, P., Shackleford, G., McMahon, A., Moon, R., Varmus, H., 1991. A new nomenclature for int-1 and related genes: the Wnt gene family. Cell 64, 231.
Nusse, R., Clevers, H., 2017. Wnt/β-Catenin Signaling, Disease, and Emerging Therapeutic Modalities. Cell 169, 985-999.
Nusslein-Volhard, C., Wieschaus, E., Kluding, H., 1984. Mutations affecting the pattern of the larval cuticle in *Drosophila melanogaster* : I. Zygotic loci on the second chromosome. Wilhelm Roux's archives of developmental biology 193, 267-282.
Oberhofer, G., Grossmann, D., Siemanowski, J.L., Beissbarth, T., Bucher, G., 2014. Wnt/beta-catenin signaling integrates patterning and metabolism of the insect growth zone. Development 141, 4740-4750.
Pan, C.L., Howell, J.E., Clark, S.G., Hilliard, M., Cordes, S., Bargmann, C.I., Garriga, G., 2006. Multiple Wnts and frizzled receptors regulate anteriorly directed cell and growth cone migrations in *Caenorhabditis elegans*. Developmental cell 10, 367-377.
Panakova, D., Sprong, H., Marois, E., Thiele, C., Eaton, S., 2005. Lipoprotein particles are required for Hedgehog and Wingless signalling. Nature 435, 58-65.
Panfilio, K.A., 2008. Extraembryonic development in insects and the acrobatics of blastokinesis. Developmental biology 313, 471-491.
Pang, K., Ryan, J.F., Mullikin, J.C., Baxevanis, A.D., Martindale, M.Q., 2010. Genomic insights into Wnt signaling in an early diverging metazoan, the ctenophore *Mnemiopsis leidyi.* EvoDevo 1, 10.
Pani, A.M., Goldstein, B., 2018. Direct visualization of a native Wnt in vivo reveals that a long-range Wnt gradient forms by extracellular dispersal. eLife 7.
Pellegrini, M., 2012. Using phylogenetic profiles to predict functional relationships. Methods in molecular biology 804, 167-177.
Percival-Smith, A., Ponce, G., Pelling, J.J., 2017. The Noncell Autonomous Requirement of Proboscipedia for Growth and Differentiation of the Distal Maxillary Palp during Metamorphosis of *Drosophila melanogaster*. Genet Res Int 2017, 2624170.
Petersen, C.P., Reddien, P.W., 2009. Wnt signaling and the polarity of the primary body axis. Cell 139, 1056-1068.

Pfeiffer, B.D., Jenett, A., Hammonds, A.S., Ngo, T.-T.B., Misra, S., Murphy, C., Scully, A., Carlson, J.W., Wan, K.H., Laverty, T.R., Mungall, C., Svirskas, R., Kadonaga, J.T., Doe, C.Q., Eisen, M.B., Celniker, S.E., Rubin, G.M., 2008. Tools for neuroanatomy and neurogenetics in *Drosophila*. Proceedings of the National Academy of Sciences 105, 9715-9720.

Piddini, E., Marshall, F., Dubois, L., Hirst, E., Vincent, J.P., 2005. Arrow (LRP6) and Frizzled2 cooperate to degrade Wingless in *Drosophila* imaginal discs. Development 132, 5479-5489.

Prakash, A., Monteiro, A., 2018a. apterous A specifies dorsal wing patterns and sexual traits in butterflies. Proceedings. Biological sciences / The Royal Society 285.

Prakash, A., Monteiro, A., 2018b. apterous A specifies dorsal wing patterns and sexual traits in butterflies. Proceedings. Biological sciences 285, 20172685.

Prud'homme, B., Lartillot, N., Balavoine, G., Adoutte, A., Vervoort, M., 2002. Phylogenetic analysis of the Wnt gene family. Insights from lophotrochozoan members. Current biology : CB 12, 1395.

Pultz, M.A., Diederich, R.J., Cribbs, D.L., Kaufman, T.C., 1988. The proboscipedia locus of the Antennapedia complex: a molecular and genetic analysis. Genes & development 2, 901-920.

Putnam, N.H., *et al*. 2008. The amphioxus genome and the evolution of the chordate karyotype. Nature 453, 1064-1071.

Raible, F., Tessmar-Raible, K., Osoegawa, K., Wincker, P., Jubin, C., Balavoine, G., Ferrier, D., Benes, V., de Jong, P., Weissenbach, J., Bork, P., Arendt, D., 2005. Vertebrate-type intron-rich genes in the marine annelid Platynereis dumerilii. Science (New York, N.Y.) 310, 1325-1326.

Ramirez-Weber, F.A., Kornberg, T.B., 1999. Cytonemes: cellular processes that project to the principal signaling center in *Drosophila* imaginal discs. Cell 97, 599-607.

Riddiford, L.M., Truman, J.W., Mirth, C.K., Shen, Y.-C., 2010. A role for juvenile hormone in the prepupal development of *Drosophila melanogaster*. Development (Cambridge, England) 137, 1117-1126.

Riddiford, N., Olson, P.D., 2011. Wnt gene loss in flatworms. Development genes and evolution 221, 187-197.

Rijsewijk, F., Schuermann, M., Wagenaar, E., Parren, P., Weigel, D., Nusse, R., 1987. The *Drosophila* homolog of the mouse mammary oncogene int-1 is identical to the segment polarity gene wingless. Cell 50, 649-657.

Robertson, A.J., Coluccio, A., Knowlton, P., Dickey-Sims, C., Coffman, J.A., 2008. Runx expression is mitogenic and mutually linked to Wnt activity in blastula-stage sea urchin embryos. PloS one 3, e3770.

Robinow, S., White, K., 1988. The locus elav of *Drosophila melanogaster* is expressed in neurons at all developmental stages. Developmental biology 126, 294-303.

Rocheleau, C.E., Downs, W.D., Lin, R., Wittmann, C., Bei, Y., Cha, Y.H., Ali, M., Priess, J.R., Mello, C.C., 1997. Wnt signaling and an APC-related gene specify endoderm in early *C. elegans* embryos. Cell 90, 707-716.

Rosenfeld, J.A., Reeves, D., Brugler, M.R., Narechania, A., Simon, S., Durrett, R., Foox, J., Shianna, K., Schatz, M.C., Gandara, J., Afshinnekoo, E., Lam, E.T., Hastie, A.R., Chan, S., Cao, H., Saghbini, M., Kentsis, A., Planet, P.J., Kholodovych, V., Tessler, M., Baker, R., DeSalle, R., Sorkin, L.N., Kolokotronis, S.O., 2016. Genome assembly and geospatial phylogenomics of the bed bug *Cimex lectularius*. 7, 10164.

Roy, S., Hsiung, F., Kornberg, T.B., 2011. Specificity of *Drosophila* cytonemes for distinct signaling pathways. Science (New York, N.Y.) 332, 354-358.

Ryan, J.F., Pang, K., Schnitzler, C.E., Nguyen, A.D., Moreland, R.T., Simmons, D.K., Koch, B.J., Francis, W.R., Havlak, P., Program, N.C.S., Smith, S.A., Putnam, N.H., Haddock, S.H., Dunn, C.W., Wolfsberg, T.G., Mullikin, J.C., Martindale, M.Q., Baxevanis, A.D., 2013. The genome of the ctenophore *Mnemiopsis leidyi* and its implications for cell type evolution. Science (New York, N.Y.) 342, 1242592.

Sander, K., 1983. The evolution of patterning mechanisms: gleanings from insect embryogenesis and spermatogenesis. Development and evolution

Schindelin, J., Arganda-Carreras, I., Frise, E., Kaynig, V., Longair, M., Pietzsch, T., Preibisch, S., Rueden, C., Saalfeld, S., Schmid, B., Tinevez, J.Y., White, D.J., Hartenstein, V., Eliceiri, K., Tomancak, P., Cardona, A., 2012. Fiji: an open-source platform for biological-image analysis. Nat Methods 9, 676-682.

Schneider, C.A., Rasband, W.S., Eliceiri, K.W., 2012. NIH Image to ImageJ: 25 years of image analysis. Nature Methods 9, 671.

Schubert, M., Holland, L.Z., Stokes, M.D., Holland, N.D., 2001. Three amphioxus Wnt genes (AmphiWnt3, AmphiWnt5, and AmphiWnt6) associated with the tail bud: the evolution of somitogenesis in chordates. Developmental biology 240, 262-273.

Schwager, E.E., *et al*. 2013. An in-silico genomic survey to annotate genes coding for early development-relevant signaling molecules in the pearl oyster, *Pinctada fucata.* Zoological science 30, 877-888.

Seto, E.S., Bellen, H.J., 2004. The ins and outs of Wingless signaling. Trends in cell biology 14, 45-53.

Sharma, R.P., 1973. Wingless a new mutant in *Drosophila melanogaster. Drosophila* information service 50, p. 134.

Shigenobu, S., Bickel, R.D., Brisson, J.A., Butts, T., Chang, C.C., Christiaens, O., Davis, G.K., Duncan, E.J., Ferrier, D.E., Iga, M., Janssen, R., Lin, G.W., Lu, H.L., McGregor, A.P., Miura, T., Smagghe, G., Smith, J.M., van der Zee, M., Velarde, R.A., Wilson, M.J., Dearden, P.K., Stern, D.L., 2010. Comprehensive survey of developmental genes in the pea aphid, *Acyrthosiphon pisum*: frequent lineage-specific duplications and losses of developmental genes. Insect Mol Biol 19 Suppl 2, 47-62.

Shingleton, A.W., 2010. The regulation of organ size in *Drosophila*. Organogenesis 6, 76-87.

Smith-Bolton, R.K., Worley, M.I., Kanda, H., Hariharan, I.K., 2009. Regenerative growth in *Drosophila* imaginal discs is regulated by Wingless and Myc. Developmental cell 16, 797-809.

Smith, J., Kraemer, E., Liu, H., Theodoris, C., Davidson, E., 2008. A spatially dynamic cohort of regulatory genes in the endomesodermal gene network of the sea urchin embryo. Developmental biology 313, 863-875.

Somorjai, I.M.L., Martí-Solans, J., Diaz-Gracia, M., Nishida, H., Imai, K.S., Escrivà, H., Cañestro, C., Albalat, R., 2018. Wnt evolution and function shuffling in liberal and conservative chordate genomes. Genome biology 19, 98-98.

Srahna, M., Leyssen, M., Choi, C.M., Fradkin, L.G., Noordermeer, J.N., Hassan, B.A., 2006. A signaling network for patterning of neuronal connectivity in the *Drosophila* brain. PLoS biology 4, e348.

Srivastava, M., Begovic, E., Chapman, J., Putnam, N.H., Hellsten, U., Kawashima, T., Kuo, A., Mitros, T., Salamov, A., Carpenter, M.L., Signorovitch, A.Y., Moreno, M.A., Kamm, K., Grimwood, J., Schmutz, J., Shapiro, H., Grigoriev, I.V., Buss, L.W., Schierwater, B., Dellaporta, S.L., Rokhsar, D.S., 2008. The Trichoplax genome and the nature of placozoans. Nature 454, 955-960.

Stamatakis, A., 2014. RAxML version 8: a tool for phylogenetic analysis and post-analysis of large phylogenies. Bioinformatics 30, 1312-1313.
Stamatakis, A., Hoover, P., Rougemont, J., 2008. A rapid bootstrap algorithm for the RAxML Web servers. Systematic biology 57, 758-771.
Stanganello, E., Hagemann, A.I.H., Mattes, B., Sinner, C., Meyen, D., Weber, S., Schug, A., Raz, E., Scholpp, S., 2015. Filopodia-based Wnt transport during vertebrate tissue patterning. Nature Communications 6, 5846.
Stefanik, D.J., Lubinski, T.J., Granger, B.R., Byrd, A.L., Reitzel, A.M., DeFilippo, L., Lorenc, A., Finnerty, J.R., 2014. Production of a reference transcriptome and transcriptomic database (EdwardsiellaBase) for the lined sea anemone, *Edwardsiella lineata*, a parasitic cnidarian. BMC genomics 15, 71.
Sullivan, J.C., Ryan, J.F., Mullikin, J.C., Finnerty, J.R., 2007. Conserved and novel Wnt clusters in the basal eumetazoan *Nematostella vectensis*. Development genes and evolution 217, 235-239.
Swarup, S., Verheyen, E.M., 2012. Wnt/Wingless signaling in *Drosophila*. Cold Spring Harbor perspectives in biology 4.
Tagle, D.A., Koop, B.F., Goodman, M., Slightom, J.L., Hess, D.L., Jones, R.T., 1988. Embryonic ε and γ globin genes of a prosimian primate (*Galago crassicaudatu*s): Nucleotide and amino acid sequences, developmental regulation and phylogenetic footprints. Journal of Molecular Biology 203, 439-455.
Takada, S., Fujimori, S., Shinozuka, T., Takada, R., Mii, Y., 2017. Differences in the secretion and transport of Wnt proteins. J Biochem 161, 1-7.
Takeshita, H., Sawa, H., 2005. Asymmetric cortical and nuclear localizations of WRM-1/beta-catenin during asymmetric cell division in *C. elegans.* Genes & development 19, 1743-1748.
Takeuchi, T., Koyanagi, R., Gyoja, F., Kanda, M., Hisata, K., Fujie, M., Goto, H., Yamasaki, S., Nagai, K., Morino, Y., Miyamoto, H., Endo, K., Endo, H., Nagasawa, H., Kinoshita, S., Asakawa, S., Watabe, S., Satoh, N., Kawashima, T., 2016. Bivalve-specific gene expansion in the pearl oyster genome: implications of adaptation to a sessile lifestyle. Zoological letters 2, 3.
Tang, X., Wu, Y., Belenkaya, T.Y., Huang, Q., Ray, L., Qu, J., Lin, X., 2012. Roles of N-glycosylation and lipidation in Wg secretion and signaling. Developmental biology 364, 32-41.
Tautz, D., Pfeifle, C., 1989. A non-radioactive *in situ* hybridization method for the localization of specific RNAs in *Drosophila* embryos reveals translational control of the segmentation gene hunchback. Chromosoma 98, 81-85.
The Honeybee Genome Sequencing, C., 2006. Insights into social insects from the genome of the honeybee *Apis mellifera*. Nature 443, 931-949.
Thorpe, C.J., Weidinger, G., Moon, R.T., 2005. Wnt/beta-catenin regulation of the Sp1-related transcription factor sp5l promotes tail development in zebrafish. Development 132, 1763-1772.
Ueno, K., Nagata, T., Suzuki, Y., 1995. Roles of homeotic genes in the *Bombyx* body plan. Cambridge University Press 1, 165-181.
Veeman, M.T., Axelrod, J.D., Moon, R.T., 2003. A second canon. Functions and mechanisms of beta-catenin-independent Wnt signaling. Developmental cell 5, 367-377.
Venter, J.C., *et al*. 2001. The sequence of the human genome. Science (New York, N.Y.) 291, 1304-1351.
Wang, X., Page-McCaw, A., 2018. *Wnt6* maintains anterior escort cells as an integral component of the germline stem cell niche. Development (Cambridge, England) 145, dev158527.

Waterhouse, A., Bertoni, M., Bienert, S., Studer, G., Tauriello, G., Gumienny, R., Heer, F.T., de Beer, T.A P., Rempfer, C., Bordoli, L., Lepore, R., Schwede, T., 2018. SWISS-MODEL: homology modelling of protein structures and complexes. Nucleic acids research 46, W296-W303.
Wickham, H., 2009. ggplot2: Elegant Graphics for Data Analysis. Springer Publishing Company, Incorporated.
Wikramanayake, A.H., Peterson, R., Chen, J., Huang, L., Bince, J.M., McClay, D.R., Klein, W.H., 2004. Nuclear beta-catenin-dependent *Wnt8* signaling in vegetal cells of the early sea urchin embryo regulates gastrulation and differentiation of endoderm and mesodermal cell lineages. Genesis 39, 194-205.
Willert, K., Brown, J.D., Danenberg, E., Duncan, A.W., Weissman, I.L., Reya, T., Yates, J.R., 3rd, Nusse, R., 2003. Wnt proteins are lipid-modified and can act as stem cell growth factors. Nature 423, 448-452.
Windsor, P.J., Leys, S.P., 2010. Wnt signaling and induction in the sponge aquiferous system: evidence for an ancient origin of the organizer. Evolution & development 12, 484-493.
Wodarz, A., Nusse, R., 1998. Mechanisms of Wnt signaling in development. Annual review of cell and developmental biology 14, 59-88.
Wu, C.H., Nusse, R., 2002. Ligand receptor interactions in the Wnt signaling pathway in *Drosophila*. J Biol Chem 277, 41762-41769.
Yamanaka, N., Rewitz, K.F., O'Connor, M.B., 2013. Ecdysone control of developmental transitions: lessons from *Drosophila* research. Annual review of entomology 58, 497-516.
Yamazaki, Y., Palmer, L., Alexandre, C., Kakugawa, S., Beckett, K., Gaugue, I., Palmer, R.H., Vincent, J.P., 2016. Godzilla-dependent transcytosis promotes Wingless signalling in *Drosophila* wing imaginal discs. Nature cell biology 18, 451-457.
Yang, Y., Mlodzik, M., 2015. Wnt-Frizzled/planar cell polarity signaling: cellular orientation by facing the wind (Wnt). Annual review of cell and developmental biology 31, 623-646.
Yang, Z., 1993. Maximum-likelihood estimation of phylogeny from DNA sequences when substitution rates differ over sites. Molecular biology and evolution 10, 1396-1401.
Yoshida, Y., Koutsovoulos, G., Laetsch, D.R., Stevens, L., Kumar, S., Horikawa, D.D., Ishino, K., Komine, S., Kunieda, T., Tomita, M., Blaxter, M., Arakawa, K., 2017. Comparative genomics of the tardigrades *Hypsibius dujardin*i and *Ramazzottius varieornatus.* PLoS biology 15, e2002266.
Zecca, M., Basler, K., Struhl, G., 1996. Direct and long-range action of a *wingless* morphogen gradient. Cell 87, 833-844.
Zhan, T., Rindtorff, N., Boutros, M., 2017. Wnt signaling in cancer. Oncogene 36, 1461-1473.
Zhang, L., Martin, A., Perry, M.W., van der Burg, K.R., Matsuoka, Y., Monteiro, A., Reed, R.D., 2017. Genetic Basis of Melanin Pigmentation in Butterfly Wings. Genetics 205, 1537-1550.
Zhang, Z., Aslam, A.F., Liu, X., Li, M., Huang, Y., Tan, A., 2015. Functional analysis of *Bombyx Wnt1* during embryogenesis using the CRISPR/Cas9 system. Journal of insect physiology 79, 73-79.
Zhou, Q., DeSantis, D.F., Friedrich, M., Pignoni, F., 2016. Shared and distinct mechanisms of atonal regulation in *Drosophila* ocelli and compound eyes. Developmental biology 418, 10-16.